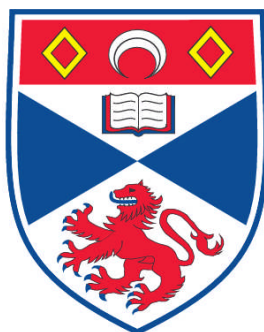


**MOLECULAR PROBES FOR THE EVALUATION OF THREE
ISOMERASE ENZYME MECHANISMS IN SECONDARY
METABOLISM**

Pitak Nasomjai

**A Thesis Submitted for the Degree of PhD
at the
University of St. Andrews**



2010

**Full metadata for this item is available in the St Andrews
Digital Research Repository
at:**

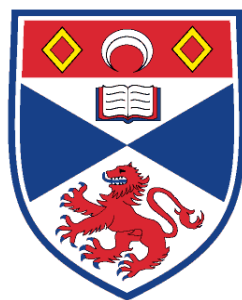
<https://research-repository.st-andrews.ac.uk/>

Please use this identifier to cite or link to this item:

<http://hdl.handle.net/10023/866>

This item is protected by original copyright

**This item is licensed under a
Creative Commons License**



University
of
St Andrews

**Molecular probes for the evaluation of
three isomerase enzyme mechanisms in
secondary metabolism**

By

Pitak Nasomjai

A thesis presented for the degree of
Doctor of Philosophy in the School of Chemistry
University of St Andrews

December 2009

I, Pitak Nasomjai, hereby certify that this thesis, which is approximately 40,000 words in length, has been written by me, that it is the record of work carried out by me and that it has not been submitted in any previous application for a higher degree.

I was admitted as a research student in August 2005 and as a candidate for the degree of Doctor of Philosophy in August 2006; the higher study for which this is a record was carried out in the University of St Andrews between 2005 and 2009.

Datesignature of candidate

I hereby certify that the candidate has fulfilled the conditions of the Resolution and Regulations appropriate for the degree of PhD in the University of St Andrews and that the candidate is qualified to submit this thesis in application for that degree.

Datesignature of supervisor.....

In submitting this thesis to the University of St Andrews we understand that we are giving permission for it to be made available for use in accordance with the regulations of the University Library for the time being in force, subject to any copyright vested in the work not being affected thereby. We also understand that the title and the abstract will be published, and a copy of the work may be made and supplied to any bona fide library or research worker, that my thesis will be electronically accessible for personal or research unless exempt by award of an embargo as requested below, and that the library has the right to migrate my thesis into new electronic forms as required to ensure continued access to the thesis. We have obtained any third-party copy right permissions that may be required in order to allow such access and migration, or have requested the appropriate embargo below.

The following is an agreed request by candidate and supervisor regarding the electronic publication of this thesis:

Access to Printed copy and electronic publication of the thesis through the University of St Andrews.

Datesignature of candidate

Datesignature of supervisor.....

To my grandma and my parents

Acknowledgements

First and foremost, I would like to thank my supervisor Professor David O'Hagan for his supervision, encouragement and advice during my PhD studies.

I would also like to thank all people that were involved in my projects: Dr Darwin W. Reed and Dr. Patrick Covello at the Plant Biotechnology Institute, Canada for “cytochrome P₄₅₀ assays of fluorolittorines”; Dr. Denis Tritsch and Prof. Michel Rohmer at the Université Louis Pasteur/Centre National de la Recherche Scientifique, France for DXR inhibition assays; Prof. David J. Tozer at the University of Durham for DFT calculations on relative energy of fluorobenzyl intermediates and ionisation potentials and Dr. Stuart M. Cross for 5-FDRP isomerase assays.

I am grateful to all the following people for technical support: Prof. Alexandra Slawin for X-ray analysis, Melanja Smith and Dr Tomas Lebl for NMR spectroscopy, and Caroline Hosburgh and Catherine Botting for mass spectrometry.

Special thanks must go to DOH members past and present: Luke, Natalie, Mayca, Matthieu, Vincent, Thomas, David, Guillaume, Stefano, Jason Schmidberger, Gildas, Daniel, Nelly, Deng and Daniel Smith. A very special thanks to Cosimo for passing on his knowledge.

Also, I would like to thank all my friends: Chamnan, Walailuck, Kannika, Sujitra and Annop for their fantastic friendships.

I am also thankful to the Royal Thai Government for financial support and the staff at the OEA, Royal Thai embassy (London) for help.

I am deeply thankful to Assoc. Somdej and Kwanjai Kanokmedhakul without them it would not be possible for me to reach this far.

Last but not least, I would like to thank all my family for their constant support.

Contents

Declaration	<i>i</i>
Acknowledgements	<i>ii</i>
Contents	<i>iii</i>
List of abbreviations	<i>xiii</i>
Abstract	<i>xvii</i>

1	Introduction	1
1.1	Carbon skeleton rearrangements in enzymology	2
1.2	Isomerisations mediated by co-enzyme B₁₂	2
1.3	Biosynthesis of tenellin	7
1.4	Isomerisation of liquiritigenin to daidzein. Isoflavonoid biosynthesis	9
1.5	Biosynthesis of cephalosporin C	11
1.6	Biosynthesis of cholesterol	13
1.7	Biosynthesis of <i>myo</i>-inositol	14
1.8	References chapter 1	17
2	Exploring the mechanism of the rearrangement of littorine to hyoscyamine	19
2.1	Introduction	20
2.2	The tropane alkaloids	20

2.3	Biosynthesis of tropane alkaloids	24
2.3.1	Total synthesis of tropine and the structural elucidation of tropine	24
2.3.2	Biosynthesis of the tropane ring	26
2.3.2.1	The amino acid derived fragment	27
2.3.2.2	The acetate derived fragment	34
2.3.2.3	The reduction of tropinone to tropine	38
2.3.3	Biosynthesis of hyoscyamine	38
2.3.3.1	Littorine as a precursor	38
2.3.3.2	Stereochemistry of the rearrangement	41
2.4	Enzymes that mediate a molecular rearrangement	44
2.4.1	Co-enzyme B ₁₂ and SAM ‘the poor man’s B ₁₂ ’ are not involved	44
2.4.2	The role of cytochrome P ₄₅₀ enzymes.	46
2.5	Reactive species involved in P₄₅₀ transformations	49
2.6	Radical or carbocation rearrangement process	52
2.7	Computational studies	54
2.8	Fluorine as mechanistic probe	56
2.8.1	Effect of fluorine on the aromatic ring	56
2.8.2	Effect of fluorine on benzylic carbocation and radical	57
2.8.3	The use of fluorine as a mechanistic probe in tropane alkaloid biosynthesis	57
2.9	Aims of the study	58
2.10	Results	59
2.10.1	DFT study on the relative energies of <i>ortho</i> -, <i>meta</i> -, and <i>para</i> - fluorobenzyl radicals and cations	59
2.10.2	Ionisation potentials	61

2.10.3	Synthesis	62
2.10.3.1	Synthesis of <i>rac</i> -fluorolittorines	
2.10.3.1.1	Synthesis of <i>rac</i> -2', 3', 4'-fluorophenyllactic acid	62
2.10.3.1.2	Synthesis of <i>rac</i> -2', 3', 4'- fluorophenyllactoyl tropines (<i>rac</i> -fluorolittorines)	62
2.10.3.2	The synthesis of enantio-enriched 2', 3', 4'-fluorolittorines	63
2.10.3.2.1	Resolution by preparation of (-)-menthol derivative	63
2.10.3.2.2	(1 <i>S</i>)-(-)-Camphanoyl chloride derivative	67
2.10.3.2.3	Resolution by preparation of amides	69
2.10.3.2.4	Resolution by D-phenylalanine methyl ester hydrochloride and (<i>S</i>)-phenylethylamine	71
2.10.3.2.5	Hydrolysis of enantio-enriched fluoroaryl amides	76
2.10.3.2.6	Determination of enantiomeric excess of the resolved fluorophenyllactic acids	78
2.10.3.2.7	Preparation of enantio-enriched fluorolittorines	80
2.10.3.3	Enzyme resolution	81
2.19.3.4	Preparation of enantio-enriched (<i>S</i>)-[3',3'- ² H ₂]-littorines and (<i>R</i>)-[3',3'- ² H ₂]-littorines	84
2.10.4	Bioassay results	86
2.10.4.1	Kinetic isotope effect study	86
2.10.4.2	Enzyme assays of <i>rac</i> -2', 3', 4'-fluorolittorines with CYP80F1	88
2.10.4.3	Enzyme assays of enantio-enriched (<i>R</i>)-2', 3', 4'-fluorolittorines	90
2.10.4.4	Enzyme assays of enantio-enriched (<i>S</i>)-2', 3', 4'-fluorolittorines	92
2.11	Discussion	94
2.12	Conclusions	97

2.13	References	98
3	Synthesis of the ribose phosphonates	106
3.1	Introduction	107
3.2	The biosynthesis of fluoroacetate and 4-fluorothreonine	107
3.3	The isomerisation of 5-FDRP to 5-FDRulP	110
3.3.1	The aldo-keto, MTR-1-P isomerase	110
3.3.2	Crystal structure of MTR-1-P isomerase from <i>Bacillus subtilis</i> .	111
3.3.3	5-FDRulP is an intermediate in fluorometabolite biosynthesis in <i>S. cattleya</i>	112
3.4	Identification of the putative isomerase gene in <i>S. cattleya</i>	115
3.5	Putative mechanisms for the isomerisation of 5-FDRP to 5-FDRulP	116
35.1	The <i>cis</i> -enediol and hydride shift mechanism	116
3.5.2	The phosphate migration mechanism	119
3.6	Aims of the project	120
3.7	Results and discussion	121
3.7.1	Synthesis	121
3.7.1.1	Synthetic plans	121
3.7.2	Preparation of phosphonates	123
3.7.2.1	The D-ribonic- γ -lactone route-Route A	123
3.7.2.2	The D-ribose route-Route B	127
3.7.2.3	Preparation of phostones	133
3.7.3	Bioassay results	135
3.8	Conclusions	137

3.9	References	138
4	Synthesis of potential DXR inhibitors	141
4.1	Introduction	142
4.2	Biosynthesis of the isoprenoid precursors IPP and DMAPP	144
4.2.1	The mevalonic acid pathway	144
4.2.2	The MEP or DOXP pathway	145
4.3	The rearrangement of DXP to MEP	148
4.3.1	The proposed mechanism of the rearrangement of DXP to MEP	148
4.3.1.1	α -Ketol rearrangement	148
4.3.1.2	The retro-aldol/aldol rearrangement	149
4.3.1.3	Hydride/methyl shift	150
4.3.2	α -Ketol or retro-aldol/aldol rearrangement mechanism	151
4.4	The structure of the DXR enzyme	153
4.5	Inhibitors of DXR enzyme	158
4.6	Aims of the project	159
4.7	Previous study on the synthesis of potential DXR inhibitors	161
4.8	Results	163
4.8.1	Synthesis	163
4.8.1.1	Preparation of 5-hydroxy-3,4-dioxo-hexyl-phosphonate	163
4.8.1.2	Preparation of [5- ¹³ C]-5-hydroxy-3,4-dioxo-hexyl-phosphonate	166
4.8.1.3	Preparation of [4- ¹³ C]-1-bromo-4-hydroxy-pent-2-yne	167
4.8.1.4	Preparation of [5- ¹³ C]- α -diketone	169
4.8.1.5	Preparation of [5- ¹³ C]- α -diketone phosphonate	171

4.8.2	Influence of pH on tautomerism of [5- ¹³ C]- α -diketone phosphonate	173
4.8.3	Incubation of 58a with <i>E. coli</i> DXR results	175
4.9	Discussion and conclusion	176
4.10	References	180
5	Chemical and biochemical experiments	184
5.1	General methods	185
5.2	Synthetic experiment for Chapter 2	187
5.2.1	(<i>RS</i>)- <i>o</i> -Fluorophenyllactic acid	187
5.2.2	(<i>RS</i>)- <i>m</i> -Fluorophenyllactic acid	188
5.2.3	(<i>RS</i>)- <i>p</i> -Fluorophenyllactic acid	188
5.2.4	(<i>rac</i>)- <i>o</i> -Fluorolittorine	189
5.2.5	(<i>rac</i>)- <i>m</i> -Fluorolittorine	190
5.2.6	(<i>rac</i>)- <i>p</i> -Fluorolittorine	191
5.2.7	Methyl (<i>RS</i>)- <i>p</i> -fluorophenyllactate	192
5.2.8	(-)-Menthyl (<i>RS</i>)- <i>m</i> -fluorophenyllactate	193
5.2.9	α -Acetyl-(-)-menthyl (<i>RS</i>)- <i>m</i> -fluorophenyllactate	195
5.2.10	(<i>S</i>)-Camphanoyl methyl (<i>RS</i>)- <i>p</i> -fluorophenyllactate	196
5.2.11	α -Acetyl-methyl-D-phenylalanyl-(<i>RS</i>)- <i>p</i> -fluorophenyllactamide	197
5.2.12	(<i>S</i>)-3-(2-Fluorophenyl)-2-hydroxyl- <i>N</i> -((<i>S</i>)-1-phenylethyl) propanamide and (<i>S</i>)-3-(2-fluorophenyl)-2-hydroxyl- <i>N</i> -((<i>S</i>)-1- phenylethyl)propanamide	199
5.2.13	(<i>S</i>)-3-(3-Fluorophenyl)-2-hydroxyl- <i>N</i> -((<i>S</i>)-1-phenylethyl)	

propanamide and (S)-3-(3-fluorophenyl)-2-hydroxyl- <i>N</i> -((S)-1-phenylethyl)propanamide	201
5.2.14 (S)-3-(4-Fluorophenyl)-2-hydroxyl- <i>N</i> -((S)-1-phenylethyl)propanamide and (S)-3-(4-fluorophenyl)-2-hydroxyl- <i>N</i> -((S)-1-phenylethyl)propanamide	202
5.2.15 (S)- <i>o</i> -Fluorophenyllactic acid	204
5.2.16 (R)- <i>o</i> -Fluorophenyllactic acid	205
5.2.17 (S)- <i>m</i> -Fluorophenyllactic acid	205
5.2.18 (R)- <i>m</i> -Fluorophenyllactic acid	206
5.2.19 (S)- <i>p</i> -Fluorophenyllactic acid	207
5.2.20 (R)- <i>p</i> -Fluorophenyllactic acid	208
5.2.21 (S)- <i>o</i> -Fluorolittorine	209
5.2.22 (R)- <i>o</i> -Fluorolittorine	210
5.2.23 (S)- <i>m</i> -Fluorolittorine	211
5.2.24 (R)- <i>m</i> -Fluorolittorine	212
5.2.25 (S)- <i>p</i> -Fluorolittorine	213
5.2.26 (R)- <i>p</i> -Fluorolittorine	214
5.2.27 (2 <i>S</i> ,2' <i>S</i>)-[3,3- ² H ₂]-3-Phenyl-2-hydroxyl- <i>N</i> -((S)-1-phenylethyl)propanamide and (2 <i>R</i> ,2' <i>S</i>)-[3,3- ² H ₂]-3-phenyl-2-hydroxyl- <i>N</i> -((S)-1-phenylethyl)	215
5.2.28 (S)-[3,3- ² H ₂]-Phenyllactic acid	216
5.2.29 (R)-[3,3- ² H ₂]-Phenyllactic acid	217
5.2.30 (S)-[3',3'- ² H ₂]-Littorine	218
5.2.31 (R)-[3',3'- ² H ₂]-Littorine	219
5.2.32 Enzymatic resolution of fluorophenyllactic acids	220

5.2.33	(<i>R</i>)-2-Acetoxy-3-(3-fluorophenyl)-2-hydroxyl- <i>N</i> -((<i>S</i>)-1-phenylethyl)propanamide	221
5.3	Synthetic experiments for Chapter 3	223
5.3.1	2,3- <i>O</i> -Isopropylidene-D-ribono-1,4-lactone	223
5.3.2	5-Deoxy-5-fluoro-2,3- <i>O</i> -isopropylidene-D-ribono-1,4-lactone	224
5.3.3	5-Deoxy-5-fluoro-2,3- <i>O</i> -isopropylidene-D-ribofuranose and (2 <i>S</i> ,3 <i>S</i> ,4 <i>S</i>)-5-fluoro-2,3-(<i>O</i> -isopropylidenedioxy)pentan-1,4-diol	225
5.3.3.1	Synthesis with NaBH ₄	225
5.3.3.2	Synthesis with DIBAL-H	226
5.3.4	5-Deoxy-5-fluoro-1-deoxy-2,3- <i>O</i> -isopropylidene-1-(dimethoxyphosphinyl)-D-ribofuranose	227
5.3.5	2,3- <i>O</i> -Isopropylidene-D-ribofuranose	228
5.3.6	2,3- <i>O</i> -Isopropylidene-5- <i>O</i> -trityl-D-ribofuranose	229
5.3.7	2,5-Anhydro-1-deoxy-2,3- <i>O</i> -isopropylidene-1-(dimethoxyphosphinyl)-5- <i>O</i> -trityl-D-altritol and D-allitol	230
5.3.8	2,5-Anhydro-1-deoxy-2,3- <i>O</i> -4-isopropylidene-1-(dimethoxyphosphinyl)-5- <i>O</i> -D-altrohexitol	232
5.3.9	2,5-Anhydro-1-deoxy-2,3- <i>O</i> -4-isopropylidene-1-(dimethoxyphosphinyl)-5- <i>O</i> -D-allohexitol	233
5.3.10	2,5-Anhydro-1-deoxy-5-fluoro-2,3- <i>O</i> -4-isopropylidene-1-(dimethoxyphosphinyl)-5- <i>O</i> -D-altrohexitol	234
5.3.11	2,5-Anhydro-1-deoxy-5-fluoro-2,3- <i>O</i> -4-isopropylidene-1-(dimethoxyphosphinyl)-5- <i>O</i> -D-allohexitol	235
5.3.12	2,5-Anhydro-1-deoxy-1-phophono-D-altritol	

	cyclohexyl ammonium salt	236
5.3.13	2,5-Anhydro-1-deoxy-1-phosphono-D-allitol	
	cyclohexyl ammonium salt	237
5.3.14	2,5-Anhydro-1-deoxy-5-fluoro-1-phosphono-D-altritol	
	cyclohexyl ammonium salt	238
5.3.15	2,5-Anhydro-1-deoxy-5-fluoro-1-phosphono-D-allitol	
	cyclohexyl ammonium salt	239
5.3.16	Phostonic acid	240
5.3.17	5-Fluorophostonic acid	241
5.4	Synthetic experiments for Chapter 4	242
5.4.1	5-Bromo-3-pentyn-2-ol	242
5.4.2	4-(Triisopropylsilanyloxy)-1-bromopent-2-yne	243
5.4.3	Diethyl 5-(triisopropylsilanyloxy)-hex-3-ynyl-phosphonate	244
5.4.4	Diethyl 5-(triisopropylsilanyloxy)-3,4-dioxohexyl-phosphonate	245
5.4.5	Deprotection of diethyl-5-(triisopropylsilanyloxy)-3,4-	
	dioxohexyl-phosphonate	246
5.4.6	[1- ¹³ C]-acetaldehyde	247
5.4.7	[2- ¹³ C]-5-Bromo-3-pentyn-2-ol	247
5.4.8	[4- ¹³ C]-4-(Triisopropylsilanyloxy)-1-bromopent-2-yne	248
5.4.9	[5- ¹³ C]-Diethyl-5-(triisopropylsilanyloxy)-hex-3-ynyl-	
	phosphonate	249
5.4.10	[5- ¹³ C]-Diethyl 5-(triisopropylsilanyloxy)-3,4-	

dioxohexyl phosphonate	249
5.4.11 Deprotection of [5- ¹³ C]-diethyl 5-(triisopropylsilanoyloxy)-3,4- dioxohexyl phosphonate	250
5.5 Biochemical experiments	251
5.5.1 Bioassay of Chapter 2	251
5.5.1.1 Preparation of yeast microsomes	251
5.5.1.2 GC/MS analysis	252
5.5.1.3 CYP80F1 enzyme assays with fluorolittorines	252
5.5.1.4 CYP80F1 enzyme assays for isotope effect experiments	253
5.5.2 Bioassay of Chapter 3	254
5.5.3 Bioassay of Chapter 4	254
5.6 References	256
<i>Appendix I</i>	258
<i>Appendix II</i>	266

List of Abbreviations

Ac	Acetyl
ACN	Acetonitrile
ATP	Adenosine triphosphate
br s	Broad singlet
BSA	N,O-bis(trimethylsilyl)acetamide
BuLi	Butyl-lithium
CI	Chemical ionization
CoA	Coenzyme A
conc.	Concentrated
d	Doublet
dd	Doublet of doublets
ddd	Doublet of doublet of doublets
dddd	Doublet of doublet of doublet of doublets
DCC	Dicyclohexylcarbodiimide
DCM	Dichloromethane
DIBAL-H	Diisobutylaluminium hydride
DFT	Density functional theory
DMAP	4-Dimethylaminopyridine
DMAPP	Dimethylallyl pyrophosphate
DMSO	Dimethyl-sulfoxide
DOXP	1-Deoxy-D-xylulose 5-phosphate
<i>de</i>	Diastereomeric excess
dec	Decompose
DXP	1-Deoxy-D-xylulose-5-phosphate

EDC	3-Ethyl-1(N,N-dimethyl)aminopropylcarbodiimide
eq.	Equivalent
Et	Ethyl
EtOAc	Ethyl acetate
ES-MS	Electrospray mass spectrometry
5'-FDA	5'-Fluoro-5'-deoxy-adenosine
5-FDR	5-Fluoro-5-deoxy-D-ribose
5-FDRP	5-Fluoro-5-deoxy-D-ribose-1-phosphate
5-FDRuIP	5-Fluoro-5-deoxy-D-ribulose-1-phosphate
g	Gram
GC-MS	Gas chromatography mass spectrometry
h	Hour
HBTU	2-(1H-Benzotriazol-1-yl)-1,1,3,3,-tetramethyluronium hexafluorophosphate
HOBt	1-Hydroxybenzotriazole
HPLC	High pressure liquid chromatography
Hz	Hertz
IPP	Isopentenyl pyrophosphate
IR	Infrared spectroscopy
<i>J</i>	Coupling constant
kDa	Kilo Dalton
KIE	Kinetic isotope effect
LDA	Lithium diisopropylamide
LLD-AVC	L- α -aminoadipyl-L-cysteinyl-D-valine
m	Multiplet

M	Molar
Me	Methyl
MEP	2-C-Methylerythritol-phosphate-2-phosphate
mg	Milligram
min	Minute
mL	Millilitre
mM	Millimolar
mmol	Millimol
mp	Melting point
MTBE	Methy <i>tert</i> -butyl ether
MTR-1-P	5-Methylthio-5-deoxy-D-ribose-1-phosphate
MVA	Mevalonic acid
μl	Microlitres
NAD ⁺	Nicotinamide adenine dinucleotide (oxidised form)
NADH	Nicotinamide adenine dinucleotide (reduced form)
NADPH	Nicotinamide adenine dinucleotide phosphate (reduced form)
NMM	N-methyl morpholine
NMR	Nuclear magnetic resonance
ODC	Ornithine decarboxylase
PEP	Phosphoenoylpyruvate
Ph	Phenyl
PLP	Pyridoxal phosphate
PMT	Putrescine methyl transferase
PPL	Porcine pancreatic lipase
PNP	Purine nucleoside phosphorylase

ppm	Parts per million
Pyr	Pyridine
q	Quartet
qt	Quintet
s	Singlet
SAM	S-Adenosyl-L-methionine
t	Triplet
TBAF	Tetrabutyl ammonium fluoride
TBTU	O-(Benzotriazol-1-yl)-N,N,N',N'-tetramethyluronium tetrafluoroborate
<i>t</i> -BuOH	<i>tert</i> -Butanol
TFA	Trifluoroacetic acid
THF	Tetrahydrofuran
TLC	Thin layer chromatography
TMS	Trimethylsilyl
Tris	Tris(hydroxymethyl)aminoethane
TrCl	Trityl chloride
UV	Ultra-violet

Abstract

This thesis is focused on an investigation of the mechanisms of three enzymatically mediated carbon skeleton isomerisation reactions.

Chapter 1 provides an overview of some representative examples of the carbon skeleton rearrangement reactions in enzymology.

Chapter 2 describes the preparation and use of fluorolittorines to explore the mechanism of the rearrangement of the tropane alkaloid littorine to hyoscyamine which is a reaction mediated by the cytochrome P₄₅₀ enzyme.

Chapter 3 describes the synthesis of D-ribose-1-phosphonates and the cyclic phosphonates (phostone) that are candidate inhibitors of the enzymatic isomerisation of 5-fluoro-5-deoxy-ribose-1-phosphate (5-FDRP) to 5-fluoro-5-deoxy-ribulose-1-phosphate (5-FDRuP), an important step in fluorometabolite biosynthesis pathway in *Streptomyces cattleya*.

Chapter 4 describes the synthesis of 5-hydroxy-3,4-dioxohexylphosphonate and [5-¹³C]-5-hydroxy-3,4-dioxohexylphosphonate. These compounds are proposed as candidates for the transition state of the retro-aldol/aldol mechanism of the enzymatic isomerisation of 1-deoxy-D-xylulose-5-phosphate (DXP) to 2-C-methylerythritol-phosphate-2-phosphate (MEP) in the biosynthesis of isopentenyl pyrophosphate (IPP) and dimethylallyl pyrophosphate (DMAPP). The influence of pH on tautomerisation of [5-¹³C]-5-hydroxy-3,4-dioxohexylphosphonate is also described.

Chapter 5 describes the general chemical and biochemical methodologies utilised in this research project.

Chapter 1

Introduction

1.1 Carbon skeleton rearrangements in enzymology

This thesis explores the mechanisms of three enzymatically mediated carbon skeleton isomerisation reactions. These are: the littorine rearrangement to hyoscyamine; the isomerisation of 5-fluoro-5-deoxy-ribose-1-phosphate to 5-fluoro-5-deoxy-ribulose-1-phosphate; and the isomerisation of 1-deoxy-D-xylulose-5-phosphate (DXP) to 2-C-methylerythritol-4-phosphate (MEP). These three reactions are representative of many unique isomerisation reactions in enzymology particularly in secondary metabolism. By way of introduction to this research some representative examples of enzymatic carbon skeleton isomerisations are discussed in this chapter. Each individual chapter, 2-4 will then introduce details of the enzymatic mechanism under investigation.

1.2 Isomerisations mediated by co-enzyme B₁₂¹⁻³

Co-enzyme B₁₂ (**1**) or adenosylcobalamine is essential to almost all living organisms but is apparently absent from plants. Co-enzyme B₁₂ has a complex structure which was solved using X-ray crystallography by D. C. Hodgkin in 1961. The structure comprises a modified porphyrin ring and a central cobalt ion (Co³⁺). The metal ion is covalently bonded with two axial ligands, the benzimidazole and adenosyl groups. The key feature of co-enzyme B₁₂ is that the Co-adenosine bond is susceptible to homolytic cleavage to generate an adenosyl radical (**2**, Figure 1.1), the initiator of co-enzyme B₁₂ dependent reactions. This adenosyl radical participates in enzymatic reactions such as carbon skeleton rearrangements, 1,2-amino group shifts, and elimination of water or ammonia from substrates (Scheme 1.1).

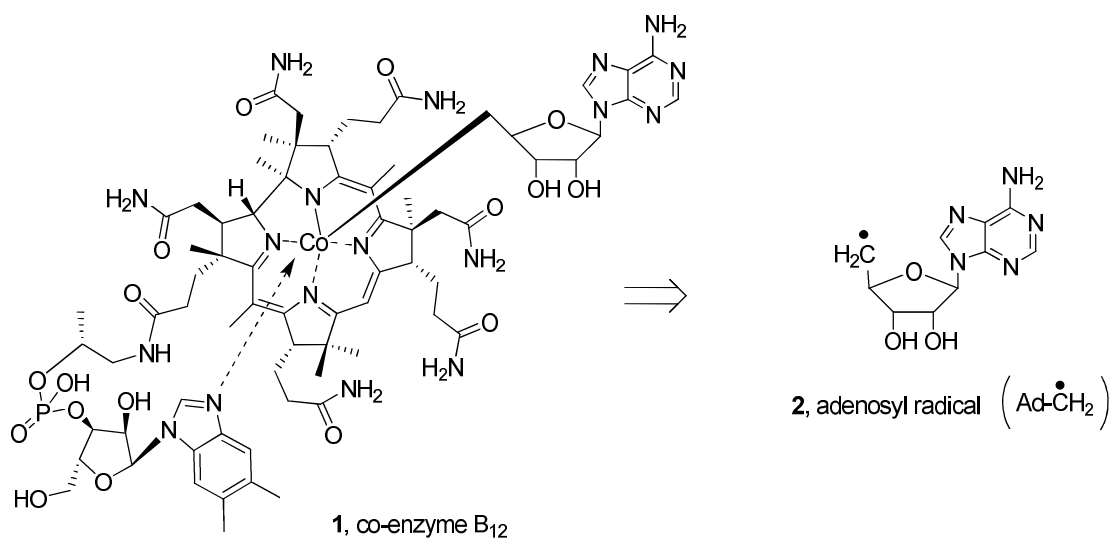
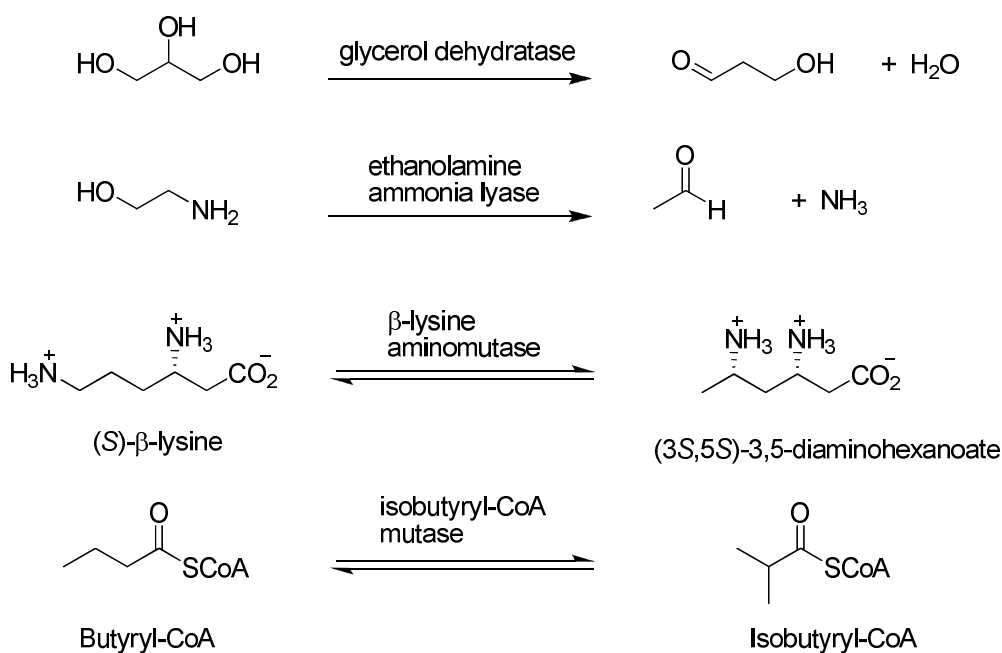


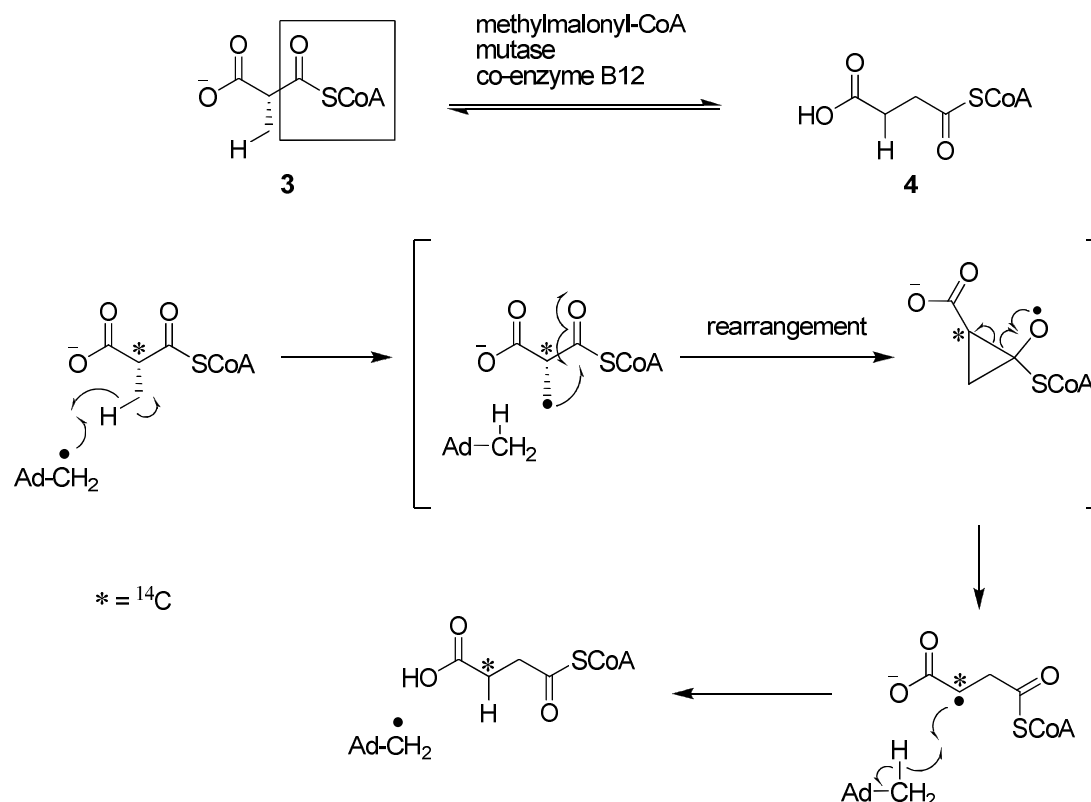
Figure 1.1 Co-enzyme B₁₂ structure and the 5'-adenosyl radical.¹



Scheme 1.1 Examples of co-enzyme B₁₂ mediated reactions.

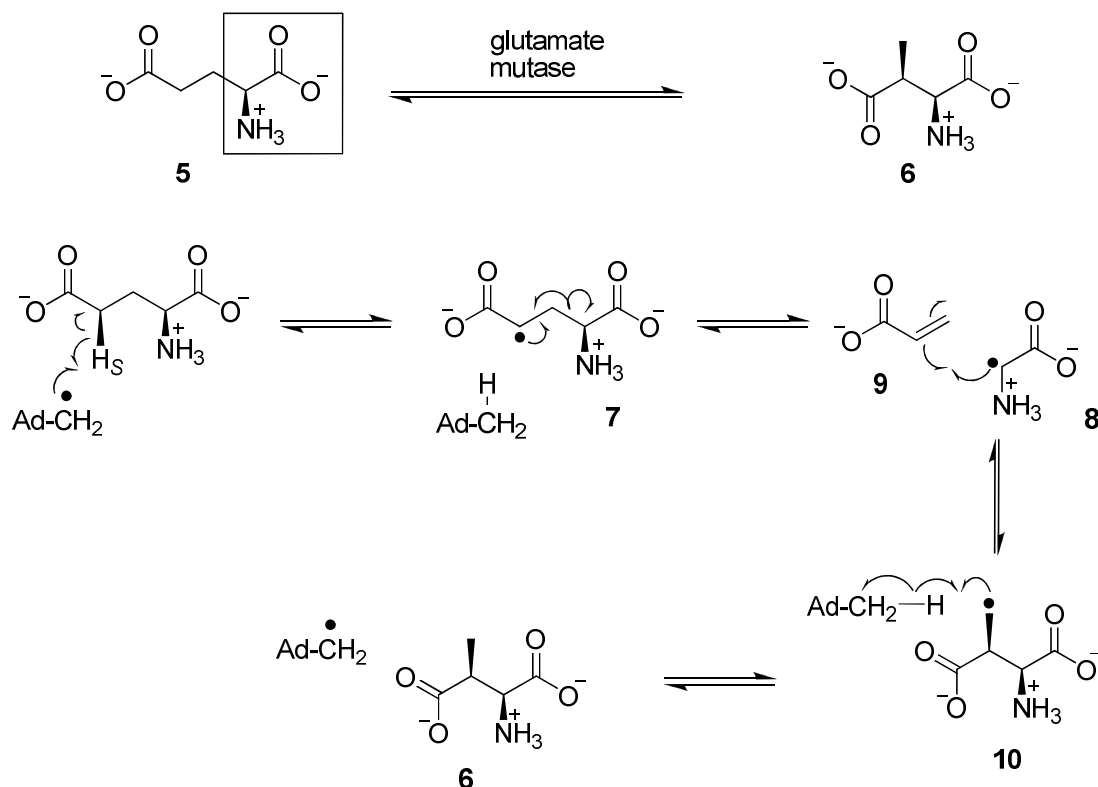
There are four families of co-enzyme B₁₂ dependent enzymes. These are methyltransferases, dehalogenases, eliminases, and mutases.¹ Only the mutase (isomerase) family is described here. Around five mutase enzymes utilise co-enzyme B₁₂ to mediate carbon skeleton rearrangements. The general mechanism involves 5'-

adenosyl radical abstraction of a hydrogen atom from the substrate to form 5'-deoxy-adenosine and a substrate-derived radical. Rearrangement of the substrate-derived radical is followed by recovery of a hydrogen atom from the 5'-methyl group of 5'-deoxy-adenosine to generate the product and regenerate the initiator. For example, methylmalonyl-CoA mutase mediates the rearrangement of (*R*)-methylmalonyl-CoA (**3**) to succinyl-CoA (**4**) a reaction which proceeds *via* radical intermediates, is shown in Scheme 1.2. This is the only mammalian B₁₂ enzyme. The intramolecular rearrangement process had been established by using [2-¹⁴C]-methylmalonyl-CoA. Chemical degradation of the resultant radioactive succinyl-CoA resulted in 80% of the radioisotope located at C-3 of succinyl-CoA, indicating that the isomerisation involved the migration of the thioester group (Scheme 1.2).⁴



Scheme 1.2 Mechanism of co-enzyme B₁₂ mediated rearrangement of methylmalonyl-CoA (**3**) to succinyl-CoA (**4**).^{2, 5}

Isomerisation of the non-essential amino acid (*S*)-glutamate (**5**) to (2*S*,3*S*)-3-methylaspartate (**6**) offers a unique example of a carbon skeleton isomerisation which is mediated by the co-enzyme B₁₂-dependent glutamate mutase. The mechanism has been proposed to proceed *via* radical intermediates and is summarised in Scheme 1.3.⁶ In a similar manner to the methylmalonyl-CoA rearrangement, the C-4 hydrogen atom of glutamate is abstracted by the 5'-adenosylradical to generate the 4-glutamyl radical (**7**) intermediate. Fragmentation of the glutamyl radical generates an intermediate glycinyl radical (**8**) and acrylate (**9**), followed by a recombination of the glycinyl radical to the other end of acrylate double bond to generate methyl aspartyl radical (**10**). Unlike the isomerisation of methylmalonyl-CoA, the migrating carbon of glutamate rearrangement is an *sp*³ and this prohibits formation of a cyclopropyl radical intermediate.^{7, 8} This radical fragmentation-recombination mechanism was supported by EPR studies. Incubations of ²H and ¹³C labelled glutamate substrates led to the identification of the 4-glutamyl radical intermediate as a radical pair with cob(II)alamin.⁹ In addition, the glycinyl radical fragment was trapped as glycine when ¹⁴C-glutamate was incubated with glutamate mutase.¹⁰



Scheme 1.3 Proposed radical fragmentation-recombination mechanism for the isomerisation of glutamate (**5**) to methylaspartate (**6**) using glutamate mutase.^{6,9}

Crystal structures of glutamate mutase bound co-enzyme B₁₂ and glutamate from *Clostridium cochlearium* have been reported.¹¹ This revealed a radical shuttling process from cobalt to the substrate by changing the conformation of the ribose moiety of adenosine. The ribose was found to be present in two conformers, C-2'-*endo* and C-3'-*endo*. The C-5' carbon of adenosine is above and points towards co(II)balamin in the C-2'-*endo* conformer whereas the C-5' of adenosine is directed towards the substrate hydrogen in the C-3'-*endo* conformer (Figure 1.2). Thus, the C-3'-*endo* is assumed to be the reactive conformer.

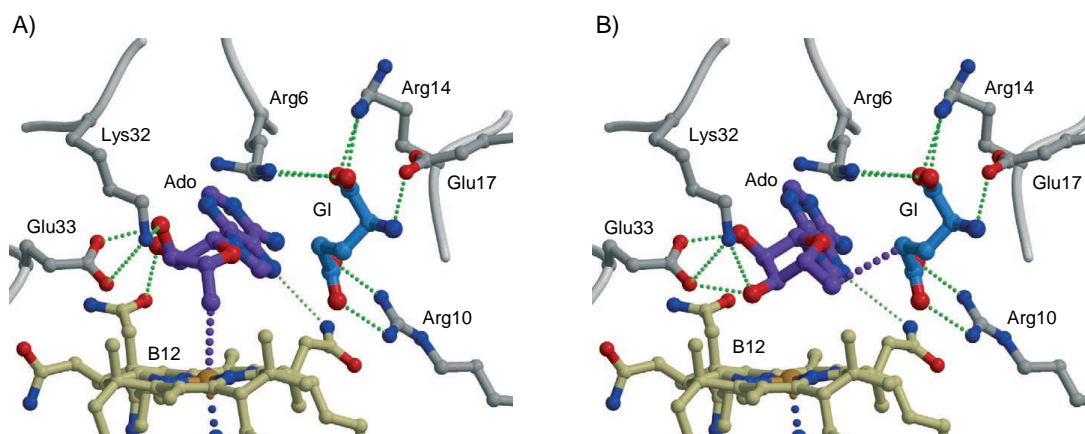
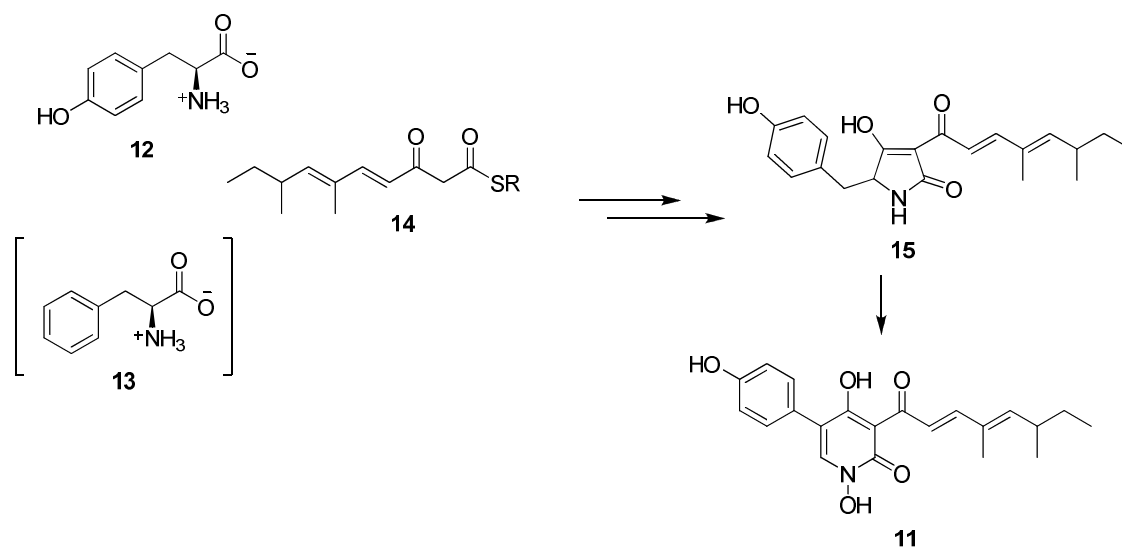


Figure 1.2 Active site of glutamate mutase bound co-enzyme B₁₂ and glutamate showing; A) C-2'-*endo* conformer and B) C-3'-*endo* conformer.^{7, 11}

1.3 Biosynthesis of tenellin (**11**)^{12, 13}

The alkaloid tenellin (**11**) is a fungal metabolite produced by *Beauveria bassiana*. This alkaloid is known to be toxic towards mammalian erythrocytes. Structurally, it comprises a 2-pyridone moiety and a branched alkenyl chain. The biosynthetic precursors to tenellin are tyrosine (**12**) (or phenylalanine, **13**), a polyketide moiety (**14**), and methyl groups which are derived from L-methionine. Tenellin is biosynthesised from a condensation of tyrosine with a β -keto polyketide intermediate to generate a five-membered pretenellin A (**15**, Scheme 1.4). This intermediate then undergoes oxidative ring expansion followed by *N*-hydroxylation to generate the 2-pyridone ring system of tenellin. This biosynthesis is catalysed by cytochrome P₄₅₀ enzymes. Recently, the tenellin biosynthesis gene cluster has been established.¹³ The cluster comprises genes *tenA*, *tenB*, *tenC*, and *tenS*. Gene *tenA* encodes a cytochrome P₄₅₀ oxidase which is responsible for the ring expansion of tetramic acid (**16**) to 2-pyridone (**17**). Gene *tenB* encodes a cytochrome P₄₅₀ monooxygenase which hydroxylates the 2-pyridone nitrogen to form tenellin. Gene *tenS* is a hybrid

polyketide synthase-nonribosomal peptide synthase (PKS-NRPS) and it is involved in the biosynthesis of pretenellin-A (**15**).

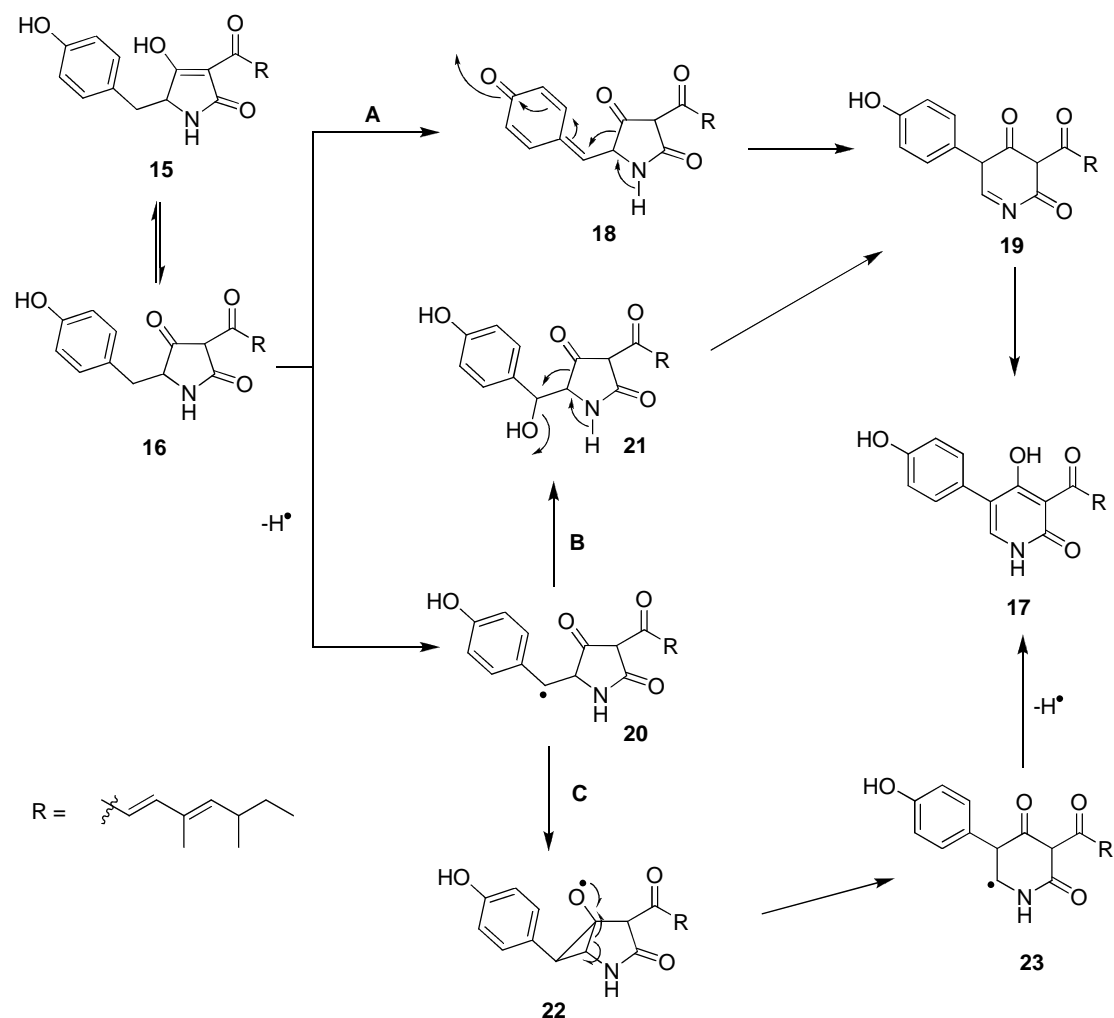


Scheme 1.4 Tenellin **11** is biosynthesised from tyrosine **12** (or phenylalanine **13**) by condensation with a polyketide intermediate, e.g. **14**.

Three mechanisms have been proposed for this oxidative ring expansion reaction and these are summarised in Scheme 1.5. The first mechanism (route A) involves oxidation of **16** to a quinomethide intermediate **18**, followed by a ring expansion and tautomerisation to generate 2-pyridone **17**. The second mechanism (route B) involves formation of a benzylic alcohol (**21**) *via* a benzylic radical (**20**), followed by ring expansion to form an imine **19**. The third proposed mechanism (route C) proceeds *via* the generation of a benzylic radical (**20**), followed by the formation of cyclopropyloxy radical **22**, which then undergoes ring expansion to generate radical **23** and then loss of a hydrogen atom to give 2-pyridone **17**.

At present, the most likely mechanism is route C. Route A cannot account for the biosynthesis of 2-pyridones which lack a *para*-hydroxyl group. Also it has been

demonstrated that prototenillin-D (**21**, route B) did not convert to 2-pyridones when incubated with cell-free extracts of *B. bassiana*.



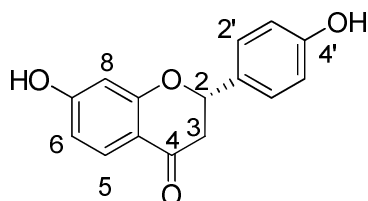
Scheme 1.5 Proposed mechanisms A-C for the rearrangement of tetramic acid **16** to 2-pyridone **17**.¹³

1.4 Isomerisation of liquiritigenin (**24**) to daidzein (**25**).^{14, 15}

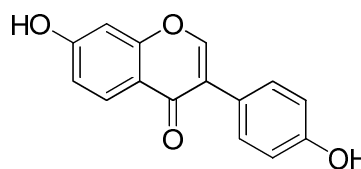
Isoflavone biosynthesis.

Isoflavones are a subclass of the flavone natural products. They have a general $\text{C}_6\text{-C}_3\text{-C}_6$ structure with a phenyl ring at C3 of a pyrone ring. The isoflavones originate from the shikimate biosynthetic pathway. These secondary metabolites are distributed in

higher plants, and particularly the Legumeminosae/Fabaceae. These plants produce isoflavones as defence substances against phytopathogenic microorganisms.

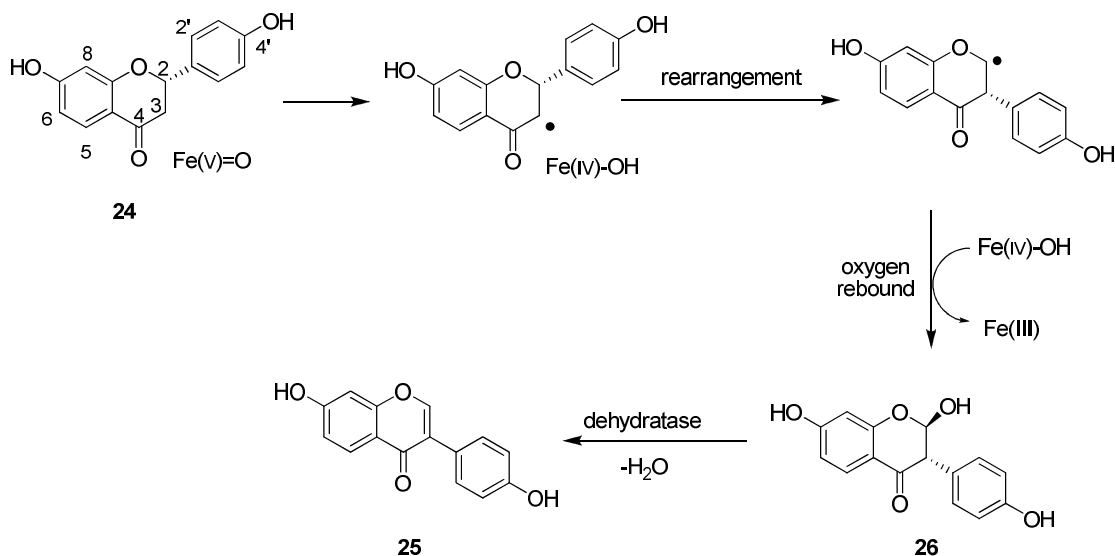


a flavone backbone



an isoflavone backbone

The isoflavone skeleton arises *via* the direct rearrangement of flavones. A cytochrome P_{450} dependent enzyme catalyses this rearrangement, an enzyme which requires NADPH and molecular oxygen. The plant *Pueraria lobata*, expresses a cytochrome P_{450} dependant isoflavone synthase which catalyses the conversion of the flavone, liquiritigenin (**24**) to the isoflavone daidzein (**25**). The process is thought to proceed *via* a radical intermediate. Abstraction of C-3 hydrogen atom, is followed by a 1,2-aryl migration to generate 2,7,4'-trihydroxyisoflavanone (**26**) as shown in Scheme 1.6. A key feature of this transformation is an “oxygen rebound” process, in which the rearranged radical intermediate is quenched by an hydroxyl radical from $Fe(IV)-OH$ to generate 2,7,4'-trihydroxyflavone. The mechanism was deduced after an oxygen-18 investigation on the origin of the oxygen atoms at 2-OH of **26** and the C-4 carbonyl of **25**. Incubation of liquiritigenin (**24**) with cytochrome P_{450} under $^{18}O_2$ resulted in the detection of 2,7,4'-trihydroxyisoflavanone (**26**) carrying 2- ^{18}OH . Oxygen-18 was not incorporated into the C4 carbonyl of **26**. Also an incubation of the cytochrome P_{450} enzyme with [4- ^{18}O]-liquiritigenin showed a retention of the ratio of $^{16}O:^{18}O$ in the product, [4- ^{18}O]-daidzein, relative to starting material. Thus the C4 carbonyl is not involved in the rearrangement process.

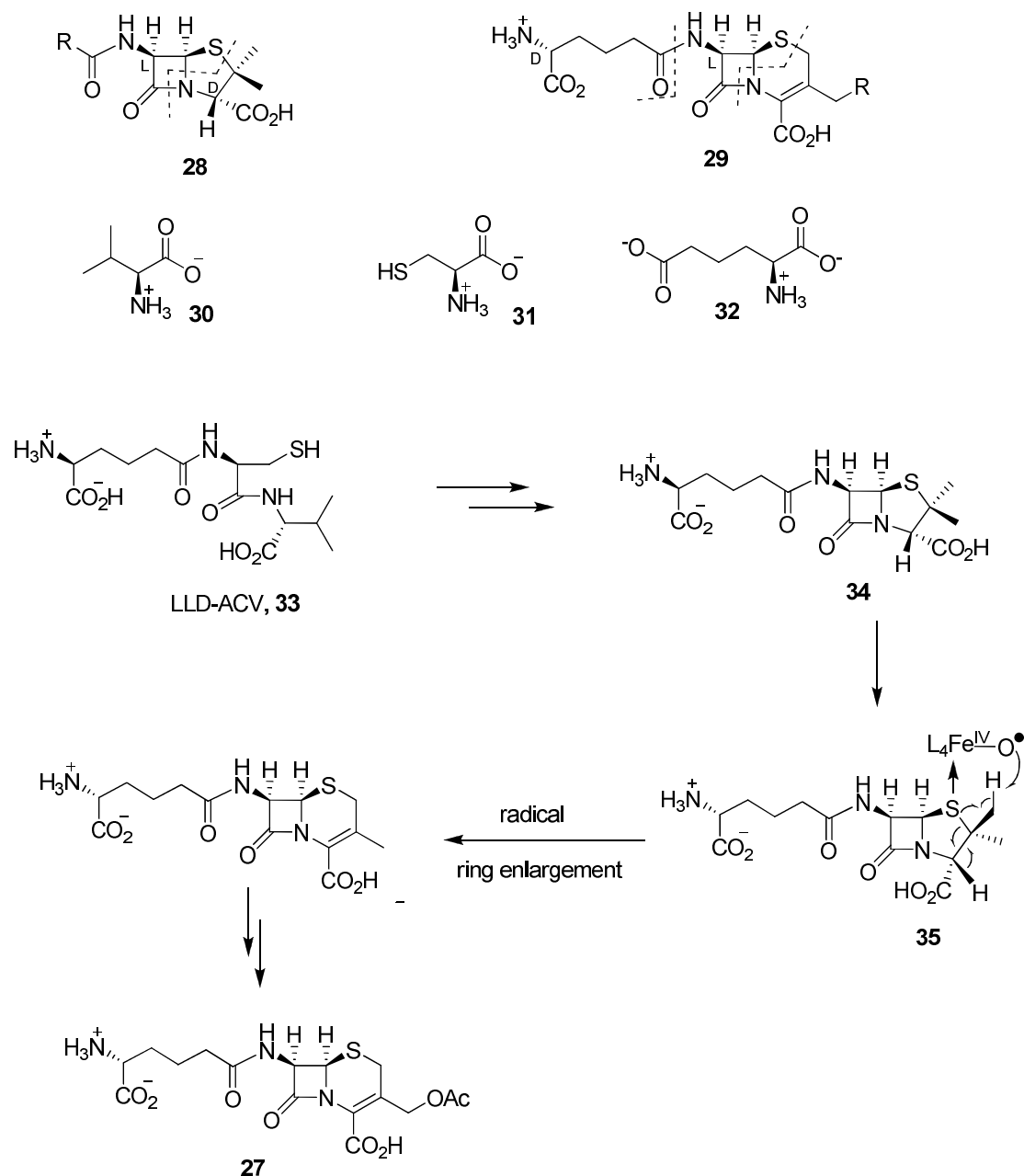


Scheme 1.6 Isomerisation of the flavonoid liquiritigenin **24** to the isoflavone daidzein **25**.^{14, 15}

1.5 Biosynthesis of cephalosporin C(27)³

Another example of an enzymatically mediated isomerisation by means of ring enlargement following from tenellin, can be found in the biosynthesis of cephalosporin C (**27**) from penicillin N (**35**). Penicillins (**28**) and cepharosporins (**29**) are important antibiotics produced by fungi such as the *Penicillium* and *Cephalosporium spp.*, respectively. These cyclic tripeptides are derived from the amino acid precursors L-valine (**30**), L-cysteine (**31**), and L- α -aminoadipate (**32**). It is noteworthy that the configuration of L-valine is inverted to D-valine during the biosynthesis and that the configuration of L- α -aminoadipate is inverted to D- α -aminoadipic acid in the cepharosporins. It has been demonstrated that the L- α -aminoadipyl-L-cysteinyl-D-valine (LLD-ACV, **33**) is the only stereoisomer that is converted to the β -lactam antibiotics.¹⁶ A summary of the biosynthesis of cephalosporin C is shown in Scheme 1.7. The intermediate LLD-ACV tripeptide is converted to isopenicillin N (**34**) and then an epimerase converts the L- α -aminoadipic

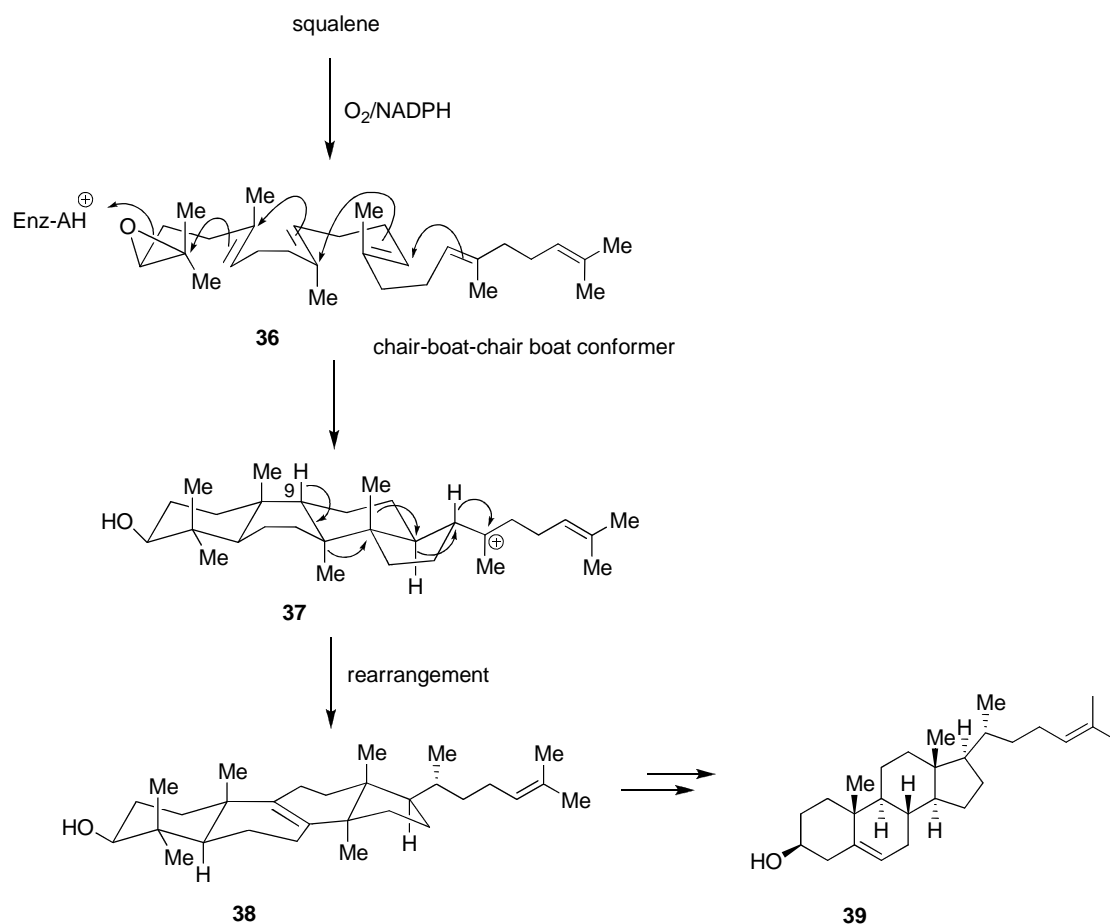
acid moiety to D- α -aminoadipic acid, to form penicillin N (**35**). In order to convert penicillin N to cephalosporin C, the five-membered thiazolidine ring is rearranged to generate the six-membered dihydrothiazine ring of the cephalosporins. This ring enlargement also proceeds *via* a radical rearrangement and is mediated by an iron-oxo species ($L_4Fe^{IV}-O^\bullet$) as illustrated in Scheme 1.7.



Scheme 1.7 Ring enlargement reaction of penicillin N **35** to cephalosporin C **27**.

1.6 Cholesterol biosynthesis ¹⁷

Steroid biosynthesis offers one of the most elaborate examples of a molecular rearrangement in enzymology. Although diverse in structure, all steroids are derived from the straight chain triterpene precursor, squalene. cholesterol is the principal animal steroid, a constituent of cell membranes, and it has been found in all animal tissues. Cholesterol is derived from a metabolite of lanosterol which itself originates from squalene. The cyclisation of squalene starts with an oxidation of the terminal double bond initiated by an epoxidase to generate squalene oxide (**36**, Scheme 1.8). This epoxidation reaction requires NADH and molecular oxygen. In the event, squalene adopts a chair-boat-chair-boat conformation on the enzyme surface. The cascade cyclisation is then catalysed by the terpene cyclases to generate the protosteryl carbocation (**37**). The rearrangement starts by an elimination of H^+ at C-9 followed by a series of Wagner-Meerwein 1,2-shifts to generate lanosterol (**38**). This steroid is then modified by a series of subsequent transformations to generate cholesterol (**39**).

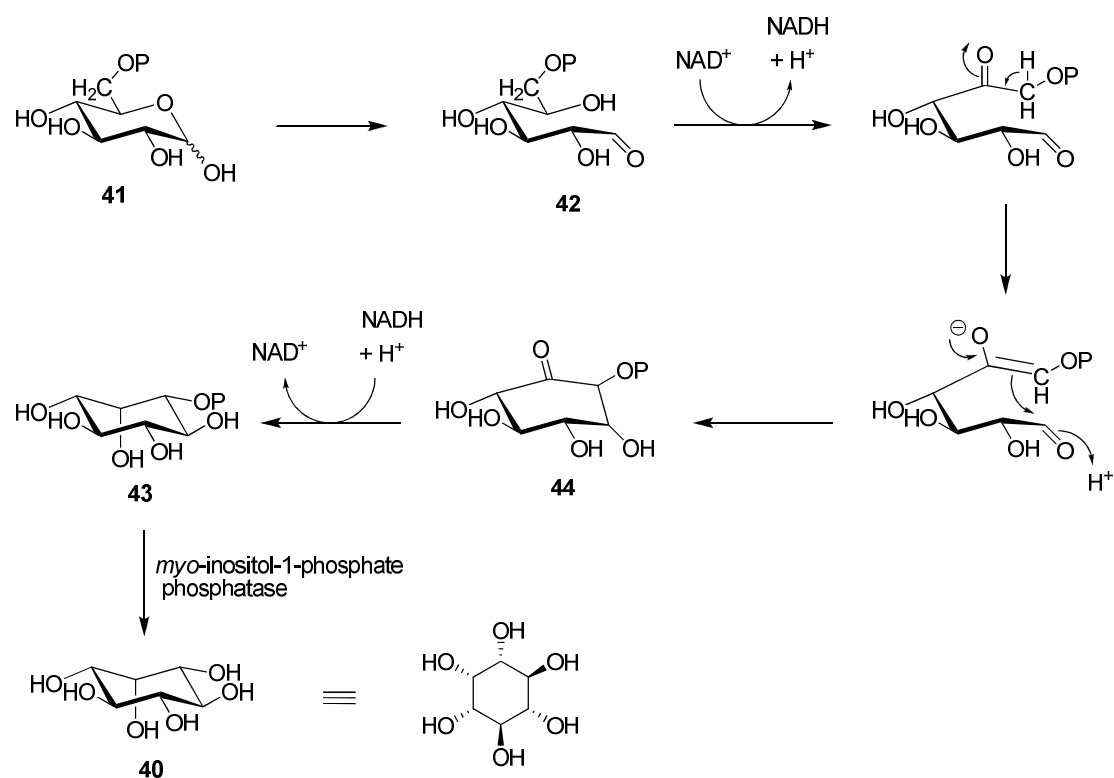


Scheme 1.8 Steroid cholesterol **39** derived from rearrangement of lanosterol **38**.¹⁷

1.7 Biosynthesis of L-*myo*-inositol^{18, 19}

An example of a carbohydrate ring isomerisation is demonstrated during the biosynthesis of *myo*-inositol (**40**). This naturally occurring cyclitol carbohydrate is the most important stereoisomer of all nine possible inositol stereoisomers. It is a precursor of all inositol containing compounds such as inositol phosphates and cell wall polysaccharides. Inositol metabolism plays an important role in growth regulation, signal transduction, and membrane biogenesis. *Myo*-inositol is biosynthesised from D-glucose-6-phosphate (**41**). The transformation is catalysed by a NAD-dependent glucose-6-phosphate-1-L-*myo*-inositol-1-phosphate cyclase. The C-5 carbon of an open form of **42** is oxidised to the corresponding carbonyl and this then

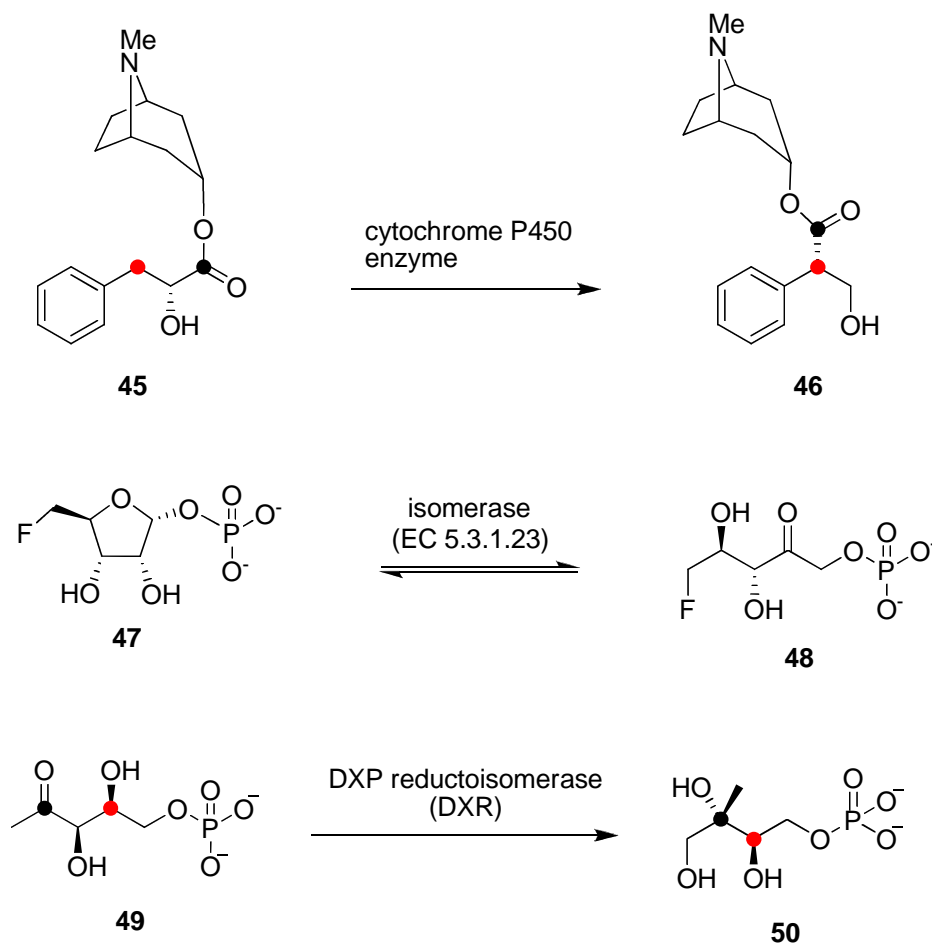
initiates an aldol condensation of C-6 to C-1 to generate cyclic ketone **44**. NADH reduction of the C-5 carbonyl generates *myo*-inositol-3-phosphate (**43**). Dephosphorylation of **43** then generates *myo*-inositol.¹⁹



Scheme 1.9 Conversion of D-glucose-6-phosphate (**43**) to *myo*-inositol (**40**).¹⁸

In summary, these carbon skeleton isomerisation reactions in enzymology are unusual in mechanisms. Particularly, unusual are the carbon skeleton rearrangements *via* radicals involving co-enzyme B₁₂ and cytochrome P₄₅₀ enzymes. This thesis is focused on investigations of the mechanism of three remarkable isomerisation reactions in secondary metabolism. The isomerisation of the alkaloid littorine (**45**) to hyoscyamine (**46**) which is catalysed by a plant cytochrome P₄₅₀ enzyme is discussed in Chapter 2. The isomerisation of 5-fluoro-5-deoxy-ribose-1-phosphate (**47**) to 5-fluoro-5-deoxy-ribulose-1-phosphate (**48**) in *Streptomyces cattleya* is discussed in

Chapter 3. The isomerisation 1-deoxy-D-xylulose-5-phosphate (DXP, **49**) to 2-C-methylerythritol-phosphate-4-phosphate (MEP, **50**) an enzyme reaction of the new biosynthetic pathway to isoprenoid precursors is discussed in Chapter 4.



Scheme 1.10 Three isomerisation reactions of secondary metabolism which constitute the focus of this research.

1.8 References

1. W. Buckel, C. Kratky and B. T. Golding, *Chem. Eur. J.*, 2006, **12**, 352-362.
2. T. Bugg, *An introduction to enzyme and coenzyme chemistry*, Blackwell Science, 1997.
3. K. B. G. Torrsell, *Natural product chemistry: A mechanistic, biosynthetic and ecological approach*, 2 edn., Apotekarsocieteten, Stockholm, 1997.
4. H. Eggerer, P. Overath, F. Lynen and E. R. Stadtman, *J. Am. Chem. Soc.*, 1960, **82**, 2643-2644.
5. S. Patterson and D. O'Hagan, *Phytochem.*, 2002, **61**, 323-329.
6. W. Buckel and B. T. Golding, *Chem. Soc. Rev.*, 1996, **26**, 329-337.
7. K. Gruber and C. Kratky, *Curr. Opin. Chem. Biol.*, 2000, **6**, 598-603.
8. R. Bunerjee, *Chem. Rev.*, 2003, **103**, 2083-2094.
9. H. Bothe, D. J. Darley, S. P. J. Albracht, G. J. Gerfen, B. T. Golding and W. Buckel, *Biochemistry*, 1998, **37**, 4105-4113.
10. H.-W. Chih and E. N. G. Marsh, *J. Am. Chem. Soc.*, 2000, **122**, 10732-10733.
11. K. Gruber, R. Reitzer and C. Kratky, *Angew. Chem. Int. Ed.*, 2001, **40**, 3377-3380.
12. K. L. Eley, L. M. Halo, Z. Song, H. Powles, R. J. Cox, A. M. Bailey, C. M. Lazarus and T. J. Simpson, *ChemBioChem.*, 2007, **8**, 289-297.
13. L. M. Halo, M. N. Heneghan, A. A. Yakasai, Z. Song, K. Williams, A. M. Bailey, R. J. Cox, C. M. Lazarus and T. J. Simpson, *J. Am. Chem. Soc.*, 2008, **130**, 17988-17996.
14. M. F. Hashim, T. Hakamatsuka, Y. Ebizuka and U. Sankawa, *FEBS*, 1990, **271**, 219-222.

15. T. Hakamatsuka, M. F. Hashim, Y. Ebizuka and U. Sankawa, *Tetrahedron*, 1991, **47**, 5969-5978.
16. G. Bahadur, J. E. Baldwin, T. Wan and M. Jung, *J. Chem. Soc. Commun.*, 1981, 1146-1147.
17. J. Mann, *Chemical aspects of biosynthesis*, Oxford University Press, Oxford, 1994.
18. D. E. Kiely and W. R. Sherman, *J. Am. Chem. Soc.*, 1975, **97**, 6810-6814.
19. A. J. Stein and J. H. Geiger, *J. Biol. Chem.*, 2002, **277**, 9484-9491.

Chapter 2

**Exploring the mechanism of the
rearrangement of littorine to
hyoscyamine**

2.1 Introduction

Alkaloids are one of the most diverse groups of secondary metabolites which are not only widely distributed in plants but also to a lesser extent in microorganisms and animals. Within the plant kingdom, 21,120 alkaloids have been identified so far.¹ As the name implies, alkali-like, the alkaloids are basic in solution, and contain at least one nitrogen atom in their structure (mostly heterocyclic). However, amino acids, peptides, nucleotides, nucleic acids, and amino acids are excluded.² Due to their pharmacological properties alkaloids have found extensive use as medicinal agents such as local anaesthetics and stimulants; e.g. cocaine **51**, caffeine **52**, the analgesic morphine **53**, and the anti-malaria agent, quinine **54**.

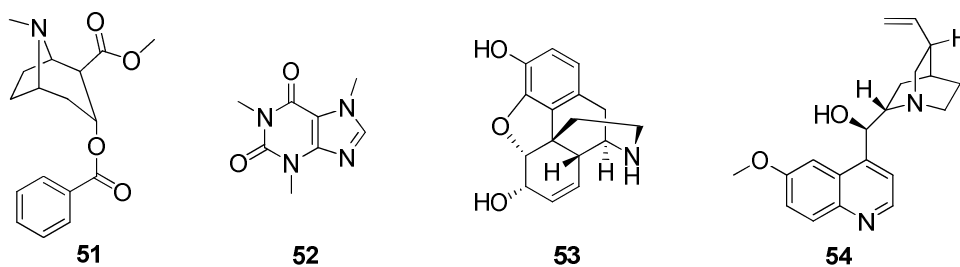


Figure 2.1 Selected medicinal alkaloids: cocaine **51**, caffeine **52**, morphine **53** and quinine **54**.

2.2 The tropane alkaloids

Structurally, the tropane alkaloids possess an 8-azabicyclo[3.2.1]octane (nortropane, **55**) skeleton which forms an ester bond with the tropic acid (**56**) moiety. Hyoscyamine **46**, atropine **58**, and scopolamine (or hyoscine **59**) have emerged as the most widely used tropane alkaloids in medicine.

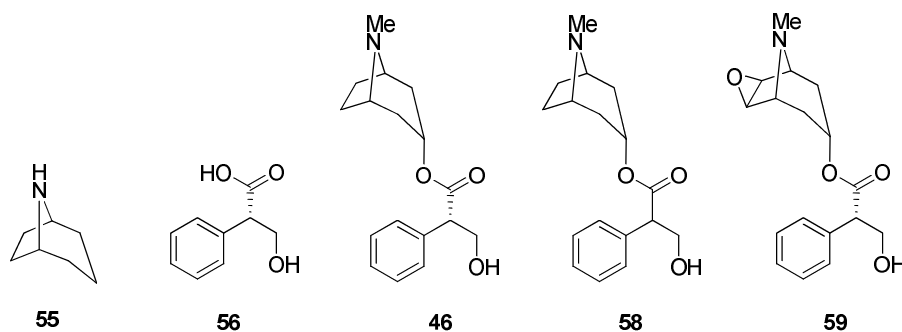


Figure 2.2 The core structure of the tropane alkaloids; nortropine **55**, tropic acid **56** and some medically important tropane alkaloids; hyoscyamine **46**, atropine **58**, and scopolamine (or hyoscine **59**).³

When (-)-hyoscyamine is extracted from plants into solvents it racemises to (±)-hyoscyamine, or atropine. The name atropine derives from Greek mythology, the god *Atropos*, one of the three Fates, who cut the thread of life. Pharmacologically, atropine and hyoscyamine act competitively as antagonists of acetylcholine (**60**) at the muscarinic receptors. Interestingly, the superimposition of atropine and acetylcholine reveals a structural similarity. Atropine comprises an ester and amine, which is protonated at physiological pH.⁴

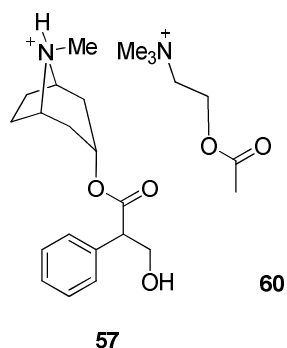


Figure 2.3 The superimposition of atropine **57** (ionised at physiological pH) and acetylcholine **60**.⁴

In low doses, atropine is used in ophthalmology to dilate the pupil (mydriasis) of the eyes prior to examination of the retina. It is also used pre-operatively to reduce mucus secretions during anesthesia and to treat bradyarrhythmias.⁵ The tropane alkaloids are also used to reduce sweating, bronchial secretions, and to dilate the bronchi. Atropine sulfate combined with obidoxime is used in combination as an injection to counteract organophosphate insecticide poisoning and nerve gases. At higher doses, the tropanes produce hallucinogenic/aphrodisiac side effects. To minimize the hallucinogenic side effects, the quaternary salt of atropine, ipratropium **61**, and the atropine analogue, atropine methonitrate **62** and amprotropine **63** are currently used clinically. Scopolamine presents a similar therapeutic profile to atropine and hyoscyamine. Its hydrobromide salt is used for its anti-depressant activity, although it causes delirium and mydriasis and in higher doses can be fatal.

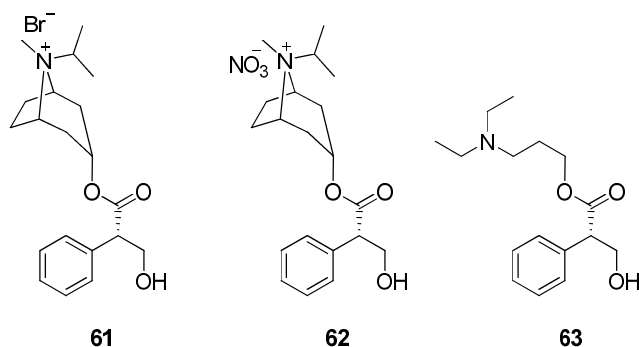


Figure 2.4 Quaternary salt of atropine; ipratropium **61**, atropine methonitrate **62** and amprotropine **63**.

Plant-containing tropane alkaloids are commonly found in three major genera. These are *Atropa*, *Datura*, and *Hyoscyamus*, of the Solanaceae family (potato family). Chiefly the tropane alkaloid constituents, hyoscyamine and scopolamine are

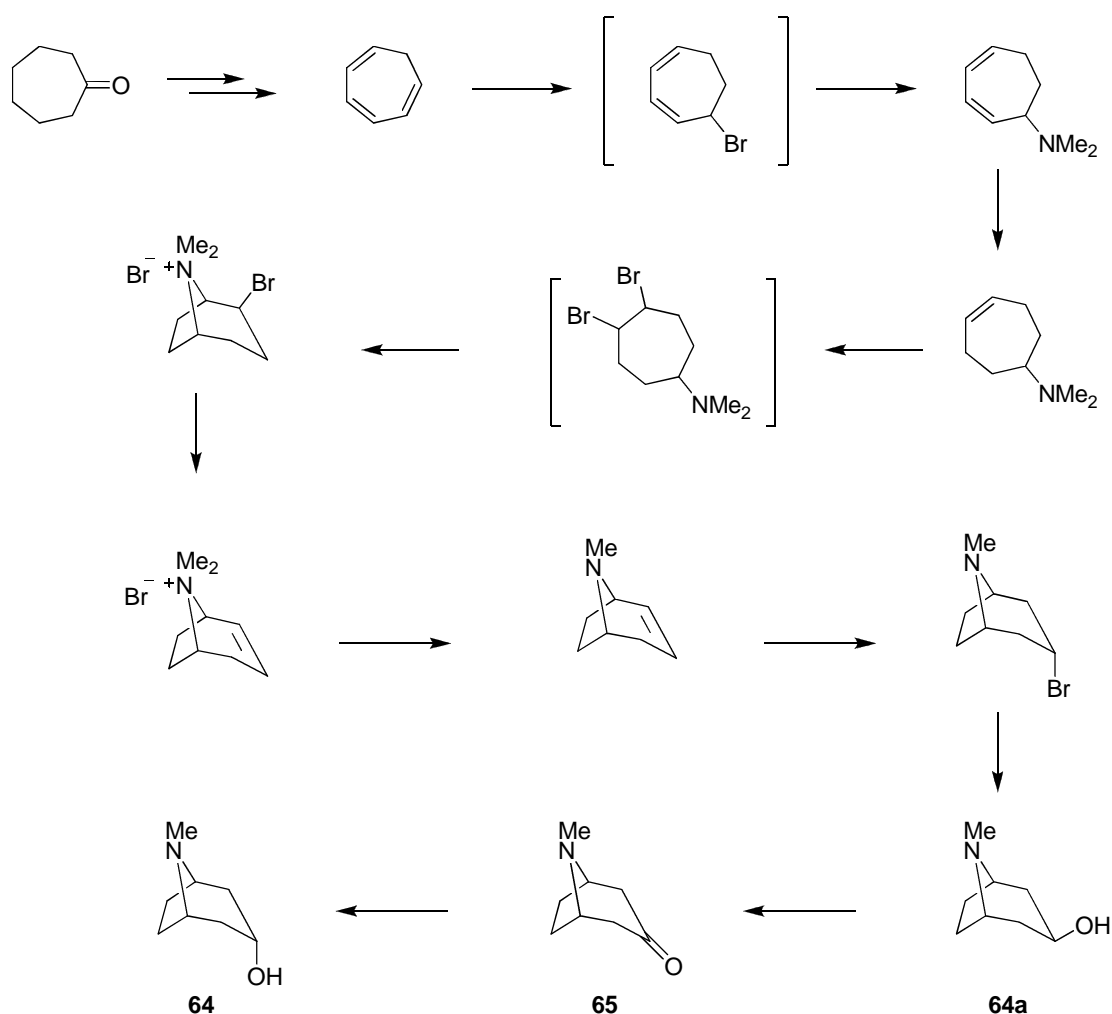
distributed in the whole plants and particularly the roots, leaves and berries. Atropine is present as a trace tropane alkaloid. Solanacea plants have long been associated with ritualistic, mystery and early medical procedures. They were essentially sources of poison, hallucinogens, and medicine in ancient and medieval times. Cleopatra systematically tested the poison of *Atropa belladonna* (the deadly nightshade) and *Hyoscyamus niger* (henbane) on her slaves in search for the best poison for suicide, although she chose the asp venom in the end. The wives of Roman emperors, Livia (wife of Augustus) and Agrippina (wife of Claudius) poisoned their husbands with the juice of deadly nightshade.⁶ Although it is poisonous, this juice was wildly used by ladies during Renaissance Italy to exaggerate the size of their eyes by dilating their pupils, hence making them more attractive to the opposite sex. The name, *Atropa belladonna* derives from this well known effect, “bella donna” meaning beautiful lady. *Datura stramonium*, known as ‘thorn apple’ or Jimson weed, is commonly distributed in Europe, North America and Asia Minor. The seeds and berries of thorn apple are particularly poisonous as they contain hyoscyamine and scopolamine at toxic levels. Ingestion of a few berries can be lethal. The seeds and plant extracts of thorn apple were used for a wide variety for medicinal purposes, including the treatment of mania, epilepsy, melancholy, rheumatism, convulsion, and madness.⁷ It was once believed that smoke from Jimson weed could relieve the respiratory symptoms of asthma and the Spanish sold it in the form of herbal cigarettes during the nineteenth century.^{6, 8} Cancer cures and motion sicknesses were reported.⁹ The Columbian Indians used *Datura* species for infanticide by smearing extracts on the nipple of the mother. The Mexican Indian rain priests chewed the roots to communicate with the spirits of the dead to intercede with the gods for rain. Extracts of tropane alkaloids are used for adolescent initiation rites for many tribes. While

others believe it possible to obtain supernatural powers through drug-induced visions.⁷ The Solanaceas plants have been closely associated with magic and witchcraft. Deadly nightshade, henbane, and mandrake (*Mandragora officinarum*) were used in witches' brews in the Middle Age. There is little doubt that the tropane alkaloids in the brew induced hallucination and produced what had been described as animal behaviour as well as experiencing a fanciful flying and inducing a frenzied dancing. In particular, mandrake has much associated folklore. Upon hearing the terrible shriek when uprooting the mandrake the collector would die.⁶ To avoid the fate the collector used dogs to uproot mandrake and plugged their ears with wax. Due to the Y-shaped root, mandrake has also been associated with enhancement of fertility.

2.3 Biosynthesis of tropane alkaloids

2.3.1 Total synthesis of tropine and the structural elucidation of tropine

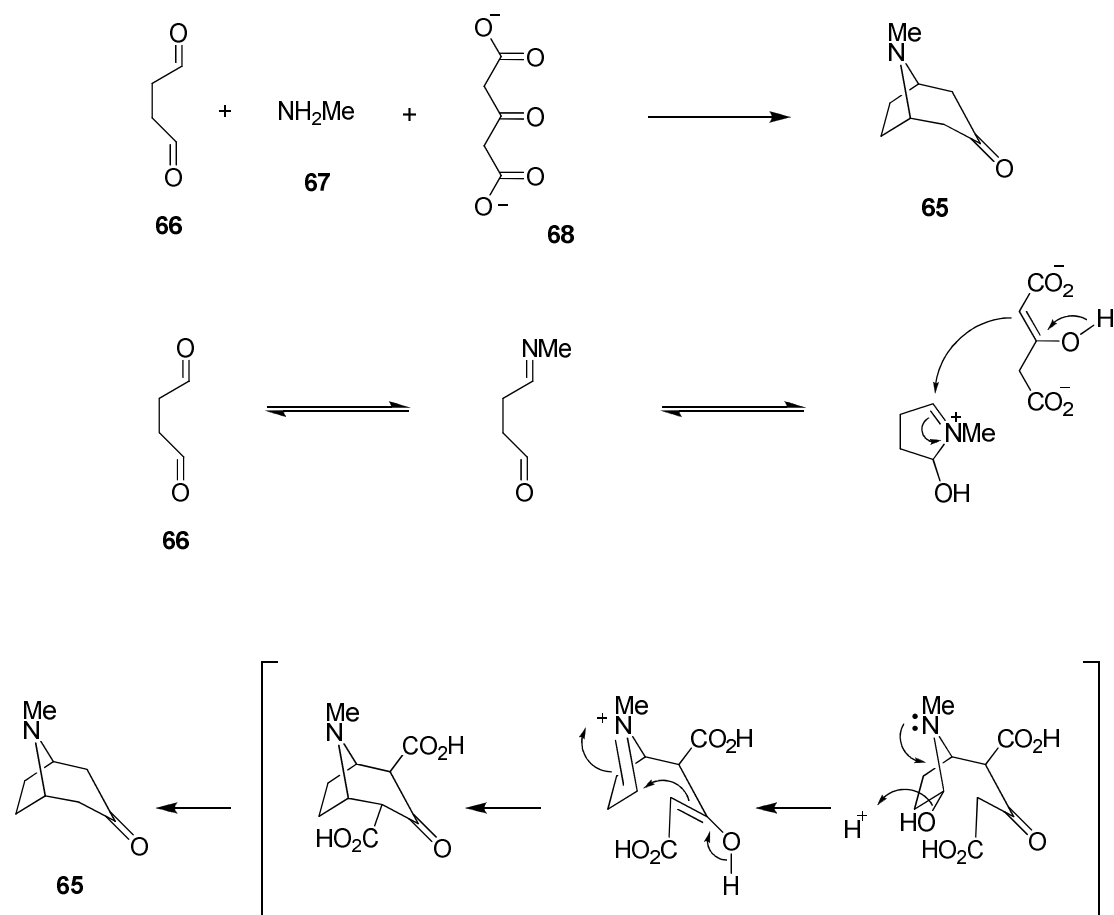
The synthesis and elucidation of the tropine structure was very much on the agenda in late nineteenth century organic chemistry. In 1863 Kraut obtained atropic acid and tropine (**64**) after boiling atropine with BaSO₄, and later Lossen showed that the initial product of the hydrolysis atropic acid, was tropic acid. The reverse synthesis was demonstrated by Ladenburg a year later, when upon treatment of tropine and atropic acid under dry hydrochloric acid conditions, he generated atropine. However, the structure was still unsettled.¹⁰⁻¹² It was not until 1903 that the first total synthesis of tropine was successfully performed by Robert Martin Willstätter, and as a consequence he successfully elucidated the structure of tropine.¹² He is also credited for the first synthesis of cocaine, another tropane alkaloid. In 1915 Willstätter received the Nobel Prize in chemistry for his work on pigments and especially chlorophyll.



Scheme 2.1 Summary of Willstätter's first total synthesis of tropine.¹²

In 1917 Robert Robinson published a one pot synthesis of tropinone (**65**) a reaction which has become a synthesis classic.¹³ The possibility that tropine might result from the condensation of succindialdehyde (**66**) and methylamine (**67**) occurred during discussions between Robinson and Lapworth.¹³⁻¹⁵ Robinson then demonstrated that by adding succindialdehyde to an aqueous solution of methylamine (**67**) and acetone he could obtain tropinone. The yield was improved significantly when the calcium salt of acetonedicarboxylic acid (**68**) was employed at physiological pH. This short and very

direct route to tropinone led Robinson to speculate that the *in vivo* biosynthesis of tropinone might parallel this chemistry.¹⁴

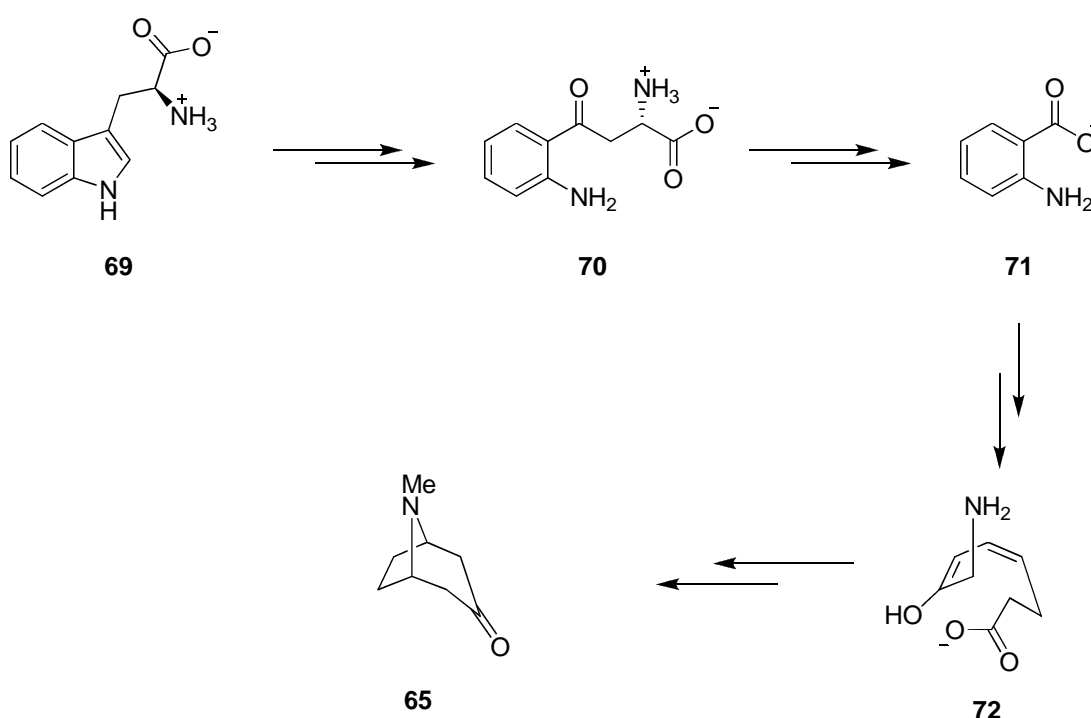


Scheme 2.2 Robert Robinson's 1917 classic one-pot synthesis of tropinone.^{13, 16}

2.3.2 Biosynthesis of the tropane ring

The biosynthesis of the tropane ring arises from two origins. The C₄N pyrrolidine, carbon atoms 1, 5, 6, 7 have an amino acid origin and the C₃ ketone fragment comprising carbon atoms 2, 3, and 4 derive from acetate. There were two hypotheses at that time on the biosynthesis of the tropane nucleus. The Robinson hypothesis suggested that the amino acid ornithine could be a precursor of succindialdehyde. The

second was presented by Mortimer based on a previous hypothesis by Dawson which suggested tryptophan as the biosynthetic precursor of the entire tropane ring *via* known biosynthetic intermediates to nicotinic acid.¹⁷ However, Robinson suggested that this was less likely as it would require the oxidative fission between C-1 and C-2 of compound **71**. Also it was known that piperidine alkaloids are related to the amino acid lysine, thus in the same way, these pyrrolidine alkaloids would be related to ornithine.¹⁸

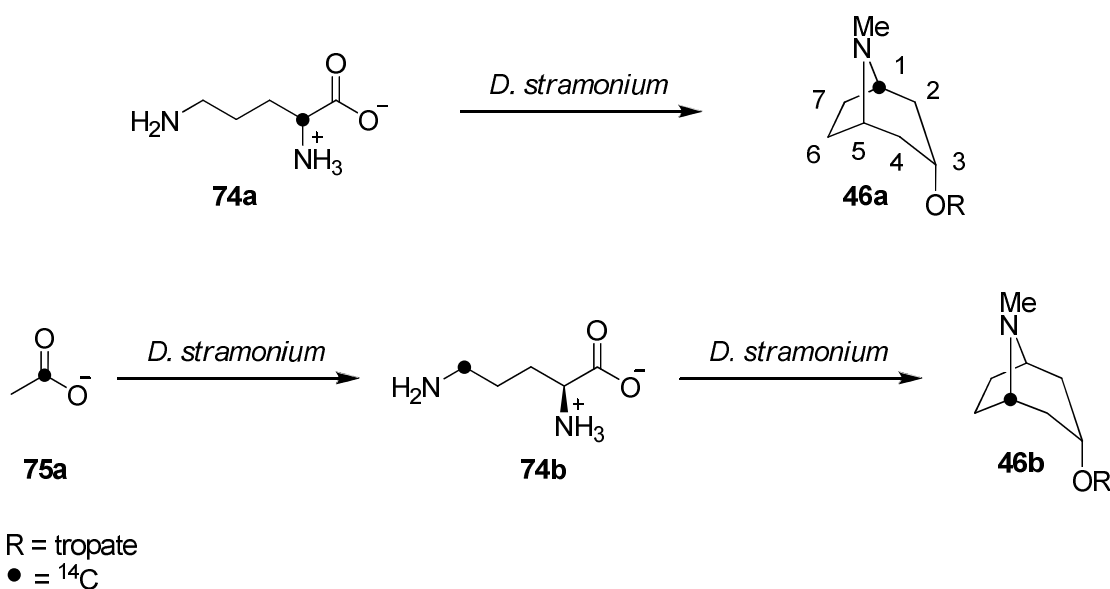


Scheme 2.3 Dawson's incorrect biosynthesis hypothesis of tropinone (**65**) from tryptophan (**69**).

2.3.2.1 The amino acid derived fragment

The amino acids argentine (**73**) and ornithine (**74**) had been suggested precursors for the biosynthesis of the pyrrolidine moiety of the tropane skeleton by Robinson, after his 1917 *in vitro* synthesis.¹⁴ Initial studies revealed that the feeding of L-(+)-argentine and L-(+)-ornithine to leaves of *A. belladonna* increased the alkaloid

content to a greater extent than other amino acids. Also ornithine was detected in the pressed juice of *A. belladonna* sprouts, supporting this hypothesis.^{19, 20} Leete's radiolabelled experiments by feeding (*RS*)-[2-¹⁴C]-ornithine (**74a**) to mature *D. stramonium* plants revealed that the radioactivity was located at C-1.²¹⁻²⁴ Complementary feeding experiments were also carried out by Bothner-By. Presumably, feeding of sodium [1-¹⁴C]-acetate (**75a**) to root culture of *D. stramonium* produced the [5-¹⁴C]-ornithine (**74b**) which then biotransformed to hyoscyamine. Chemical degradation of hyoscyamine revealed that radioactivity was found to be located at C-5 of the pyrrolidine moiety of hyoscyamine (**46a**, **46b**).²⁵

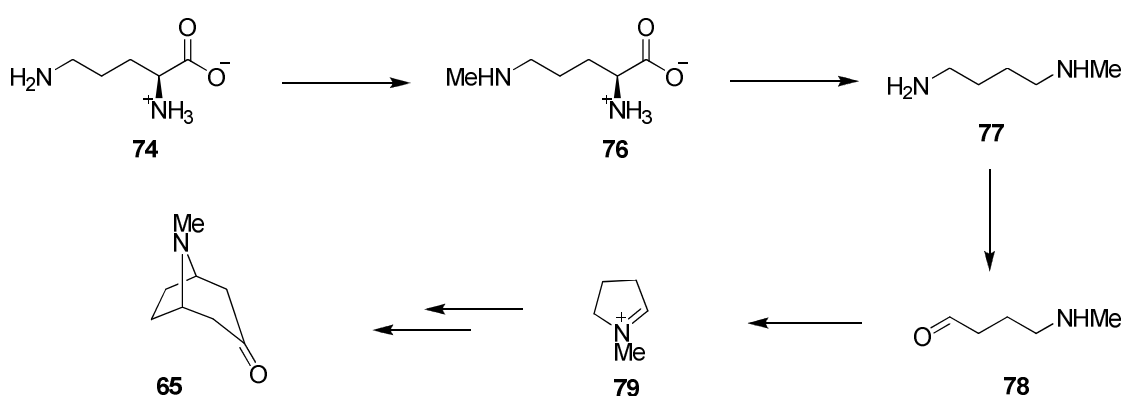


Scheme 2.4 Leete's feeding experiment demonstrated the regiospecific incorporation of radioactivity into C-1 and C-5 of the pyrrolidine ring of hyoscyamine (**46a**, **46b**).²⁴ This was also supported by Bothner-By's feeding experiments of sodium [1-¹⁴C]-acetate (**75a**).²⁵

Other intermediates in the biosynthesis of the tropane alkaloids have been revealed. Feeding of radiolabelled [*N*-methyl-¹⁴C,2-¹⁴C]-ornithine (**74c**) to *Datura* plants

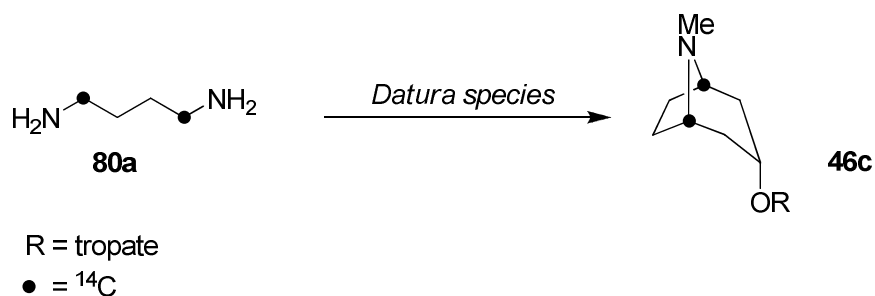
indicated *N*-methylputrescine as a precursor of the tropanone ring.²⁶ Also administration of DL-[5-¹⁴C]- and DL-[5-³H]-ornithine (**74d**, **74e**)²⁷ to *A. belladonna* supported the involvement of *N*-methylornithine (**76**) as a biosynthetic precursor of the pyrrolidine moiety, and **76** was also identified as a natural metabolite by isolation.²⁷ *N*-Methylputrescine (**77**) had been found to be an intermediate of the tropanes in *Datura metel*,²⁸ whilst radioactive 4-methylaminobutanal (**78a**) had been detected in *Datura* plants which were fed with [2-¹⁴C]-ornithine (**74a**).²⁹

Leete's early proposal of the biosynthetic pathway is shown in Scheme 2.5.²⁶ The amino acid ornithine (**74**) is first methylated, followed by decarboxylation to yield *N*-methylputrescine (**77**). Oxidative deamination would then deliver 4-aminobutylaldehyde **78**, a substrate for cyclisation to *N*-methylpyrrolinium salt (**79**). Condensation of **79** with an acetate derived fragment (see below) would then generate tropanone **65**. It is noteworthy that intermediates after **76** in this biosynthetic proposal are asymmetric.

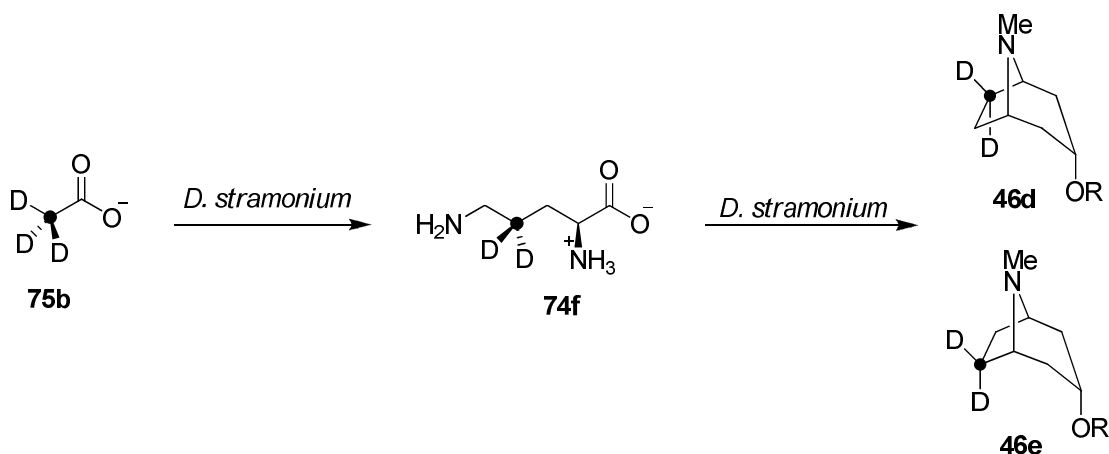


Scheme 2.5 Leete's early proposal for the biosynthetic pathway to tropanone.²⁶

Leete's proposal required ornithine and other intermediates to become incorporated in an asymmetric manner into the pyrrolidine moiety of the tropane ring. However, symmetrical incorporations of radiolabelled substrates into the tropane alkaloids in *Datura* plants³⁰, *Hyoscyamus niger*³¹, *H. niger*,³² and *Erthroxylon coca*³³ have been reported. The doubly labelled [1,4-¹⁴C]-putrescine (**80a**) feeding experiment with *D. mentel* incorporated equally into C-1 and C-5 of the pyrrolidine moiety.³⁴ Additionally, feeding experiments of [2-¹³C, ²H₃]-acetate (**75b**) to root cultures of *D. stramonium* confirmed the symmetrical incorporation into hyoscyamine (**46d**, **46e**) as shown in Scheme 2.7.³⁵

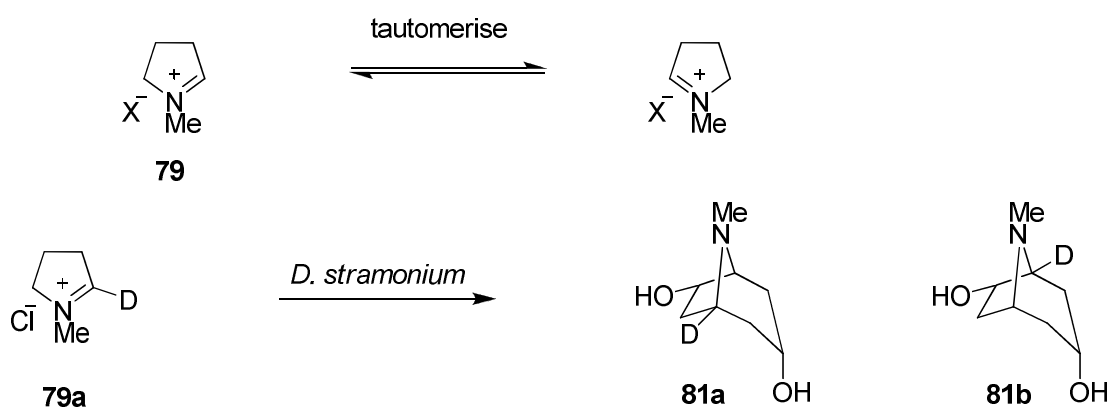


Scheme 2.6 Feeding experiment demonstrating the regiospecific incorporation of [1,4-¹⁴C]-putrescine (**80a**) into C-1 and C-5 of hyoscyamine (**46c**).³⁴

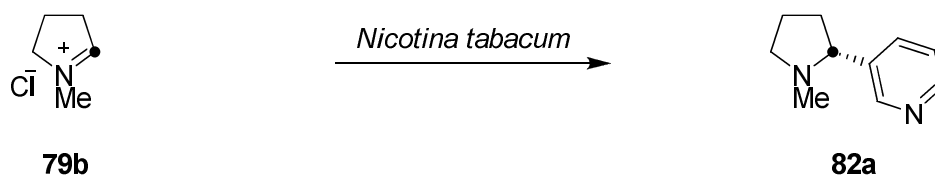


Scheme 2.7 Feeding of [2-¹³C, ²H₃]-acetate (**75b**) into root cultures of *D. stramonium* revealed the symmetrical incorporation into C-6 and C-7 of hyoscyamine (**46d**, **46e**).³⁵

These apparent inconsistent results from feeding experiments were rationalised.¹² Pyrrolinium (**79**) may tautomerise *in vivo* to result in a symmetrical incorporation. This was shown when deuterium in [2-²H]-*N*-methylpyrrolinium chloride (**79a**) was incorporated into both C-1 and C-5 of the tropane ring of 7β-hydroxytropane (**81a**, **81b**) after feeding experiments to *D. stramonium*.^{12, 36} However, in a contradictory study, radioactivity was only located at C-2' of nicotine (**82a**) when *Nicotina tabacum* was fed with *N*-methyl-[2-¹⁴C]-pyrrolidinium chloride (**79b**), inconsistent with an *in vivo* tautomerisation.³⁷



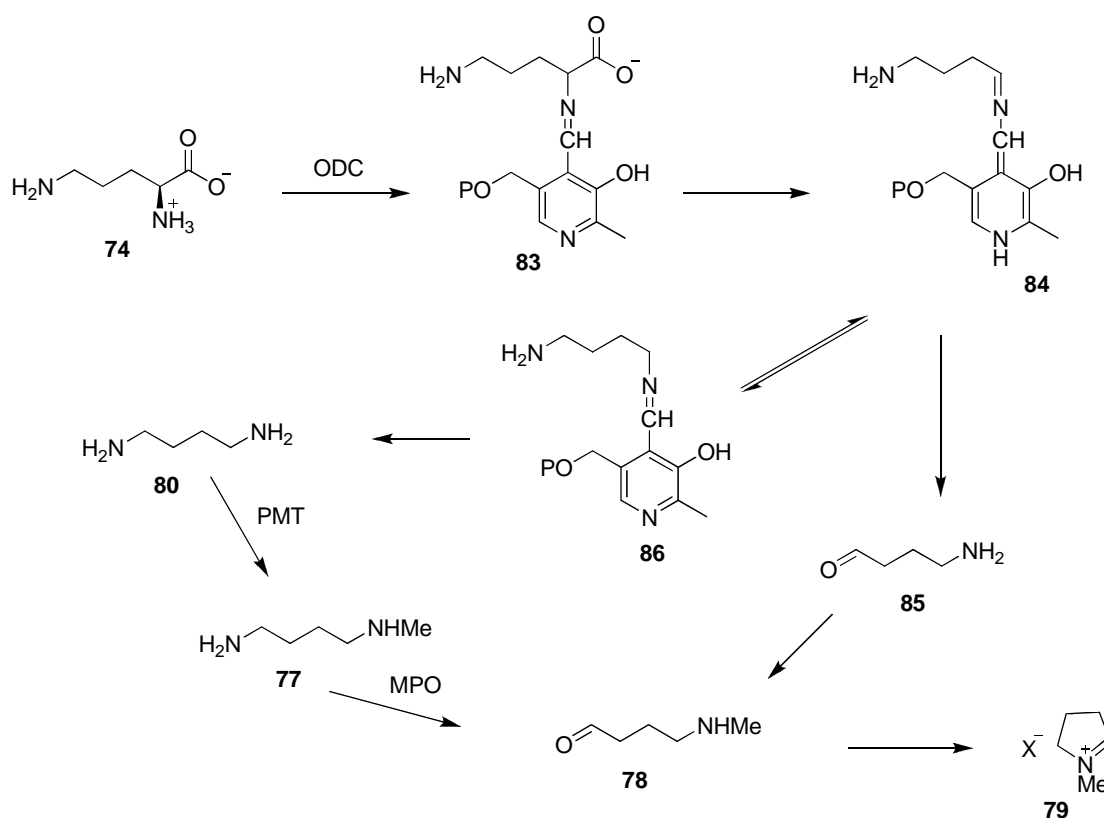
Scheme 2.8 Tautomerism in *N*-methylpyrrolidinium (**79**) salt would lead to the observed symmetrical labelling.³⁶



Scheme 2.9 [¹⁴C]-Feeding experiments in *Nicotiana tabacum* showed asymmetric labelling into nicotine (**82a**).³⁷

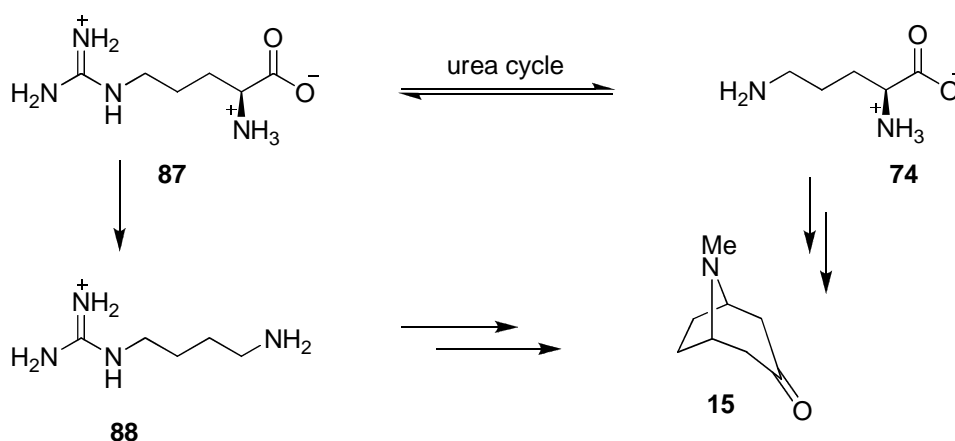
Alternatively, Leete has proposed³⁸ the involvement of PLP in the biosynthesis of the tropane alkaloids and more recent studies^{32, 39} on enzyme activities involved in the

biosynthesis of hyoscyamine support this hypothesis (Scheme 2.10). Decarboxylation of ornithine by ornithine decarboxylase (ODC, EC 4.1.1.17) will generate Schiff base (**84**). Hydrolysis of **84** would give the aminoaldehyde (**85**), followed by methylation to generate 4-*N*-methylaminobutanal (**78**). Tautomerisation of **84** to Schiff base **86** followed by hydrolysis would however result in a loss of the symmetry in the labelling of putrescine (**80**). Methylation mediated by putrescine *N*-methyltransferase (PMT, EC 2.1.1.53)^{32, 39} would then form *N*-methylaminobutyraldehyde (**78**), followed by cyclisation to generate **79**. Recent investigations have shown *S*-adenosyl-L-methionine acts as a methyl donor for PMT.⁴⁰ This was proven by the administering [²H₃-methyl]-methionine to transformed root cultures of *D. stramonium*.³⁵



Scheme 2.10 Proposed involvement of PLP dependent ornithine decarboxylase in the biosynthesis of tropane.³⁸

L-ornithine is an accepted precursor for the biosynthesis of tropane alkaloids and more recent studies suggest a role for arginine (**87**) since ornithine and arginine are metabolically inconvertible *via* the urea cycle. An investigation with *H. albus*, feeding with L-[2,3- $^3\text{H}_3$]-arginine (**87a**), found that radioactivity in *N*-methylputrescine became incorporated into hyoscyamine.⁴¹ Tracer studies in *Datura* cultures feeding DL-[5- ^{14}C]-ornithine (**74a**), L-[U- ^{14}C]-arginine (**87b**), [U- ^{14}C]-agmatine (**88a**), all showed incorporations into hyoscyamine. Interestingly, hyoscyamine production was substantially inhibited by the arginine-decarboxylase inhibitor, DL- α -difluoromethylarginine (**89**), but not by the corresponding ornithine decarboxylase inhibitor, DL- α -difluoromethylornithine (**90**). This suggests that arginine is the more direct precursor of tropane biosynthesis by decarboxylation to agmatine **88**.³⁹



Scheme 2.11 Ornithine (**74**) and arginine (**87**) are interconvertable *via* the urea cycle

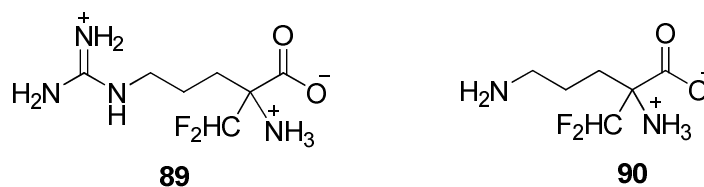
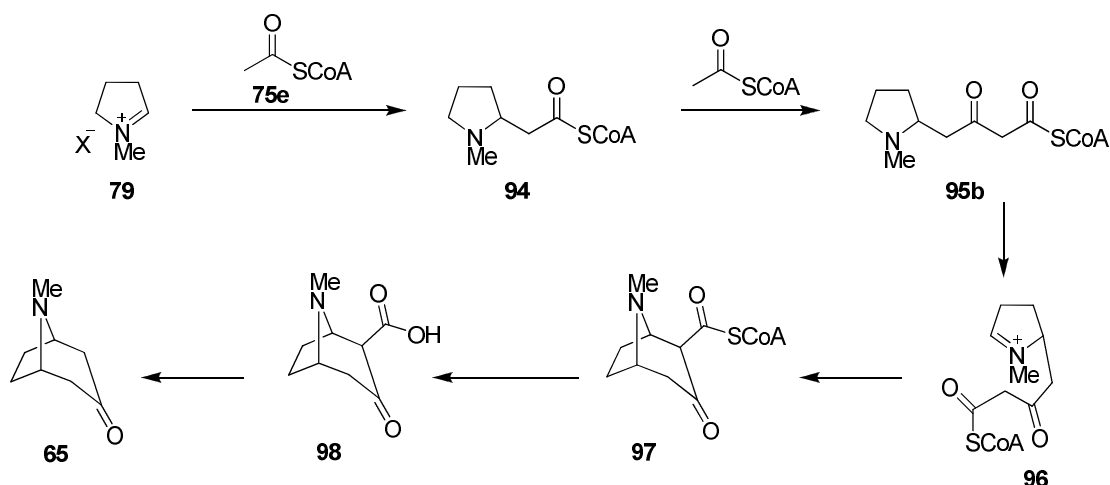


Figure 2.5 DL- α -difluoromethylarginine (**89**), an arginine decarboxylase inhibitor and DL- α -difluoromethylornithine (**90**), an ornithine decarboxylase inhibitor.³⁹

2.3.2.2 The acetate derived fragment

It is obvious that the biosynthesis of the tropane alkaloids requires the condensation of *N*-methylpyrrolinium (**79**) with an acetate derived unit. Either acetone, acetate (**75**) or acetoacetate (**91**) have been discussed as candidate intermediates in Robinson's hypothesis.¹⁴ Early studies involving radiolabelling experiments by feeding sodium [1-¹⁴C]-acetate (**75a**), sodium [2-¹⁴C]-acetate (**75c**), and [2-¹⁴C]-ornithine (**74a**) pointed to the involvement of the alkaloid hygrine (**92**) as an intermediate in tropane alkaloid biosynthesis.⁴²⁻⁴⁴ In addition, feeding experiments with (*RS*)-[*N*-methyl-¹⁴C,2'-¹⁴C]-hygrine (**92a**), (2*R*)-[2'-¹⁴C]-hygrine (**92b**) and (2*S*)-[2'-¹⁴C]-hygrine (**92c**) with *D. innoxia*, *H. niger*, and *A. belladonna* all resulted in radioactive hyoscyamine.^{43, 45, 46} However, there were inconsistencies in stable isotope labelling studies indicating that hygrine may not be involved hyoscyamine biosynthesis. This was revealed by the feeding of [1,2,3,4-¹³C]-acetoacetate (**91a**) which showed a similar labelling pattern to feeding sodium [1,2-¹³C₂]-acetate (**75d**).^{36, 47} Additionally, the incorporation of (*RS*)-[2',3'-¹³C₂]-hygrine (**92d**) into hyoscyamine and scopolamine *D. innoxia* was very low.⁴⁸ Ethyl (*RS*)-[2,3-¹³C₂,3-¹⁴C]-4-(1-methyl-2-pyrrolidinyl)-3-oxobutanone (**95a**) was successfully incorporated into scopolamine and hyoscyamine at high levels in both *D. innoxia*⁴⁸ and *D. stramonium*.⁴⁹ Presumably, the ethyl ester was hydrolysed *in vivo* and was incorporated as its free acid or perhaps as a co-enzyme A ester (**95b**). Interestingly, the feeding, by hydroponics to *D. innoxia* roots showed no preference for (*R*)- or (*S*)- **95** into scopolamine (**59**). Also the possibility that (*RS*)-[2,3-¹³C₂,3-¹⁴C]-4-(1-methyl-2-pyrrolidinyl)-3-oxobutanone (**95a**) could undergo decarboxylation to (*RS*)-[2',3'-¹³C₂,2'-¹⁴C]-hygrine (**92e**) was ruled out, since labelled (*RS*)-[2',3'-¹³C₂]-hygrine (**92d**) was incorporated at a very low level.⁴⁸ The hypothesis is shown in Scheme 2.12.

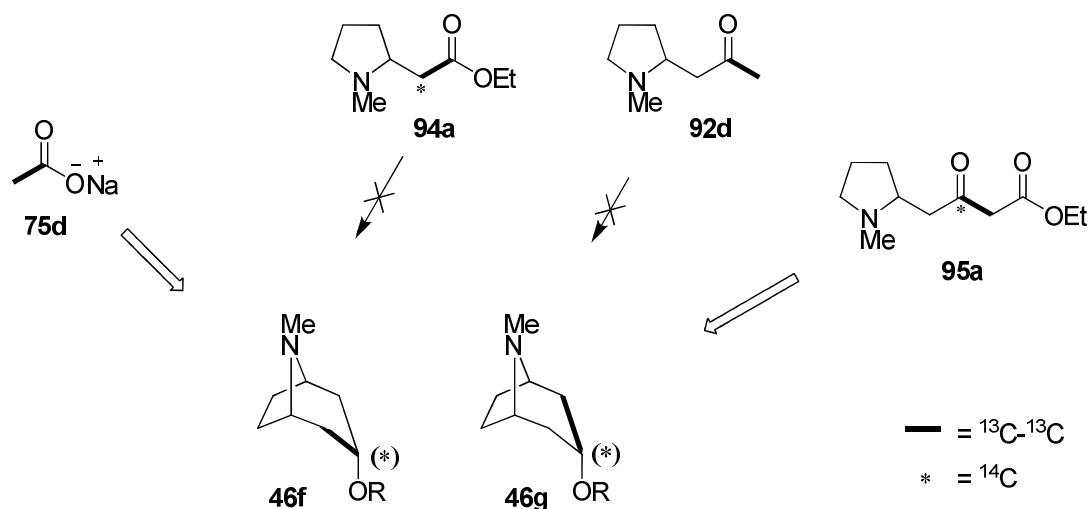
Pyrrolinium salt (**79**) reacts consecutively with two acetate (or acetyl-CoA, **75e**) units to form thioester (**95b**), as suggested by Hemscheidt and Spenser.³⁶ Cyclisation *via* the pyrrolinium salt (**96**) forms the thioester of 2-carboxy-3-tropinone (**97**), followed by hydrolysis and decarboxylation to deliver tropinone (**65**).



Scheme 2.12 Proposed biosynthesis of tropinone *via* the consecutive incorporation of acetyl-CoA (**75e**). Hygrine is not an intermediate.^{48, 49}

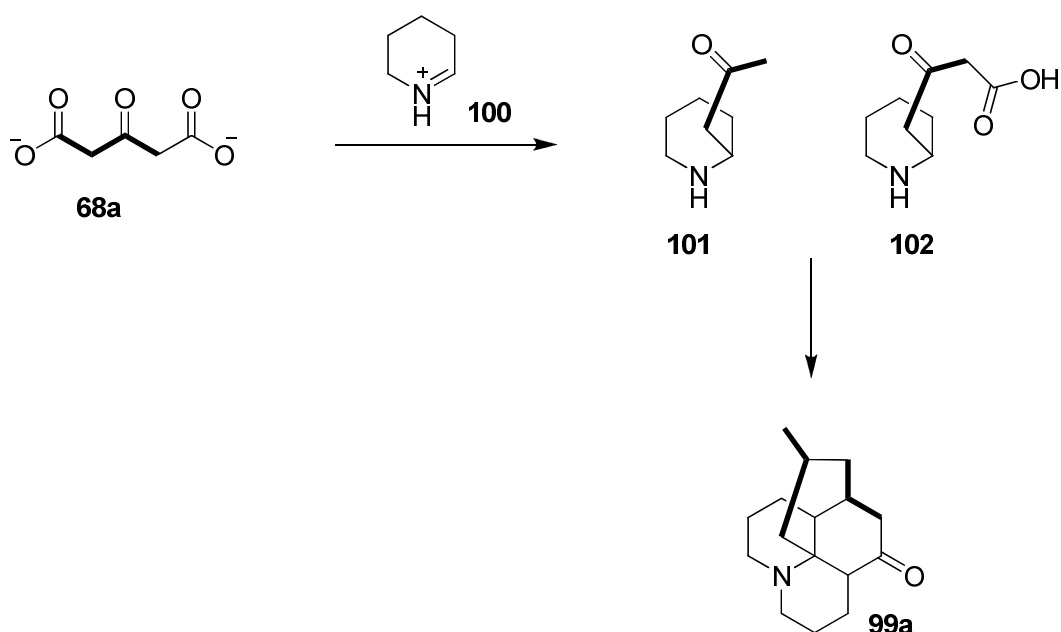
Richard Robins and co-workers⁴⁹ re-evaluated the intermediacy of ethyl (*RS*)-[2,3-¹³C₂,3-¹⁴C]-4-(1-methyl-2-pyrrolidinyl)-3-oxobutanone (**95a**) in transformed root cultures of *D. stramonium*. The results confirmed that hygrine (**92**) was not incorporated into hyoscyamine. There was no preference for the (*R*)- over the (*S*)-isomer of (*RS*)-[2,3-¹³C₂,3-¹⁴C]-4-(1-methyl-2-pyrrolidinyl)-3-oxobutanone (**95a**) or its thioester (**95b**). However, a feeding experiment with sodium [1,2-¹³C₂]-acetate (**75d**) suggested the involvement of an intact C₃ unit because this gave an incorporation of label at C-2 and C-4 in hyoscyamine, but there was also a significant level of triply-labelled molecules. Also, the shorter monoacetate derivative **94a** did

not become incorporated into the tropane ring, so a stepwise process as shown in Scheme 2.12, is not supported by this experiment.

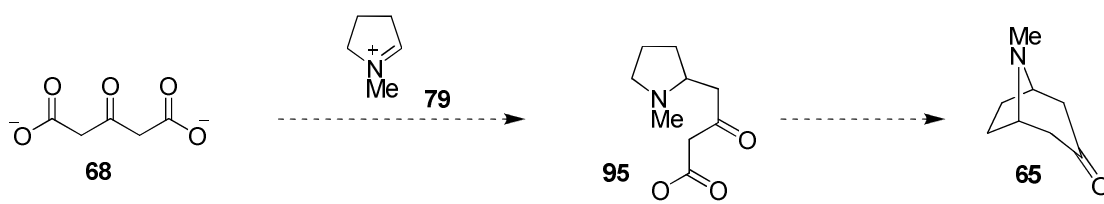


Scheme 2.13 Re-evaluation of β -ketoester **95a** in tropane biosynthesis.⁴⁹

Alternatively, there has been a suggestion that 1,3-acetonedicarboxylic acid (**68**) could be a precursor to the acetate derived fragment of the tropane ring.^{12, 36, 50, 51} A closely related biosynthesis had been explored for lycopodine (**99**) in *Lycopodium tristachyum*. Feeding of [1,2,3,4- $^{13}\text{C}_4$]-1,3-acetonedicarboxylate (**68a**) resulted in the incorporation of an intact C_3 unit into two separate fragments (Scheme 2.14).⁵² The condensation of piperidinium ion (**100**) with acetonedicarboxylate would generate intermediates **101** and **102** which would then condense to generate lycopodine. A condensation of the pyrrolinium salt (**79**) with acetondicarboxylate (**68**) for tropane biosynthesis would mirror this observation (Scheme 2.15), however this hypothesis has yet to be proven experimentally.



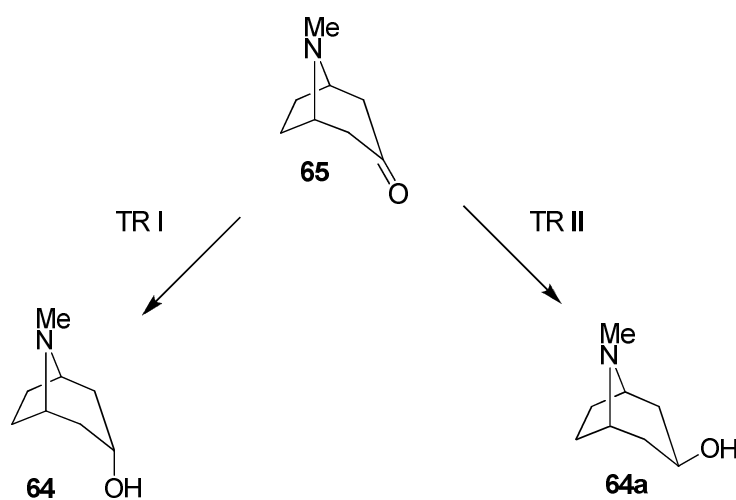
Scheme 2.14 The incorporation of [1,2,3,4-¹³C]-acetonedicarboxylate (**68a**) into lycopodine (**99a**) in *L. trischyum*.⁵²



Scheme 2.15 Proposed incorporation of acetonedicarboxylate (**68**) into tropinone (**65**).^{12, 36, 50, 51}

2.3.2.3 The reduction of tropinone to tropine

[Methyl- ^{14}C]-Tropinone is an established precursor to tropine.⁵³ Two NADPH dependent enzymes have been isolated and purified from transformed root cultures of *D. stramonium*. Tropinone reductase I converts tropinone to tropine, whereas tropinone reductase II generates pseudotropine (ψ -tropine,).⁵⁴ The structures of TR-II has been solved by X-ray structure analysis.⁵⁵



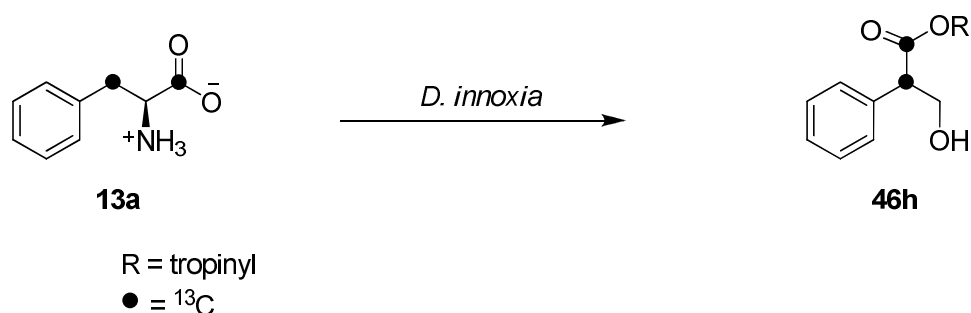
Scheme 2.16 The reduction of tropinone by tropane reductases (TR I and II).⁵⁴

2.3.3 Biosynthesis of hyoscyamine

2.3.3.1 Littorine as a precursor

Robinson recognised that tropic acid is an isomer of the phenylpropanoic acid skeleton and he proposed that tropic acid may originate by a rearrangement of the phenylpropanoid skeleton.⁵⁶ Several researchers have shown that the phenylpropionate moiety of littorine (**45**) is derived from phenylalanine (**13**).⁵⁷⁻⁵⁹ Further feeding experiments by administering [1,3- $^{13}\text{C}_2$]-phenylalanine (**13a**) to *D. innoxia* have demonstrated the incorporation of ^{13}C into C-1 and C-2 of the tropic acid moiety of hyoscyamine, as evident by ^{13}C -NMR satellites peaks due to ^{13}C - ^{13}C

coupling.⁶⁰ Remarkably this experiment demonstrated an intramolecular rearrangement where the two isotopes become contiguous in the resultant tropate.

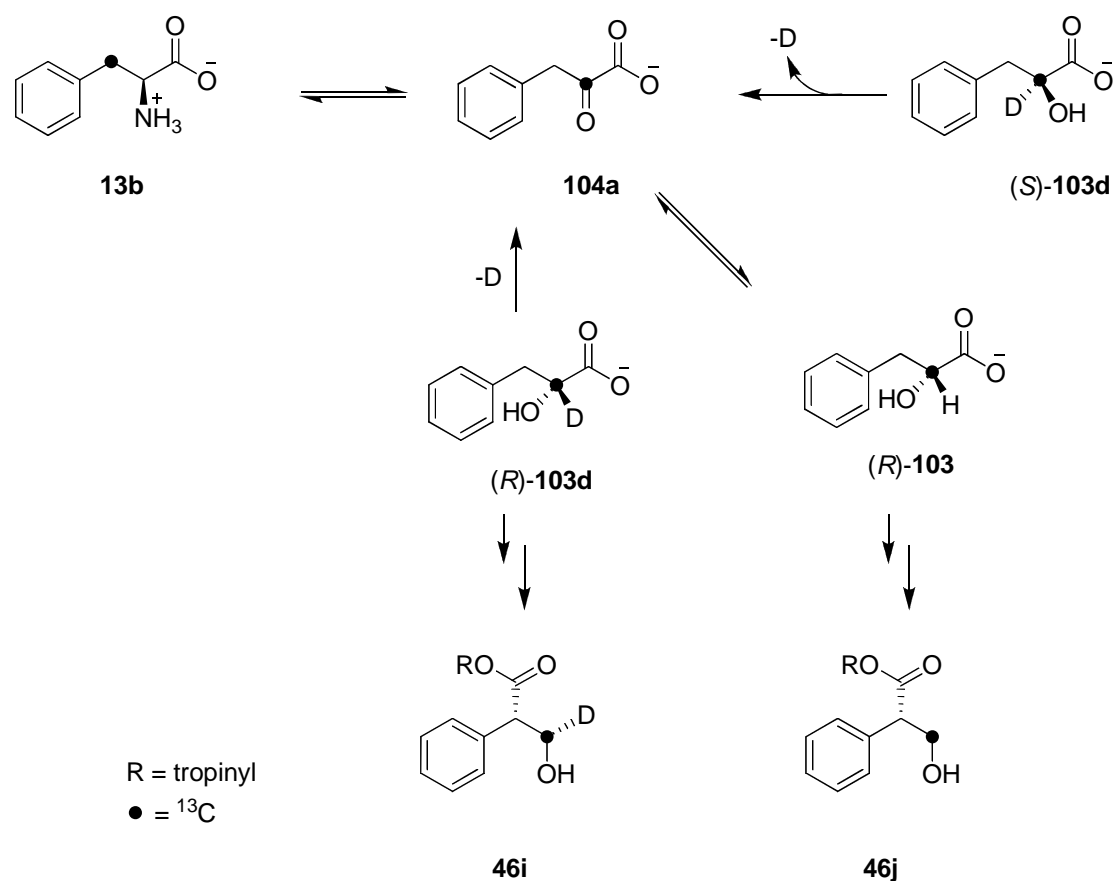


Scheme 2.17 Leete's feeding of [1,3- $^{13}\text{C}_2$]-phenylalanine (**13a**) proved an intramolecular rearrangement in the biotransformation of the tropate ester.⁶⁰

It is known that phenylalanine is metabolically interconvertible *in vivo* with phenyllactate (**103**) presumably *via* phenylpyruvate (**104**), so the role of phenyllactate in the biosynthesis of the tropane alkaloids then attracted attention. Phenyllactate was shown to incorporate into tropic acid in *D. sanguinea*⁶¹ and a radiolabelled study showed that the $^3\text{H}:$ ^{14}C ratio from feeding of (*RS*)-phenyl-[1- ^{14}C ,2- ^3H]-lactate (**103a**) remained essentially constant in the recovered hyoscyamine and scopolamine.⁶² Further, feeding experiments with phenyl-[1,3- $^{13}\text{C}_2$]-lactic acid (**103b**)⁶³ in *D. stramonium* resulted in the similar spin-spin couplings by ^{13}C -NMR at C-1 and C-2 of the tropic acid recovered by hydrolysis of hyoscyamine and scopolamine. These findings clearly suggested that phenyllactate is an obligatory intermediate in the biosynthesis of tropic acid and that the rearrangement of the side chain takes place at the phenyllactate level, not the phenylpyruvate level.⁶² Feeding experiments supplementing *D. stramonium* transformed root cultures with sodium (*R,S*)-phenyl-[2- ^{13}C ,2- ^2H]-lactate (**103c**) resulted in a substantial retention of ^{13}C -D attached to C-3' of tropate ester.⁶⁴ Further experiments with (*R*)- [2- ^{13}C , ^2H] and (*S*)- [2- ^{13}C , ^2H]-

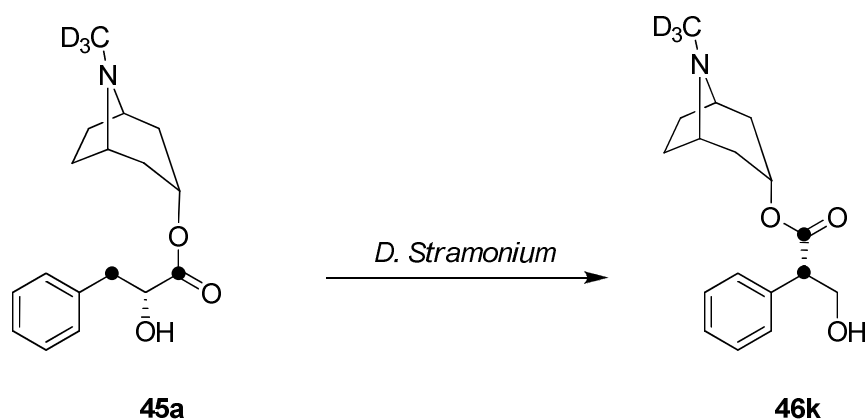
phenyllactates (*R*-**103d**, *S*-**103d**) showed that only the (*R*)-isomer resulted in hyoscyamine containing a dual labelled ^{13}C -D (28.9%) indicating that the bond remained intact during the biosynthesis (Scheme 2.18). For the (*S*)-isomer the deuterium was lost, indicating this bond had been broken during hyoscyamine formation. Presumably, (*S*)-phenyllactate is converted *in vivo* to (*R*)-phenyllactic acid perhaps *via* phenylpyruvate, prior to incorporation into hyoscyamine biosynthesis.^{65,}

66



Scheme 2.18 An *in vivo* interconversion between (*R*)- [2- ^{13}C , ^2H] and (*S*)- [2- ^{13}C , ^2H]-phenyllactate (*R*-**103d**, *S*-**103d**) *via* phenylpyruvate (**104a**) resulted in a loss of ^{13}C -D bond in hyoscyamine for the (*S*)-isomer and remaining intact for the (*R*)-isomer.^{65, 66}

The most direct precursor of tropane biosynthesis emerged when the quintuply labelled of littorine, (*RS*)-phenyl-[1,3- $^{13}\text{C}_2$]-lactoyl-[methyl- $^2\text{H}_3$]-tropine (**45a**), was fed to transformed root cultures *D. stramonium*. This revealed an intact incorporation of the quintuply labelled precursor into hyoscyamine.^{67, 68} Additionally, the intramolecular rearrangement was again confirmed by NMR with ^{13}C spin-spin coupling due to the adjacent enriched C-1' and C-2' carbons of hyoscyamine (**46k**). These experiments clearly suggest that littorine is the true substrate for rearrangement to hyoscyamine.

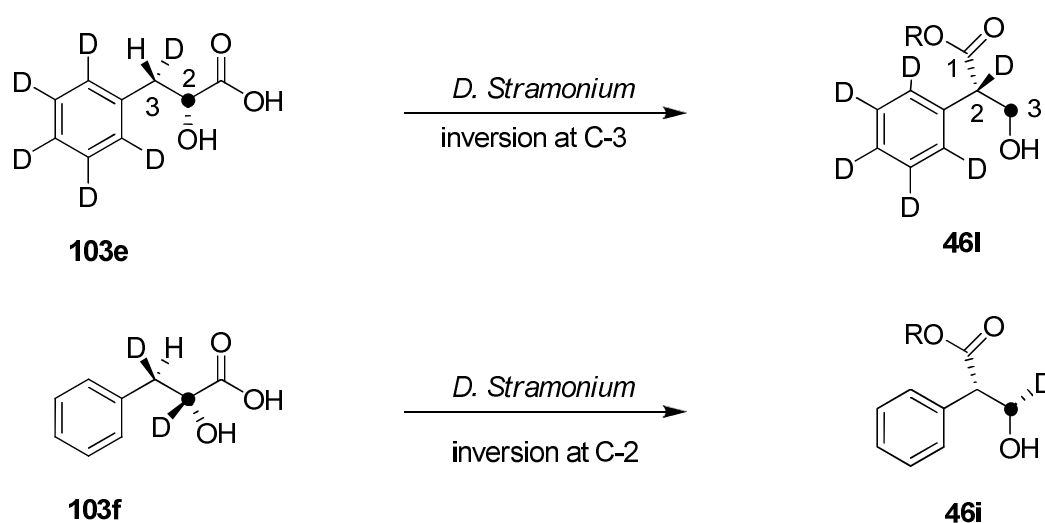


Scheme 2.19 The feeding of (*RS*)-phenyl-[1,3- $^{13}\text{C}_2$]-lactoyl-[methyl- $^2\text{H}_3$]-tropine (**45a**) to *D. stramonium* resulted in the quintuply labelled hyoscyamines (**46k**) securing littorine (**45**) as a direct precursor to hyoscyamine (**46**).^{67, 68}

2.3.3.2 Stereochemistry of the rearrangement

The studies described above have shown the intramolecular rearrangement of phenylalanine to tropane alkaloids.^{60, 69, 70} In order to establish the stereochemical course of the rearrangement of littorine (**45**) to hyoscyamine (**46**), isotopic labelling experiments were carried out in *D. stramonium*. Initially, the migration centre at C-3 of littorine to C-2 of hyoscyamine was investigated by feeding (2*R*,3*R*)-[2- ^{13}C ,3-

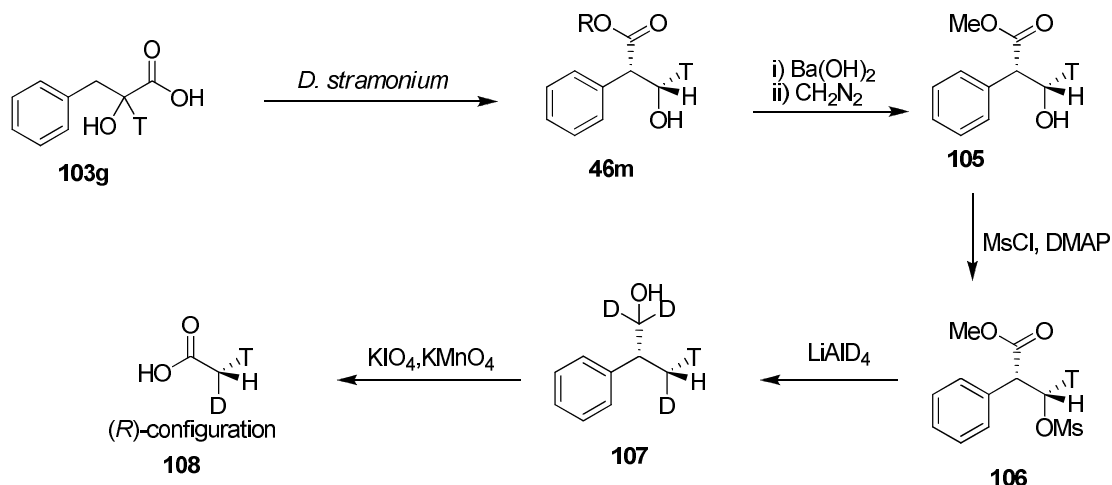
$^2\text{H}_{1,\text{phenyl}}\text{-}^2\text{H}_5\text{]-phenyllactate (103e)}$ carrying deuterium at the 3-*pro-S* site, and separately (2*R*, 3*S*)-[2- ^{13}C ,3- $^2\text{H}_1\text{]-phenyllactate (103f)}$, carrying deuterium at the 3-*pro-R* site. These experiments revealed that the 3-*pro-R* deuterium was lost during the transformation and that the 3-*pro-S* deuterium was retained. The resultant tropate ester has the (*S*)-configuration so it was deduced that there is an overall inversion of configuration at C-3 of (*R*)-phenyllactate during the rearrangement.⁷¹



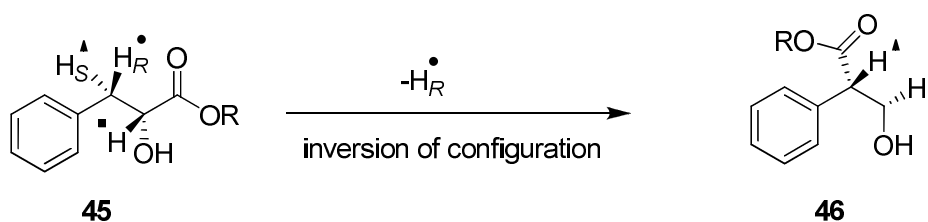
Scheme 2.20 Exploring the stereochemistry of C-3 of phenyllactic acid during its conversion to tropic acid in *D. stramonium*.⁷¹

The stereochemical course at C-2 of littorine as it progressed to C-3 of hyoscyamine was established by feeding (*RS*)-[2- ^3H]-phenyllactate (**103g**) to generate radiolabelled hyoscyamine (**46m**) with tritium located at C-2.⁷² After *in vivo* isomerisation the radiolabelled hyoscyamine was isolated and the resultant configuration of the C-T bond was revealed by oxidation to acetic acid and then chiral acetic acid analysis. The resultant [^2H , ^3H]-acetic acid (**108**) had the (*R*)-configuration (Scheme 2.21). Thus, by deduction, the tritium must have occupied the 3-*pro-S* site in the isolated

hyoscyamine. Clearly, again, there is an overall inversion of stereochemistry in going from littorine to hyoscyamine at this migratory terminus. This was consistent with a previous study by Haslam which indicated inversion of configuration at C-2'.⁷³ A summary of the stereochemical course of the rearrangement is shown in Scheme 2.22.



Scheme 2.21 Incorporation of (RS)-[2-³H]-phenyllactate (**103g**) to *D. stramonium* and the chemical manipulation of hyoscyamine (**46m**) to chiral acetic acid (**108**).⁷²

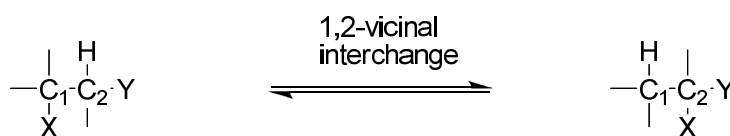


Scheme 2.22 Summary of the stereochemical course of the rearrangement of littorine (**45**) to hyoscyamine (**46**).^{65, 72}

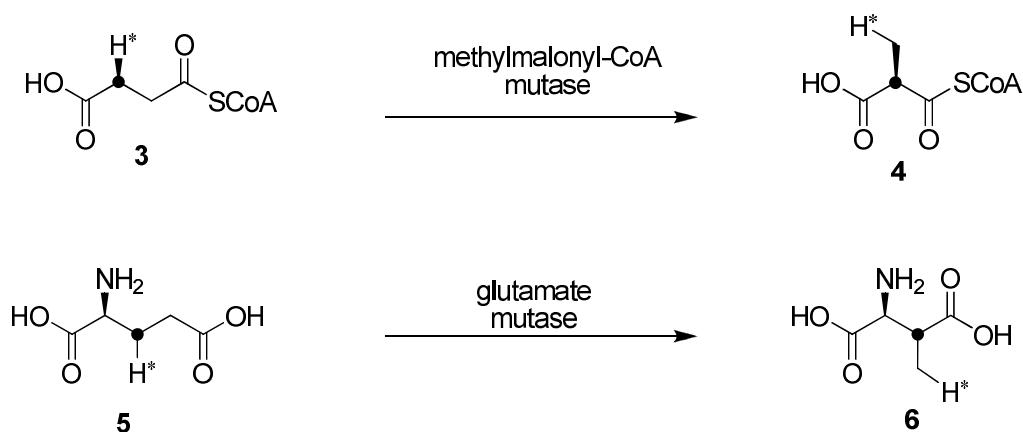
2.4 Enzymes that mediate a molecular rearrangement.

2.4.1 Co-enzyme B₁₂ and SAM. 'Poor man B₁₂' is not involved.

The carbon skeleton rearrangement of littorine to hyoscyamine finds some precedence in B₁₂ mediated isomerisations such as that catalysed by methylmalonyl-CoA mutase^{74, 75} and glutamate mutase (Section 1.2, Chapter 1).⁷⁶ These rearrangements involve a vicinal interchange between a carboxyl moiety with the subsequent 1,2-back migration of a hydrogen atom. The similarity of the littorine rearrangement process to that of the conversion of methylmalonyl-CoA (**3**) to succinyl-CoA (**4**)⁷⁰ led to the hypothesis that co-enzyme B₁₂ may mediate this process. However, no co-enzyme B₁₂ dependent enzymes have been identified in plants to date.



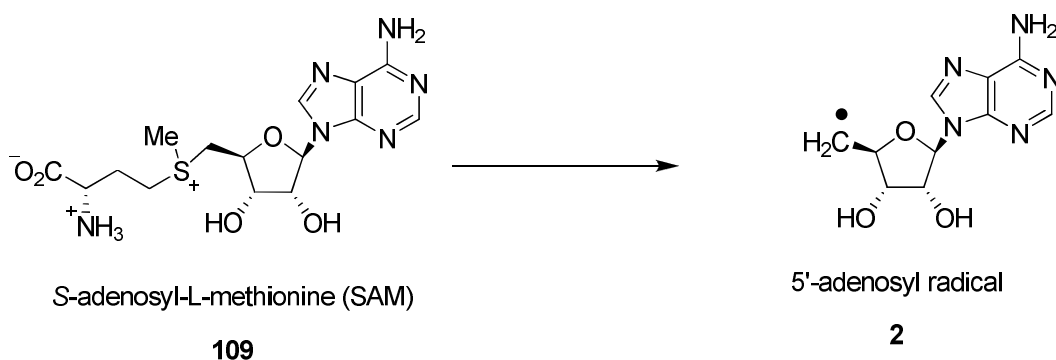
Scheme 2.23 Vicinal interchange mediated by co-enzyme B₁₂.



Scheme 2.24 1,2-Vicinal interchanges mediated by co-enzyme B₁₂.^{74, 76}

Nature utilises the 5'-deoxyadenosyl radical (**2**) to abstract a hydrogen atom from non-activated positions. In animals and bacteria, co-enzyme B₁₂ is the major source for

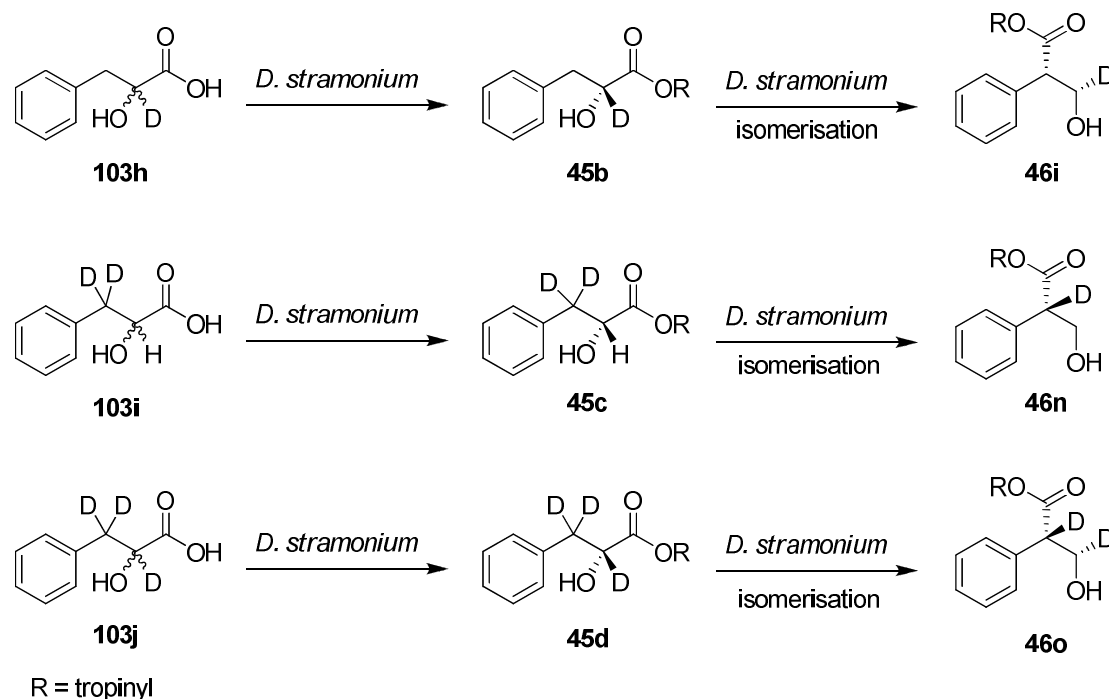
this radical, however it has been reported that SAM (**109**) mediated lysine 2,3-aminomutase from *Clostridia* catalyses the interconversion of L-lysine to L- β -lysine.^{77, 78} The enzyme contains iron-sulphur clusters and is activated by the 5'-deoxyadenosyl radical (**2**) and pyridoxal 5'-phosphate. This led researchers to call SAM “poor man’s B₁₂”. In an effort to demonstrate⁷⁹ the transfer of hydrogen from the methylene group of the adenosyl radical into the alkaloid, [2,8,5'-³H] SAM (**109a**) (65% ³H at 5' position) was administered to cell free extracts of *D. stramonium*. However, only a very low incorporation of tritium into littorine or hyoscyamine was observed.



Scheme 2.25 5'-Adenosyl radical (**2**) generates from SAM (**109**).

More recent studies using stable isotope methodology failed to detect any back migration of the deuterium isotope.⁷¹ The re-investigation by feeding (*RS*)-[2-²H]-, (*RS*)- [3,3-²H₂]-, and (*RS*)-[2,3,3-²H₃]-phenyllactic acids (**103h**, **103i**, **103j**) to *D. stramonium* did not provided evidence of a vicinal interchange process (Scheme 2.26). The complete loss of deuterium at C-3' of **46n** during the isomerisation to hyoscyamine and the absence of deuterium redelivery back to C-3' of hyoscyamine, is inconsistent with a vicinal interchange process.⁸⁰ These experiments ruled out the role

a vicinal interchange process and the involvement of co-enzyme B₁₂ or SAM. This also illustrated the shortcoming of radiolabelled experiments, particularly in interpreting low levels of incorporation.

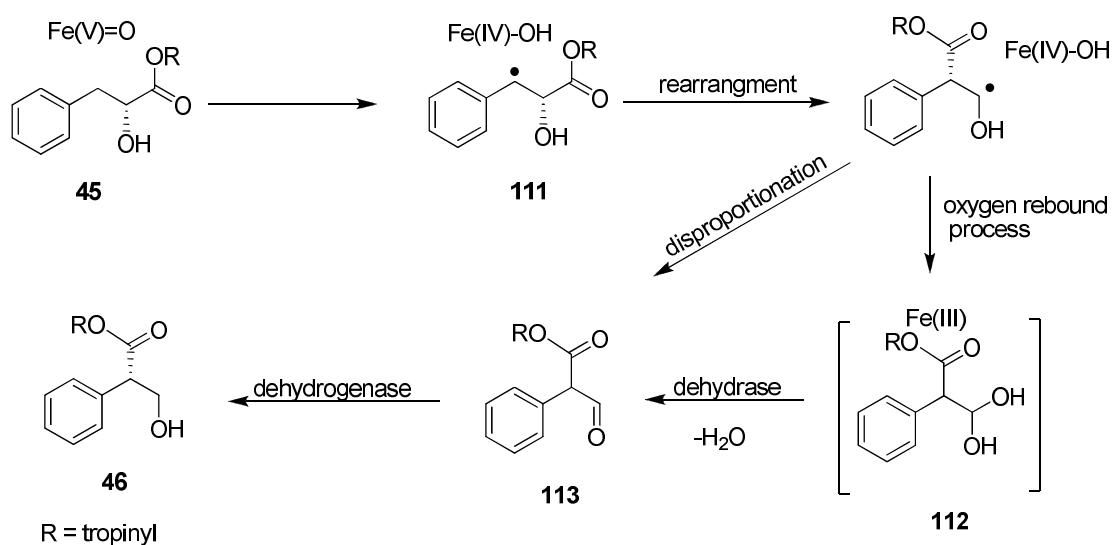


Scheme 2.26 A series of feeding experiments did not provide any evidence for a 1,2-vicinal interchange operating in the rearrangement of littorine to hyoscyamine.⁸⁰

2.4.2 The role of cytochrome P₄₅₀ enzymes.

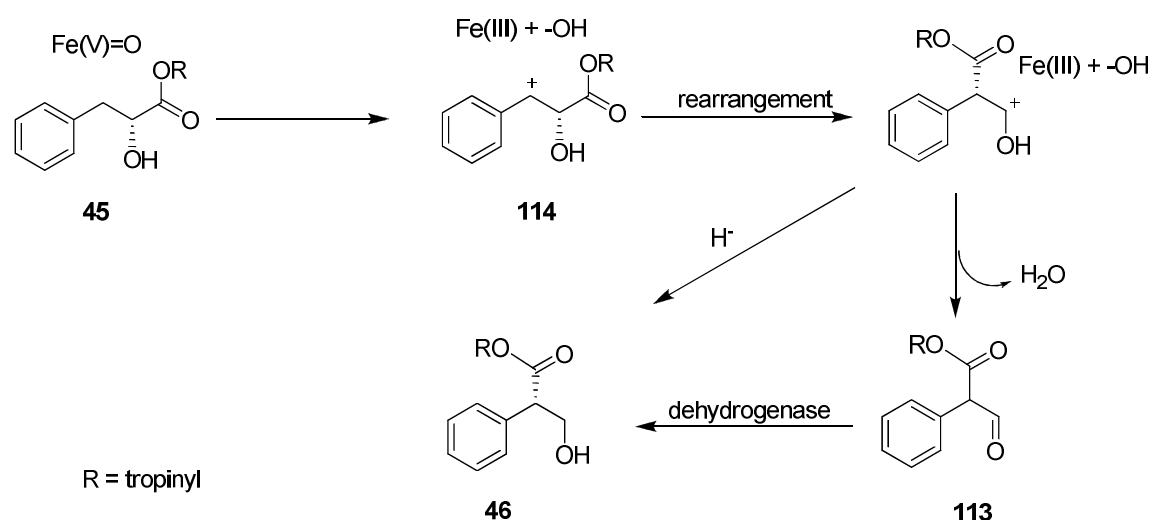
It has been reported that some plants utilise cytochrome P₄₅₀, iron-oxo enzymes, to mediate isomerisation processes.^{81, 82} Also the P₄₅₀ inhibitor chlortrimazole suppresses the conversion of littorine to hyoscyamine in *D. stramonium* transformed root cultures. This implicates P₄₅₀ involvement in the biotransformation.⁸³ In recent studies,⁸⁴ a virus silencing cytochrome P₄₅₀ gene, identified CYP80F1 P₄₅₀ the gene/enzyme from *H. niger* (black henbane) responsible for the conversion of littorine to hyoscyamine. Hyoscyamine was observed when CYP80F1 was expressed in tobacco hairy roots supplemented with (*R*)-littorine. Expression in yeast confirmed

that CYP80F1 catalysed the oxidation of (*R*)-littorine to form the hyoscyamine aldehyde, the putative precursor to hyoscyamine, along with the side product 3'-hydroxylittorine (**110**). A mechanism for the rearrangement of littorine to hyoscyamine involving radicals has been proposed by analogy to the study in *Pueraria lobata* plants (Section 1.4, Chapter 1).^{66, 82} Abstraction of the benzylic proton of littorine (**45**) generates radical **111**. Rearrangement of this radical intermediate, followed by an “oxygen rebound” process would give gem-diol **112**. Dehydration to an aldehyde and subsequent reduction by a dehydrogenase then gives hyoscyamine. The feeding of (*R,S*)-[2-²H, ¹⁸O] phenyllactic acid to root cultures of *D. stramonium* had shown that 25-29% of the ¹⁸O isotope was lost during the rearrangement.⁸⁵ The proposed oxygen rebound process requires the intermediacy of aldehyde (**113**). Exchange of the aldehyde oxygen with the aqueous medium prior to reduction could account for some loss of the isotope. In addition a partially stereoselective dehydration of the gem-diol could lead also to some loss of the isotope.



Scheme 2.27 A putative cytochrome P 450 dependent mechanism for the rearrangement of littorine (**45**) to hyoscyamine (**46**) via a radical process.⁶⁶

Alternatively a carbocation type migration, arising from a P_{450} mediated two electron oxidation could occur. The resultant benzylic carbocation could undergo a carbon skeleton rearrangement by 1,2-sigma bond migration. This would result in the direct formation of a product carbocation which could collapse to an aldehyde intermediate. Reduction would then give hyoscyamine (Scheme 2.28).



Scheme 2.28 An alternative carbocation mechanism for hyoscyamine biosynthesis.⁶⁶

Although, the cytochrome P_{450} enzyme, CYP80F1 gene responsible for the rearrangement of littorine to hyoscyamine has been identified by Covello and co-workers,⁸⁴ mechanistic details of the rearrangement of littorine to hyoscyamine remain unknown. It is not clear whether the mechanism involves a carbocation or a radical.

2.5 Reactive species involved in P₄₅₀ transformations.

Cytochrome P450's (CYP450 or P₄₅₀) are a superfamily of heme-containing monooxygenase enzymes which are present in all aerobic organisms. They exhibit a characteristic absorption band at 450 nm when coordinated to carbon monoxide, thus they are dubbed P450's. Structurally, the prosthetic group of cytochromes P₄₅₀ consists of an iron(III) protoporphyrin IX which links to a cysteine residue by a covalent bond as shown in Figure 2.6.⁸⁶ Probably the most remarkable reactions mediated by cytochromes P₄₅₀ are hydroxylation of unactivated C-H bonds and epoxidation of double bonds. The generally accepted catalytic cycle for the hydroxylation of C-H bond is shown in Scheme 2.29.⁸⁷⁻⁸⁹ The resting state of the P₄₅₀ has iron(III) coordinated to water as a distal ligand and thiolate as a proximal ligand. The approaching substrate induces an electron transfer process from NADP(H) *via* an electron transfer chain (flavin reductase-Fe₂S₂ system, or without Fe₂S₂ system) to generate an iron(II), allowing this species to bind with dioxygen and form iron(III)-superoxide. A second single electron transfer and protonation generates an iron(III)-peroxide, the so-called Compound 0 (Cpd 0). The second protonation allows water to leave, generating the high-valent ferryl moiety [Fe(IV)=O] and a porphyrin radical cation, Compound I (Cpd I). Abstraction of a hydrogen atom from the substrate by Cpd I, followed by the return of a hydroxyl radical in an 'oxygen rebound process', regenerates the iron(III) species.

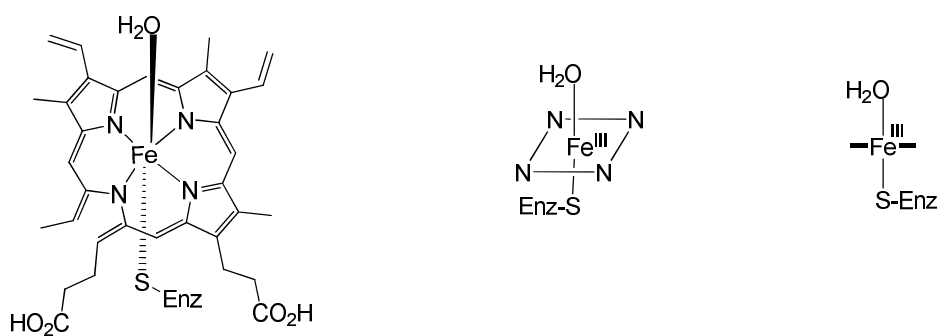
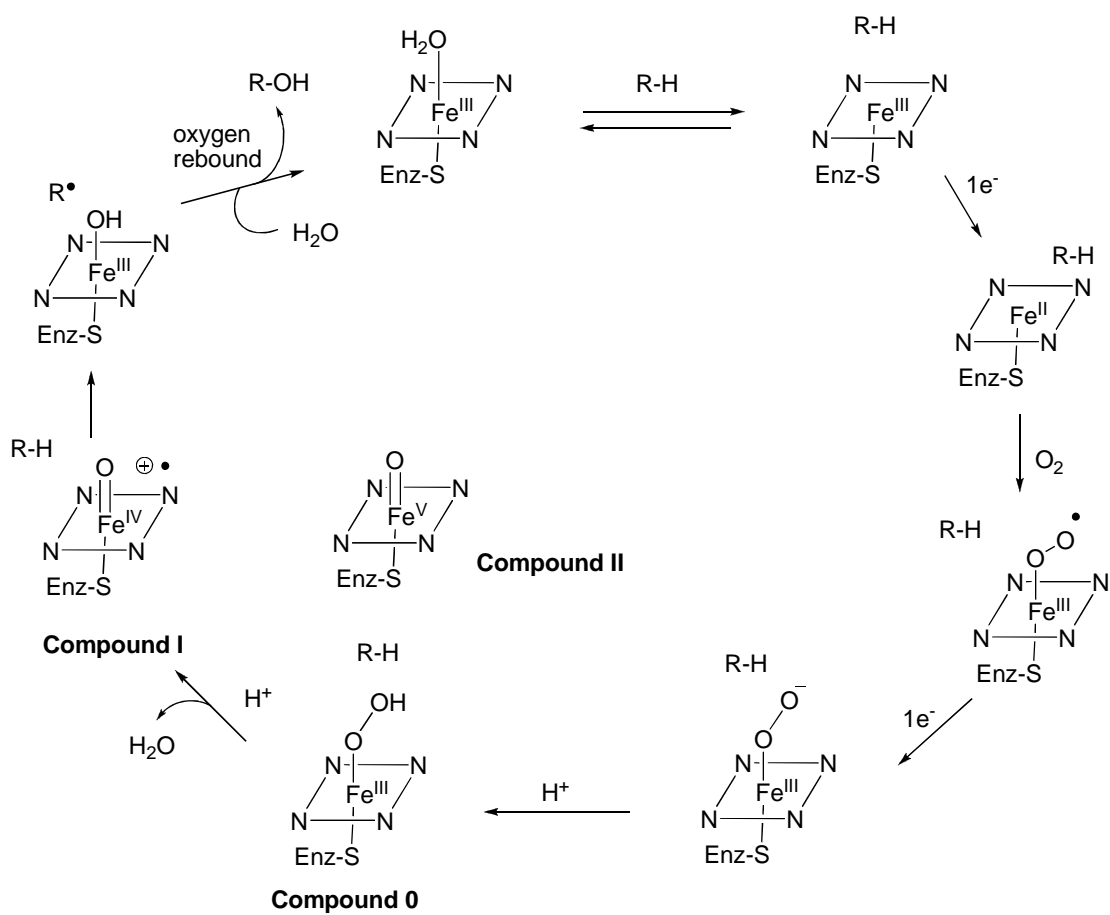
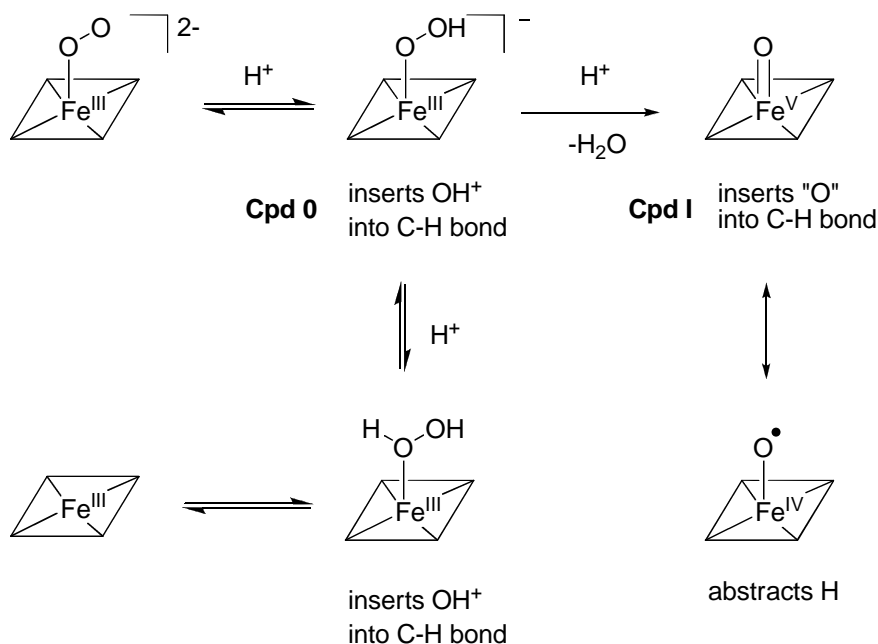


Figure 2.6 Structure of iron (III)-protoporphyrin IX.^{86, 89}



Scheme 2.29 P₄₅₀ cycle for substrate hydroxylation.⁸⁷⁻⁸⁹

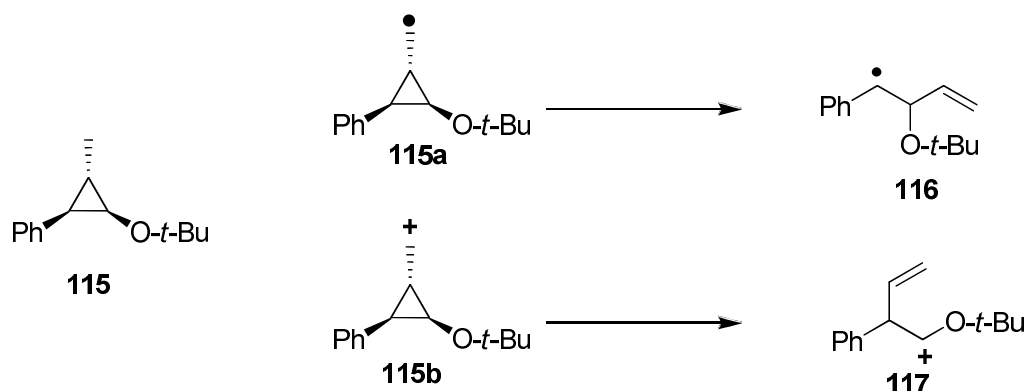
The intermediates in the catalytic cycle have been extensively studied both computationally and experimentally, however Cpd I, has not yet been fully characterised. Generation of Cpd I has recently been accomplished by photooxidation of Cpd II to perform hydroxylation.⁹⁰ Recently, radical clock experiments by Newcomb have cast doubt on the true oxidant species utilised by P₄₅₀ enzymes.⁹¹⁻⁹⁵ He proposed a two oxidant hypothesis.⁹⁶ Newcomb observed oxidation of a substituted cyclopropane **115** by a cationic rearrangement process along with the expected hydroxylation product (Scheme 2.31). It is well known that Cpd I is the primary oxidant in P₄₅₀ enzymes, operating *via* a radical process. Newcomb, therefore suggested that Cpd 0 might act as the secondary oxidant responsible for the insertion of hydroxonium ion (⁺OH) into C-H to initiate a cation rearrangement. This is summarised in Scheme 2.30.



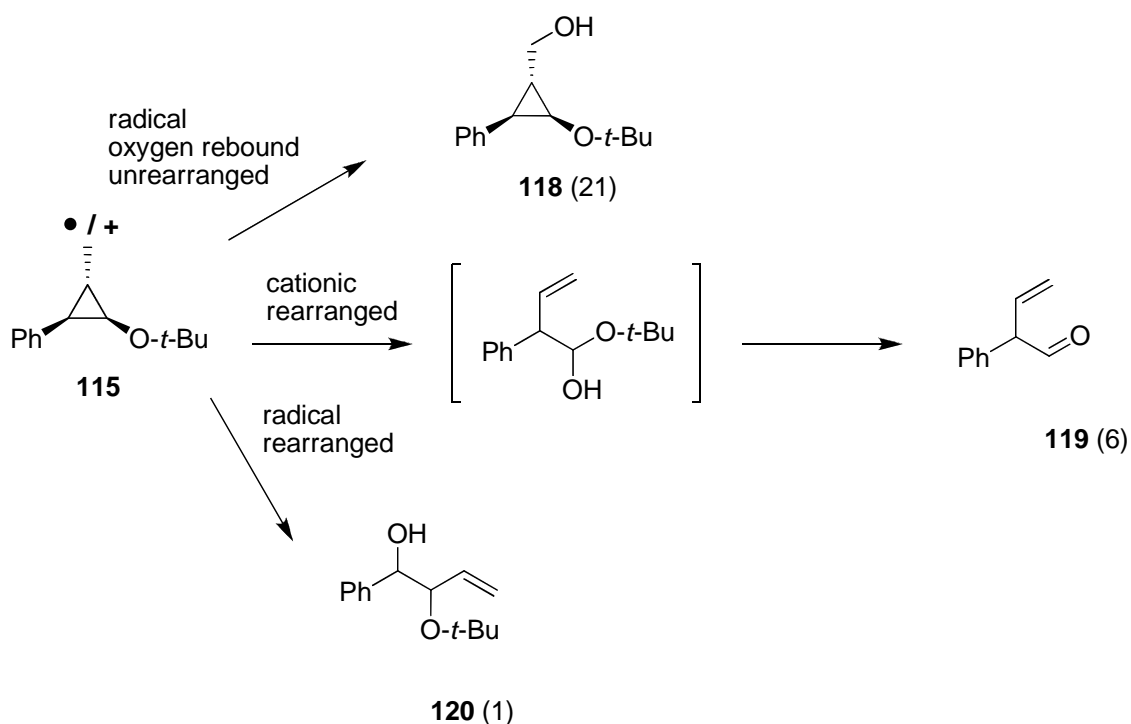
Scheme 2.30 Reactive species in P₄₅₀ mediated hydroxylation reactions⁹⁶

2.6 Radical or carbocation rearrangement process

In order to discriminate radical and carbocation intermediates in P₄₅₀ enzymes, a mechanistic probe has been developed.⁹⁷ The cyclopropylcarbinyl cation **115b** opens preferably towards the oxygen in a ratio of 1000:1. This has a similarity to the rearrangement process of littorine to hyoscyamine in the forward direction. On the other hand the cyclopropylcarbinyl radical **115a** opens preferentially towards the aryl ring with a ratio of 170:1. This is opposite to the direction of the rearrangement. In addition, these probes were applied to *in vivo* incubations with cytochrome P₄₅₀ enzymes.⁹³ The unrearranged product (**118**) predominated in those experiments along with small amounts of rearranged products (**119** and **120**). The 6:1 preference of cationic rearranged product (**119**) over radical derived product (**120**) implied that the P₄₅₀ enzymes could generate carbocations and lends support to the intermediacy of carbocations, e.g. in the rearrangement of littorine to hyoscyamine.

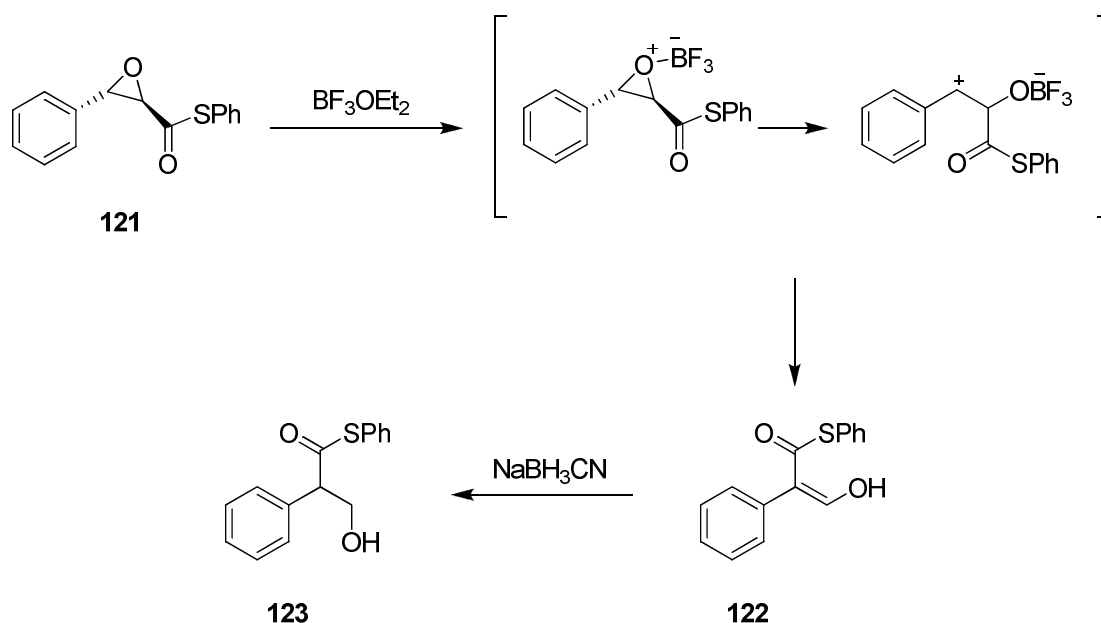


Scheme 2.31 A mechanistic probe to partition radicals from carbocations as devised by Newcomb.⁹⁷



Scheme 2.32 Cytochrome P₄₅₀ mediates hydroxylation and rearrangement to give **118**, **119** and **120** with ratios shown in parentheses, suggesting significant cationic character in P₄₅₀ processes.⁹³

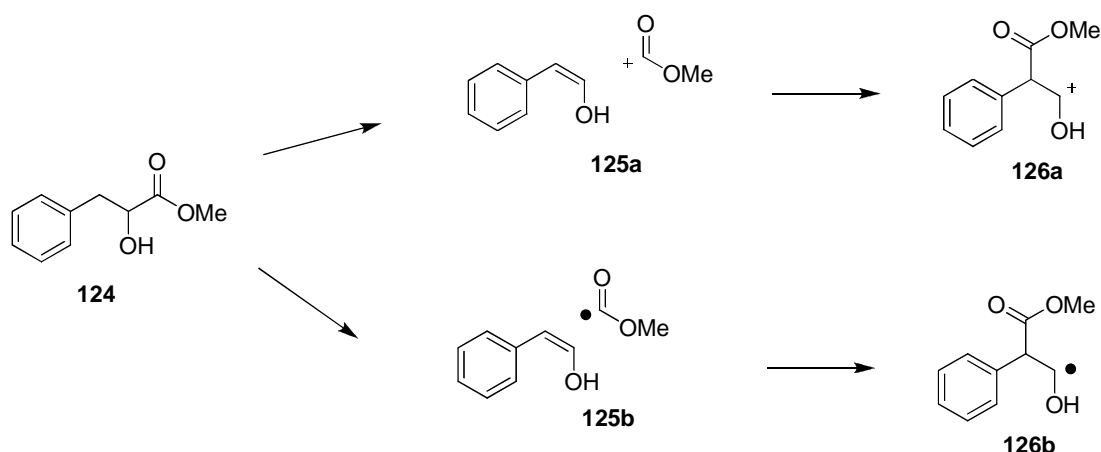
In a biomimetic model reaction, a carbocation isomerisation has been demonstrated *in vitro* by Wemple.^{98, 99} The rearrangement was mediated by Lewis acid catalysis and reaction resulted in the α -formylphenylthioacetate (**122**). This product was then converted into the thioester of tropic acid (**123**) by treatment with sodium cyanoborohydride (Scheme 2.33).



Scheme 2.33 α -Formylphenylthioacetate (**122**) is converted to a thioester of tropic acid (**123**) *via* a cationic rearrangement.

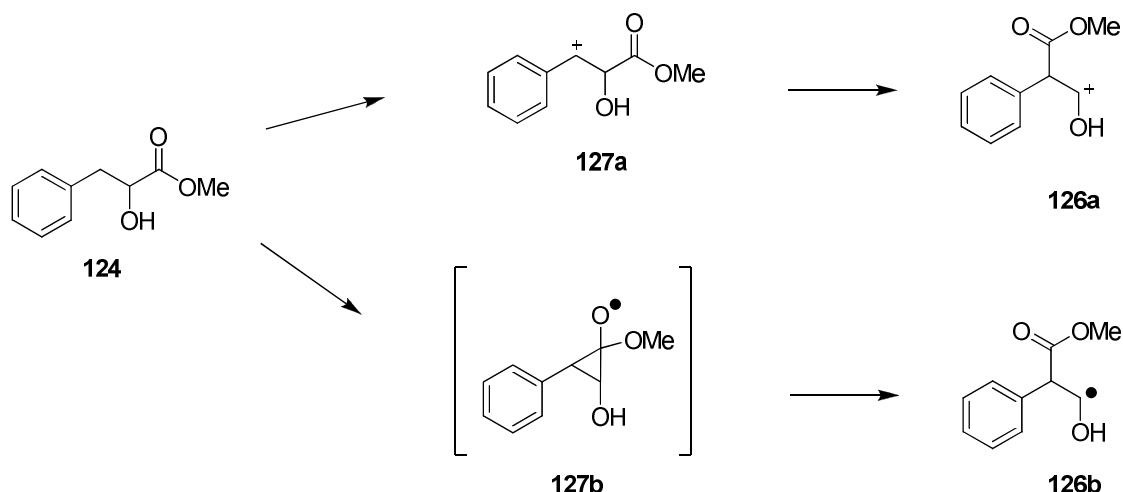
2.7 Computational studies

Recently in a computational study in 2008 Radom *et. al.*, the rearrangement of methyl phenyllactate (**124**) to methyl tropic acid was explored.¹⁰⁰ The high-level quantum chemistry calculation (G3(MP2)-RAD, level) considered two possible pathways, a stepwise and a concerted rearrangement. In the stepwise process (Scheme 2.34) the energy barrier to form radical **125b** from **124** was calculated to be $136.3 \text{ kJ mol}^{-1}$ and the recombination of **125b** to form the radical product **126b** was 106 kJ mol^{-1} , but the overall reaction for the radical rearrangement was calculated to be endothermic by 29.4 kJ mol^{-1} . For the carbocation process, the relative energy barrier to form **125a** was slightly higher at $170.9 \text{ kJ mol}^{-1}$, however the overall reaction for this process was calculated to be exothermic by 26.8 kJ mol^{-1} .



Scheme 2.34 High-level quantum chemistry calculations using G3(MP2)-RAD considered the stepwise rearrangement *via* radical and cationic intermediates.¹⁰⁰

For the concerted rearrangement process (Scheme 2.35), the energy barrier for radical rearrangement was calculated to be similar in magnitude to the stepwise radical process. On the other hand, the barrier associated with cationic concerted rearrangement (**124** to **127a**) was calculated to be as low as 47.4 kJ mol^{-1} and the overall reaction was calculated to be exothermic by 26.8 kJ mol^{-1} . The ionization energy of the substrate-derived radical to generate a carbocation was calculated to be 7.01 eV , suggesting that its oxidation to generate the substrate-derived carbocation ought to be facile. These calculations led the authors to suggest that a concerted rearrangement mechanism involving a carbocation constitutes a more viable pathway for carbon skeleton rearrangement in tropane alkaloid biosynthesis.



Scheme 2.35 High-level quantum chemistry calculations using G3(MP2)-RAD considered the concerted rearrangement *via* radical and cationic pathways.¹⁰⁰

2.8 Fluorine as a mechanism probe

2.8.1 Effect of fluorine on the aromatic ring.

Fluorine is the most electronegative element (4.0) in chemistry. Its size is similar to that of hydrogen (the Van der Waal's radii of fluorine: 1.35 Å; of hydrogen: 1.1 Å). Thus, the substitution of hydrogen by fluorine in an organic compound does not change the steric profile of a molecule, although the electronic profile alters significantly. For aromatics, the replacement of hydrogen by fluorine is deactivating but *ortho*-, *para*-directing in electrophilic substitution reactions. This can be explained by donation of the fluorine lone pairs into the aromatic ring system stabilising reaction intermediates. The short C-F bond and similar size of the orbitals result in a maximal *p*- π interaction. However, the powerful inductive effect of fluorine which acts most strongly at the *ortho*-position relative to the *para*- position, leads to a preference for *para*- substitution in electrophilic substitution reactions of fluorobenzene.¹⁰¹

2.8.2 Effect of fluorine on benzylic carbocation and radical intermediates.

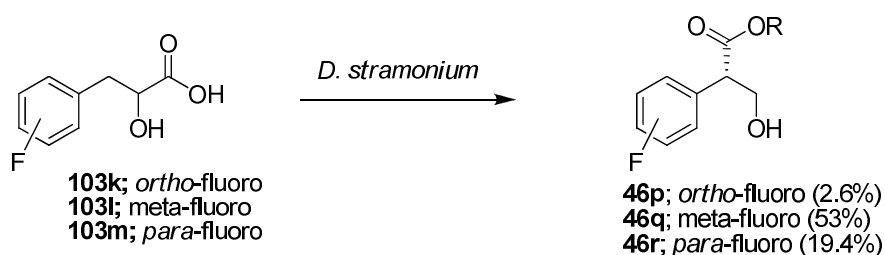


Benzylic carbocations are stabilised by *ortho*- and *para*- fluoro substituents *via* donation of electron density from fluorine lone pairs into the aromatic π -system with a significant stability preference of *para*- over *ortho*-. *Meta* substitution does not significantly stabilise the benzylic carbocation since electron resonance and inductive effects are small.¹⁰¹⁻¹⁰³ Unfortunately, there is very little in the literature on the influence of aryl fluorine substituents and their ability to stabilise a benzylic radical. It appears that a *meta*-fluoro and *para*-fluoro substituents will destabilise the benzylic radical although the effect is small.¹⁰⁴⁻¹⁰⁷ There was no information prior to this research, on the behavior of a 2-fluoro substituents on the stability of a benzylic radical. Theory calculations on the effect of fluorine on benzylic intermediates will be discussed in Section 2.10.1.

2.8.3 The use of fluorine as a mechanism probe in tropane alkaloids biosynthesis

O'Hagan and co-worker¹⁰⁸ have demonstrated that 2'-, 3'- and 4'- fluorophenyl-DL-lactic acids (**103k**, **103l**, **103m**) were esterified *in vivo* with tropine in *D. stramonium* root cultures. The resultant fluorinated littorines were then isomerised to the corresponding fluorinated hyoscyamines (**46p**, **46q**, **46r**). If the mechanistic intermediate is a carbocation, then *ortho*-, *meta*-, and *para*-fluorinated littorines would be anticipated to rearrange in the order 4F-littorine > 3F-littorine > 2F-littorine.

However, interestingly, the efficiency of the conversion of fluorolittorine to fluorohyoscyamine was in the order 3'-F-lit > 4'-F-lit >> 2'-F-lit. Clearly, the inductive effect of fluorine is greatest at the *ortho*- position, but the result did not indicate a progressive inductive effect for substitution at the other sites and surprisingly the *meta* fluorine was most efficient. So it was suggested that different binding affinities of the isomers to the isomerase may also contribute to this overall activity profile, and this complicates a straightforward analysis of the results.



Scheme 2.36 The conversions of *rac*-fluorophenyllactic acids in *D. stramonium* showed the production of fluoroaryhyoscyamines with the *in vivo* conversions (at day 17) shown in parentheses.¹⁰⁸

2.9 Aims of the study

The availability of a cytochrome P₄₅₀ enzyme involved in hyoscyamine biosynthesis from *H. niger* in Prof. Patrick Covello's laboratory, provided an opportunity to explore the mechanism of the rearrangement of littorine to hyoscyamine. Therefore the objectives of this study were:

1. Preparation of the *rac*-(**45e-g**) and enantio-enriched fluorolittorines (*S*-**45e-g**, *R*-**45e-g**).
2. Preparation of enantio-enriched dideuterio-littorines (*S*-**45h**, *R*-**45h**) for measurement of the kinetic isotope effect of this intriguing rearrangement reaction.

3. DFT calculations on fluorine substituent effects particularly exploring the stability of benzylic carbocations and radicals. (Carried out by David J. Tozer at Durham University)

4. The enzyme assays carried out in Prof. Covello's laboratory in Canada.

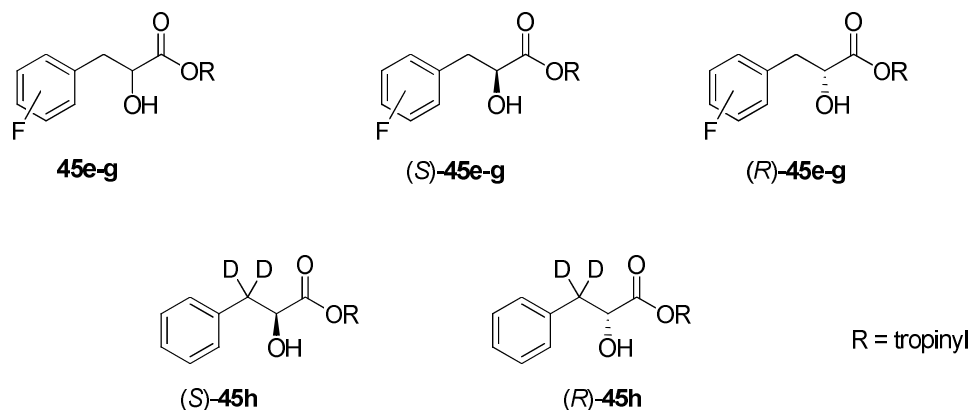


Figure 2.7 Target molecules to explore the mechanism of hyoscyamine formation.

2.10 Results

2.10.1 DFT study on the relative energies of *ortho*-, *meta*- and *para*- fluorobenzyl radicals and cations.

The results from the DFT calculations carried out at Durham University are shown in Table 2.1. These were consistent with the literature in that fluorine can stabilise a benzylic carbocation. The stability order of fluorobenzyl carbocations is *para*- > *ortho*- > *meta*- as expected. Calculation of the relative stabilities of benzyl radicals revealed that there was no significant difference in relative energy between these three isomers, but it appears that the *meta*-fluorobenzyl radical is the most stable, with the *para*- and *ortho*- only a little higher in energy. In this case the stability order appears as *meta*-, *ortho*-, and *para*-. Interestingly, the relative energy differences for the three benzyl radicals are small compared with that of the benzylic cations (and anions). Additionally, the relative stability of the *ortho*-, *meta*- and *para*- fluorobenzyl anions

was calculated and showed the reverse order, but similar in magnitude to that of the fluorobenzylic cations. The calculated C-F bond lengths are shown in Table 2.1 and are consistent with the conjugative interactions expected for fluorine. Generally, the C-F bond lengths are shorter in the cations and longest in the anions, and the C-F bond length in the *p*-fluorobenzylic cation is shortest, consistent with its conjugative stabilising influence.

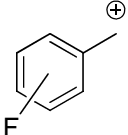
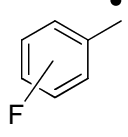
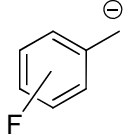
Fluorobenzylic intermediate	Relative energy (kcalmol ⁻¹)	C-F bond length (Å)
Carbocation <i>ortho</i> - <i>meta</i> - <i>para</i> - 	+3.57 +6.75 0.00	1.308 1.319 1.301
Radical <i>ortho</i> - <i>meta</i> - <i>para</i> - 	+0.20 0.00 +0.15	1.345 1.347 1.344
Anion <i>ortho</i> - <i>meta</i> - <i>para</i> - 	+2.18 0.00 +5.67	1.376 1.377 1.385

Table 2.1 The relative energies of *o*-, *m*- and *p*- fluorobenzylic cations, radicals and anions. Relative values from DFT calculations are indicated in kcal mol⁻¹. Calculated C-F bond lengths are in shown (Å). (D. J. Tozer, the University of Durham)

2.10.2 Ionisation potentials

The ionization energies required for the oxidation of the benzylic radicals to benzylic carbocations was also calculated (Table 2.2). The oxidation potentials of the *o*-, *m*- and *p*- fluoro radicals to carbocations is predicted to be facile since the oxidation potentials were found to be low at 7-7.35 eV. The potential trend reflects the relative stability of the fluorobenzylic carbocations. Clearly, the electronegative fluorine exerts a small but significant effect on the oxidation potential relative to the non-fluorinated benzyl case.

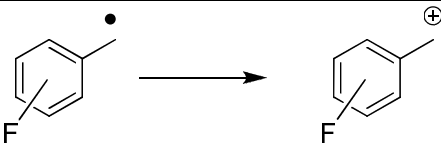
fluorobenzylic radical	Ionization energy (eV)
<i>ortho</i> - <i>meta</i> - <i>para</i> - 	7.21 7.35 7.05
benzylic radical	7.09

Table 2.2 Ionisation potentials (eV) for the oxidation of benzyl radicals to cations. (D. J. Tozer, the University of Durham)

2.10.3 Synthesis

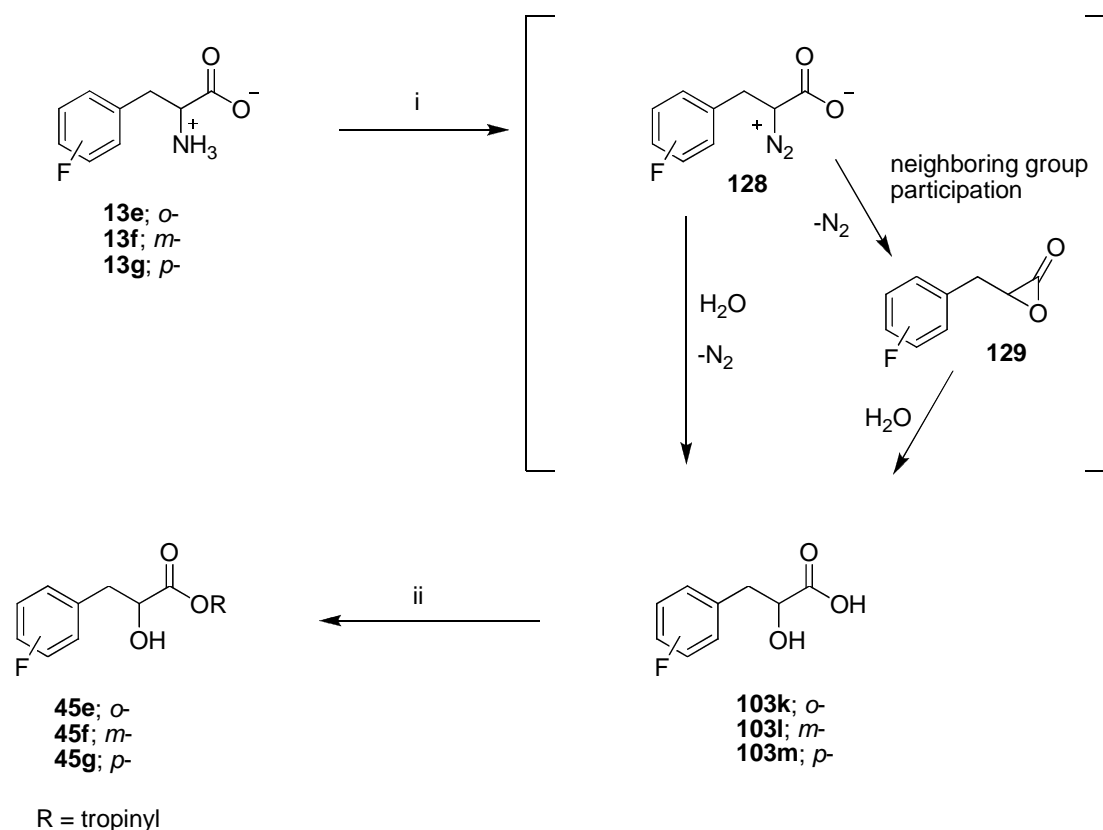
2.10.3.1 The synthesis of *rac*-fluorolittorines

2.10.3.1.1 Synthesis of *rac*-2', 3' and 4'-fluorophenyllactic acid (**103k**, **103l**, **103m**)

Preparation of *rac*-fluorophenyllactic acids followed the method previously described by Wong.¹⁰⁹ Starting from commercially available *rac*- 2', 3' and 4'-fluorophenylalanines (**13c**, **13d**, **13e**), each isomer of fluorophenyllactic acid (**103k**, **103l**, **103m**) was synthesized in a racemic form *via* a diazotization reaction, with sodium nitrite and concentrated hydrochloric acid (Scheme 2.37). The mechanism proceeds with the formation of a diazonium ion (**128**) which decomposes to release N₂, assisted by the neighboring carboxylate group, to form an intermediate α -lactone (**129**). Nucleophilic attack by water then opens the α -lactone to generate *rac*-fluorophenyllactic acid. In all cases the yields were low (20-32%). This was the consequence of incomplete reaction, as starting material was recovered in the individual reactions.

2.10.3.1.2 Synthesis of *rac*-2', 3' and 4'-fluorophenyllactoyl tropines (*rac*-fluorolittorine)

Following a previously described procedure,⁵¹ each of the *rac*-fluorophenyllactic acids was mixed intimately with tropine under a stream of dry HCl gas at 135 °C. The crude product was then worked-up and purified by preparative TLC and extracted into methanol to give each of the three isomers of *rac*-fluorolittorine.



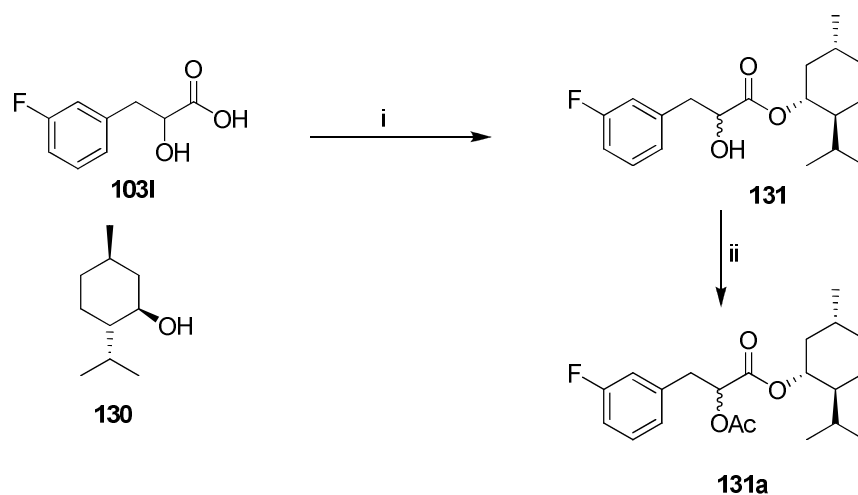
Scheme 2.37 Synthesis of *rac*-fluorolittorines (**45e**, **45f**, **45g**): *Reagents and conditions*: i) cHCl, NaNO₂, H₂O, 20-32% ; ii) tropine, dry HCl_(g), 20-48%.

2.10.3.2 The synthesis of enantio-enriched 2', 3', and 4'fluorolittorines (*S*-**45e-g**, *R*-**45e-g**)

2.10.3.2.1 Resolution by preparation of (-)-menthyl derivatives (**131**)

The resolution of the racemic esters was explored by derivatisation with (-)-menthol. Such an approach has been successfully applied to the resolution of atrolactic and α -hydroxy- β -phenylpropionic acids.¹¹⁰ The acids and (-)-menthol (**130**) were esterified by acid catalysed reaction and the diastereoisomeric mixture was then worked-up and each diastereoisomer was purified by means of crystallization. Accordingly the *m*-fluorophenyllactic acid (**103l**) was mixed with (-)-menthol and heated at 120 °C,

periodically passing a stream of dry HCl gas over the reaction. After work-up, the product was analysed by ^1H and ^{19}F NMR spectroscopy. The ^{19}F NMR spectrum exhibited two sets of *ddd* at -113.9 ppm and -114.2 ppm in a 1:1 ratio as shown in Figure 2.8. Despite considerable effort crystallisation and conventional chromatography failed to separate the diastereoisomers. An attempt to reduce the polarity of the stereoisomers was made by acetylation of the 2'-OH group using acetic anhydride, however the mixture still co-eluted in all common eluting systems.



Scheme 2.38 Synthesis of menthyl *m*-fluorophenyllactate (**131**) and α -acetyl derivative (**131a**). *Reagents and conditions:* i) dry HCl (g), 120 °C, 6 h; 73.2% ii) Ac₂O, dry pyridine, overnight, 89%.

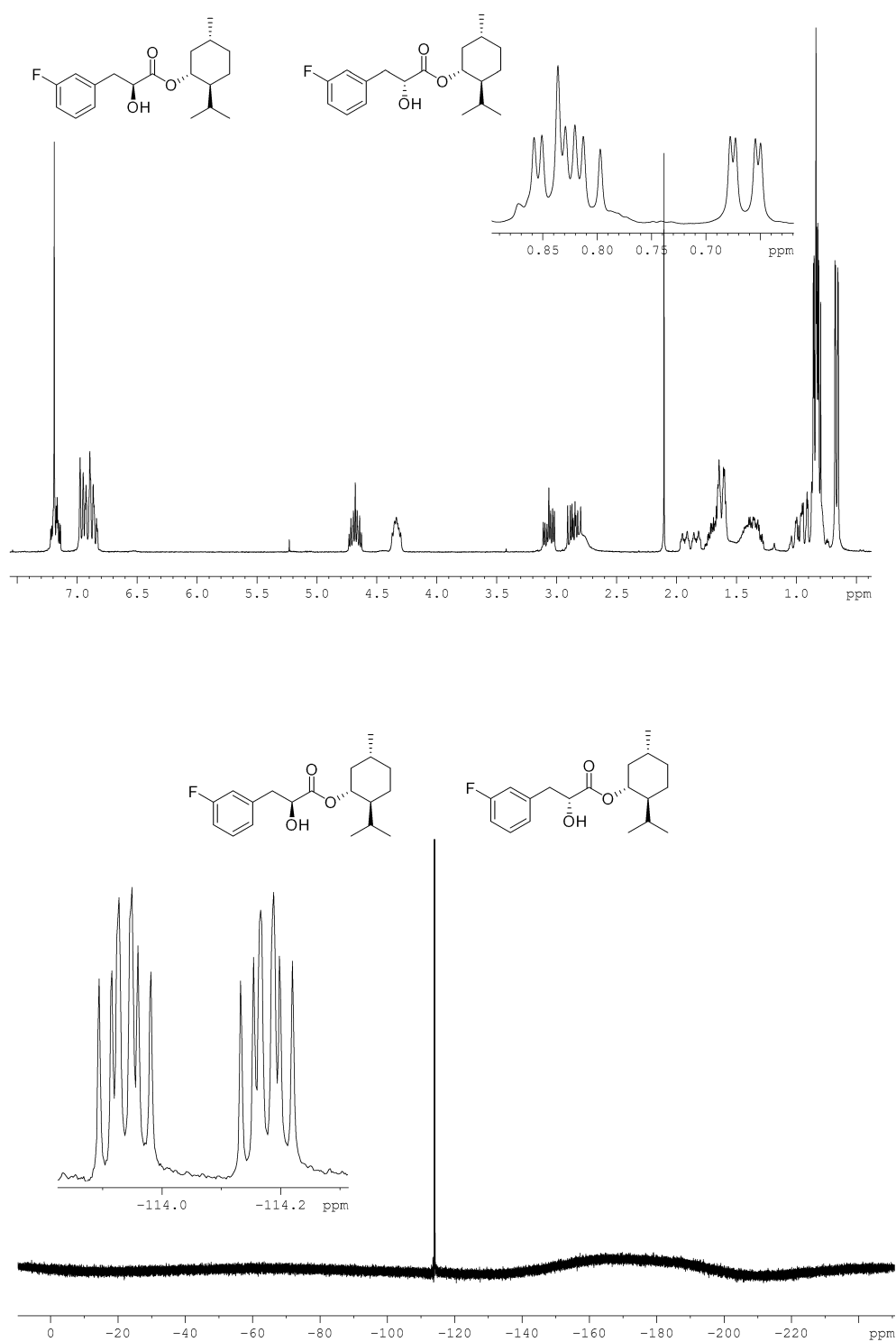


Figure 2.8 ^1H and ^{19}F NMR of menthyl *m*-fluorophenyllactate (131).

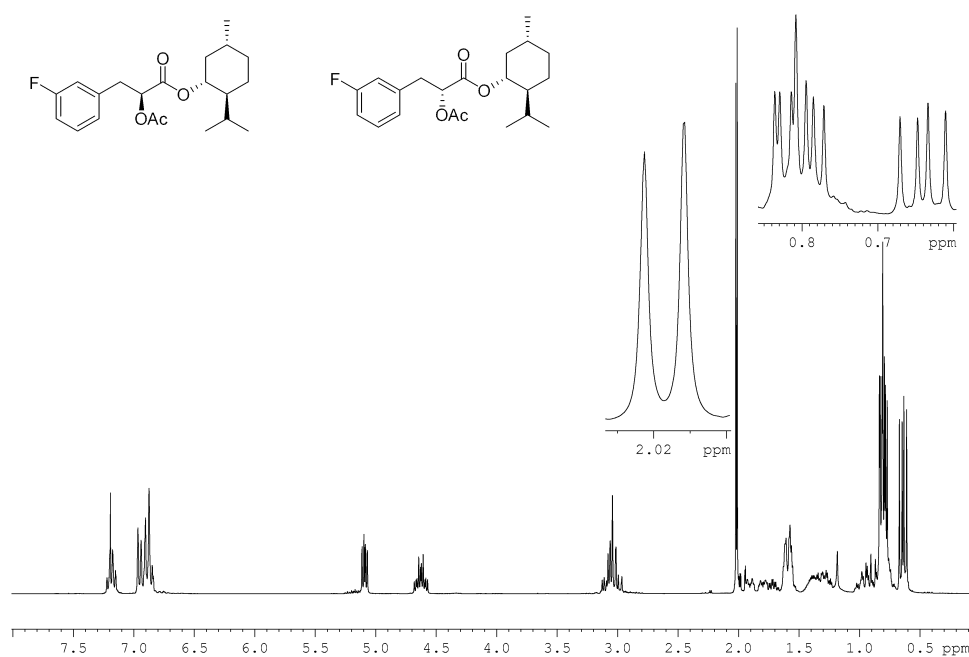
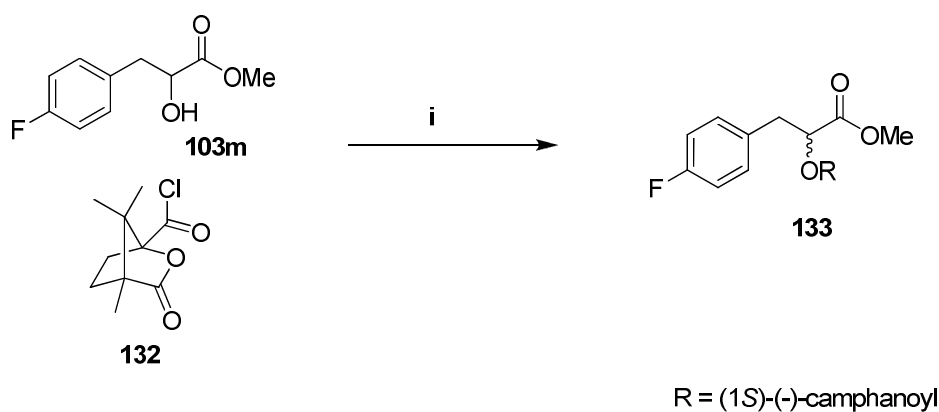


Figure 2.9 ^1H NMR of α -acetyl menthyl *m*-fluorophenyllactate (**131a**).

2.10.3.2.2 (1*S*)-(-)-Camphanoyl chloride derivative (**133**)

Due to the failure to separate the menthyl ester stereoisomers, another chiral resolving reagent, (1*S*)-(-)-camphanoyl chloride was explored. The free carboxylate of *rac*-*p*-fluorophenyllactic acid (**103m**) was first esterified with methanol and was then treated with (1*S*)-(-)-camphanoyl chloride (**132**) in dry pyridine/DCM. The reaction went smoothly and was completed within 2 hrs. After work-up, the ^{19}F and ^1H NMR (Figure 2.10) clearly indicated a mixture of two diastereoisomers. Unfortunately, however, separation of these mixtures (**133**) by chromatography was also unsuccessful.



Scheme 2.39 Synthesis of (-)-camphanoyl methyl fluorophenyllactate (**133**).

Reagents and conditions: i) dry pyridine, DCM, 0 °C, 90%.

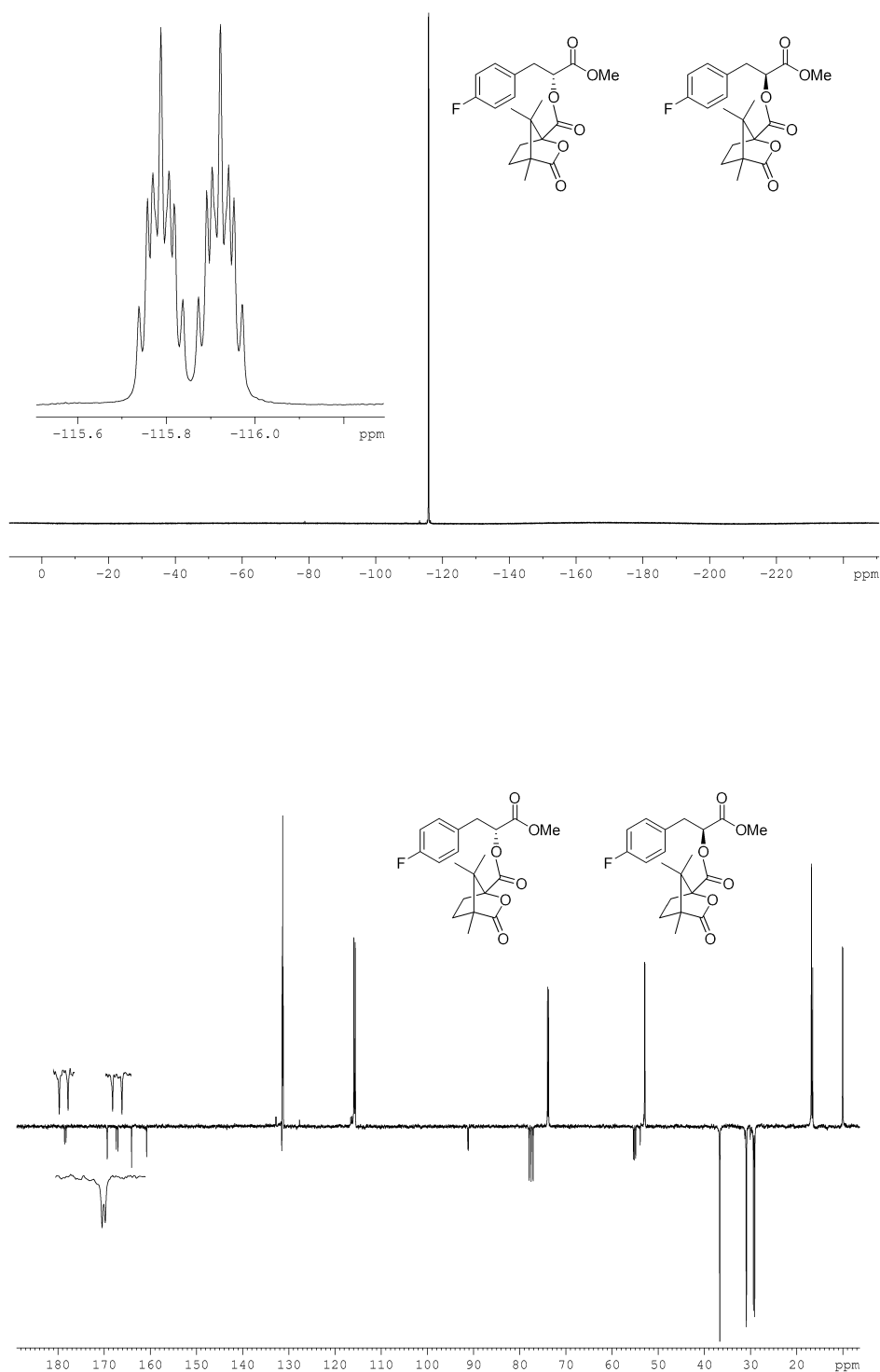


Figure 2.10 ^{19}F NMR and ^{13}C NMR of camphanoyl methyl fluorophenyllactate (**133**). The carbonyl signals in the lower ^{13}C -NMR spectrum are expanded to show the pair of signals.

2.10.3.2.3 Resolution by preparation of amides

Attention then turned to the generation of amide diastereoisomers for this resolution. There are various coupling methods to form an amide bond in the literature.¹¹¹ Carbodiimide-mediated coupling has been regularly used since first introduced into peptide synthesis by König and Greiger.¹¹² A disadvantage of the DCC/HOBt (**134/136**) coupling system is that the urea by-product of the reaction is highly insoluble in most solvents and can cause purification problems. So, new additives such as EDCI (**135**), HBTU (**137a**), and TBTU (**137b**) have been developed. The urea by-products in these cases are most easily removed by an acid wash during the work-up.

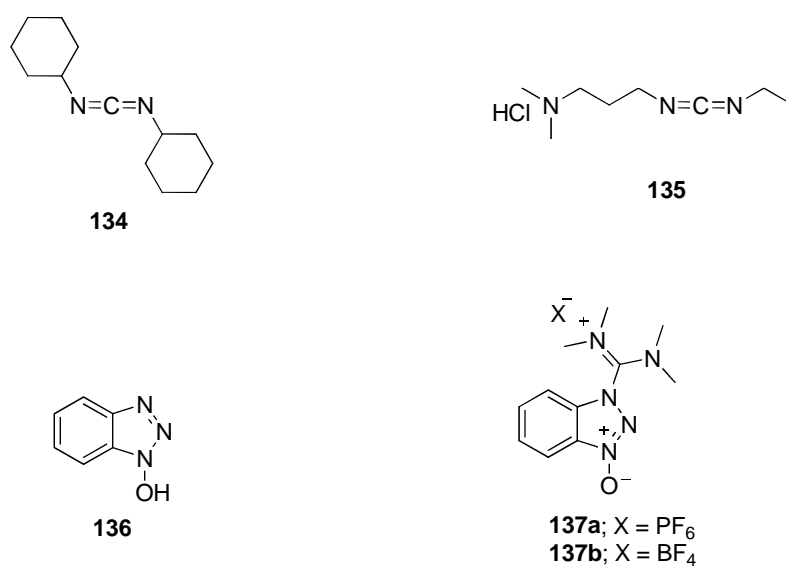
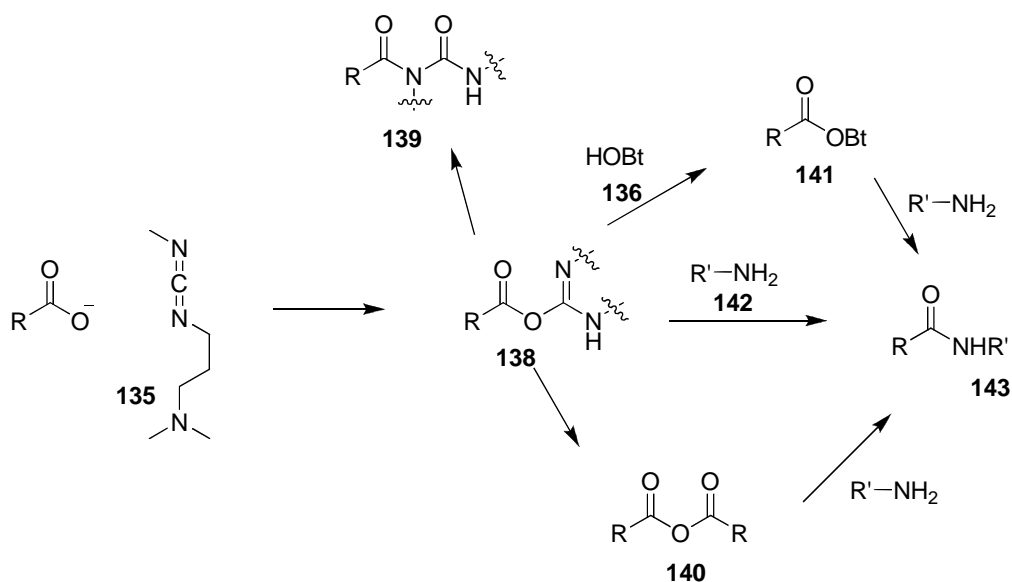


Figure 2.11 Common coupling reagents for amide formation.¹¹³

The accepted mechanism (Scheme 2.40) for the coupling reaction involves a rapid reaction of the carboxylate group with the carbodiimide to generate a highly reactive *O*-acylisourea (**138**). This intermediate can undergo either aminolysis to give a

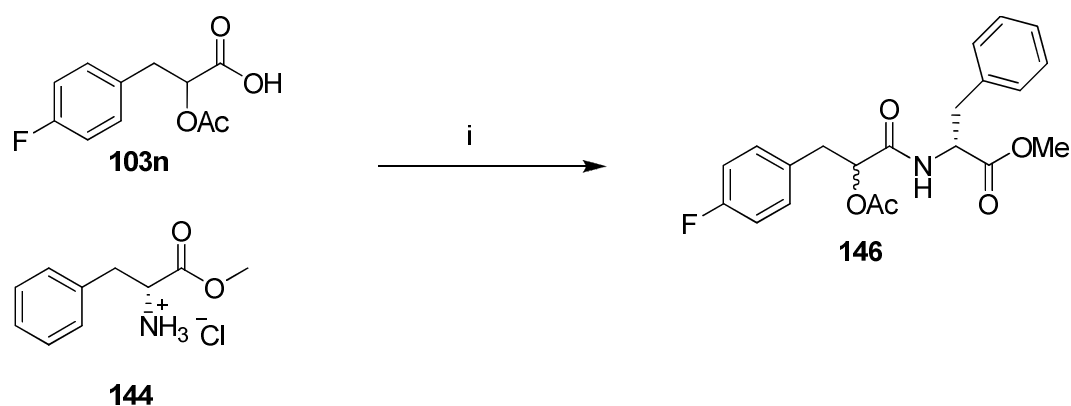
corresponding amide (**143**) or it can react with another acid to form a symmetric anhydride (**140**). The highly reactive *O*-acylisourea can isomerise to form a stable *N*-acylurea (**139**) *via* an intramolecular acyl transfer. This side reaction may compete with aminolysis, lowering the yield of the reaction and causing purification problems. However this difficulty can be avoided by the addition of HOBt (**136**) which is able to react rapidly with the *O*-acylisourea to form an acyl-OBt adduct (**141**). This adduct has been reported to exist in two isomeric forms where both isomers react with amine to form an amide.^{114, 115}



Scheme 2.40 A general mechanism for peptide coupling.¹¹¹

2.10.3.2.4 Resolution by D-phenylalanine methyl ester hydrochloride (**144**) and (*S*)-phenylethylamine (**145**)

D-Phenylalanine methyl ester hydrochloride (**144**) and (*S*)-phenylethylamine (**145**) were chosen to explore the methodology. According to a procedure previously described by M. Shuller,¹¹⁶ (*RS*)- α -acetyl-*p*-fluorophenyllactic acid (**103n**) was treated with D-phenylalanine methyl ester hydrochloride (**144**), using HOBt/EDCI·HCl as coupling system. The amide (**146**) was obtained in high yield after work-up, although the diastereoisomers could not be separated by chromatography. The ¹H NMR (Figure 2.12) analysis of the purified diastereoisomers showed well separated signals for the –OMe groups at 3.61 ppm and 3.64 ppm. Interestingly the –NH protons also appeared as two sets of doublets at 6.29 ppm and 6.37 ppm with the same coupling constant (6.9 Hz). The ¹⁹F NMR spectrum (Figure 2.12) revealed two sets of *dddd* at -116.2 and -116.4 ppm. The individual diastereoisomers could not be assigned.



Scheme 2.41 Preparation of diastereoisomers amide **146**. *Reagents and conditions:* i) DMF, NMM, HOBt, EDCI, CHCl₃, rt, overnight, 75%.

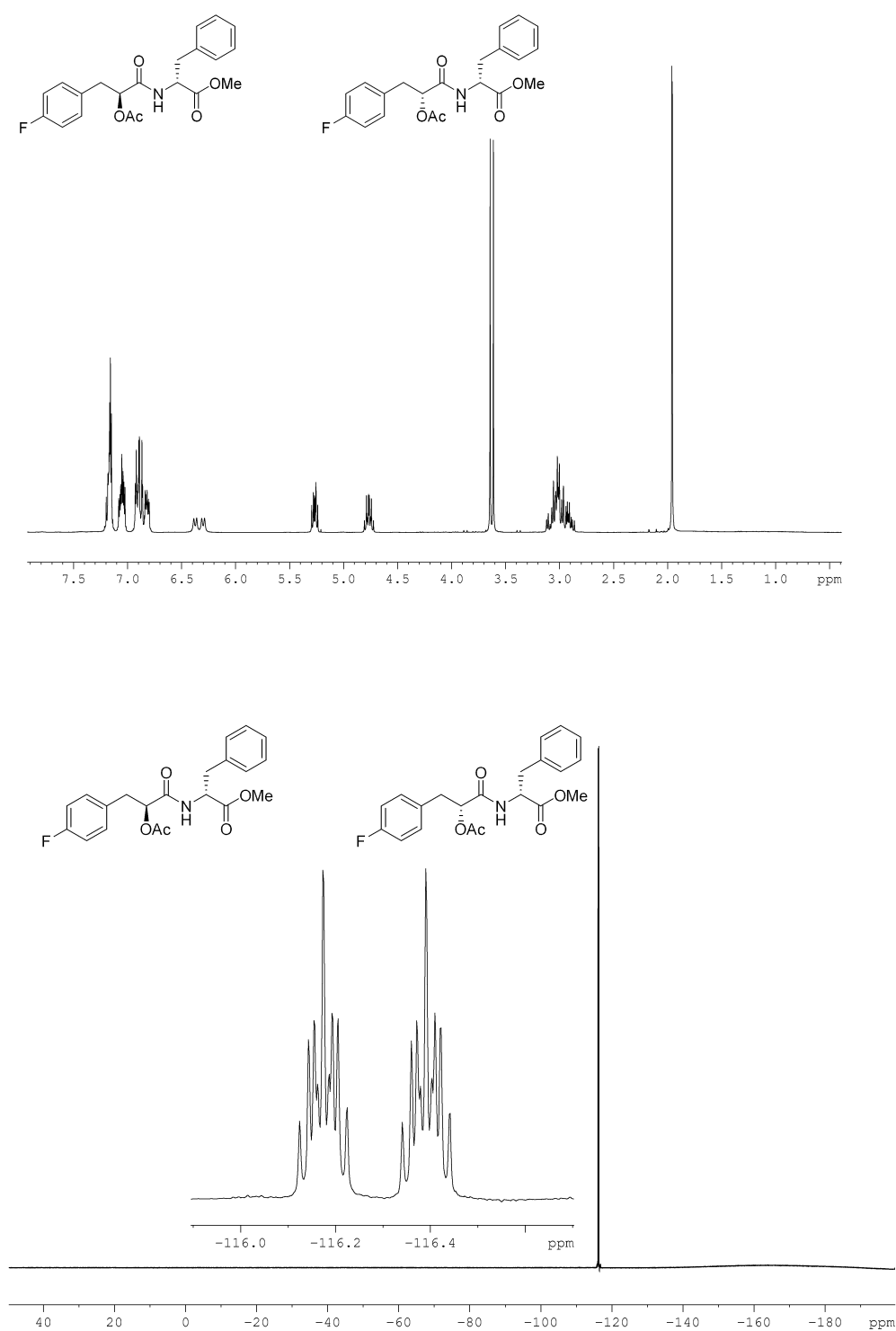
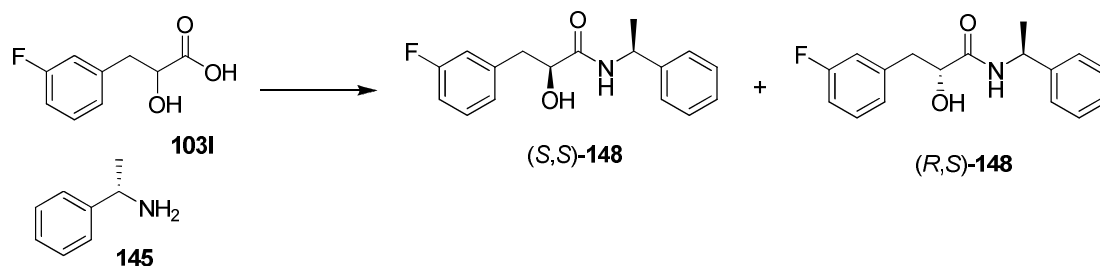


Figure 2.12 ^1H and ^{19}F NMR of the α -acetyl diastereoisomers of **146**.

In a similar manner to that previously described, (*RS*)- α -acetyl-*p*-fluorophenyllactic acid (**103n**) acid was also coupled with (*S*)-phenylethylamine (**145**) and the amide product was obtained in high yield. Attempts to separate these diastereoisomers by chromatography were however unsuccessful. In a continuous search for a system to separate the isomers, the free α -hydroxy acids were explored. According to the standard coupling procedure, *m*-fluorophenyllactic acid (**103l**) was treated with (*S*)-phenylethylamine (**145**) and the amide product was obtained with a good conversion. This time the diastereoisomers showed a promising resolution by chromatography in a system of 80% EtOAc/20% cyclohexane. Subsequent purification over silica gel eluting with 60% EtOAc/40% cyclohexane finally led to a successful separation of (*S,S*)-**148** and (*R,S*)-**148** as single stereoisomers.



Scheme 2.42 Resolution of *m*-fluorophenyllactic acid (**103l**). *Reagents and conditions:* HOBt, EDCI·HCl, CHCl₃, DMF, rt, overnight, (*S,S*)-**148**; 46.8% and (*R,S*)-**148**; 44%.

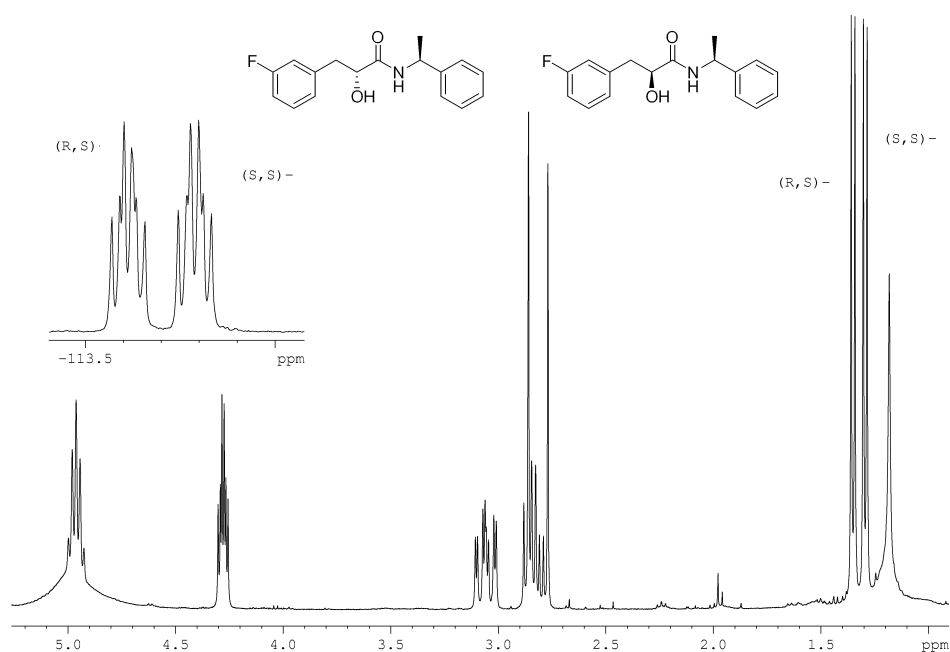
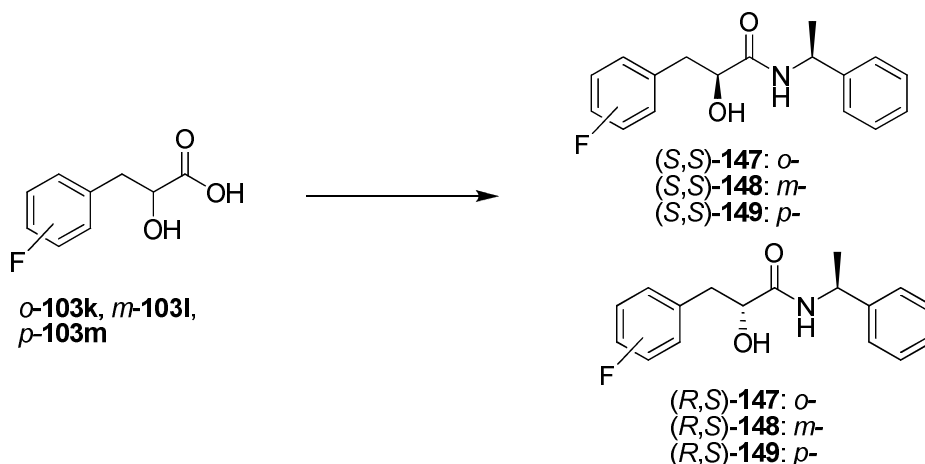


Figure 2.13 ^1H and ^{19}F NMR of the amide diastereoisomers of **148**.

This protocol proved to be very straightforward and was general for all three of the isomers. Thus the *ortho*-, *meta*-, and *para*- fluorophenyllactic acid stereoisomers were prepared as single stereoisomers of each enantiomeric series, by converting the corresponding *rac*-fluoroaryl acids into these amide diastereoisomers, followed by chromatographic separation.



Scheme 2.43 Resolution of *rac*-fluoroaryl acids by amide formation. *Reagents and conditions:* (*S*)-phenylethylamine, HOBT, EDCI·HCl, CHCl₃, DMF, rt, overnight, 84-91%.

The absolute configuration of the amides was assigned by X-ray crystallographic analysis. Re-crystallisation of all six enantio-enriched fluoroaryl amides from the hexane/DCM system yielded two crystals which were suitable for X-ray structure analysis. Separation of *o*-fluoroaryl amides (**147**) afforded a crystal of the higher polarity diastereoisomer. This emerged with the (*S,S*)- absolute configuration. A crystal of the lower polarity amide was obtained from *p*-fluoroaryl amides (**149**) and this indicated an absolute configuration as (*R,S*)-**149** after X-ray structure analysis. Thus, it appeared that the (*S,S*)-fluoroaryl amide eluted first in these two cases using a 60%EtOAc/20%cyclohexane solvent system. The absolute stereochemistry of the *meta*- fluoroarylamides was assumed relative to these two experimentally determined cases.

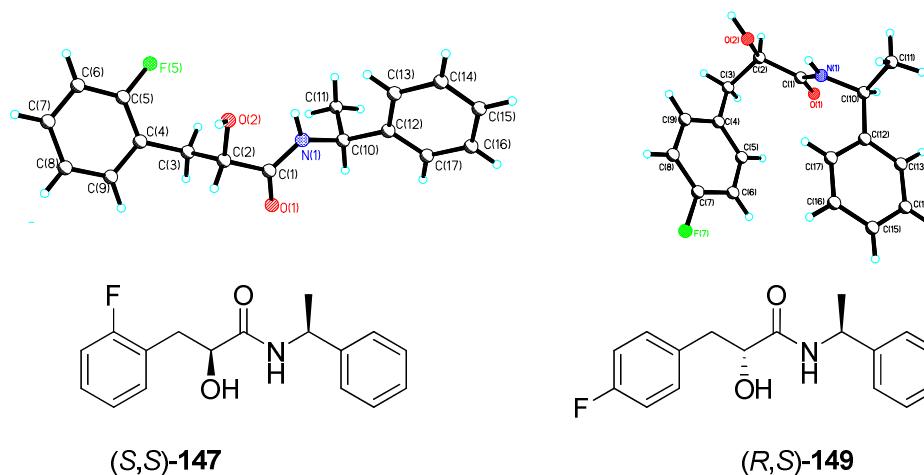
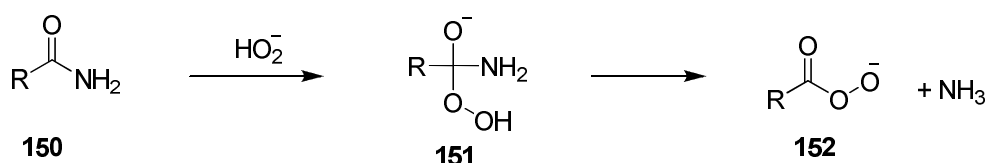


Figure 2.14 X-ray crystal structures of (*S,S*)-*o*-fluoroaryl amide (*S,S*-**147**) and (*R,S*)-*p*-fluoroaryl amide (*R,S*-**149**) were used to confirm the absolute stereochemistry.

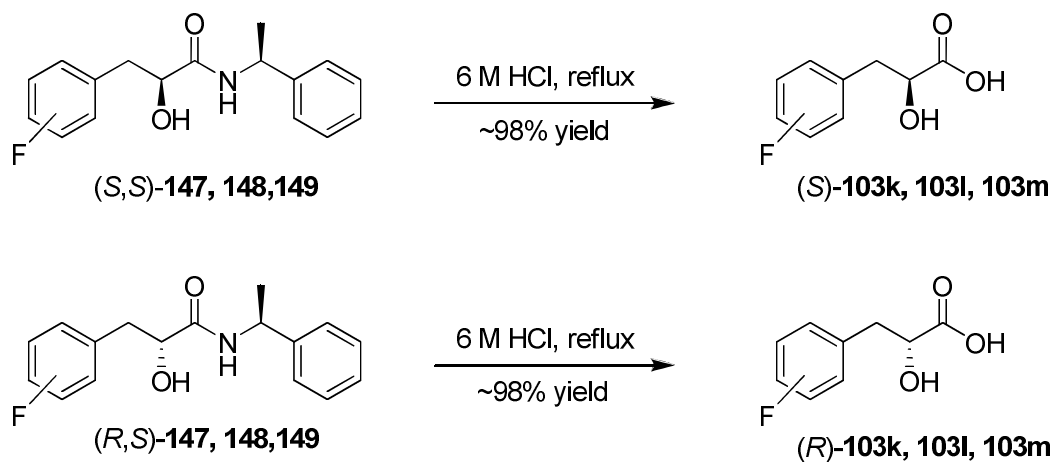
2.10.3.2.5 Hydrolysis of the enantio-enriched fluoroarylamides

In order to obtain the enantio-enriched fluoroaryl acids, amide hydrolysis conditions were explored. Initially, *m*-fluoroarylamide (*S,S*-**148**) was heated under reflux with 2M H₂SO₄ for 24 hrs, but only starting material was recovered. Treatment with 2M HCl under reflux for 20 h also gave only recovery of starting material. A basic hydrolysis with 10% NaOH was also unsuccessful. Interestingly, a facile and mild hydrolysis of amides has been reported^{117, 118} involving sodium peroxide (Na₂O₂). This method efficiently converted both primary and secondary amides to their corresponding acids along with small amounts of decarboxylated products. The mechanism has been suggested as shown in Scheme 2.44. Therefore *m*-fluoroarylamide (*S,S*-**148**) was treated with aq. solution of Na₂O₂ at 50 °C for 2 hrs. Unfortunately, these conditions proved unsuccessful with only starting material recovered.



Scheme 2.44 Proposed mechanism for hydroperoxide mediated hydrolysis.^{117, 118}

Failure to hydrolyse the amides under the above conditions forced a re-evaluation of acidic hydrolysis. Fortunately, with 6M HCl and under refluxing condition for 24 hrs, the hydrolysis of the *m*-fluoroarylamide (*S,S*-**148**) was achieved in high yield after work-up. Purification of the product by re-crystallisation from EtOAc/hexane gave the carboxylic acid as a white solid. All six of the fluoroaryl acid stereoisomers were recovered by this method and in good yields (> 98%).



Scheme 2.45 Hydrolysis of enantio-enriched fluoroarylamides yielded enantio-enriched fluoroaryl carboxylic acids in good yields (>98%).

2.10.3.2.6 Determination of enantiomeric excess of the resolved fluorophenyllactic acids (*S*-103k, 103l, 103m) and (*R*-103k, 103l, 103m)

It was important to determine the enantiomeric excess (ee) of the resolved fluorophenyllactic acids, particularly due to the harsh hydrolysis conditions. Since, the diastereoisomers of fluoroaryl amides exhibited distinguishable signals by ^1H and ^{19}F NMR (Figure 2.13), the free fluoroaryl acids were subjected to enantiomeric assay by re-forming the amides with (*S*)-phenylethylamine. Therefore, the crude reaction products after recoupling the fluorophenyllactic acids with (*S*)-phenylethylamine were subject to ^1H or ^{19}F NMR analysis. The %ee in each case was calculated from the integration of signals from each diastereoisomer.

For instance, the enantio-enriched (*R*)-**103l** and (*S*)-**103l** isomers were independently coupled with (*S*)-phenylethylamine (**145**) and the crude amides were directly subjected to ^1H NMR spectroscopy. The crude (*S,S*)-amide **148** showed a single doublet for the methyl group at 1.36 ppm (J 6.92 Hz) and no apparent signal for the other diastereomer appeared (Figure 2.15, A), indicating that the diastereoisomeric purity of this amide was >95% de. Thus, the enantiomeric excess of the starting (*S*)-*m*-fluorophenyllactic acid was at least >95%. The crude (*R,S*)-amide **148** product also showed a doublet at 1.39 ppm (J 6.92 Hz) and the diastereoisomeric purity was also calculated to be >95%ee (Figure 2.15, B). This procedure was re-evaluated by mixing equal amounts of the crude (*S,S*)-amide **148** and crude (*R,S*)-amide **148**. The resultant ^1H NMR spectrum clearly showed two doublets for the methyl groups at 1.35 and 1.28 ppm (Figure 2.16). According to this protocol, the enantiomeric excesses for the rest of the fluorophenyllactic acids was shown to be >95%ee.

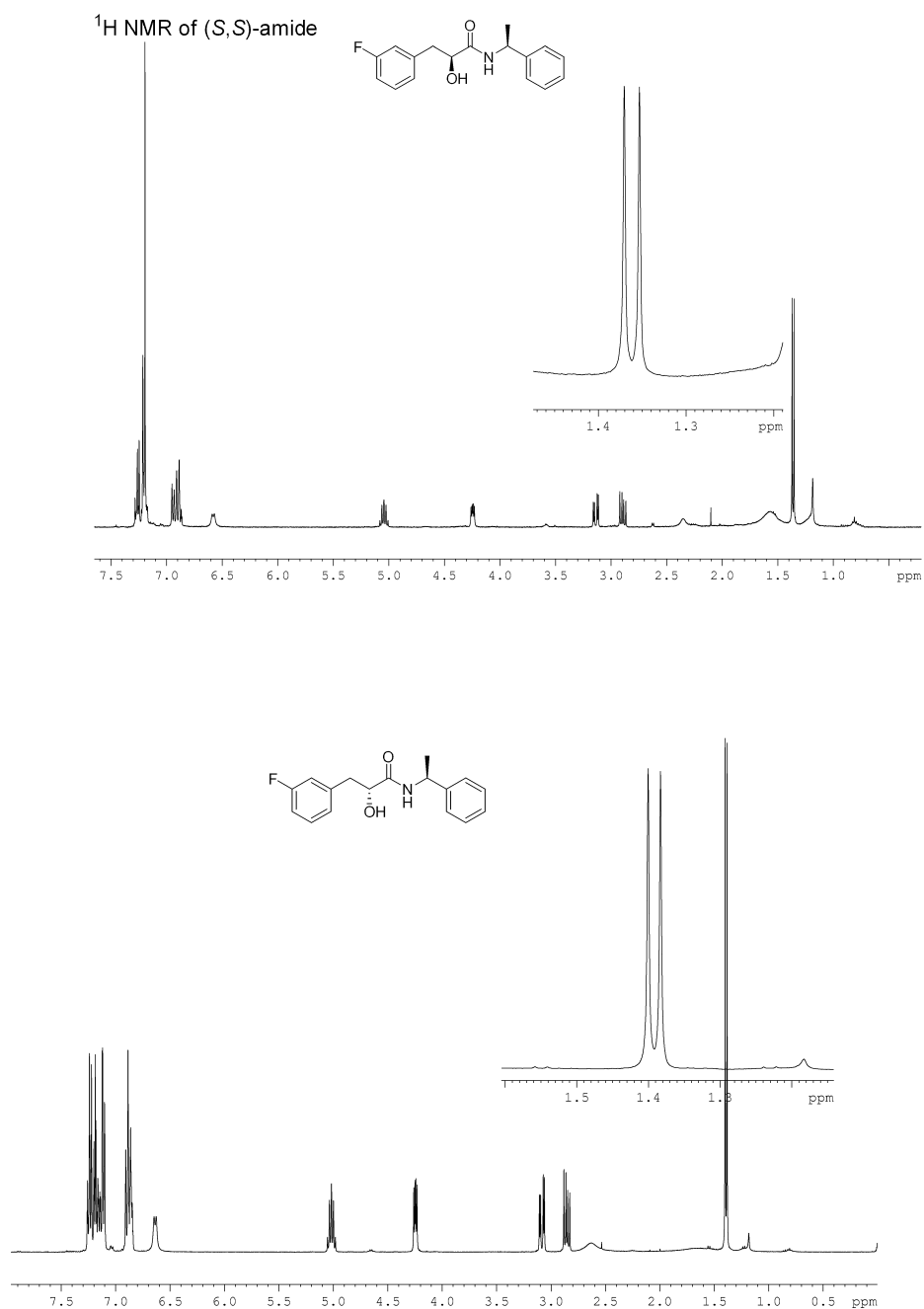


Figure 2.15 ¹H NMR of the crude coupled product of; A) (S,S)-*m*-fluoroarylamide **148** and B) (R,S)-*m*-fluoroarylamide **148**.

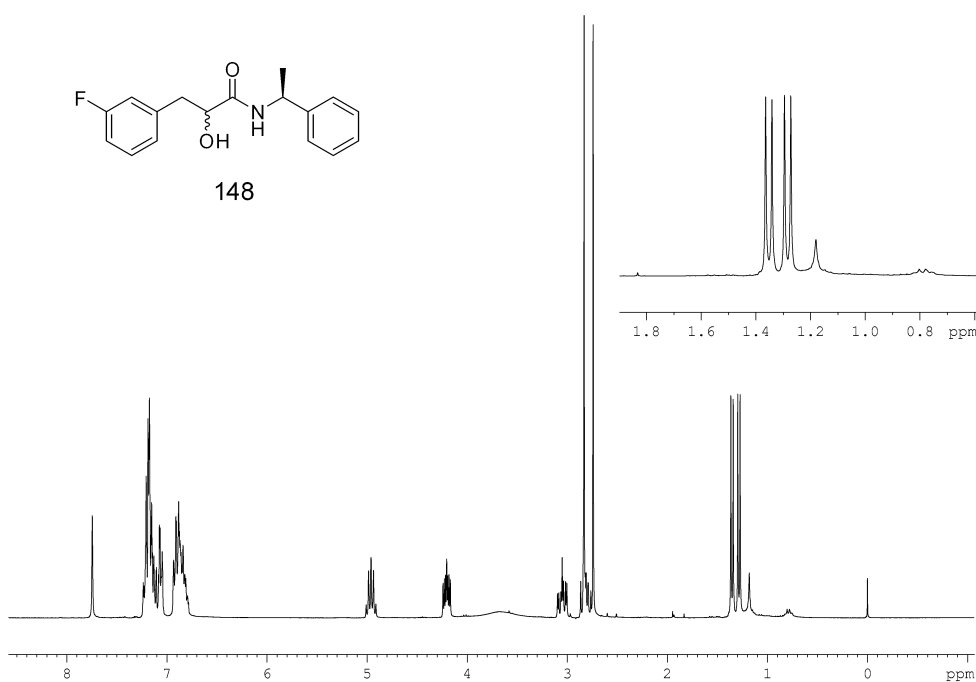
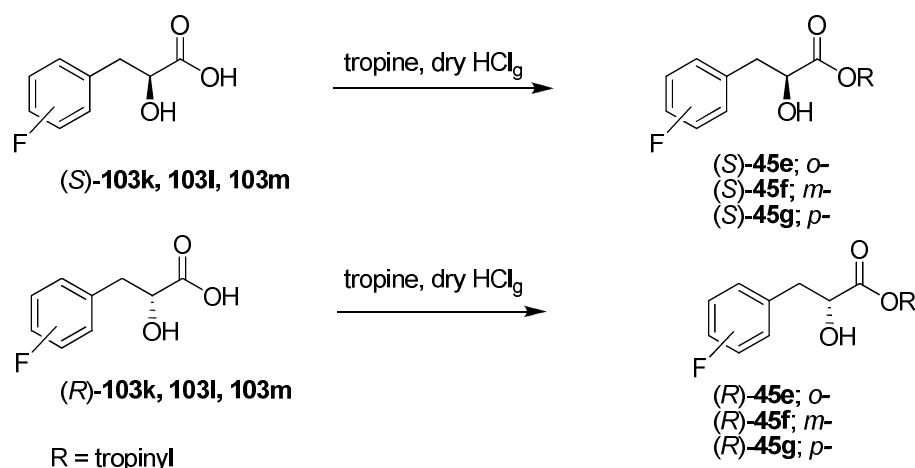


Figure 2.16 ¹H NMR obtained by mixing the crude (*S,S*)-**148** and (*R,S*)-**148**.

2.10.3.2.7 Preparation of enantio-enriched fluorolittorines.

In a similar manner to that previously described for the preparation of *rac*-fluorolittorines, the individual fluoroaryl acid diastereoisomer were coupled to tropine as previously described in the preparation of *rac*-fluorolittorines. This gave preparative samples of enantio-enriched (>95% ee) fluorolittorines in moderate yields (32-51%) after chromatography.



Scheme 2.46 The synthesis of enantio-enriched fluorolittorines.

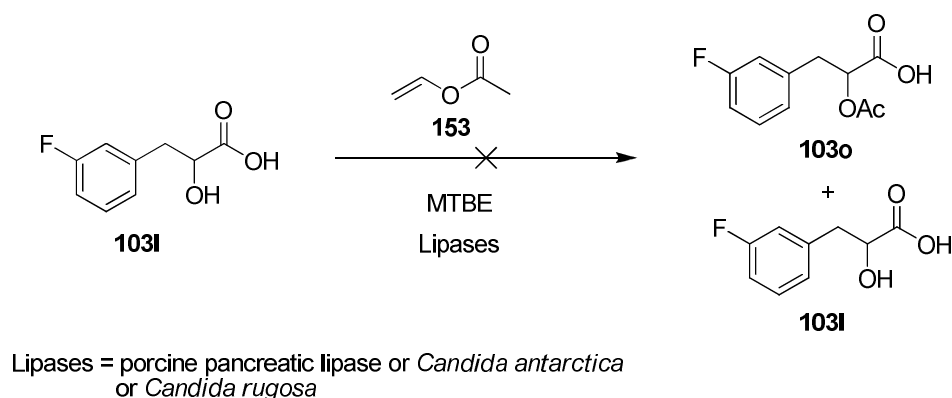
2.10.3.3 Enzymatic resolution

During the resolutions described in the previous section, a lipase resolution strategy was also expanded as a measure to resolve the fluorophenyllactic acids into their individual enantiomers.

Lipases (triacylglycerol acylhydrolases EC 3.1.1.3) are probably the most frequently used enzymes in the kinetic resolution of racemic alcohols and carboxylic acids. The wide substrate range of lipases and the ability of such processes to be carried out in organic solvents make lipases particularly attractive for the preparation of enantiomerically pure substances. Either dry powder enzymes or enzymes in an immobilized form have been widely employed. The kinetic resolution can be successful if the two enantiomers react with the enzyme at substantially different rates. The theoretical yield of such a kinetic resolution is 50% and high optical purity of organic substances can be achieved if conditions and enzymes are optimised.¹¹⁹

Three commercially available lipase enzymes were explored in this study. These were the porcine pancreatic lipase (PPL), the *Candida rugosa* lipase, and the *Candida*

antarctica lipase. Initially the transesterification of *rac*-fluorophenyllactic acid was performed. Vinyl acetate (**153**) has been used as acyl donor in such reactions and methyl *t*-butyl ether (MTBE) is a solvent of choice. This system has an advantage since the vinyl alcohol formed as a by-product is then tautomerised to acetaldehyde, making the reaction irreversible. Following a previously described protocol,¹²⁰ *rac-m*-fluorophenyllactic acid (**103l**) was treated separately with PPL, *Candida antarctica* (fraction-B, CAL-B), and *Candida rugosa* using MTBE as the solvent. The reactions were stirred at ambient temperature for 4 days. Following the reactions by TLC or ¹H NMR spectroscopy did not indicate any conversion after 4 days, so the reaction was stopped and the starting material was recovered.



Scheme 2.47 Attempted kinetic resolution by lipase enzymes.

Alternatively, lipases are regularly used to perform kinetic resolutions of racemates by ester hydrolysis.¹²¹ Accordingly the *rac-m*-fluorophenyllactic acids were treated with acetic anhydride to obtain the 2-acetyl ester derivatives and then these were used as resolution substrates. The racemate acetates were dissolved in acetone and each was treated separately with PPL, CAL-B, or *Candida rugosa* in a phosphate buffer (pH 7) with shaking at 30 °C. The progress of the reactions was monitored by TLC and ¹H

NMR spectrum (Figure 2.17). This showed that hydrolysis occurred only with the PPL.

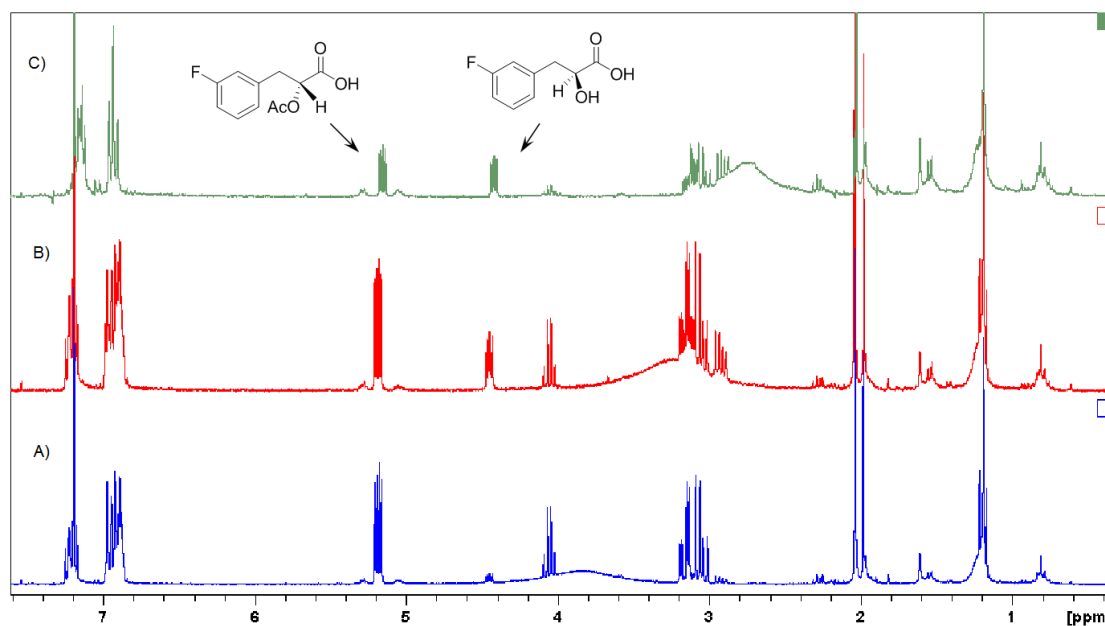
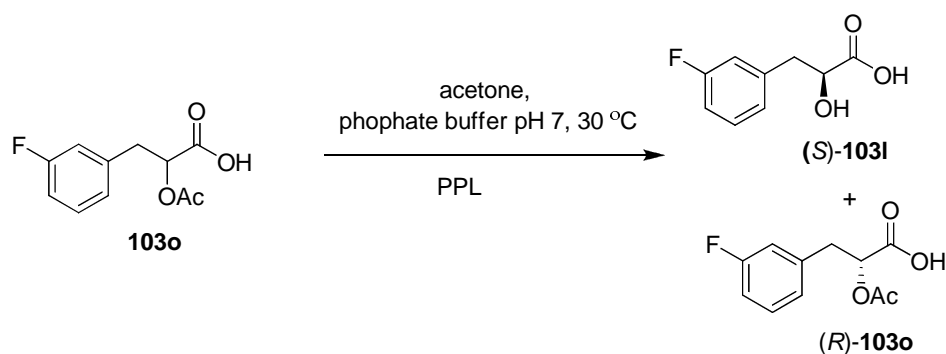


Figure 2.17 The ^1H NMR of the kinetic resolution of acetyl *m*-fluorophenyllactic acid recorded at; A) 6h, B) 12h and C) 20 h.

After 20 hrs, the reaction was quenched by centrifugation of the enzyme. Careful chromatography ($\times 3$) gave the resultant carboxylic acid but with a low recovery. Crystallization of the resultant stereoisomer from EtOAc/hexane gave colourless needles and the X-ray crystal structure is shown in Figure 2.18. However the absolute configuration could not be assigned. Instead, the unreacted enantiomer was coupled with (*S*)-phenylethylamine to give another suitable crystal for structure analysis after re-crystallisation from DCM/hexane. The resultant X-ray structure is shown in Figure 2.18 which revealed the absolute configuration of the amide as (*R,S*)-**148a**. Therefore, the PPL hydrolyses the (*S*)-enantiomer in preference to the (*R*)-enantiomer. This result is consistent with the previously demonstrated kinetic resolution of *rac*-phenyllactic.¹²¹ Due to the difficulty encountered in the purification process, the

resolution of the hydroxy acids was achieved by the chemical resolution method as described in the previous section 2.10.3.2.4.



Scheme 2.48 Kinetic resolution of (*RS*)- α -acetyl-*m*-fluorophenyllactic (**103o**) acid by porcine pancreatic lipase.

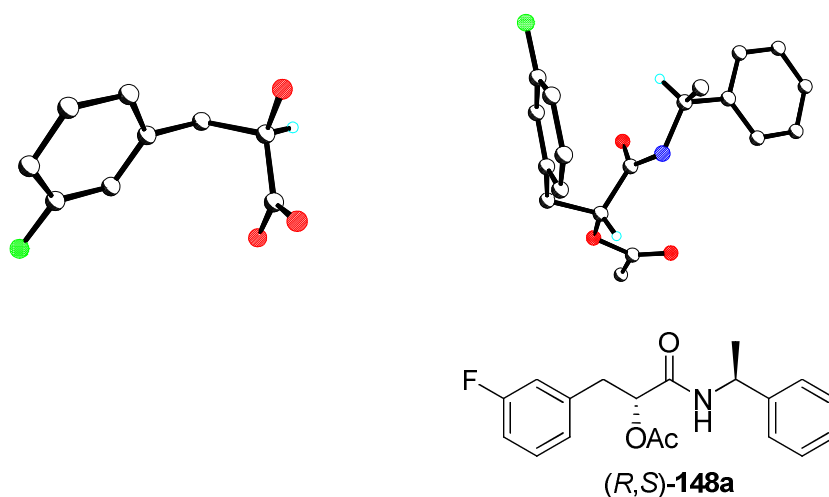
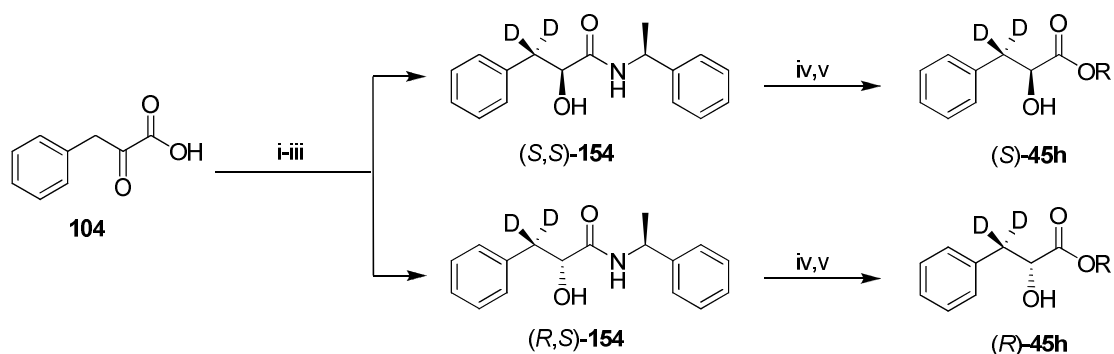


Figure 2.18 X-ray crystal structure of (*S*)-*m*-fluorophenyllactic acid and an amide derivative of (*R*)- α -acetyl-*m*-fluorophenyllactic acid (**103o**).

2.10.3.4 The preparation of enantio-enriched (*S*)-[3',3'-²H₂]-littorine (*S*-45h) and (*R*)-[3',3'-²H₂]-littorine (*R*-45h)

rac-[3,3-²H₂]-Phenyllactic acid had previously been prepared by N. C. J. E. Chesters in the research group in 1995.¹²² In order to prepare an enantio-enriched [3,3-²H₂]-phenyllactic acid, that method was employed again. According to the literature, the commercially available phenylpyruvate (**104**) was dissolved in D₂O and the pH

adjusted to 11. The reaction was kept stirring at ambient temperature. The progress of the deuterium exchange was monitored by ^1H NMR. The benzylic hydrogen completely disappeared indicating an efficient exchange process. The reaction mixture was then neutralised by careful addition of D_2SO_4 . The resultant phenylpyruvic acid was treated directly with NaBH_4 to afford the *rac*-[3,3- $^2\text{H}_2$]-phenyllactic acid. Subsequently *rac*-[3,3- $^2\text{H}_2$]-phenyllactic acid was treated with (*S*)-phenylethylamine to afford (*R,S*)- and (*S,S*)-amides (12-14% in three steps) such that the individual diastereoisomers could be separated. Hydrolysis (6 M HCl) then gave the desired enantio-enriched (*S*)- and (*R*)- [3,3- $^2\text{H}_2$]-phenyllactic acids ((*S*)-**103i** and (*R*)-**103i**, 95 and 96%). Again the enantiomeric purity of the acids was assayed in the same manner as that for the preparation of the enantio-enriched fluoraryl acids. The diastereoisomeric purity was again found to be >95%. Finally, the free acids were coupled with tropine to yield (*S*)-[3',3'- $^2\text{H}_2$]-littorine and (*R*)-[3',3'- $^2\text{H}_2$]-littorine (40 and 41%).



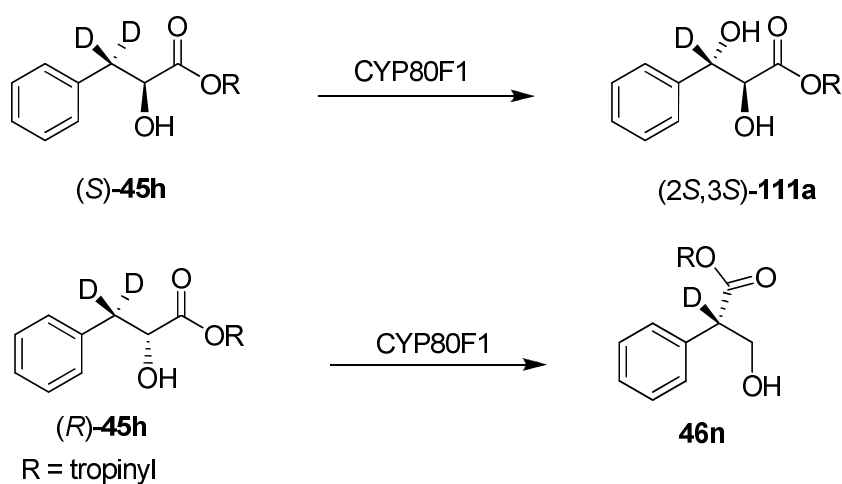
Scheme 2.49 Preparation of enantio-enriched (*S*)- and (*R*)-[3',3'- $^2\text{H}_2$]-littorine (*S*-**45h**, *R*-**45h**) from phenylpyruvic acid (**104**). *Reagents and conditions*: i) D_2O , K_2CO_3 ; ii) NaBH_4 ; iii) (*S*)-phenylethylamine, HOBt, EDCI, DMF, rt, 16h, 11.5% over 3 steps. iv) 6 M HCl, 100 °C, 24 h, 95%, > 95%ee; v) tropine, dry $\text{HCl}_{(\text{g})}$, 130 °C, 4 h, 40-41%.

2.10.4 Bioassay results

The bioassays were carried out by Dr. Darwin W. Reed in the laboratory of Dr. Patrick Covello at the Plant Biotechnology Institute, 110 Gymnasium Place, Saskatoon, SK, Canada, S7N 0W9.

2.10.4.1 Kinetic isotope effect study

The enantio-enriched (*S*)-[3',3'-²H₂] and (*R*)-[3',3'-²H₂]-littorines were assayed in incubations with CYP80F1 and the kinetic isotope effects on the hydroxylation and the rearrangement processes were evaluated by direct competitive and indirect comparative methods. The hydroxylation of (*S*)-[3',3'-²H₂]-littorine (*S*-**45h**) showed a similar primary KIE when measured by the different methods (2.55 and 2.86, Scheme 2.51 and Table 2.3). The KIE for the (*R*)-[3',3'-²H₂]-littorine (*R*-**45h**) from the direct competitive experiments could not be measured due to the enolisation of hyoscyamine aldehyde. For the rearrangement, the non-competitive experiments showed a KIE of 3.81, a value which agrees, within experimental error, with the hydroxylation results. The primary KIE's from these experiments confirm that the removal of the 3'-*pro-R* hydrogen is the rate limiting step for both rearrangement of (*R*)-littorine to hyoscyamine aldehyde and hydroxylation of the unnatural (*S*)-substrate at the 3'-position.



Scheme 2.50 The hydroxylation reaction of (*S*)-[3',3'-²H₂]-littorine (**R-45h**) and rearrangement reaction of (*R*)-[3',3'-²H₂]-littorine (**R-45h**) mediated by the CYP80F1.

Assay	Substrate	Reaction	KIE
CYP80F1	littorine		
Non-competitive	(<i>S</i>)-[3', 3'- ² H ₂]- 45h	3'-hydroxylation	2.86 (0.23)
	(<i>R</i>)- [3', 3'- ² H ₂]- 45h	hydroxylation/ Rearrangement	3.81 (1.1)
Competitive	(<i>S</i>)-[3', 3'- ² H ₂]- 45h	3'-hydroxylation	2.55 (0.14)

Table 2.3 KIE data for CYP80F1 incubations of (*S*)-[3',3'-²H₂] and (*R*)-[3',3'-²H₂]-littorine. Means and standard deviations (in parentheses) are indicated for five (non-competitive) and nine (competitive) replicates. (D. W. Reed and P. Covello; Plant Biotechnology Institute, 110 Gymnasium Place, Saskatoon, SK, Canada, S7N 0W9)

2.10.4.2 The enzyme assays of *rac*-2', 3' and 4'-fluorolittorines (**45e**, **45f**, **45g**) with CYP80F1.

The *rac*-fluorolittorines (**45e**, **45f**, **45g**) were incubated independently with CYP80F1 expressed in yeast microsomes. The natural substrate (*R*)-littorine was mostly converted to hyoscyamine aldehyde as expected and its fluorinated analogues also underwent rearrangement to the corresponding fluorohyoscyamine aldehydes (Figure 2.19). The fluorine substituents at the *ortho*, *meta*- and *para*- position did not have a significant effect on the production. All three isomers were almost equally rearranged to fluorohyoscyamine aldehyde. However their efficiencies were approximately half that of the non-fluorinated (natural) substrates.

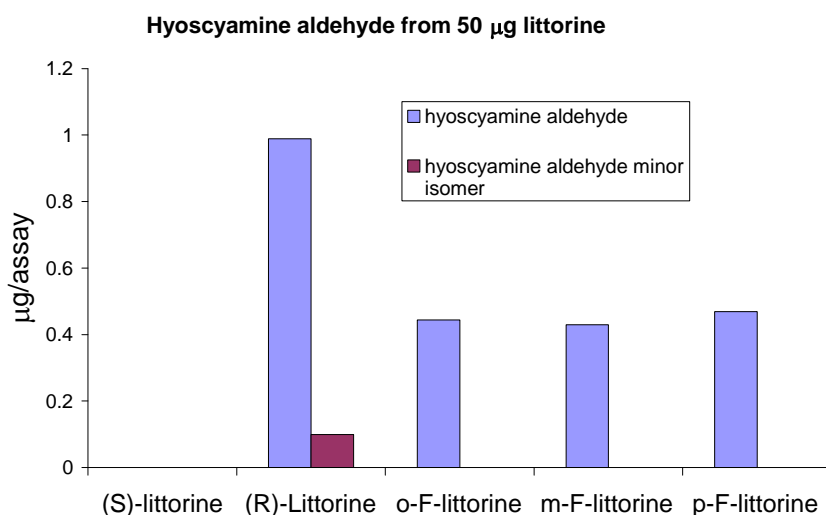


Figure 2.19 The incubation of *rac*-fluorolittorines with CYP80F1.

Interestingly, for the unnatural substrates, (*S*)-littorine was hydroxylated at the C3' position to release hydroxylittorine in the CYP80F1 assay as shown in Figure 2.20. The *rac*-fluorinated analogues produced the corresponding fluorinated 3'-hydroxylittorines. Clearly, the fluorine substituents appear to exert a clear effect on the efficiency of fluoro 3'-hydroxylittorine production. The *meta*- fluorine strongly

suppressed the hydroxylation reaction whereas the *ortho*- and *para*- fluorines showed a much higher efficiency. Nearly three times the level of fluorohydroxylittorine production was observed. As shown in the theory calculation (Table 2.1), the ability of *ortho*-/*para*- fluorine to stabilise benzylic intermediates, suggests a carbocation type mechanism operating in the hydroxylation reaction.

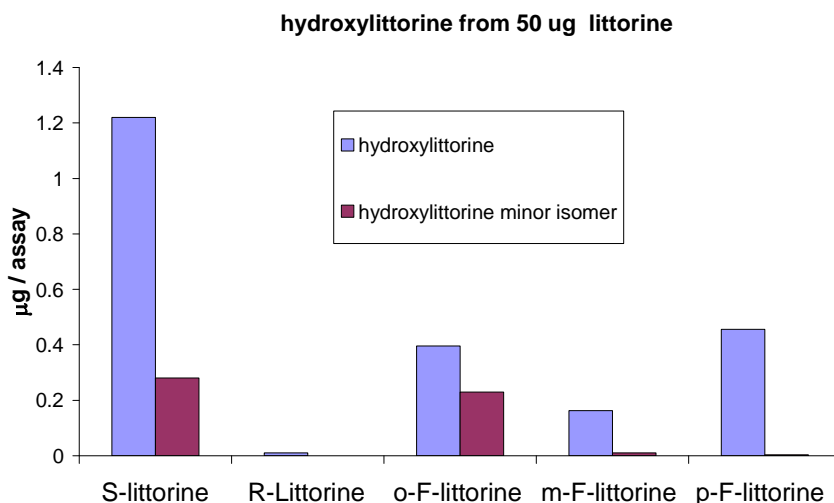
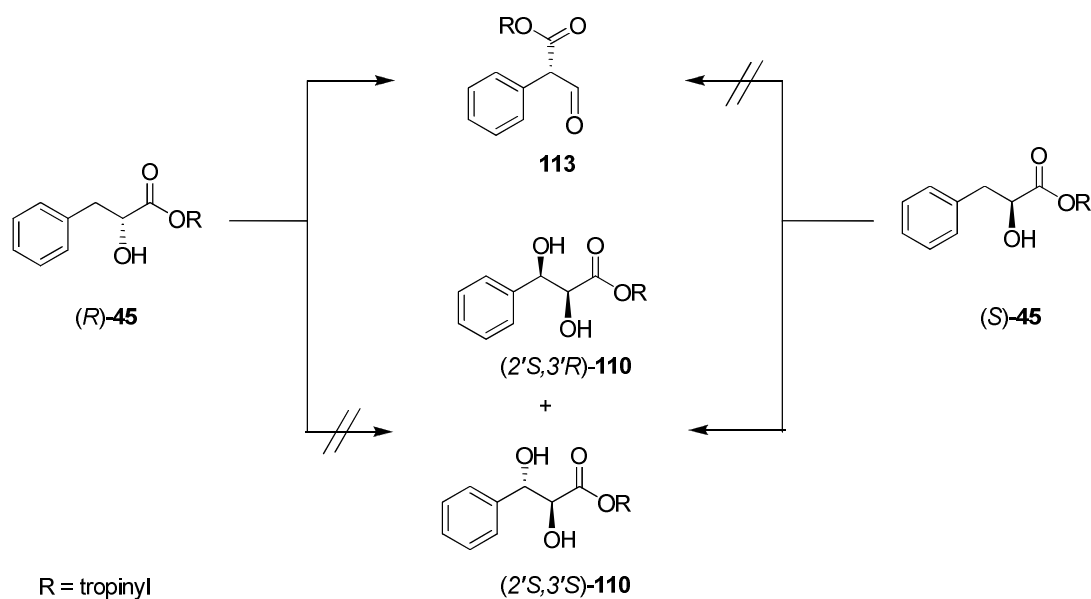


Figure 2.20 The incubation of *rac*-fluorolittorines with CYP80F1.

Clearly, the unnatural substrate, (*S*)-littorine is hydroxylated by CYP80F1 to give 3'-hydroxylittorine. The (*R*)-enantiomer rearranges to hyoscyamine aldehyde as summarized in Scheme 2.51.



Scheme 2.51 The products obtained from the feeding of (*R*)-littorine and (*S*)-littorine (**45**) to CYP80F1.

2.10.4.3 Assay on enantio-enriched (*R*)-fluorolittorines (*R*-**45e**, **45f**, **453g**)

Incubation of (*R*)-littorine and its arylfluorinated analogues with CYP80F1 revealed that not only the expected aldehydes (**113a-c**) were formed but also that hydroxylittorines (*R,S*-**113b-d**) were detected. With the natural substrate (Figure 2.21), hyoscyamine was predominantly formed along with only a trace of the 3'-hydroxylittorine as a minor product. For the *ortho/para*-(*R*)-fluorolittorines, however almost equal amounts of fluorohydroxylittorines and fluorohyoscyamine aldehydes were generated, indicating a significant competition between the hydroxylation and the rearrangement processes promoted by fluorine. On the other hand the *meta*-fluorine strongly suppressed the hydroxylation process and rearrangement to fluorohyoscyamine aldehyde was the primary process. This tendency to hydroxylation reflects the ability of the *ortho/para* fluorine substituents to stabilise a fluorobenzylic cation. For the rearrangement process, the *meta*-fluorine suppressed hydroxylation

relative to the rearrangement. This outcome is consistent with hydroxylation by a carbocation process, but rearrangement *via* a benzylic radical intermediate.

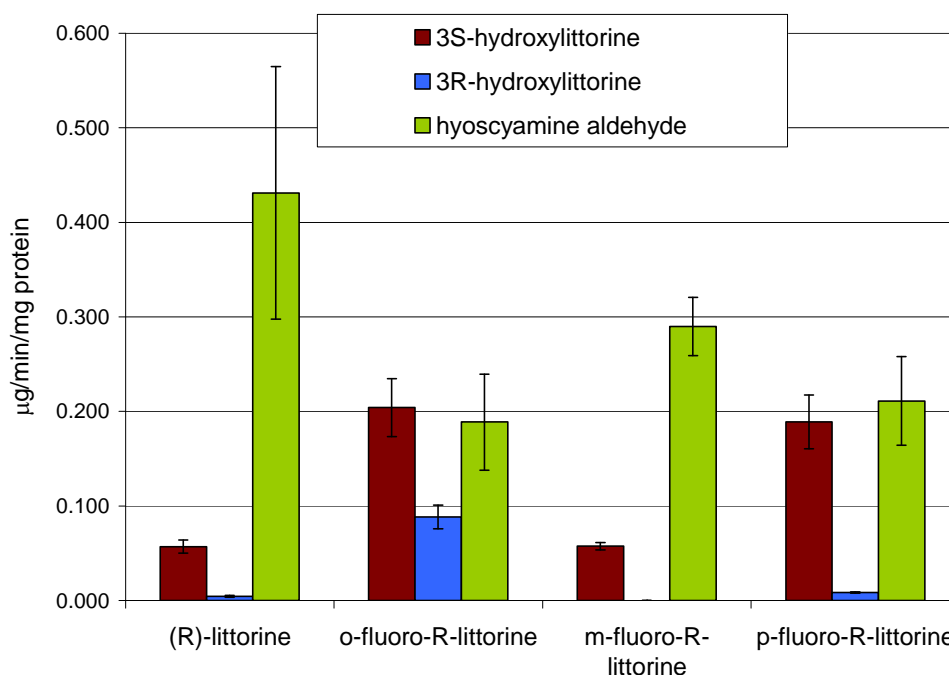
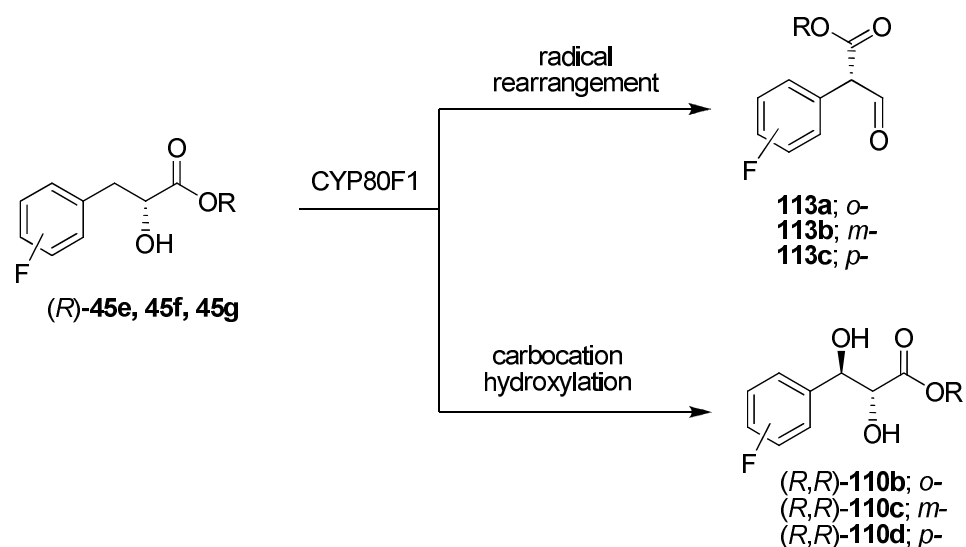


Figure 2.21 Production profiles after incubation of (*R*)-fluorolittorines with CYP80F1 expressed in yeast microsomes.



Scheme 2.52 The products from the bioassay suggest that hydroxylation occurs *via* a carbocation whereas rearrangement occurs *via* a benzylic radical.

2.10.4.4 Assays on the enantio-enriched (*S*)-fluorolittorines (*S*-45e, 45f, 45g)

Incubation of the unnatural (*S*)-littorines isomers and its arylfluorinated analogues with CYP80F1 showed similar productivity profiles to that of the *rac*-fluorolittorines (Figure 2.22). The (*S*)-littorine was predominantly hydroxylated to (2'*S*,3'*S*)-hydroxylittorine (2'*S*,3'*S*-110). The other diastereoisomer (2'*S*,3'*R*)-hydroxylittorine (2'*S*, 3'*R*-110) was only a minor product. Interestingly a trace of hyoscyamine aldehyde was also detected. For the (*S*)- fluorolittorine substrates, the fluorine substituents clearly exert a significant influence on the product profile. The *ortho/para*-fluorine promoted the hydroxylation reaction whereas the *meta*-fluorine suppressed hydroxylation. In particular, the *para*-fluorine was the most efficient substrate for hydroxylation and was surprisingly even better than the non-fluorinated substrate. Clearly, hydroxylation efficiency reflects the stability trend of the fluorobenzyl carbocations as indicated by the theory calculations (Table 2.1).

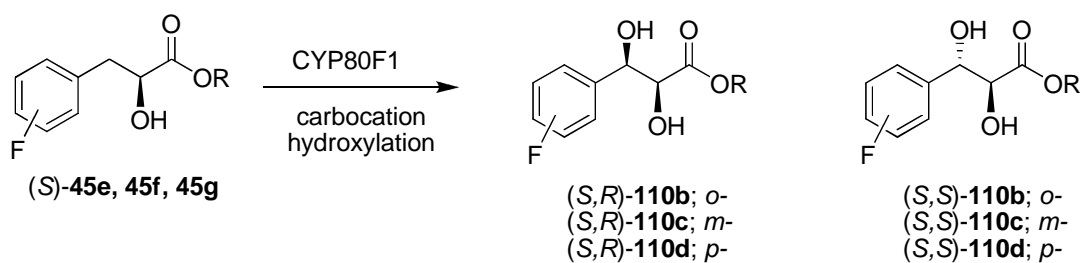
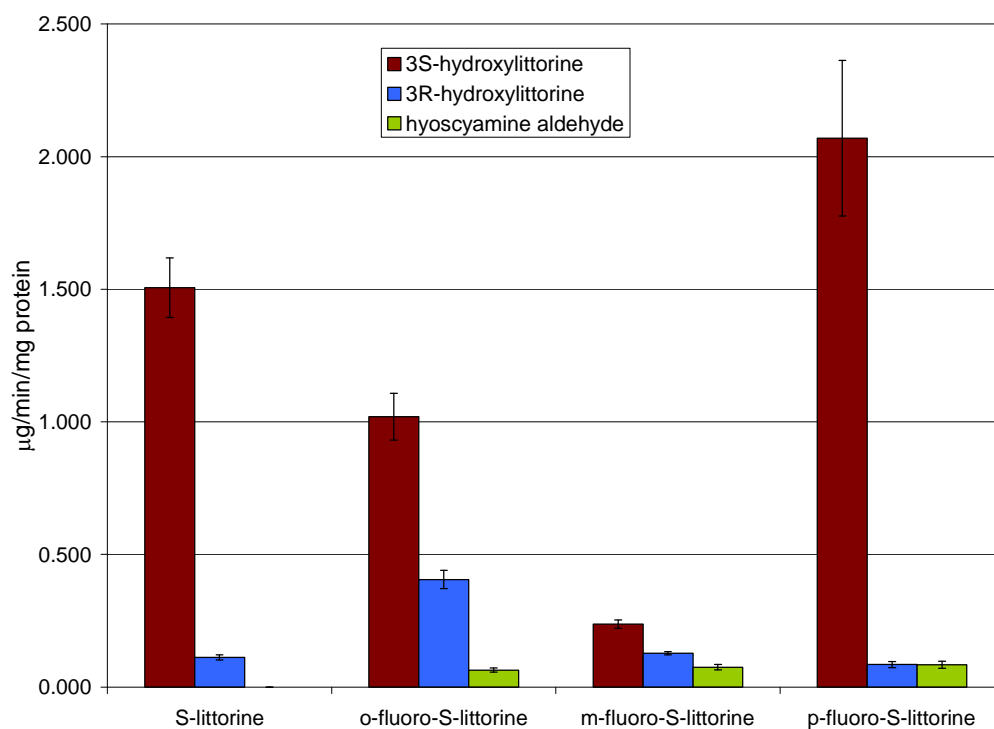


Figure 2.22 Production profiles from the incubation of (S)-fluorolittorines CYP80F1 suggest the hydroxylation of (S)-fluorolittorines occurs *via* a carbocation.

2.11 Discussion

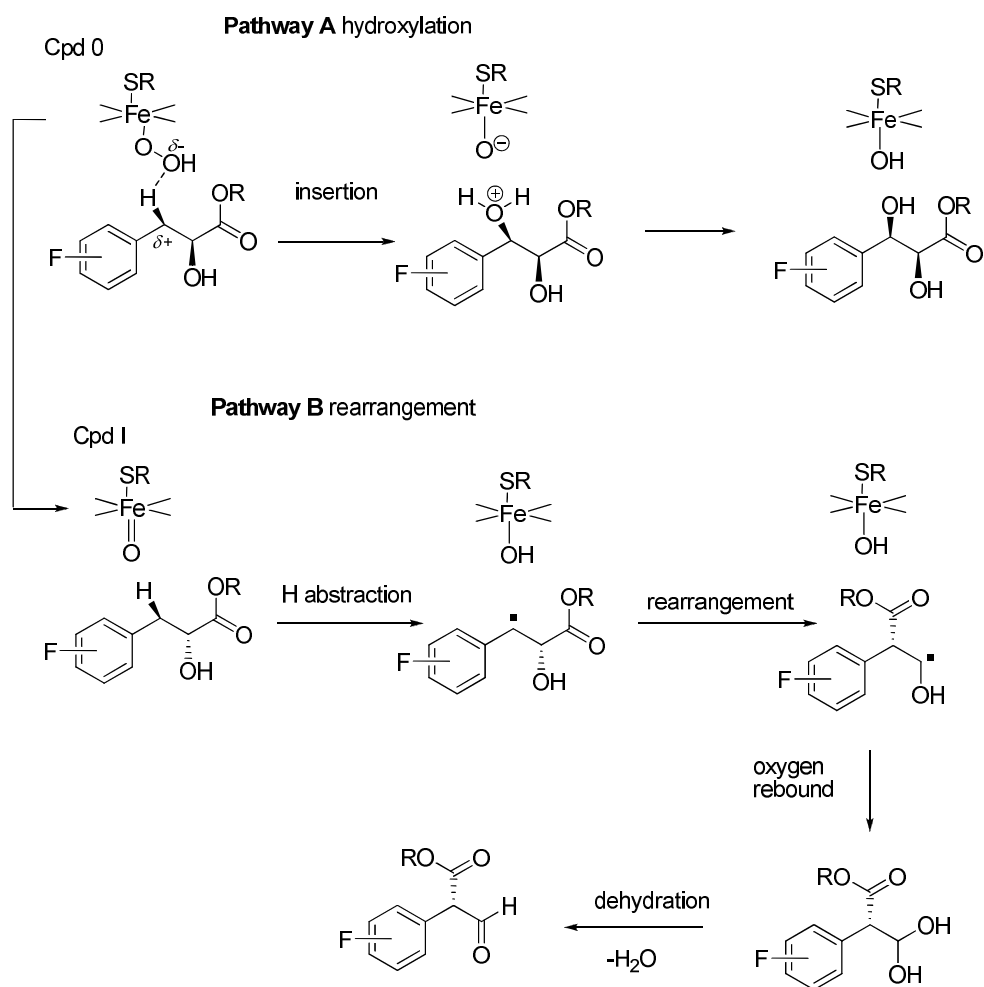
In order to explore the mechanism of the rearrangement of littorine to hyoscyamine *rac*- and enantio-enriched fluorolittorines were prepared and incubated with the CYP80F1 enzyme expressed in yeast microsomes. The unnatural (*S*)-littorine and its fluorinated analogues were hydroxylated by the CYP80F1 to give the corresponding 3'-hydroxylittorines (2'*S*, 3'*R*-**110b-d**). The fluorohydroxylittorine product profiles are clearly influenced by the nature of the fluorine substituent. The *para*-fluorine is the best substrate followed by the *ortho*-substate, whereas the *meta*-substrate had the lowest efficiency. This convincingly indicates the involvement of a benzylic carbocation mechanism operating during the 3'-hydroxylation reaction.

Incubations of the (*R*)-enantiomers (natural series) with CYP80F1 revealed competing hydroxylation and rearrangement reactions. The hydroxylation reaction is strongly suppressed by the *meta*- fluorine substituent and significantly promoted in the *ortho/para* isomers, also suggesting a carbocation process operating. On the other hand, the product profile for the competing rearrangement reaction suggests a radical stability trend, i.e. *meta*- is the most efficient relative to the *ortho/para*-substrates.

Conventional wisdom suggests that cytochrome P₄₅₀ enzymes hydroxylate *via* a radical process, however the present experiments point to a cationic hydroxylation pathway. The observation that the *para*- and *ortho*- fluorine substituents promote 3'-hydroxylation relative to the *meta*-, is consistent with the involvement of a benzylic carbocation.

It has been suggested that P₄₅₀ enzymes utilise multiple oxidants during mono-oxygenation reactions. The two-state reactivity hypothesis⁹⁶ proposes Cpd I as an oxidant which equilibrates between high and low spin states. Also there are suggestions from Newcomb that Cpd I may act as the primary oxidant and that the iron hydroperoxy intermediate Cpd 0 is a secondary oxidant.^{95, 96} The insertion of a hydroxonium species into the C-H bond by Cpd 0 would fit our experimental observations for hydroxylation. The cationic character developing during the reaction course would be stabilised by the *ortho/para*-fluorine substituents, hence the high production of *ortho/para*-fluorohydroxylittorines.

On the other hand, Cpd I mediates mono-oxygenation by inserting oxygen into the C-H bond by the abstraction of hydrogen generating a radical intermediate. The radical is then quenched by the well known “oxygen rebound” process. This circumstance would fit our experimental outcome for the rearrangement process. Homolytic abstraction of the 3'-*pro-R* hydrogen would generate a benzylic radical. The stability would not differ much between the *ortho*-, *meta*-, and *para*-fluoro substituents. The fact that Cpd I can be generated from Cpd 0, suggests the possibility that these two reactive species may be partitioned as shown in Scheme 2.53. For hydroxylation (pathway A) Cpd 0 inserts ⁺OH into 3' *pro-R*-hydrogen to generate 3'-fluorohydroxylittorine. The competitive rearrangement reaction (pathway B) is promoted by the Cpd I where the 3' *pro-R*-hydrogen is removed, generating a radical intermediate, which then rearranges and is quenched by an oxygen rebound process. Following collapsing of the resultant hydrate this gives fluorohyoscyamine aldehyde.



Scheme 2.53 Working hypothesis for partitioning between Cpd 0/Cpd I for reaction on fluorolittorine stereoisomers.

2.12 Conclusion

(*rac*)-Fluorolittorine isomers and enantio-enriched fluorolittorine isomers were prepared as a tool to explore the mechanism of the rearrangement of littorine to hyoscyamine by the P₄₅₀ CYP80F1 enzyme. Incubations of (*rac*)-fluorolittorines isomers with CYP80F1 enzyme indicated that the (*S*)-enantiomer is hydroxylated to give 3'-hydroxylittorine whereas the (*R*)-enantiomer rearranges to hyoscyamine. Incubation of enantio-enriched (*R*)- and (*S*)- fluorolittorines isomers suggest that the hydroxylation reaction to 3'-hydroxylittorine occurs *via* a carbocation intermediate whereas the rearrangement to hyoscyamine is a radical process.

Incubations with enantio-enriched (*S*)-[3',3'-²H₂]-littorine and (*R*)-[3',3'-²H₂]-littorine with CYP80F1 showed a primary KIE. This also suggests the abstraction of the C3' benzylic hydrogen of littorine as the rate determining step.

2.13 References

1. G. A. Cordell, M. L. Quinn-Beattie and N. R. Farnsworth, *Phytother. Res.*, 2001, **15**, 183-205.
2. IUPAC, *Compendium of chemical terminology internet edition*, <http://old.iupac.org/goldbook/A00220.pdf>, Accessed 29, 2009.
3. P. M. Dewick, *Medicinal natural products: A biosynthetic approach*, 2 edn., John Wiley & Sons Ltd, Chichester, 2001.
4. G. L. Patrick, *Introduction to Medicinal Chemistry*, 3 edn., Oxford University Press, 1995.
5. G. B. Wood, *A Treatise on Therapeutics, and Pharmacology or Meteria Medica.*, J. B. Lippincott and Co., London, 1856.
6. J. Mann, *Murder, Magic, and Medicine*, Oxford University Press, 1992.
7. W. H. Lewis and M. P. F. Elvin-Lewis, *Medical Botany plants affecting man's health*, john-wiley & sons, 1977.
8. G. Pinn, *Herbal Medicine "A Practical Guide for Medical Practitioners"*, Blackwell, 2003.
9. P. C. Blackett, *An Essay on the use of the Atropa Belladonna or Solanum Lethale, and The solanum Hortense with practical observations on their effects in the cure of scirrous , cancer, stricture, and various other complaints*, 1826
10. J. Schmidt, *Organic Chemistry*, 4 edn., Gurney and Jackson, Edinburgh, 1943.
11. A. Ladenburgh, *Ber. Dtsch. Chem. Ges.*, 1879, **12**, 941-944.
12. A. J. Humphry and D. O'Hagan, *Nat. Prod. Rep.*, 2001, **18**, 494-502.
13. R. Robinson, *J. Chem. Soc., Trans.*, 1917, **111**, 762-768.

14. R. Robinson, *J. Chem. Soc., Trans.*, 1917, **111**, 876-899.
15. A. J. Birch, *Notes and Records of the Royal Society of London*, 1993, **47**, 277-296.
16. K. C. Nicolaou, D. Vourloumis, N. Winssinger and P. S. Baran, *Angew. Chem. Int. Ed.*, 2000, **39**, 44-122.
17. P. I. Mortimer, *Nature*, 1953, **172**, 74-75.
18. R. Robinson, *Nature*, 1953, **172**, 344-345.
19. W. O. James, *New Phytologist*, 1949, **48**, 172-185.
20. W. O. James, *Nature*, 1946, **158** 654-656.
21. E. Leete, L. Marion and I. D. Spencer, *Nature*, 1954, **174**, 650-651.
22. E. Leete, L. Marion and I. D. Spencer, *Can. J. Chem.*, 1954, **32**, 1116-1123.
23. E. Leete, *J. Am. Chem. Soc.*, 1962, **84**, 55-57.
24. E. Leete, *Tetrahedron Lett.*, 1964, **24**, 1619-1622.
25. A. A. Bothner-By, R. S. Schutz, R. F. Dawson and M. L. Solt, *J. Am. Chem. Soc.*, 1962, **84**, 52-54.
26. A. Ahmad and E. Leete, *Phytochemistry*, 1970, **9**, 2345-2347.
27. S. H. Hedges and R. B. Herbert, *Phytochemistry*, 1981, **20**, 2064-2065.
28. H. W. Liebisch, W. Maier and H. R. Schutte, *Tetrahedron Lett.*, 1966, **34**, 4079-4082.
29. S. Mizusake, T. Kisaki and E. Tamaki, *Plant Physiol.*, 1968, **43**, 93-98.
30. H. W. Liebisch, H. R. Schutte and K. Mothers, *Annalen*, 1963, 139-144.
31. T. Hashimoto, Y. Yukimune and Y. Yamada, *J. Plant Physiol.*, 1986, **124**, 61-75.
32. T. Hashimoto, Y. Yulimune and Y. Yamada, *Planta*, 1989, **178**, 123-130.
33. E. Leete, *J. Am. Chem. Soc.*, 1982, **104**, 1403-1408.

34. J. Kaczkowski and L. Marion, *Can. J. Chem.*, 1963, **41**, 2651-2653.
35. R. Duran-Patron, D. O'Hagan, J. T. G. Hamilton and C. W. Wong, *Phytochemistry*, 2000, **53**, 777-784.
36. T. Hemscheidt and I. D. Spenser, *J. Am. Chem. Soc.*, 1992, **114**, 5472-5473.
37. E. Leete, *J. Am. Chem. Soc.*, 1967, **89**, 7081-7084.
38. T. Hashimoto, Y. Yamada and E. Leete, *J. Am. Chem. Soc.*, 1989, **111**, 1141-1142.
39. N. J. Walton, R. J. Robins and A. C. J. Peerless, *Planta*, 1990, **182**, 136-141.
40. N. J. Walton, A. C. J. Peerless, R. J. Robins, M. J. C. Rhodes, H. D. Boswell and D. J. Robins, *Planta*, 1994, **193**, 9-15.
41. T. Hashimoto, Y. Yukimune and Y. Yamada, *Planta*, 1989, **178**, 131-137.
42. J. Kaczkowski, H. R. Schütte and K. Mothes, *Biochem. Biophys. Acta.*, 1961, **46**, 588-594.
43. D. G. O'Donovan and M. F. Keogh, *J. Chem. Soc. Chem. Commun.*, 1969.
44. H. W. Liebisch, K. Peisker, A. S. Radwal and H. R. Schuette, *Pflanzenphysiol.*, 1972, **67**, 1-9.
45. B. A. McGaw and J. G. Woolley, *Phytochemistry*, 1978, **17**, 257-259.
46. B. A. McGaw and J. G. Woolley, *Phytochemistry*, 1979, **18**, 189-190.
47. U. Sankawa, H. Noguchi, T. Hashimoto and Y. Yamada, *Chem. Pharm. Bull.*, 1990, **38**, 2066-2068.
48. T. W. Abraham and E. Leete, *J. Am. Chem. Soc.*, 1995, **117**, 8100-8105.
49. R. J. Robins, T. W. Abraham, A. J. Parr, J. Eagles and N. J. Walton, *J. Am. Chem. Soc.*, 1997, **119**, 10929-10934.
50. T. Hemscheidt, *Topics in Current Chemistry*, 2000, **209**.
51. S. Patterson, University of St Andrews, 2003.

52. T. Hemscheidt and I. D. Spencer, *J. Am. Chem. Soc.*, 1996, **118**, 1799-1800.
53. M. E. Landgrebe and E. Leete, *Phytochemistry*, 1990, **29**, 2521-2524.
54. A. Portsteffen, B. Draeger and A. Nahrstedt, *Phytochemistry*, 1992, **31**, 1135-1138.
55. A. Yamashita, H. Kato, S. Wakatsuki, T. Tomizaki, T. Nakatsu, K. Nakajima, T. Hashimoto, Y. Yamada and J. Oda, *Biochemistry*, 1999, **38**, 7630-7637.
56. R. Robinson, *Proceeding of the University of Durham Philosophical Society*, 1927-1932, **8**, 14-19.
57. E. Leete, *J. Am. Chem. Soc.*, 1960, **82**, 612-614.
58. M. L. Louden and E. Leete, *J. Am. Chem. Soc.*, 1962, **84**, 1510-1511.
59. M. L. Louden and E. Leete, *J. Am. Chem. Soc.*, 1962, **84**, 4507-4509.
60. E. Leete, N. Kowando and R. A. Newmark, *J. Am. Chem. Soc.*, 1975, **97**, 6826-6830.
61. W. C. Evans and V. A. Woolley, *Phytochemistry*, 1969, **8**, 2183-2187.
62. M. Ansarin and J. G. Woolley, *Phytochemistry*, 1993, **32**, 1183-1187.
63. M. Ansarin and J. G. Woolley, *Phytochemistry*, 1994, **35**, 935-939.
64. N. C. J. E. Chesters, D. O'Hagan and R. J. Robins, *J. Chem. Soc. Perkin Trans. I*, 1994, 1159-1162.
65. N. C. J. E. Chesters, D. O'Hagan and R. J. Robins, *J. Chem. Soc. Chem. Commun.*, 1995, 127-128.
66. D. O'Hagan and R. J. Robins, *Chem. Soc. Rev.*, 1998, **27**, 207-212.
67. R. J. Robins, P. Bachmann and J. G. Woolley, *J. Chem. Soc. Perkin Trans. I*, 1994, 615-619.
68. R. J. Robins, N. C. J. E. Chesters, D. O'Hagan, A. J. Parr, N. J. Walton and J. G. Woolley, *J. Chem. Soc. Perkin Trans. I*, 1995, 481-485.

69. E. Leete, *J. Am. Chem. Soc.*, 1984, **106**, 7271-7272.
70. E. Leete, *Can. J. Chem.*, 1987, **65**, 226-228.
71. N. C. J. E. Chesters, K. Walker, D. O'Hagan and H. G. Floss, *J. Am. Chem. Soc.*, 1996, **118**, 925-926.
72. N. C. J. E. Chesters, D. O'Hagan, R. J. Robins, A. Kastle and H. G. Floss, *J. Chem. Soc. Chem. Commun.*, 1995, 129-130.
73. V. R. Platt, C. T. Opie and E. Haslam, *Phytochemistry*, 1984, **23**, 2211-2217.
74. M. Sprecher, M. J. Clark and D. B. Sprinson, *J. Biol. Chem.*, 1966, **241**, 872-877.
75. H. Eggerer, P. Overath, F. Lynen and E. R. Stadtman, *J. Am. Chem. Soc.*, 1960, 2643-2644.
76. M. Sprecher, M. J. Clark and D. B. Sprinson, *J. Biol. Chem.*, 1966, **241**, 864-867.
77. J. L. Kilgore and D. J. Alberhart, *J. Chem. Soc. Perkin Trans. 1*, 1996, 79-84.
78. C. H. Chang, M. D. Ballinger, G. H. Reed and P. A. Frey, *Biochemistry*, 1996, **35**, 11081-11084.
79. S. Ollagnier, E. Kervio and J. Retey, *FEBS Letters*, 1998, **437**, 309-312.
80. S. Patterson and D. O'Hagan, *Phytochemistry*, 2002, **61**, 323-329.
81. M. F. Hashim, T. Hakamatsuka, Y. Ebizuka and U. Sankawa, *FEBS Letters*, 1990, **271**, 219-222.
82. T. Hakamatsuka, M. F. Hashim, Y. Ebizuka and U. Sankawa, *Tetrahedron*, 1991, **47**, 5969-5978.
83. I. Zebetakis, R. Edwards, J. T. G. Hamilton and D. O'Hagan, *Plant Cell Reports*, 1998, **18**, 341-345.

84. R. Li, D. W. Reed, E. Liu, J. Nowak, L. E. Pelcher, J. E. Page and P. S. Covello, *Chem. Biol.*, 2006, **13**, 513-520.
85. C. W. Wong, J. T. G. Hamilton, D. O'Hagan and R. J. Robins, *J. Chem. Soc. Chem. Commun.*, 1998, 1045-1046.
86. T. Bugg, *An Introduction to Enzyme and Coenzyme chemistry*, Blackwell Science, 1997.
87. M. Sono, M. P. Roach, E. D. Coulter and J. H. Dawson, *Chem. Rev.*, 1996, **96**, 2841-2887.
88. B. Meunier, S. P. d. Visser and S. Shaik, *Chem. Rev.*, 2004, **104**, 3947-3980.
89. S. Shaik, H. Hirao and D. Kumar, *Nat. Prod. Rep.*, 2007, **24**, 533-552.
90. M. Newcomb, R. Zhang, R. E. P. Chandrasena, J. A. Halgrimson, J. H. Horner, T. M. Makris and S. G. Sligar, *J. Am. Chem. Soc.*, 2006, **128**, 4580-4581.
91. M. Newcomb, M.-H. L. Tadic-Biadatti, D. L. Chestney, E. S. Robert and P. F. Hollenberg, *J. Am. Chem. Soc.*, 1995, **117**, 12085-12091.
92. M. Newcomb and P. H. Toy, *Arch. Biochem. Biophys*, 2000, **33**, 449-455.
93. M. Newcomb, R. Shen, S.-Y. Choi, P. H. Toy, P. F. Hollenberg, A. D. N. Vaz and M. J. Coon, *J. Am. Chem. Soc.*, 2000, **122**, 2677-2686.
94. R. E. P. Chandrasena, K. P. Vatsis, M. J. Coon, P. F. Hollenberg and M. Newcomb, *J. Am. Chem. Soc.*, 2004, **126**, 115-126.
95. X. Sheng, H. Zhang, P. F. Hollenberg and M. Newcomb, *Biochemistry*, 2009, **48**, 1620-1627.
96. M. Newcomb, P. F. Hollenberg and M. J. Coon, *Arch. Biochem. Biophys*, 2003, **409**, 72-79.
97. M. Newcomb and D. L. Chestney, *J. Am. Chem. Soc.*, 1994, **116**, 9753-9754.

98. J. Wemple, *J. Am. Chem. Soc.*, 1970, **92**, 6694-6695.
99. J. Domagala and J. Wemple, *Tetrahedron Lett.*, 1973, **14**, 1179-1182.
100. G. M. Sandala, D. M. Smith and L. Radom, *J. Am. Chem. Soc.*, 2008, **130**, 10684-10690.
101. J. Rosenthal and D. I. Schuster, *J. Chem. Ed.*, 2003, **80**, 679-690.
102. G. A. Olah, R. D. Porter, C. L. Jeuell and A. M. White, *J. Am. Chem. Soc.*, 1972, **94**, 2044-2052.
103. D. A. Forsyth, P. Lucas and R. M. Burk, *J. Am. Chem. Soc.*, 1982, **104**, 240-245.
104. J. E. Hodgkins and E. D. Megarity, *J. Am. Chem. Soc.*, 1965, **87**, 5322-5326.
105. J. M. Dust and D. R. Arnold, *J. Am. Chem. Soc.*, 1983, **105**, 1221-1227.
106. T. H. Fisher, S. M. Dershem and M. L. Prewitt, *J. Org. Chem.*, 1989, **55**, 1040-1043.
107. R. A. Jackson and M. Sharifi, *J. Chem. Soc. Perkin Trans. 2*, 1996, 775-778.
108. D. O'Hagan, R. J. Robins, M. Wilson, C. W. Wong, M. Berry and I. Zebetakis, *J. Chem. Soc., Perkin Trans. 1*, 1999, 2117-2120.
109. C. W. Wong, University of Durham, 1999.
110. H. Wren and E. Wright, *J. Chem. Soc. Trans.*, 1921, **119**, 798-803.
111. J. Jones, *Amino Acid and Peptide Synthesis*, Oxford Science Publications, 2000.
112. W. Konig and R. Geiger, *Chem. Ber.*, 1970, **103**, 788-798.
113. S.-Y. Han and Y.-A. Kim, *Tetrahedron*, 2004, **60**, 2447-2467.
114. P. Li and J. C. Xu, *J. Chem. Soc. Perkin Trans. 2*, 2001, 113-120.
115. K. A. Mahmoud, Y.-T. Long, G. Schatte and H.-B. Kraatz, *Eur. J. Inorg. Chem.*, 2005, 173-180.

- 116. M. Schueler, The University of St Andrews.
- 117. H. L. Vaughn and M. D. Robins, *J. Org. Chem*, 1975, **40**, 1187-1189.
- 118. B. Gomez-Reyes and A. K. Yatsimirsky, *Org. Lett.*, 2005, **5**, 4831-4834.
- 119. A. Ghanem and H. Y. Aboul-Enein, *Tetrahedron: Asymmetry*, 2004, **15**.
- 120. W. Adam, M. Lazarus, A. Schmerder, H.-U. Humpf, C. R. Saha-Moller and P. Schreier, *Eur. J. Org. Chem.*, 1998, 2013-2018.
- 121. B. Larissegger-Schnell, S. M. Glueck, W. Kroutil and K. Faber, *Tetrahedron*, 2006, **62**, 2912-2916.
- 122. N. C. J. E. Chesters, University of Durham, 1995.

Chapter 3

Synthesis of ribose phosphonates

3.1 Introduction

Streptomyces cattleya is one of only two bacteria which have been identified that are capable of elaborating organofluorine metabolites.¹ This soil bacterium is known to produce the β -lactam antibiotic, thienamycin.² Remarkably, *S. cattleya* also produces fluoroacetate (**155**) and an antibiotic 4-fluorothreonine (**156**) when a fluoride ion is available.³ Fluoroacetate is a well known mammalian toxin. Presumably, these two fluorinated compounds are produced as defence substances. Uncovering the fluorometabolic pathway to these metabolites attracted much intention over the last 15 years and the details have largely been elucidated. Most of the enzymes are now known and recently, the whole biotransformation was demonstrated by reconstitution *in vitro* in *St Andrews*.⁴

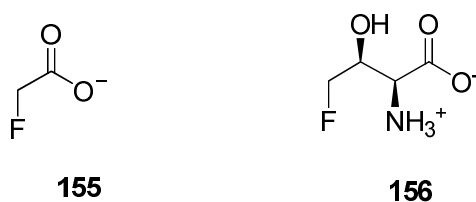
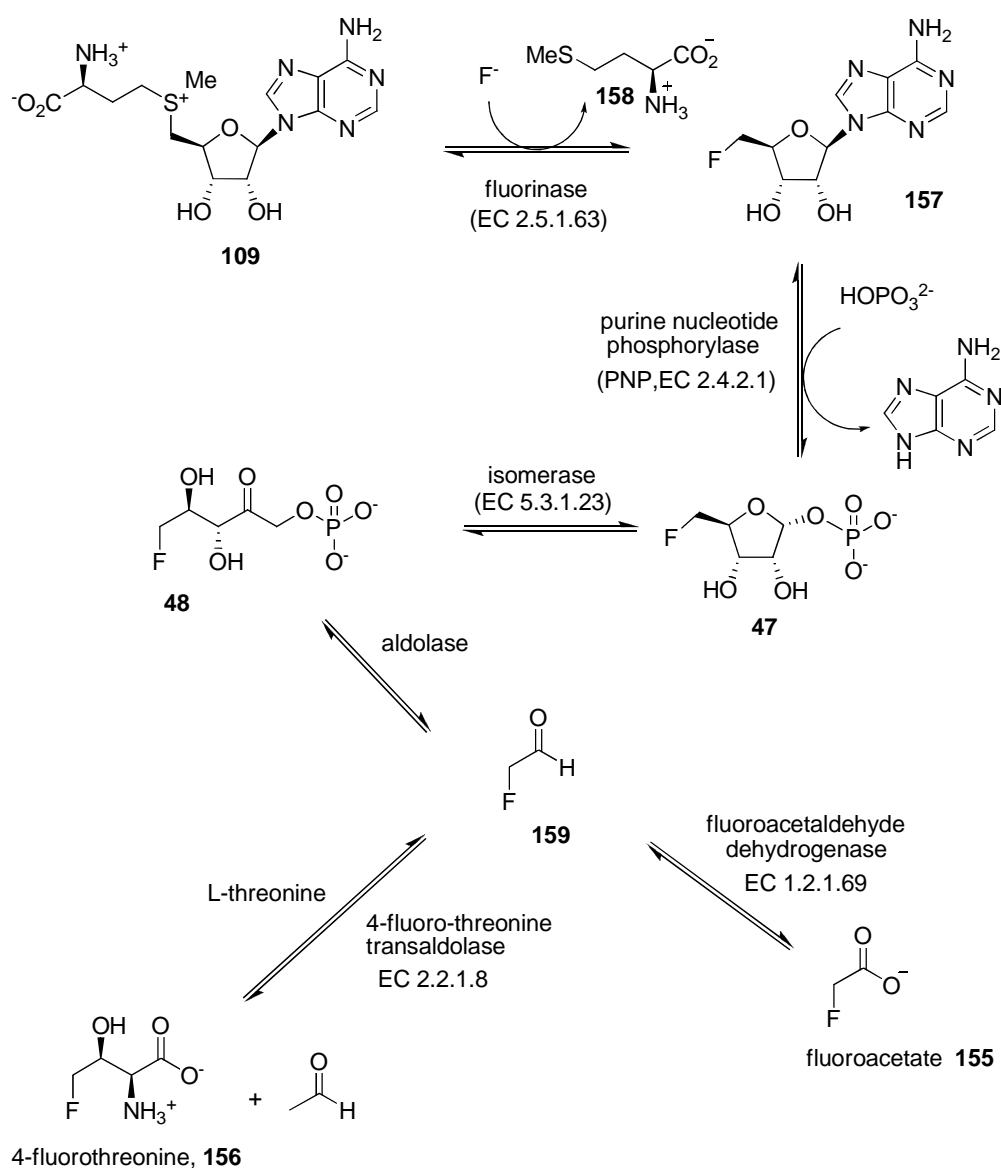


Figure 3.1 Fluoroacetate (**155**) and 4-fluorothreonine (**156**) are secondary metabolites produced by *S. cattleya*.

3.2 The biosynthesis of fluoroacetate (**155**) and 4-fluorothreonine (**156**) in *S. cattleya*

An overview of the biosynthetic pathway is summarised in Scheme 3.1. The first committed step in the biosynthesis of fluoroacetate (**155**) and 4-fluorothreonine (**156**) involves the conversion of SAM **109** to 5'-FDA **157**. The reaction is mediated by a 5'-fluoro-5'-deoxyadenosine synthase (5'-FDA synthase, EC 2.5.1.63), an enzyme which has been informally named the “fluorinase”.^{5, 6} In the event, inorganic fluoride ion

attacks the C5' carbon of SAM (**109**) to form a C-F bond in an S_N2 type reaction, releasing L-methionine (**158**). Studies have shown that the fluorinase can also utilise a chloride ion to produce a 5'-ClDA, however, bromide and iodide ion do not appear to be substrates.⁷ In the next enzymatic step, the adenosine moiety of 5'-FDA (**157**) is replaced by a phosphate group to generate 5-fluoro-5-deoxyribose-1-phosphate (5-FDRP, **47**). This phosphorolysis reaction is catalysed by a purine nucleotide phosphorylase (PNP) and is a reversible process.⁸ This type of enzyme is found quite widely in nucleotide metabolism. An isomerase then mediates a ring opening isomerisation reaction of **47** to generate 5-fluoro-5-deoxyribulose-1-phosphate (**48**).⁹ This ribulose-phosphate is then acted upon by an aldolase, which catalyses the cleavage of **48** in a retro-aldol reaction to give fluoroacetaldehyde (**159**),¹⁰ a precursor to both **155** and **156**. Fluoroacetaldehyde (**159**) is oxidised by a NAD⁺ dependent fluoroacetaldehyde dehydrogenase to generate fluoroacetate (**156**).¹¹ Separately, a pyridoxal phosphate (PLP) dependent enzyme (4-FTase) mediates a trans-aldol addition reaction of fluoroacetaldehyde with L-threonine to form the antibiotic, 4-fluorothreonine (**156**) and acetaldehyde.¹²

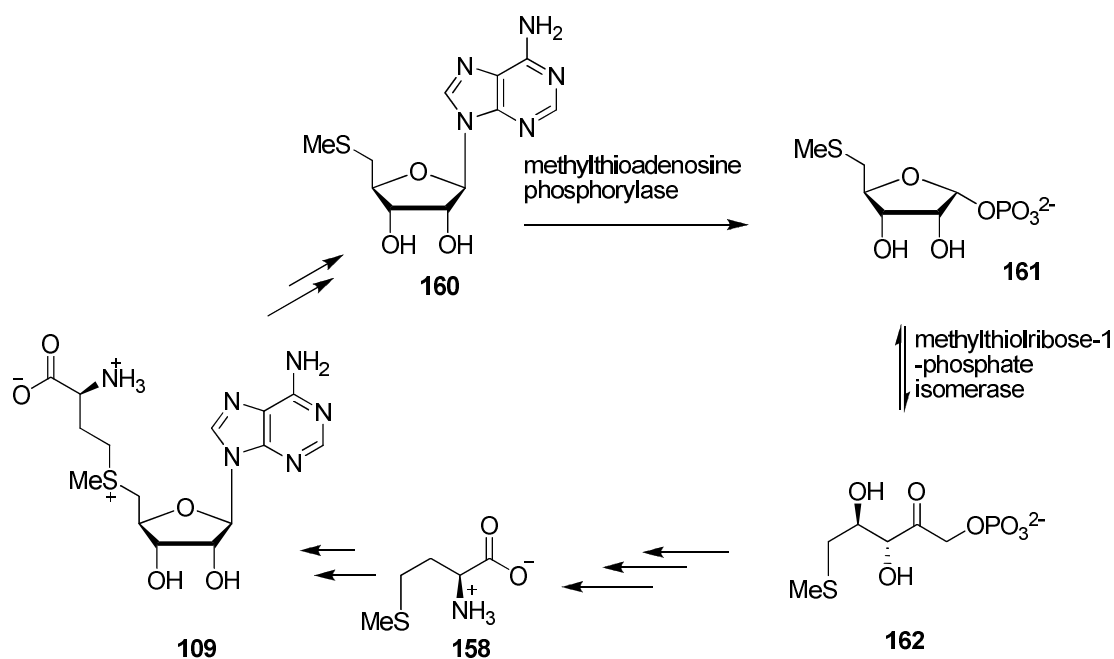


Scheme 3.1 Overview of the biosynthesis of fluoroacetate (**155**) and 4-fluorothreonine (**156**) in *Streptomyces cattleya*.

3.3 The isomerisation of 5-fluoro-5-deoxyribose-1-phosphate (5-FDRP, 47) to 5-fluoro-5-deoxyribulose-1-phosphate (5-FDRulP, 48)

3.3.1 The aldo-keto, MTR-1-P isomerase

There is an isomerase enzyme involved in fluorometabolite biosynthesis that has similarity to an enzyme on the L-methionine salvage pathway. The L-methionine salvage pathway is essential for bacteria, yeast, plants, and animals. These organisms utilise this pathway to regulate L-methionine levels. This essential amino acid is involved in many cellular functions, including methylation of DNA and rRNA, and the biosynthesis of L-cysteine. Studies¹³ in *Bacillus subtilis* have established details of the complete pathway which is summarised in Scheme 3.2.



Scheme 3.2 L-Methionine salvage pathway in *B. subtilis*.¹³

5-Deoxy-5-methylthioribulose 1-phosphate isomerase (MTR-1-P isomerase) is a key enzyme of the methionine salvage pathway. This aldose-ketose isomerase mediates the interconversion of MTRP-1-P (**161**) to MTRul-1-P (**162**). The isomerisation of **161** to **162** in *B. subtilis* is analogous to the isomerisation from **47** to **48** in the fluorometabolite pathway of *S. cattleya*. The only variation is that the -SMe group is replaced by a fluorine atom.

3.3.2 Crystal structure of 5-deoxy-5-methylthio- α -D-ribose-1-phosphate isomerase from *Bacillus subtilis*.

Several 5-deoxy-5-methylthio- α -D-ribose-1-phosphate isomerase (MTR-1-P isomerase) enzymes have been structurally characterised from bacteria¹⁴ and yeast.¹⁵ Recently, the MTR-1-P isomerase from *B. subtilis* has been isolated¹⁶ and was co-crystallised with the ring open product, 5-MTRul-1-P (Figure 3.2).¹⁷ The active site of this enzyme can be divided into three regions; that involving hydrogen bonding with the phosphate group, that which forms a hydrogen bond to backbone oxygens or hydrogens of the ribulose, and that involving hydrophobic interactions with the thiomethyl group. The putative catalytic residues that are involved in the isomerisation of MTR-1-P to MTRul-1-P are thought to be the highly conserved amino acids Asp240 and Cys160. During the catalysis, Asp240 appears to play a role as a proton donor/acceptor, whilst Cys160 may be present in a deprotonated form at the optimal pH (8.1) of MTRPI. Thus, Cys160 may stabilise a transient positive charge developing at C1 (Scheme 3.6).

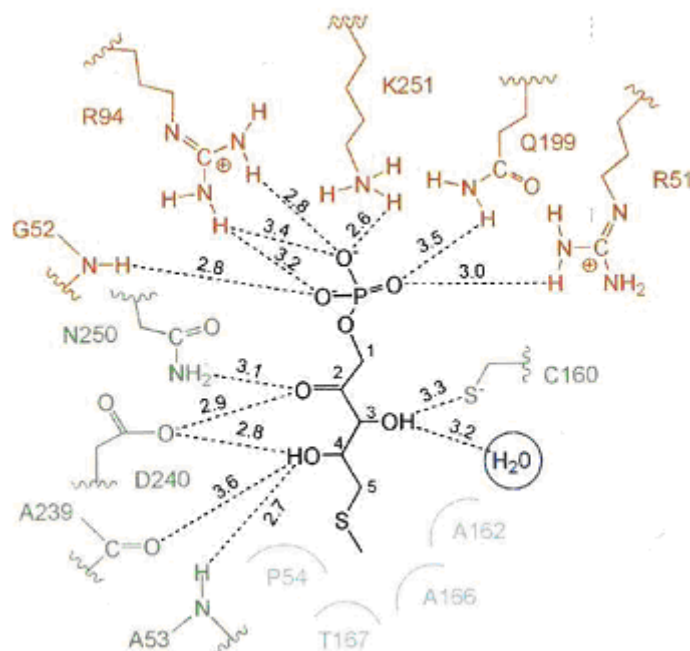
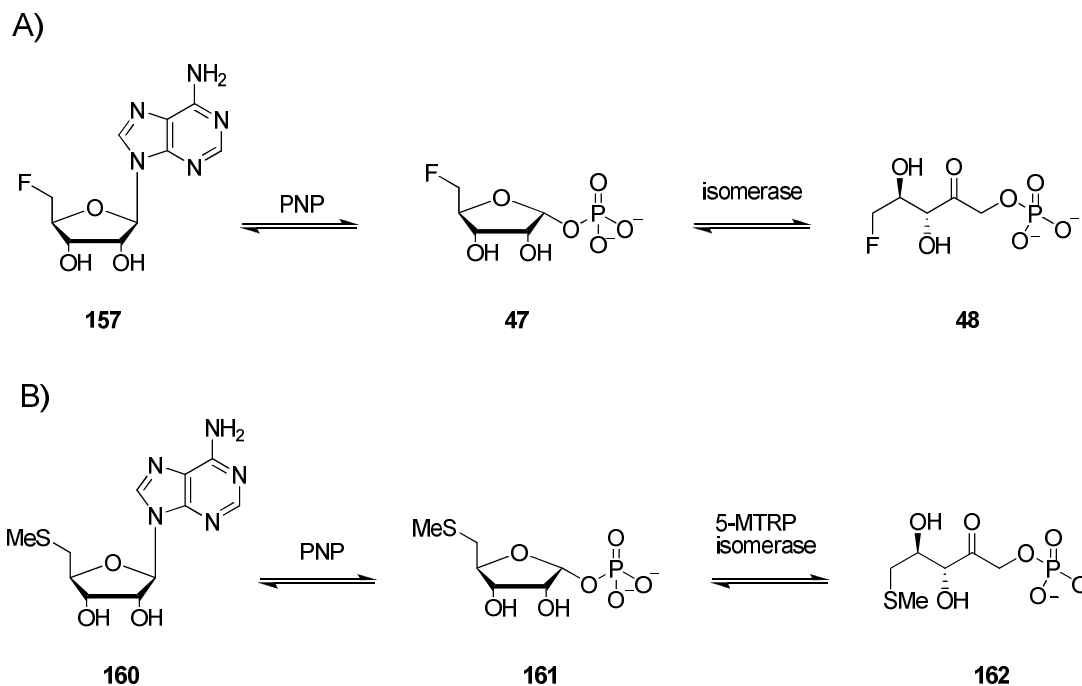


Figure 3.2 Active site residues and product, bound to MTR-1-P isomerase from *B. subtilis* (distances are given in Å).¹⁷

3.3.3 5-FDRulP is an intermediate in the fluorometabolite biosynthesis in *S. cattleya*

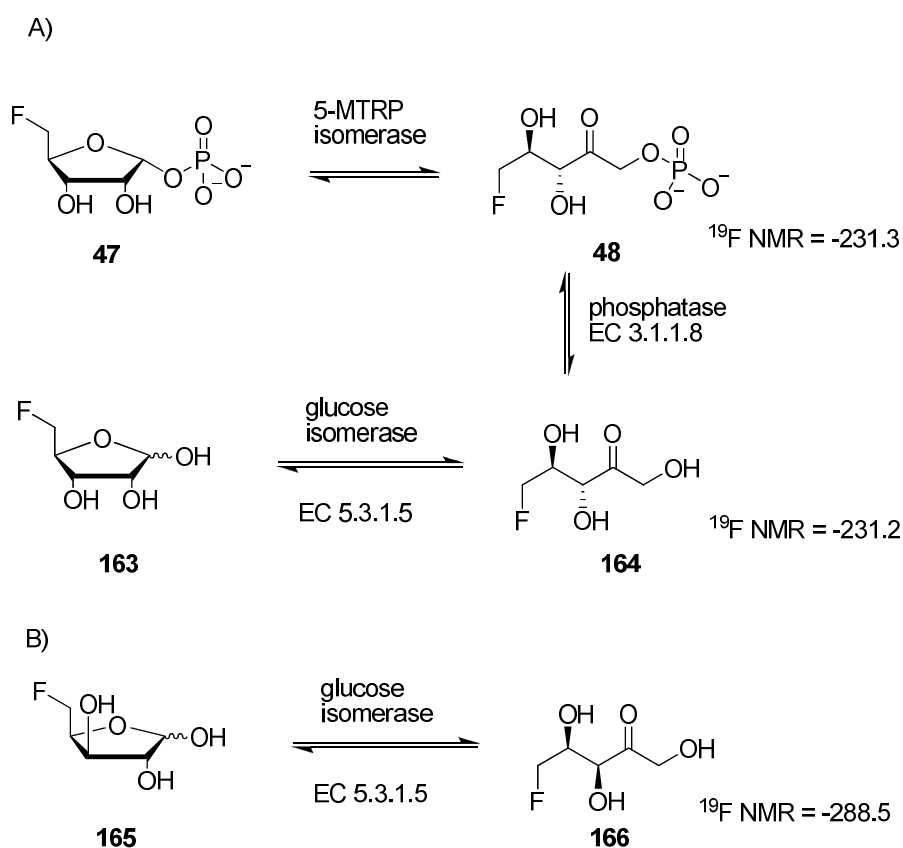
It has been established that 5-FDRP (**47**) is the second formed intermediate on the fluorometabolite pathway in *S. cattleya* and that it undergoes isomerisation to 5-FDRulP (**48**) in a similar manner to the MTR-1-P isomerase.^{18, 19}



Scheme 3.3 Conversion of 5-fluoro-5-deoxyribose-1-phosphate (**47**) to generate 5-fluoro-5-deoxyribulose-1-phosphate (**48**) in *S. cattleya* (Pathway A) and conversion of 5'-methioadenosine to ribose phosphate and ribulose in mammals (Pathway B).^{18, 19}

When 5-FDRP (**47**) was incubated with cell-free extracts of *S. cattleya* then 5-FDRulP (**48**) was obtained,⁹ clearly by the action of a related isomerase (5-FDRPi). The stereochemistry of 5-FDRulP was confirmed by comparative structural studies (Scheme 3.4). Firstly, the produced 5-FDRulP (**48**) was incubated with a commercial phosphatase to obtain the free 5-FDRul (**164**) sugar. This was apparent by a shift of the ¹⁹F NMR signal from -231.3 ppm to -231.2 ppm (**164**) which indicated that the phosphate moiety had cleaved. Separately, 5-FDR (**163**) was incubated with glucose isomerase in a reaction known to mediate an isomerisation to ribulose. These experiments gave identical diastereoisomers as determined by ¹⁹F NMR. Moreover, as a control, 5-FDX (**165**) was treated in a similar manner with glucose isomerase and this resulted in a different ¹⁹F NMR signal (-228.5 ppm) which belongs to

diastereoisomer **166**. Therefore, the stereochemistry and intermediacy of 5-FDRP (**47**) and 5-FDRuP (**48**) in fluorometabolite biosynthesis in *S. cattleya* was secured.⁹ The mechanism of the isomerisation is intriguing, and several possibilities emerge which will be discussed in due course in Section 3.4. The actual mechanism remains to be elucidated.



Scheme 3.4 The absolute stereochemistry of **48** was deduced by comparative structural studies.⁹

3.4 Identification of the putative isomerase gene in *S. cattleya*⁴

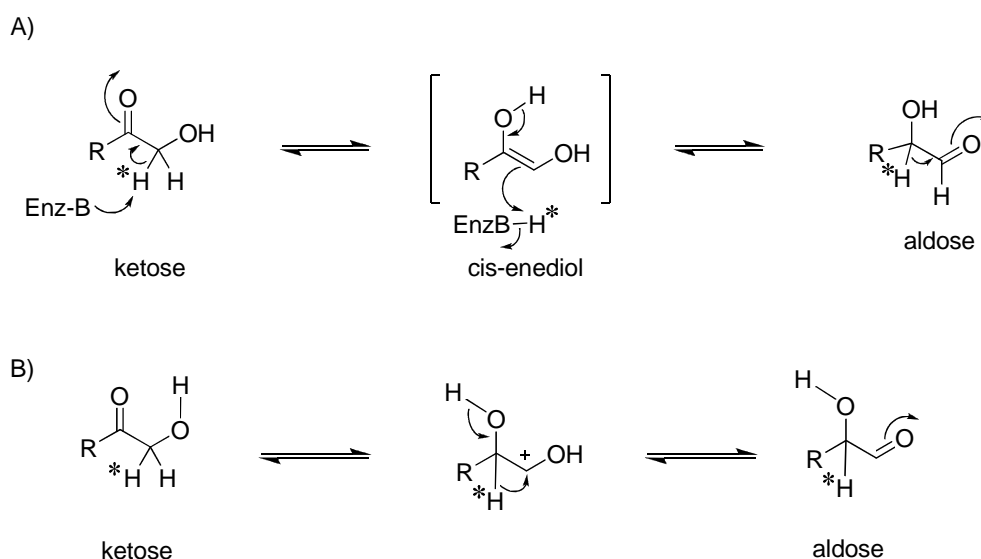
A homology search of the MTRPI gene of *B. subtilis* with the full genome sequences of *S. coelicolor* and *S. avermitilis* revealed two genes which had a 35% amino acid identity. These were the SCO3014 (*S. coelicolor*) and SAV6658 (*S. avermitilis*) genes. Initially, these two genes had been annotated as eukaryotic translation initiation factors 2B (eIF2B), however they are now correctly assigned as isomerases. The over-expression of the SCO3014 gene product in *E. coli* led to the isolation of the protein. This enzyme clearly exhibited the ability to catalyse the isomerisation of 5-FDRP (**47**) to 5-FDRuP (**48**). These findings have led to the design of a primer that is now much more homologous to *S. cattleya*, and the identification of the putative *MTR-Sc*. This enzyme was over-expressed and the purified protein has 1161 base pairs and a 75% amino acid identity to the isomerase from *S. coelicolor*. As expected, this protein showed the ability to catalyse the conversion of **47** into **48** and thus the activity was identified now in *S. cattleya*. The abilities of these isomerases indicated that the original 'translation initiation factors' designations had been misassigned.

3.5 Putative mechanisms for the isomerisation of 5-FDRP (47) to 5-FDRuIP (48)

Three mechanisms for the isomerisation of 5-MTRP to 5-MTRuIP have been proposed. These involve enediol, hydride shift, and phosphate migration processes. These are discussed below.

3.5.1 The *cis*-enediol and hydride shift mechanisms

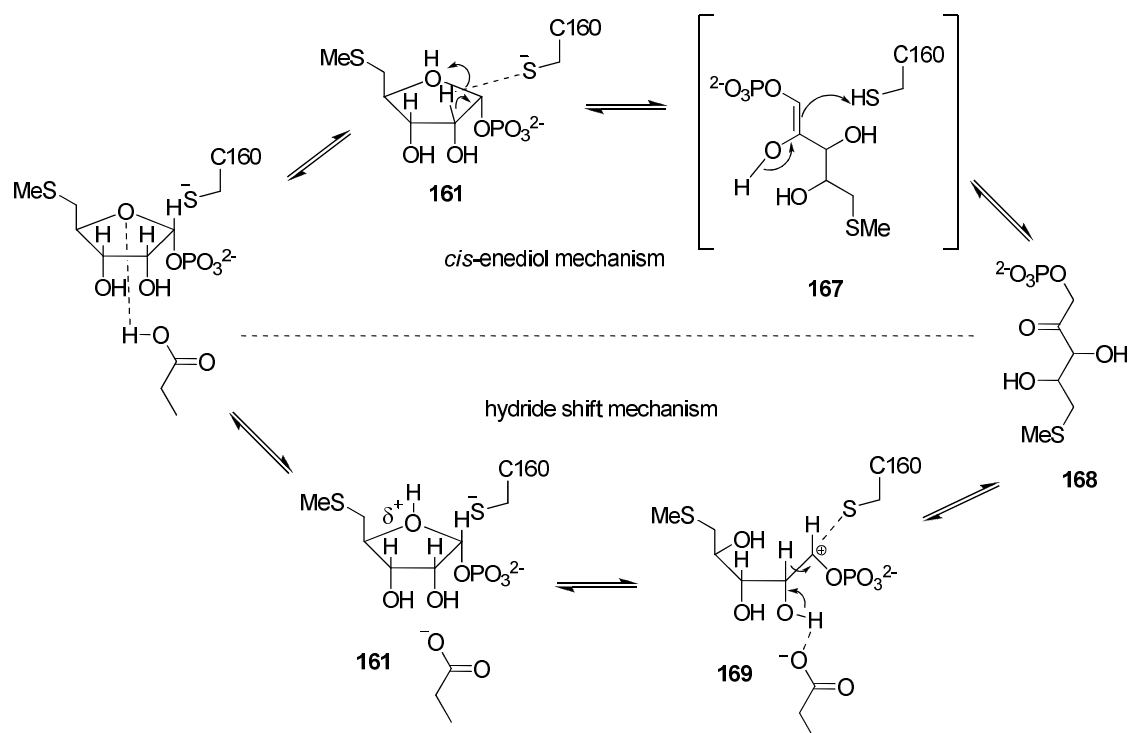
Cis-enediol and hydride shift mechanisms have been proposed for the interconversion of aldose and ketose sugars mediated by the aldose-ketose isomerase enzymes. These mechanisms are shown in Scheme 3.5.



Scheme 3.5 Proposed mechanisms for aldose (A) and ketose (B) isomerisations.

MTRPI is also a aldo-keto isomerase enzyme, however its substrate bears a phosphate group at C1 whereas the other aldose-ketose isomerase enzymes utilise a free anomeric hydroxyl group. The proposed *cis*-enediol and the hydride shift mechanism are shown in Scheme 3.6. A *cis*-enediol proton transfer requires to be triggered by deprotonation of the C2 hydroxyl. Cys160 is a candidate base for this deprotonation and would generate a *cis*-enediol (phosphoenolate). Asp240 would then mediate a simultaneous transfer of a proton between O2 and O4. The catalytic cycle would complete by redonation of the abstracted proton from Cys160 to generate MTRu-1-P.

The hydride transfer mechanism (Lower side, Scheme 3.6) would require a nucleophilic attack at C2 of the substrate. A candidate for this nucleophile is Asp240, triggering ring opening of the substrate. The transient positive charge which would develop on C1 would be stabilised by Cys160, now as a thiolate. The hydride on C2 would then migrate to C1, generating the product with release of 5-MTRu-1-P.



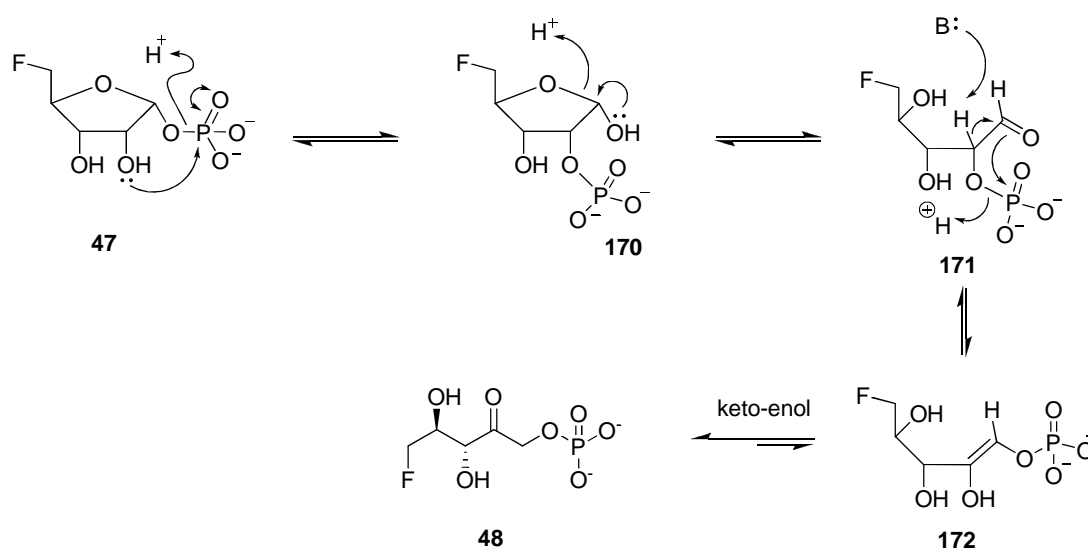
Scheme 3.6 Putative mechanism for the isomerisation of 5-MTR-1-P (**161**) to 5-MTRul-1-P (**168**) via the *cis*-enediol (upper side) and the hydride shift (lower side).

A study on the mechanism of D-xylose isomerase (XI) from *Streptomyces olivochromogenes* has revealed that the ketose-aldolase mediated isomerisation of D-xylose to D-xylulose operates via a hydride shift mechanism.²⁰ The D-xylose isomerase is a metalloenzyme requiring a divalent cation to assist hydride transfer. It has however been established that the MTR-1-P isomerase from *B. subtilis* does not require divalent ions such as Zn^{2+} or Mg^{2+} . Such divalent cations are required for keto-aldolases and in those cases the isomerisation proceeds via a *cis*-enediol mechanism.¹⁶ In this case, incubations in D_2O did not support the *cis*-enediol mechanism, since there was no apparent incorporation of deuterium from the medium into the products. Although, a negative result, this does suggest that the isomerisation

reaction of *B. subtilis* may adopt a hydride transfer process. It is noteworthy that the isomerase does not require divalent cations.

3.5.2 The phosphate migration mechanism.

A third mechanistic hypothesis for the isomerisation envisages an intramolecular phosphate migration. This mechanism would be triggered by the migration of the phosphate group from C1 to C2 in **47** to generate **170**. Epimerisation of **170** would then result in an equilibrium between **170** and **171**, followed by a back migration of the phosphate group from C2 to C1 to generate **172**. The keto-enol tautomerisation of **172** would then deliver 5-FDRuP (**48**).



Scheme 3.7 Putative phosphate group migration during the isomerisation of 5-FDRP (**47**) to 5-FDRuP (**48**).

3.6 Aims of the project

This aspect of the research is focused on the synthesis of an isosteric analogue of **47** by the preparation of D-ribose-1-phosphonates **173a-b** and **174a-b** where the linking phosphate oxygen has been replaced by a methylene group. These phosphonates are envisaged to be potential inhibitors for either the PNP or the isomerase enzymes involved in fluorometabolite biosynthesis (Scheme 3.1). They have potential utility as tools to explore these enzyme mechanisms by inhibition studies and as candidate inert substrate analogues for enzyme co-crystallisation studies.

The cyclic phosphonates **175a-b** were also targeted. These phosphonates were viewed as potential reaction intermediate analogues for co-crystallisation studies, and particularly to explore the phosphate migration mechanism of the isomerase enzyme.

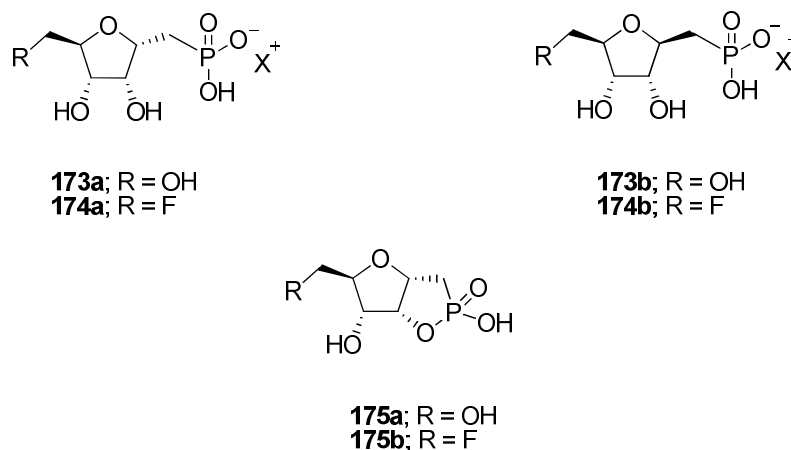


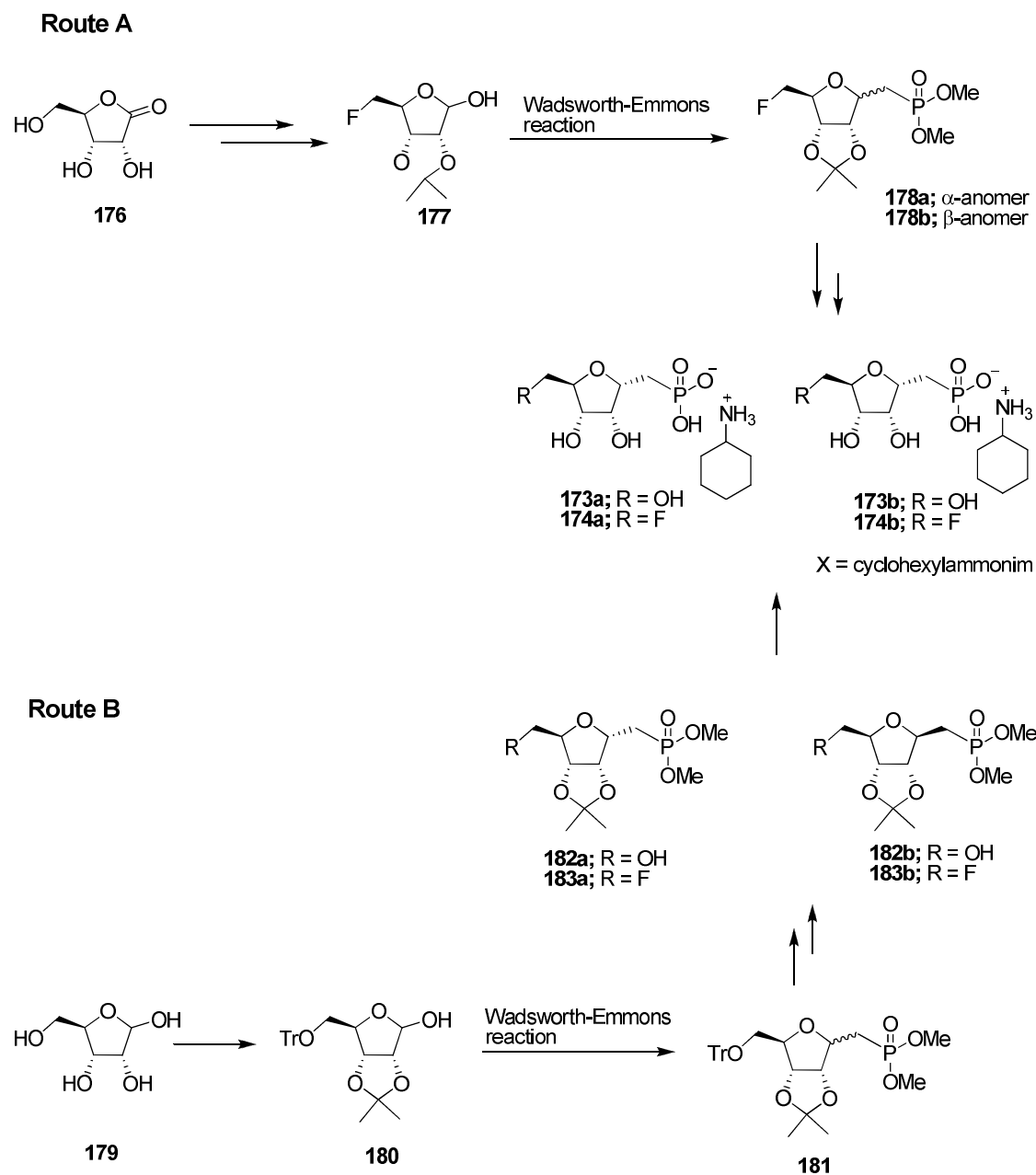
Figure 3.3 Target phosphonate analogues of D-ribose-1-phosphate **173a-b** and **174a-b** and the cyclic phosphonates **175a-b**.

3.7 Results and discussion

3.7.1 Synthesis

3.7.1.1 Synthetic plans

The target phosphonates **173a-b** and **174a-b** were prepared by routes A and B as shown in Scheme 3.8. The synthetic routes start either from D-ribonic- γ -lactone **176** or D-ribose **177**. For each route the key synthetic step involves installation of the methylenephosphonate moiety on a 2,3-isopropylidene ribofuranoside *via* a Wadsworth-Emmons reaction. The 5-OH can be replaced by fluorine, prior (route A) or after (route B) installation of the diethyl methylenephosphonate ester moiety. Deprotections of **178a-b**, **182a-b** and **183a-b** would then yield the free phosphonic acids. The phosphonic acids are anticipated to be highly hygroscopic and therefore they will be treated with cyclohexylamine to afford the target compounds **173a-b** and **174a-b** as non-hygroscopic salts.



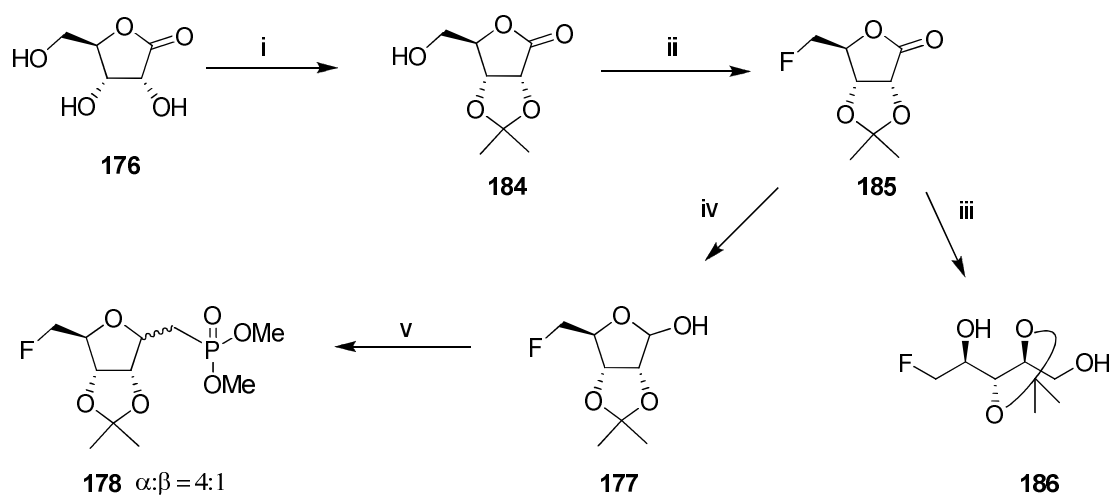
Scheme 3.8 Synthetic routes for the preparation of phosphonates **173a-b** and **174a-b**. Route A starts with D-ribonic lactone and route B starts with D-ribose.

3.7.2 Preparation of phosphonate **173a-b** and **174a-b**

At first glance, route A appears to offer the shorter synthetic route, since the involvement of a protection/deprotection step of the 5-hydroxyl group is not required. Accordingly, route A was explored at the outset.

3.7.2.1 The D-ribonic- γ -lactone route-Route A.

The synthetic route (Route A Scheme 3.9) started with the protection of D-ribonic- γ -lactone **176** as its acetonide to generate 2,3-isopropylidene **184**.²¹ Fluorination of the free 5-hydroxyl group of **184** was accomplished directly with Deoxo-fluorTM to afford 5-deoxy-5-fluoro-2,3-isopropylidene-D-ribonic- γ -lactone (**185**) in good yield. Subsequent reduction of lactone **185** with NaBH₄ resulted in the generation of (2*S*,3*R*,4*S*)-5-fluoro-2,3-(*O*-isopropylidenedioxy)-pentan-1,4-diol (**186**). Diol **186** has previously been synthesised,²² however this route appears to offer a more efficient preparation. Reduction of **185** with limiting NaBH₄ (0.5 eq.) was found to be incomplete with only about 60% of the lactone **185** converted to the desired product, along with the diol **186**, in a ratio of 1:5 as determined by ¹⁹F NMR (Figure 3.4). Reduction of **185** with DIBAL-H at -78 °C and at -40 °C failed to give the desired product,²³ and only starting material were recovered in each case. However at the elevated temperature (40 °C), DIBAL-H²⁴ smoothly reduced the lactone **185** to 5-fluoro-ribofuranoside **177**, in good yield.



Scheme 3.9 Synthetic route A. *Reagent and conditions:* i) Acetone, cH_2SO_4 (cat.), 6h, 86%; ii) Deoxo-fluorTM, DCM, 40°C, 30 min, 84%; iii) NaBH_4 , ethanol, 0°C, 2 h, 65%; iv) DIBAL-H, toluene, 40°C, 64%; v) $\text{CH}_2[\text{P}(\text{O})(\text{OMe})_2]_2$, DCM, 50% aq.NaOH, 60%.

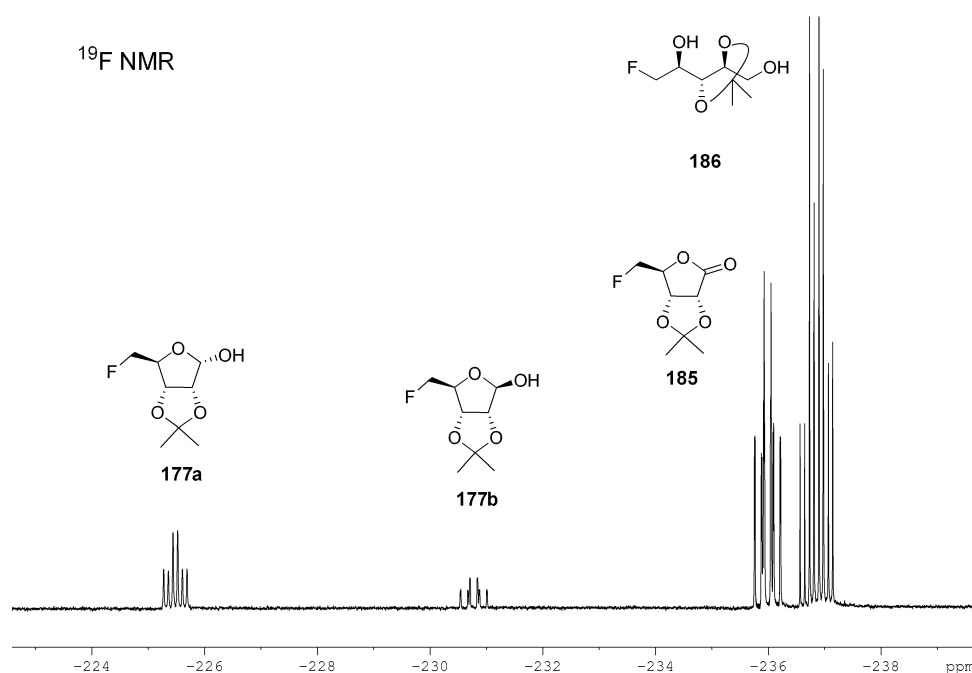
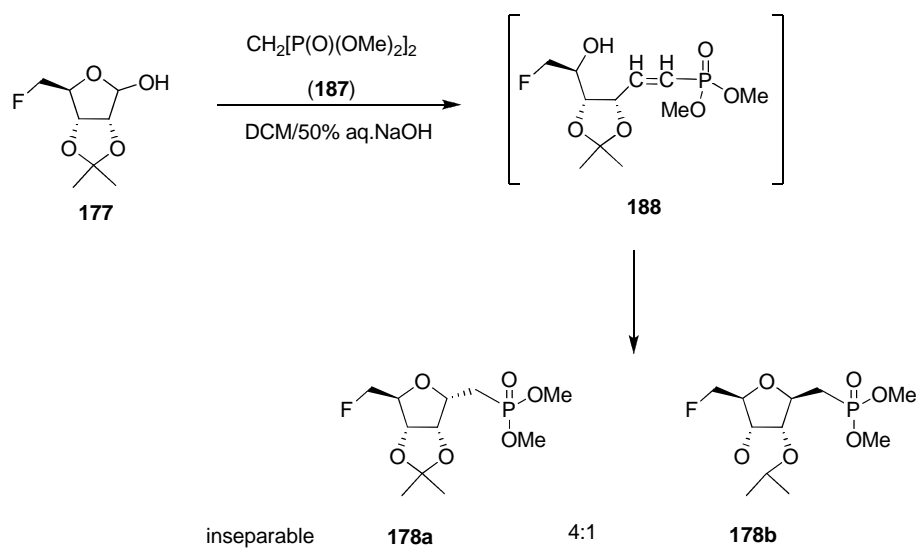


Figure 3.4 ¹⁹F NMR of the product obtained when lactone **185** was treated with NaBH₄ (0.5 eq.) at 40 °C.

The next step involved a Wadsworth-Emmons reaction of **177** with tetramethyl methylenediphosphonate (**187**) in DCM/50% aq. NaOH.²⁵ This gave a clean reaction to yield the 5-fluoro-phosphonate **178** which had an α : β ratio of 4:1 as determined by ¹⁹F and ³¹P NMR (Figure 3.5). The reaction is believed to generate an intermediate olefin **188**, which subsequently undergoes a Michael-type addition to give the cyclic methylenephosphonates **178a-b** (Scheme 3.10). Unfortunately, the diastereoisomers were inseparable by conventional chromatography.



Scheme 3.10 Formation of an anomeric mixture of phosphonates **178a** and **178b** via a Wadsworth-Emmons reaction.

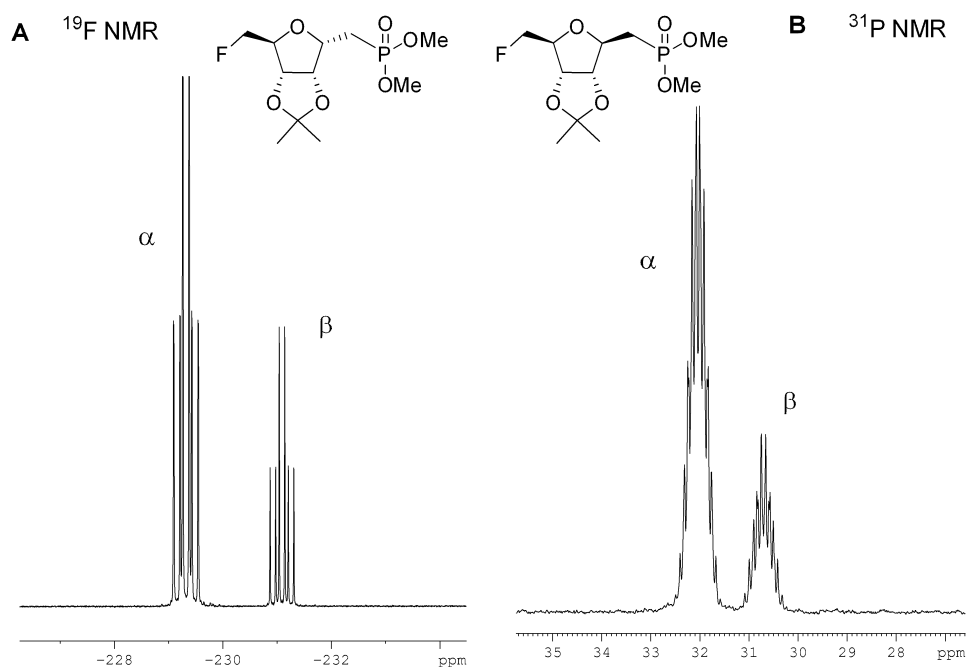
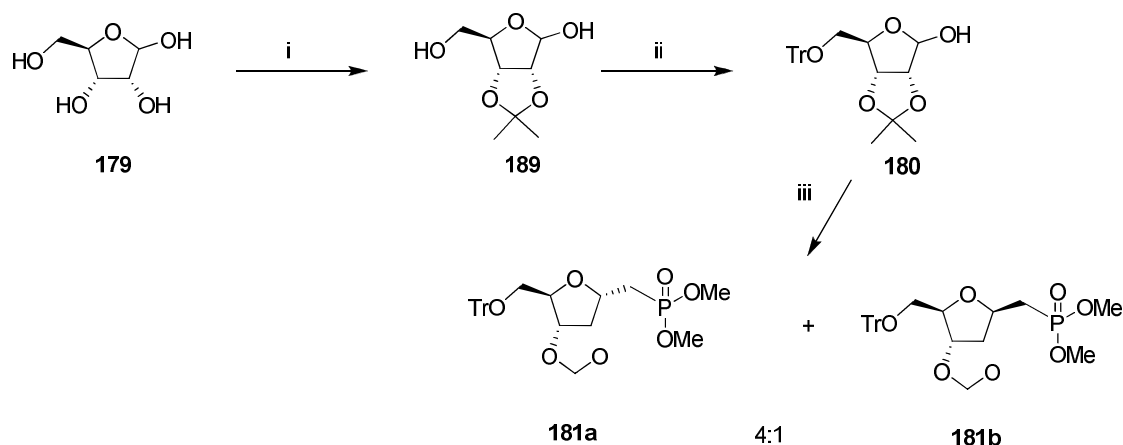


Figure 3.5 A) ^{19}F and B) ^{31}P NMR of the phosphonate **178** showing the α : β ratio as 4.1.

3.7.2.2 The D-ribose route – Route B

Due to the inability to separate α -**178** from β -**178**, Route B (Scheme 3.11) was explored as an alternative. Following the previously described protocol by Meyer *et.al.*,²⁵ the free hydroxyl group at C5 of 2,3-isopropylidene-D-ribose (**189**) was now protected as a trityl group after treating **189** with trityl chloride and DMAP. This gave **180** with an epimer ratio (α : β) of 1:2.5 as determined by ^1H NMR spectroscopy. In a similar manner to Route A, the dimethyl methylenephosphonate ester moiety was installed by a Wadsworth-Emmons protocol to obtain 5-*O*-trityl-phosphonates **181a** and **181b** as individual epimers, after chromatographic separation of the initial product mixture (α : β of 4:1, Figure 3.6). Apparently, the bulky 5-OTr group influences the anomeric ratio of **181** favouring the α -epimer over the β -epimer, as previously shown by Ohrui *et al.*²⁶



Scheme 3.11 Preparation of phosphonates **181a-b** via a Wadsworth-Emmons reaction. *Reagents and conditions:* i) Acetone, CH_2SO_4 (cat.), 4 h, 90%; ii) TrCl , pyridine, DMAP, rt, 16h, 94%; iii) $\text{CH}_2[\text{P}(\text{O})(\text{OMe})_2]_2$, 50% aq. NaOH; DCM, 64%;

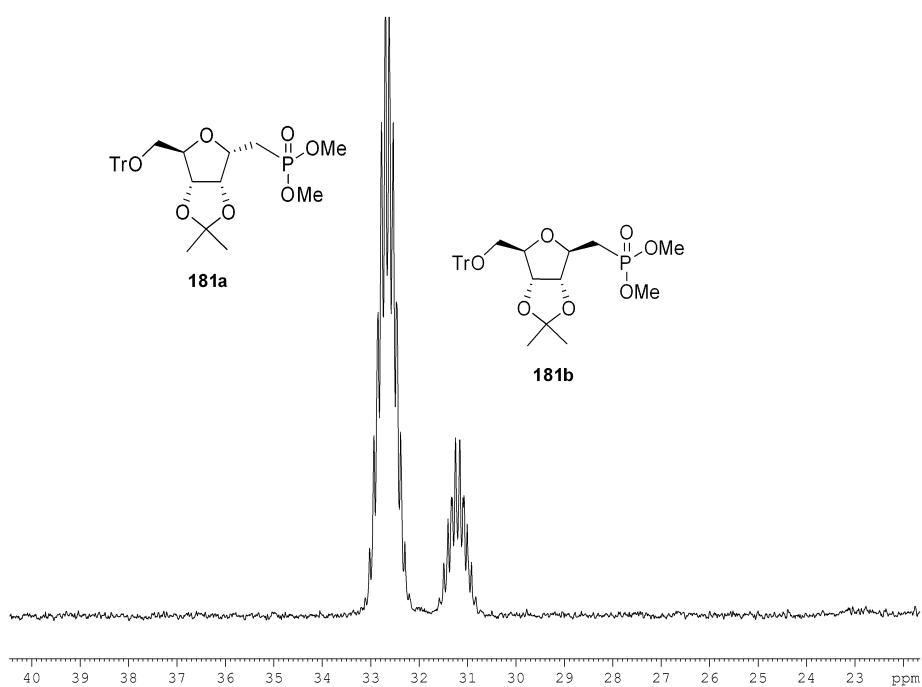


Figure 3.6 ^{31}P NMR of **181a/181b** product mixture indication an $\alpha:\beta$ ratio of 4:1.

The ^1H NMR of the α -**181** and β -**181** epimers was assigned based on a NOSEY experiment (Figure 3.7 and 3.8). Selective irradiation of H-3 of **181a** resulted in an enhancement of the H-2 signals (Figure 3.7), corresponding to the α -epimer whereas irradiation of the H-3 proton of **181b** resulted in an enhancement of the H-1 signals (Figure 3.8). These results are consistent with literature.²⁵

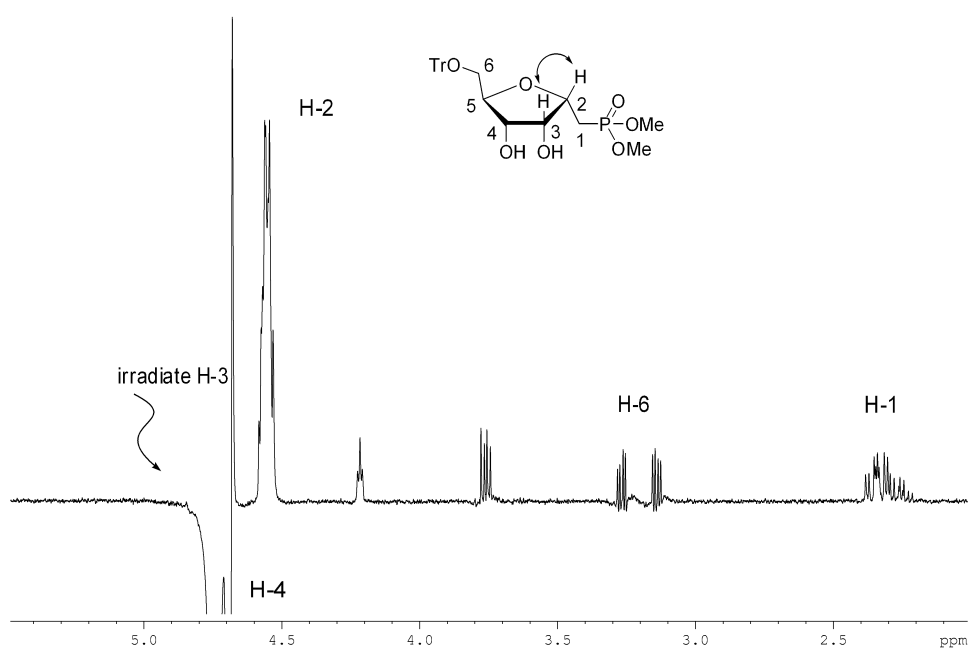


Figure 3.7 ^1H NMR NOE experiment showing the correlation between H-2 and H-3 in **181a**.

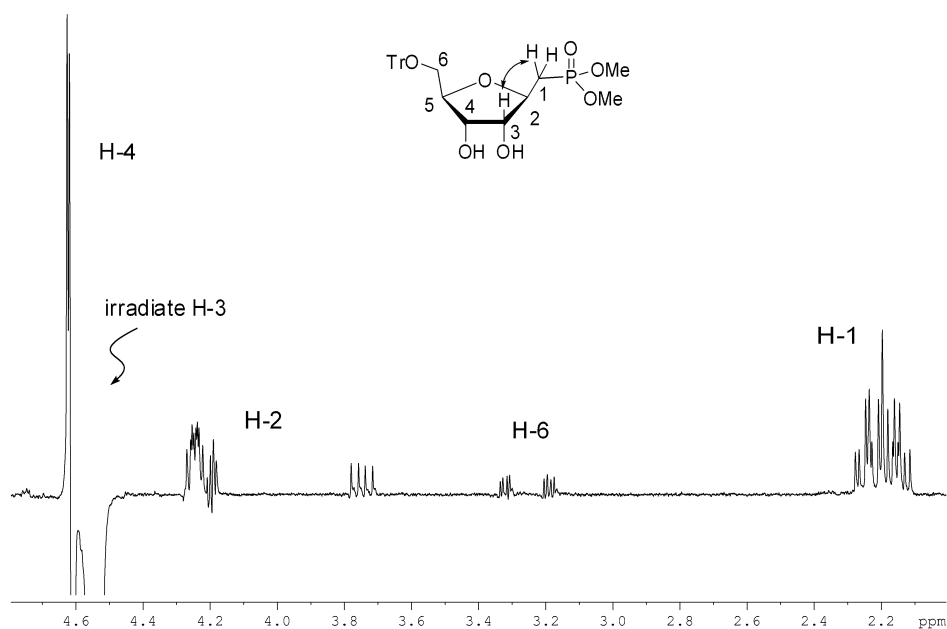


Figure 3.8 ^1H NMR NOE experiment showing the correlation between H-1 and H-3 in **181b**.

For the next step, selective deprotection of the 5-OTr was explored (Schemes 3.12 and 3.13). Detritylation of **181a-b** with formic acid is reported to efficiently remove the trityl group from C5 of some similarly protected carbohydrates and nucleic acids.²⁷ However, this proved to be ineffective in this case. However, deprotection was achieved by treatment of **181** with ZnCl_2 ²⁸ to generate the 5-hydroxy phosphonates **182a** and **182b** in a good yield. The free alcohol of both epimers was then directly fluorinated by using tosylfluoride and TBAF under refluxing THF.^{29, 30} Finally phosphonate esters, **182a-b**, and the 5-deoxy-5-fluoro **183a-b** were sequentially deprotected with TMSBr and then TFA/ H_2O to yield the free phosphonic acids. These phosphonic acids were dissolved in water and the pH of the solution was adjusted to ~11 with cyclohexylamine.³¹ After removal of water, the non-hygroscopic salts **173a-b** and **174a-b** were obtained by precipitation from MeOH/acetone. Recrystallisation of the amine salts **173a-b** and **174a-b** from MeOH/acetone was explored. Fortunately, a sample of colourless needles was obtained for phosphonate **174a**. This allowed X-Ray structure analysis to be carried out (Figure 3.9). The resultant crystal structure of **174a** confirmed its structure and its stereochemical relationship to the intermediate ribose-1-phosphate metabolite **47**. Phosphonate **174a** formed a 1:1 salt with the amine in the crystal structure.

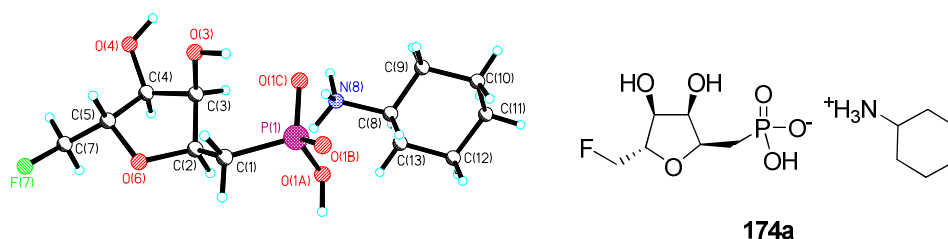
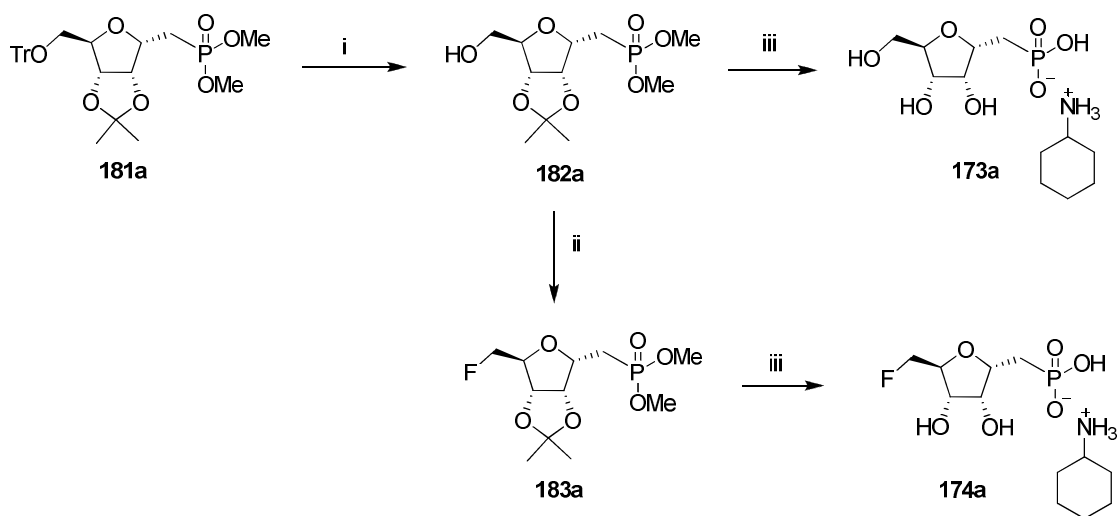
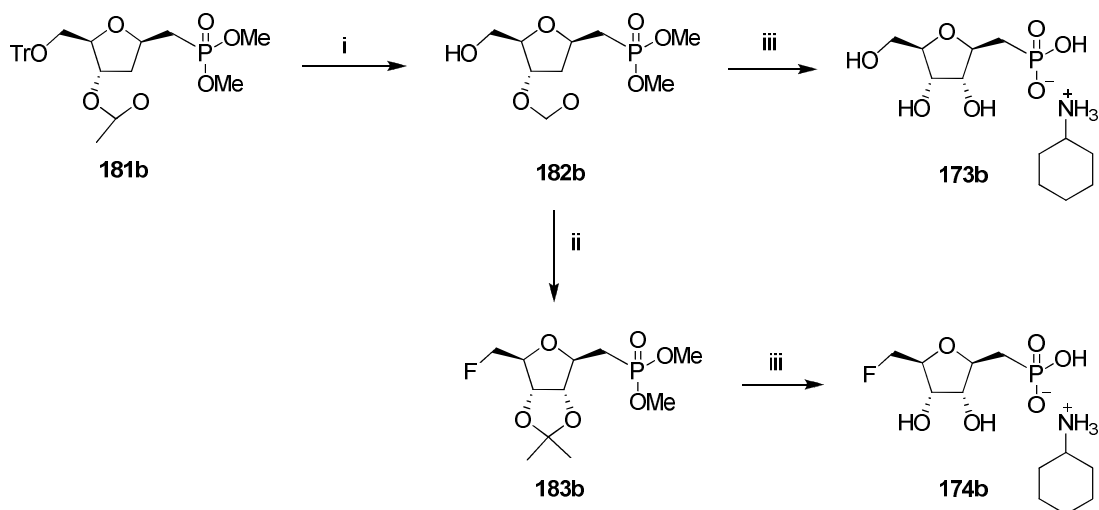


Figure 3.9 X-ray Crystal structure of cyclohexylammonium salt of phosphonate **174a**.



Scheme 3.12 Preparation of **173a** and **174a**; *Reagents and conditions*: i) ZnCl_2 , DCM, rt, 2h, 78-81%; ii) TsF, TBAF, THF, reflux, 16h, 83-92%; iii) a) TMSBr, DCM, rt; b) TFA: H_2O (1:1), c) cyclohexylamine, pH~11, 84-87%;



Scheme 3.13 Preparation of **173b** and **174b**; *Reagents and conditions*: i) ZnCl_2 , DCM, rt, 2h, 78-81%; ii) TsF, TBAF, THF, reflux, 16h, 83-92%; iii) a) TMSBr, DCM, rt; b) TFA: H_2O (1:1), c) cyclohexylamine, pH~11, 84-87%;

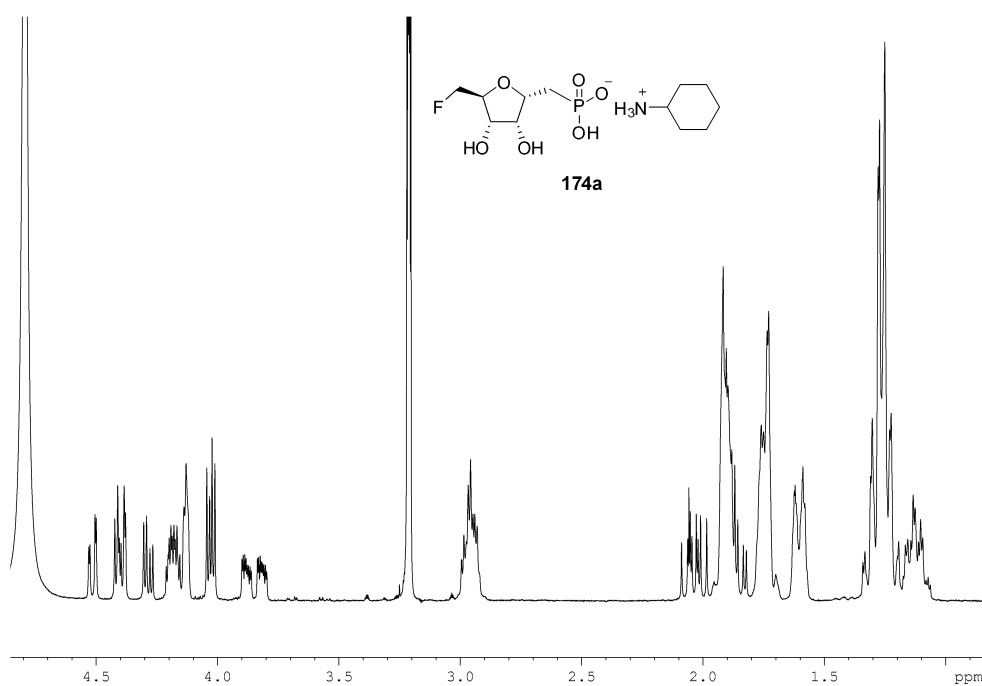


Figure 3.10 ^1H NMR of the amine salt **174a**.

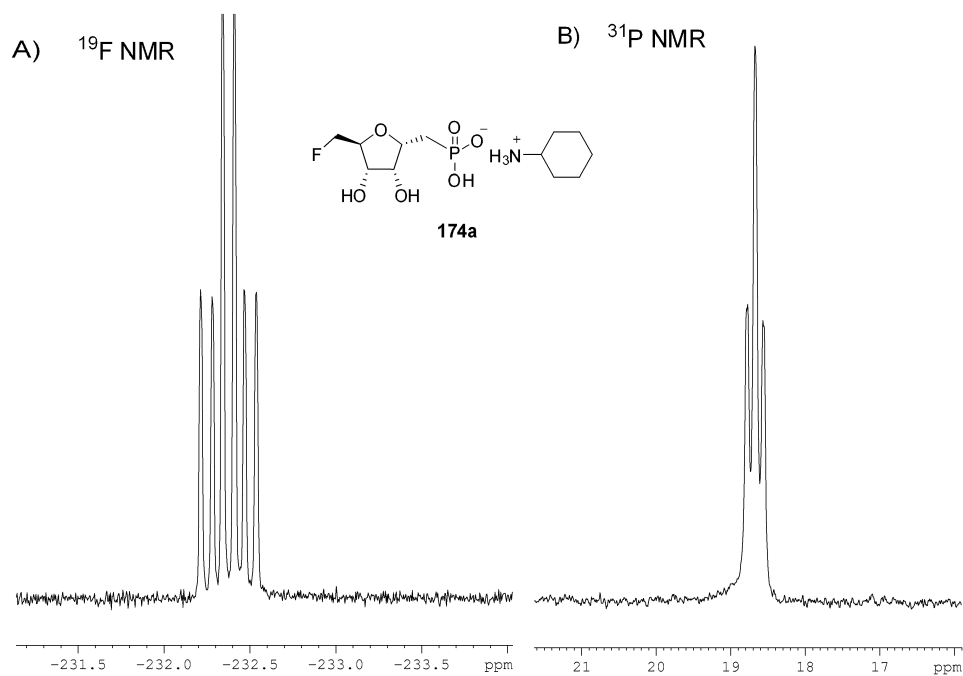
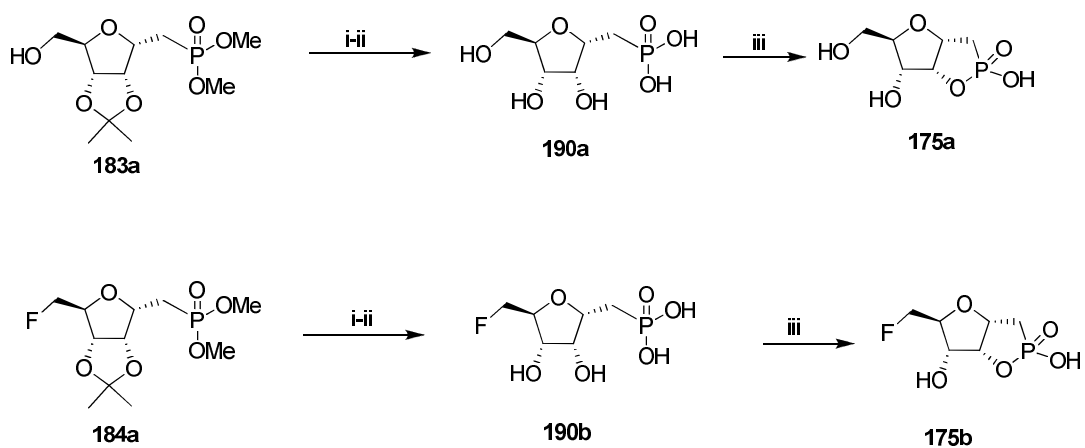


Figure 3.11 A) ^{19}F NMR and B) ^{31}P NMR of the amine salt **174a**.

3.7.2.3 Preparation of phostones **175a** and **175b**

In order to prepare the phostonic acids **175a**, phosphonate **182a** was treated with TMSBr, followed by TFA:H₂O to give the phosphonic acid **190a** (Scheme 3.14). The phosphonic acid was then treated with acetic anhydride in dry pyridine to afford the cyclic phostone **175a**.³² The conversion from phosphonic acid to a 5-membered ring phostonic acid could be conveniently followed by a change in the ³¹P-NMR resonance from 27 ppm (phosphonate) to 44 ppm (Figure 3.12), characteristic of a 5-membered ring phostone.^{31, 33, 34} The product was also confirmed by HRMS. Purification by chromatography allowed the recovery of phostone **175a** as a white amorphous solid in moderate yield. By treating the 5-fluoro phosphonate **183a** in a similar manner, the 5-fluoro phostone **175b** was similarly obtained as a white amorphous solid. Attempts to recrystallise **175a** and **175b** from acetone/MeOH or EtOAc/MeOH were unfortunately unsuccessful. With these compounds in hand inhibition assay was conducted with the 5-FDRP isomerase enzyme.



Scheme 3.14 Preparation of phostone **175a-b**; *Reagents and conditions*: i) TMSBr, DCM, rt; ii) TFA:H₂O (1:1), iii) Ac₂O, pyridine, 16h, 40-47%.

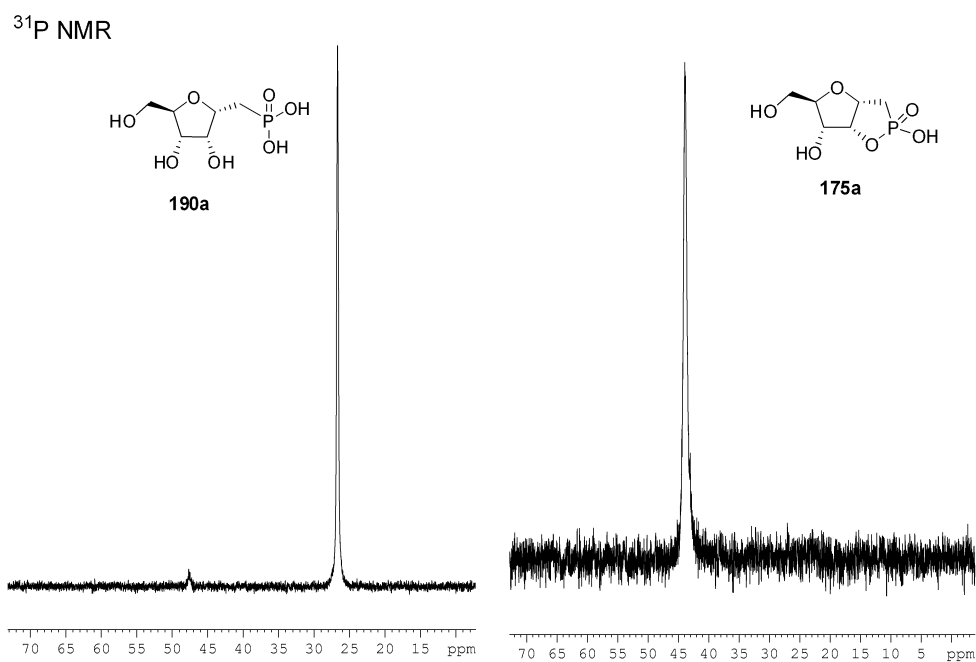


Figure 3.12 ³¹P NMR of phosphonic acid (**190a**) and cyclic phosphonic (phostone, **175a**).

3.7.3 Bioassay results

Incubation with 5-FDRP isomerase

Incubation assays of the phosphonate salt **173a-b** and **174a-b** with the *S. cattleya* 5-FDRP isomerase from *S. cattleya* were performed in our research group by Dr. S. Cross. In each assay, the *S. cattleya* isomerase was incubated with its natural substrate 5-FDR-1-P (**47**) and then the appropriate phosphonate was added. The reaction was conveniently monitored by ^{19}F NMR. 5-FDR-1-P (**47**) shows a signal at -231.4 ppm whereas the product 5-FDRuIP (**48**) exhibits a signal at -231.8 ppm. In the event, incubation with the phosphonate salts **173a-b** and **174a-b** did not show any inhibitory effect on the isomerisation reactions (Figure 3.13) even at 4 mM concentrations. In all cases, the conversions of **47** to **48** were similar to that of the control experiment.

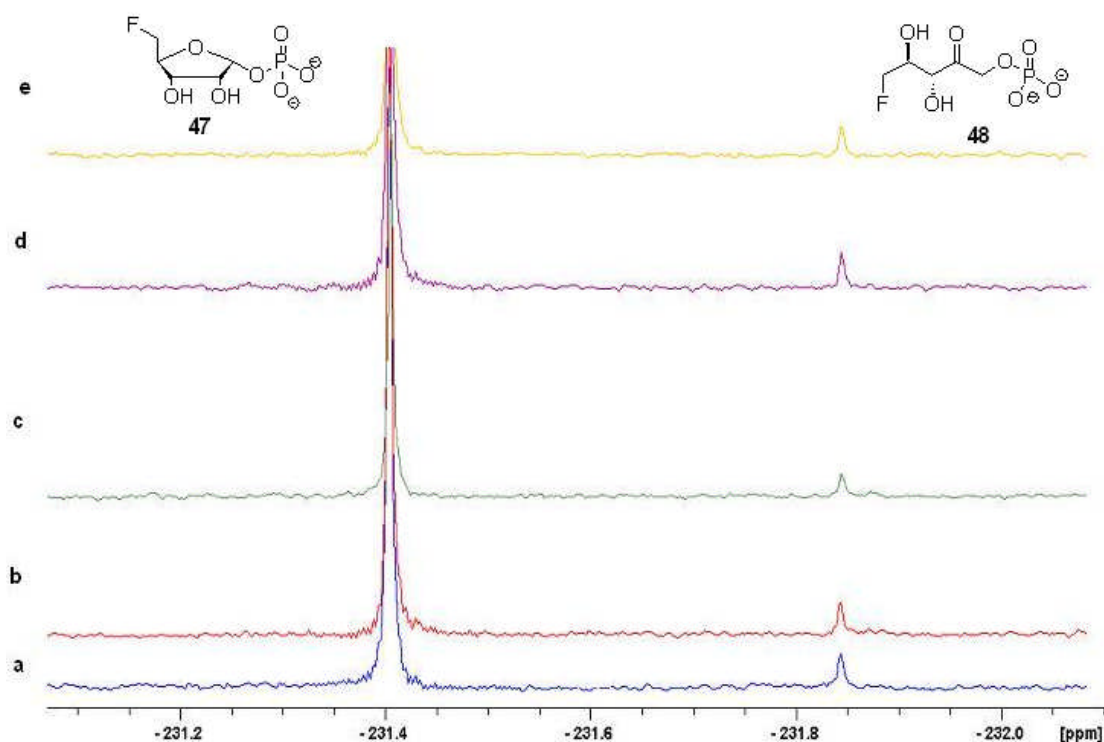


Figure 3.13 Incubation of 5-FDRP isomerase with 5-FDRP (**47**) and the synthetic phosphonates: a) Control; b) with **173a**; c) with **173b**; d) with **174a**; e) with **174b**. There was no apparent inhibitory effect with any of the phosphonates.

Phostones **175a** and **175b** are currently being employed to explore crystal structures of the *S. cattleya* 5-FDRP isomerase by co-crystallisation. Also the phosphonates **173a-b** and **174a-b** will be used to co-crystallise with the 5-FDRP isomerase in an attempt to explore their binding and interactions to the surface of the enzyme in the University of St Andrews.

3.8 Conclusions

Synthetic phosphonate analogues of D-ribose-1-phosphate phosphonate **173a-b** and **174a-b** have been successfully synthesised. Incubations of the phosphonates **173a-b** and **174a-b** with the 5-FDRP isomerase have shown that these phosphonates were not inhibitors of the isomerase at 4mM concentration. However, these analogues are currently being used to explore co-crystallisation studies with the enzyme to try to obtain a structure with a cyclic substrate.

The photones **175a-b** were designed based on a putative phosphate migration mechanism for the isomerisation of 5-FDRP (**47**) to 5-FDRulP (**48**). These photones were considered as potential inhibitors for the 5-FRRP isomerase enzyme with potential utility as tools to explore the mechanism of this biosynthetic enzyme. Their co-crystallisation is on going.

3.9 References

1. H. Deng, D. O'Hagan and C. Schaffrath, *Nat. Prod. Rep.*, 2004, **21**, 773-784.
2. J. S. Kahan, F. M. Kahan, R. Goegelman, S. A. Currie, M. Jackson, E. O. Stapley, T. W. Miller, A. K. Miller, D. Hendlin, S. Mochales, S. Hernandez, H. B. Woodruff and J. Birnbaum, *J. Antibiot.*, 1979, **32**, 1-12.
3. M. Sanada, T. Miyano, S. Iwadare, J. M. Williamson, B. H. Arison, J. L. Smith, A. W. Douglas, J. M. Liesch and E. Inamine, *J. Antibiot.*, 1986, **39**, 259-265.
4. H. Deng, S. M. Cross, R. P. McGlinchey, J. T. G. Hamilton and D. O'Hagan, *Chem. Biol.*, 2008, **15**, 1268-1276.
5. D. O'Hagan, C. Schaffrath, S. L. Cobb, J. T. G. Hamilton and C. D. Murphy, *Nature*, 2002, **416**, 279.
6. C. Schaffrath, H. Deng and D. O'Hagan, *FEBS Lett.*, 2003, **547**, 111-114.
7. H. Deng, S. L. Cobb, A. R. McEwan, R. McGlinchey, J. H. Naismith, D. O'Hagan, D. A. Robinson and J. B. Spencer, *Angew. Chem. Int. Ed.*, 2006, **45**, 759-762.
8. S. L. Cobb, H. Deng, J. T. G. Hamilton, R. P. McGlinchey and D. O'Hagan, *Chem. Commun.*, 2004, 592-593.
9. M. Onega, R. P. McGlinchey, H. Deng, J. T. G. Hamilton and D. O'Hagan, *Bioorg. Chem.*, 2007, **35**, 375-385.
10. S. J. Moss, C. D. Murphy, J. T. G. Hamilton, W. C. MaRoberts, D. O'Hagan, C. Schaffrath and D. B. Harper, *Chem. Commun.*, 2000, 2281-2282.
11. C. D. Murphy, S. J. Moss and D. O'Hagan, *Appl. Environ. Microbiol.*, 2001, **67**, 4919-4921.

12. C. Schaffrath, C. D. Murphy and D. O'Hagan, *Angew. Chem. Int. Ed.*, 2001, **40**, 4479-4481.
13. F. R. Tabita, T. E. Hanson, H. Li, S. Satagopan, J. Singh and S. Chan, *Microbiol. Mol. Biol. Rev.*, 2007, **71**, 576-599.
14. H. Ashida, Y. Saito, C. Kojima, K. Kobayashi, N. Ogasawara and A. Yokota, *Science*, 2003, **302**, 286-290.
15. T. E. Hanson and F. R. Tabita, *Proc. Natl. Acad. Sci. USA*, 2001, **98**, 4397-4402.
16. Y. Saito, H. Ashida, C. Kojima, H. Tamura, H. Matsu, Y. Kai and A. Yokota, *Biosci. Biotechnol. Biochem.*, 2007, **71**, 2021-2028.
17. H. Tamura, Y. Saito, H. Ashida, T. Inoue, Y. Kai, A. Yokota and H. Matsumura, *Protein Sci.*, 2008, **17**, 126-135.
18. J. Wrey and R. H. Abeles, *J. Biol. Chem.*, 1995, **270**, 3147-3153.
19. E. S. Furfine and R. H. Abeles, *J. Biol. Chem.*, 1988, **263**, 9598-9606.
20. T. D. Fenn, D. Ringe and G. A. Petsko, *Biochemistry*, 2004, **43**, 6464-6467.
21. A. A. Kandil and K. N. Slessor, *J. Org. Chem.*, 1985, **50**, 5649-5662.
22. D. T. Fox and C. D. Poulter, *J. Org. Chem.*, 2005, **70**, 1978-1985.
23. F. Freeman and K. D. Robarge, *Carbohydr. Res.*, 1985, **137**, 89-97.
24. S. J. Baker and D. W. Young, *J. Labelled Cpd. Radiopharm.*, 2000, **43**, 1023-1032.
25. R. B. Meyer, T. E. Stone and P. K. Jesthi, *J. Med. Chem.*, 1984, **27**, 1095-1098.
26. H. Ohrui, G. H. Jones, J. G. Moffatt, M. L. Maddox, A. T. Christensen and S. K. Byram, *J. Am. Chem. Soc.*, 1974, **97**, 4602-4613.
27. M. Bessodes, D. Komiotis and K. Antonakis, *Tetrahedron Lett.*, 1986, **27**, 579-580.

28. V. Kohli, H. Blocker and H. Koster, *Tetrahedron Lett.*, 1980, **21**, 2683-2686.
29. M. Shimizu, Y. Nakamura and H. Yoshioka, *Tetrahedron Lett.*, 1985, **26**, 4207-4210.
30. T. D. Ashton and P. J. Scammells, *Bioorg. Med. Chem. Lett.*, 2005, **15**, 3361-3363.
31. R. W. McClard and J. F. Witte, *Bioorg. Med. Chem. Lett.*, 1994, **4**, 1537-1538.
32. M. Bosco, P. Bisseret and J. Eustache, *Tetrahedron Lett.*, 2003, **44**, 2347-2349.
33. R. W. McClard and J. F. Witte, *Bioorg. Chem.*, 1990, **18**, 165-178.
34. M. Morr, C. Kakoschke and L. Ernst, *Tetrahedron Lett.*, 2001, **42**, 8841-8843.

Chapter 4

Synthesis of potential DXR inhibitors

4.1 Introduction

Isoprenoids are one of the most abundant, diverse and important families of naturally occurring compounds found in nature. They contribute to biological functions including electron transport in respiration and photosynthesis (ubiquinone (**191**), plastoquinone (**192**), the phytol residue (**193**) of chlorophyll and carotenoids), and growth and development regulation (vitamin A, D, E (**194**), K; steroid hormone; phytohormone; abscisic acid (**195**), insect juvenile hormones). In addition, isoprenoids constitute a structural component of cell membranes (hopanoid (**196**) in prokaryote and cholesterol (**39**) in eukaryotes).^{1, 2} The fundamental precursors of isoprenoids are C-5 units derived from isopentenyl pyrophosphate (IPP, **197**) and dimethylallyl pyrophosphate (DMAPP, **198**). These precursors originate from two different biosynthetic pathways, the mevalonic acid (MVA) and methylerythritol phosphate (MEP) pathways. The classic mammalian pathway to the steroids proceeds *via* mevalonic acid as a key intermediate, the so-called the MVA pathway. This pathway had been known since the 1950s and for many years it was assumed to be the sole pathway used for isoprenoid biosynthesis in all organisms.³

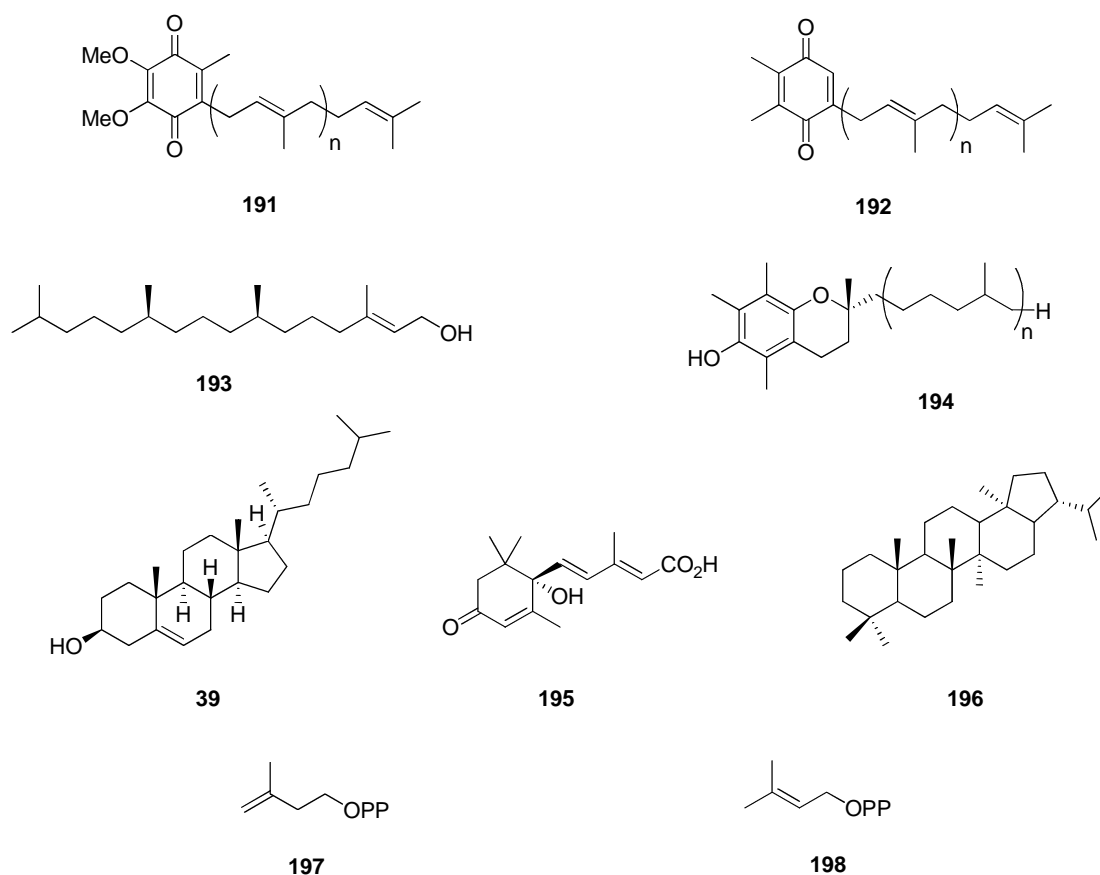


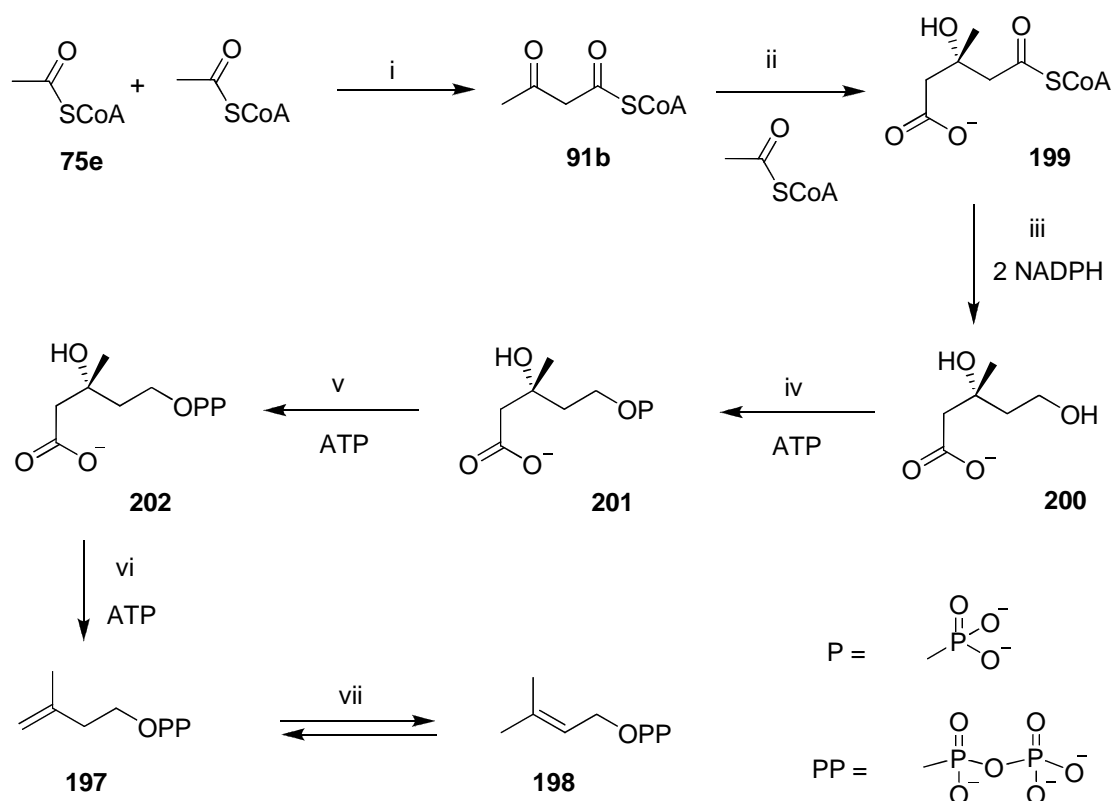
Figure 4.1 Example of isoprenoids; ubiquinone (**191**), plastoquinone (**192**), phytol (**193**), vitamin E (**194**), cholesterol (**39**), abscisic (**195**), and hopane (**196**) and the biosynthetic precursors IPP (**197**) and DMAPP (**198**)

In the early 1990's an alternative biosynthetic pathway was discovered.⁴ This novel pathway proceeds *via* the key intermediate methylerythritol phosphate, the so-called MEP pathway (or DOXP, the first substrate of the pathway). It was found to operate in eubacteria, all photosynthetic organisms such as higher plants, and algae, as well as in cyanobacteria and diatoms.⁵⁻⁸ In addition, the MEP pathway is also found operating in *Plasmodium falciparum*,⁹ the malaria parasite, and it is utilised by *Mycobacterium tuberculosis*. However the MEP pathway is not functional in humans, animals and archaeobacteria.³

4.2 Biosynthesis of the isoprenoid precursors IPP and DMAPP

4.2.1 The mevalonic acid pathway (MVA pathway)¹

The biosynthesis of IPP and DMAPP *via* the MVA pathway (Scheme 4.1) starts with a Claisen condensation between two molecules of acetyl-CoA (**75e**) to generate acetoacetyl-CoA (**91b**). A third molecule of acetyl-CoA condenses *via* an aldol addition to form the branched chain ester, β -hydroxy- β -methylglutaryl-CoA (HMG-CoA, **199**). Reduction of HMG-CoA generates mevalonic acid (**200**), a transformation catalysed by HMG-CoA reductase. This step is the rate determining step of the MVA pathway. The last two steps involve sequential phosphorylation where two ATP molecules generate a diphosphate (**202**), which is then combined with a third ATP, followed by decarboxylation to generate IPP (**197**). The resulting IPP is then isomerised to DMAPP (**198**) by the action of an IPP isomerase enzyme.

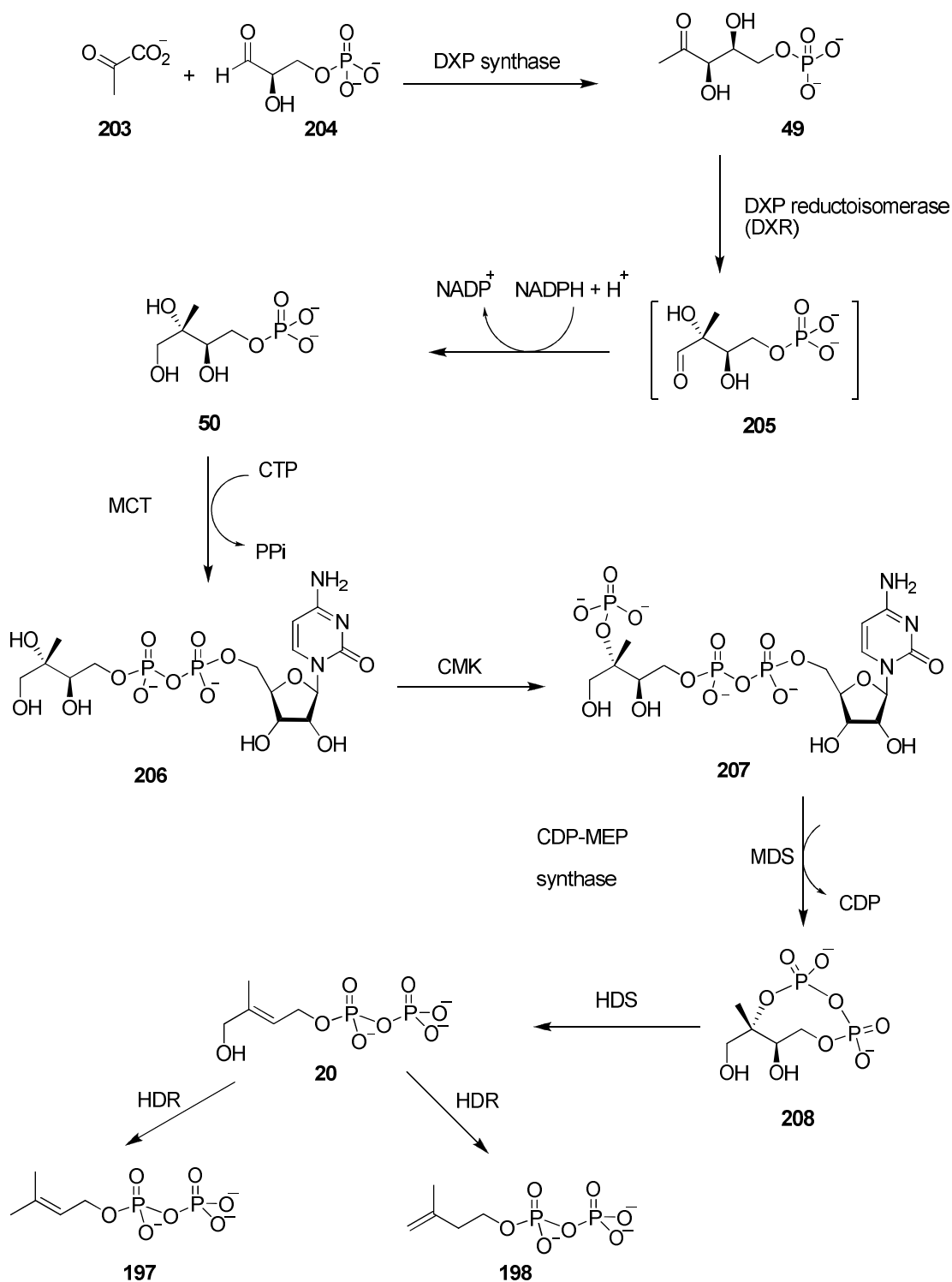


Scheme 4.1 The biosynthesis of IPP (**197**) and DMAPP (**198**) *via* the MVA pathway, showing the enzymes involved; i) acetoacetyl CoA thiolase; ii) HMG-CoA synthase; iii) HMG-CoA reductase; iv) mevalonate kinase; v) phosphomevalonate kinase; vi) mevalonate 5-phosphate decarboxylase; vii) IPP isomerase.

4.2.2 The 2-C-methyl-D-erythritol 4-phosphate pathway or 1-deoxy-D-xylulose 5-phosphate pathway (the MEP or DOXP pathway).

The biosynthesis of isoprenoids *via* the alternative non-mevalonate pathway comprises seven enzymatic reaction steps which are catalysed by eight enzymes (Scheme 4.2). The initial step is the formation of 1-deoxy-D-xylulose 5-phosphate (DXP, **49**) by condensation of pyruvate (**203**) and glyceraldehyde 3-phosphate (**204**). This step is catalyzed by the thiamine-dependent enzyme, DXP synthase (DXS, EC

2.2.1.7).^{10, 11} The DXP also serves as a biosynthetic precursor of vitamins B₁ (thiamine) and B₆ (pyridoxal).¹² The second biosynthetic step involves the conversion of **49** to the branched chain polyol, 2-*C*-methyl-D-erythritol 4-phosphate (MEP, **50**). A pinacol-like rearrangement of **49** generates a transient intermediate 2-*C*-methyl-D-erythrose 4-phosphate (**205**) which is then converted to MEP by delivery of the *pro-S* hydrogen of NADPH to the *re* face of aldehyde intermediate **205**. This biotransformation step is a reversible process^{13, 14} and is mediated by the enzyme DXP reducto-isomerase (DXR, EC 1.1.1.267).¹⁵ In the third step, 4-diphosphocytidyl-2-*C*-methyl-D-erythritol (CDP-MEP, **206**)^{16, 17} is formed from the reaction of MEP with CTP, which is catalyzed by the ATP-dependent enzyme, 2-*C*-methyl-D-erythritol-4-phosphate cytidyltransferase (MCT, EC 2.7.7.60). The CDP-MEP (**206**) is then converted to 4-diphosphocytidyl-2-*C*-methylerythritol 2-phosphate (**207**)^{18, 19} by an ATP-dependent enzyme, 4-(cytidine5-diphospho)-2-*C*-methyl-erythritol kinase (CMK, EC 2.7.1.148). In the fifth step intermediate **207** is converted to MECP (**208**),^{20, 21} catalysed by 2-*C*-methyl-D-erythritol-2,4-cyclodiphosphate synthase (MDS, EC 4.6.1.12). In the last two steps, the cyclic diphosphate **208** undergoes consecutive reduction and then elimination to form 1-hydroxy-2-methyl-2-(*E*)-butenyl 4-diphosphate (HMBPP, **209**).²² NADPH dependent 2-methyl-2-(*E*)-butenyl diphosphate reductase (HDR, EC 1.17.1.2) then converts intermediate **209** to IPP and DMAPP.^{23, 24} Most of these enzymes have now had their X-ray structures solved.²⁵



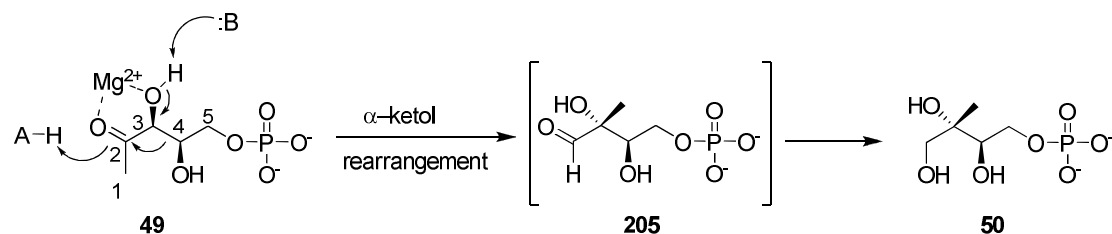
Scheme 4.2 Summary of the biosynthesis of DMAPP (**197**) and IPP (**198**) via the MEP pathway.

4.3 The rearrangement of DXP to MEP

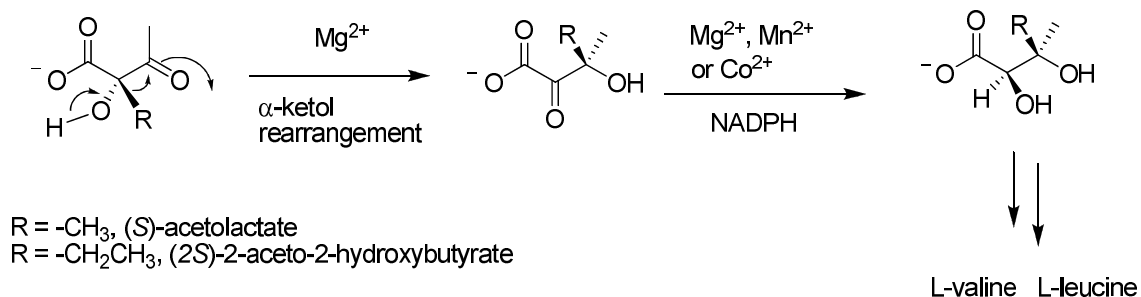
4.3.1 The proposed mechanism of the rearrangement of DXP to MEP^{7, 13, 26}

4.3.1.1 α -Ketol rearrangement

The conversion of DXP to MEP, the first step of the MEP pathway, involves an intramolecular rearrangement process. This α -ketol rearrangement (Scheme 4.3) is initiated by deprotonation of the hydroxyl group at C3 of DXP (**49**), followed by a migration of the C4-C5 phosphate-bearing subunit to C2, generating the transient intermediate methylerythrose phosphate (**205**). Subsequent reduction of **205** by NADPH then delivers MEP (**50**). It is noteworthy that C3 of **49** is rehybridised from sp^3 to sp^2 in its conversion from **205** whilst C4 remains sp^3 hybridised. The α -ketol rearrangement has an analogy with the biosynthesis of the amino acids valine and leucine,²⁷ where α -ketol rearrangements are also involved (Scheme 4.4).



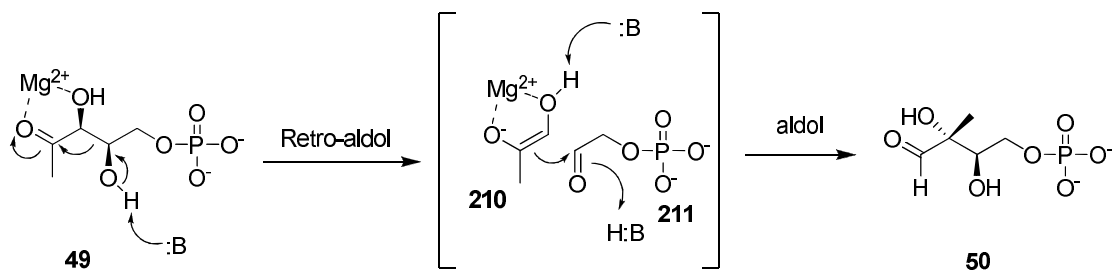
Scheme 4.3 Proposed α -ketol rearrangement mechanism of DXP (**49**) to MEP (**50**).²⁶



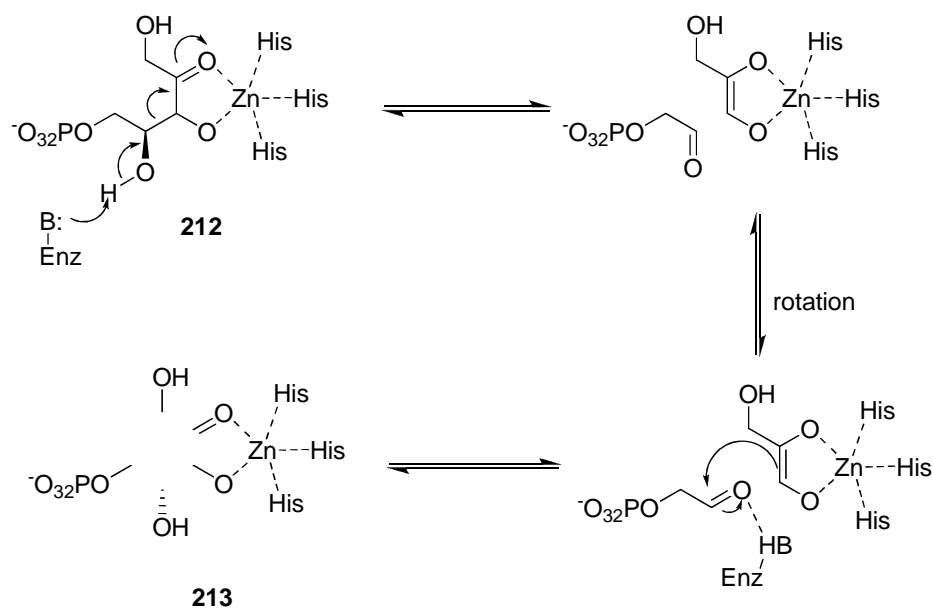
Scheme 4.4 The α -ketol rearrangement reported for acetoxy acid isomeroreductase.²⁷

4.3.1.2 The retro-aldol/aldol rearrangement

The alternative retro-aldol/aldol rearrangement mechanism involves deprotonation of the hydroxyl group at C4 of **49**, followed by cleavage of C3-C4 bond to generate the enolate of hydroxyacetone (**210**) and glycoaldehyde phosphate (**211**). Recombination of fragments **210** and **211** via an aldol reaction generates **205** with a new C-C bond derived from C-2 and C-4 of **49**. In this event, the C3 and C4 carbon atoms are both rehybridised from sp^3 to sp^2 in **205**. Such a reaction has been reported for the epimerization of L-ribulose 5-phosphate (L-Ru5P, **212**) and D-xylulose-5-phosphate (D-Xu5P, **213**) which is catalysed by the enzyme L-ribulose-5-phosphate 4-epimerase.²⁸



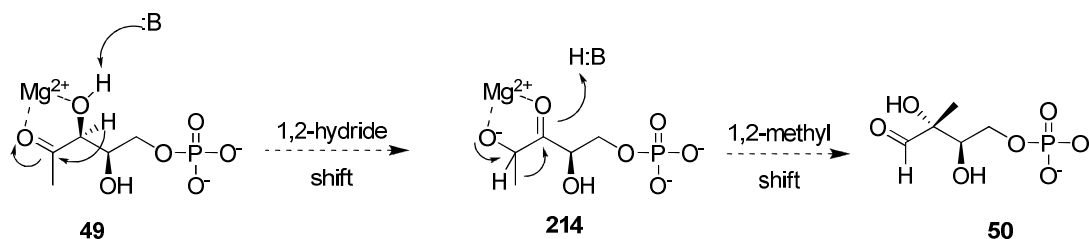
Scheme 4.5 Proposed retro-aldol/aldol rearrangement mechanism of DXP to MEP.



Scheme 4.6 Epimerization between L-ribulose-5-phosphate (L-Ru5P, **212**) and D-xylulose-5-phosphate (D-Xu5P, **213**) via a retro-aldol/aldol mechanism.²⁸

4.3.1.3 Hydride/methyl shift

The third mechanistic hypothesis for this rearrangement involves a 1,2-hydride shift from C3 to C2 to form **214**, followed by a 1,2-methyl shift. However, the results from labelling studies^{7, 13} are inconsistent with this mechanism, so the hydride/methyl migration mechanism is ruled out. Either α -ketol and retro-aldol/aldol mechanisms remain candidates for the rearrangement of DXP to MEP.



Scheme 4.7 Hydride shift mechanism for the rearrangement of DXP to MEP catalysed by DXR. However this mechanism is not supported by isotope labelling studies.

4.3.2 α -Ketol rearrangement or retro-aldol/aldol rearrangement mechanism

In order to differentiate the mechanisms between the α -ketol and retro-aldol/aldol rearrangement mechanisms for the DXP to MEP isomerisation, 3-deoxy and 4-deoxy MEP (**215**, **216**) were explored as inhibitors of DXR.^{13, 29} They were partial inhibitors,¹³ and Proteau found that they were non-competitive inhibitors.²⁹ For the retro-aldol/aldol reaction, the putative fragments, hydroxyacetone (**217**) and glycoaldehyde phosphate (**218**), were incubated with DXR. Neither **217** nor **218** inhibited enzyme catalysis.¹³

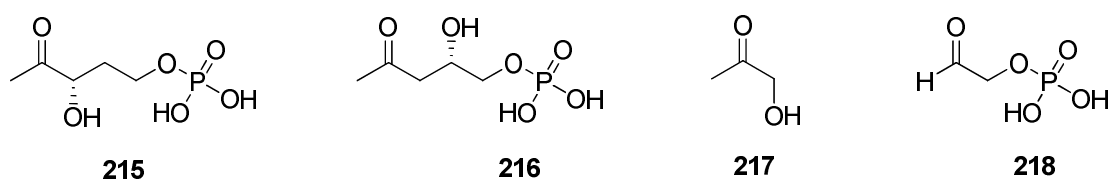


Figure 4.2 The 3-deoxy and 4-deoxy MEP (**215**, **216**) are partial inhibitors of DXR, whereas hydroxyacetone (**217**) and glycoaldehyde phosphate (**218**) are not inhibitors.

Fluorinated analogues of MEP have been analysed as inhibitors of DXR. Both **219** and **220** proved to be inhibitors. Fluorinated analogues with one, two and three fluorines at C1 were also tested with DXR. Interestingly, **221** and **222** were poor

substrates whereas **219** was a good substrate for DXR.³⁰ Incubation of **219** with (4*S*)-[²H]NADPH and DXP showed a normal KIE compared to that of the natural substrate case.³¹

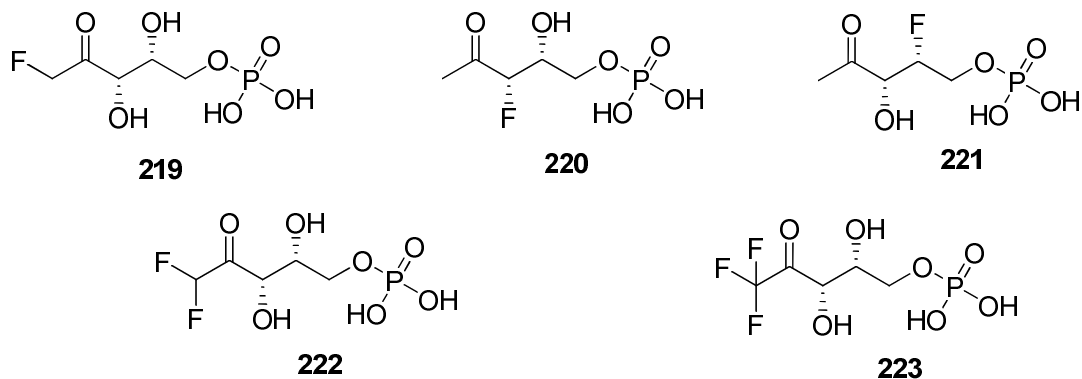


Figure 4.3 Fluorinated analogues of DXP which have been explored as substrates for DXR.

Recently, two independent studies have shown evidence for a retro-aldol/aldol mechanism, as deduced by kinetic isotope labelling studies.^{32, 33} Incubations of [3-²H]DXP (**49a**) and [4-²H]DXP (**49b**) allowed the observation of a secondary KIE on the intramolecular rearrangement process. During the retro-aldol/aldol reaction, both C3 and C4 are rehybridised from sp^3 to sp^2 thus a secondary KIE should be observed for both of these isotopically labelled substrates. On the other hand, only C3 is rehybridised from sp^3 to sp^2 if a α -ketol rearrangement is occurring, so a secondary KIE would be observed only for **49a**.



Figure 4.4 Labelling probes to measure the KIE of the rearrangement of DXP to MEP.

Interestingly, both substrates exhibited similar KIEs during incubations with DXR. These results supported the retro-aldol/aldol reaction mechanism. However, in a separate study an inverse (0.92, 0.86 for **49a** and **49b**)³² and normal secondary KIE (1.04, 1.11 for **49a** and **49b**)³³ was reported. The different KIE observations between these two studies may arise from the purity of the substrates. In the first study, the synthetic route to prepare labelled substrates **49a** and **49b** gave only 74-84% ee. An inverse KIE would be observed if the unlabelled DXP had a lower ee% than that of isotopically labelled substrates.^{29, 33}

4.4 The structure of the DXR enzyme

Four crystal structures of DXR from *E. coli* have been reported. These are the apo-enzyme,³⁴ a binary complex with NADPH,³⁵ a complex with fosmidomycin (**224**) and manganese,³⁶ and a complex with a biphosphonate inhibitor and manganese.³⁷ In addition, a ternary complex of DXR, fosmidomycin and NADPH has also been reported.³⁸ Also the crystal structure of DXR from *Zmomonas mobilis* has recently been reported as has the apoenzyme and a binary complex with NADPH.³⁹

The first reported structure of DXR was the *E. coli* apoenzyme without a bound substrate.³⁴ The structure revealed that the enzyme is present as a homodimer. Each monomer (42-45 kDa) displays a V-like shape (Figure 4.5). This monomer composes three distinct domains: an amino-terminal dinucleotide NADPH binding domain, a central connective domain, and a carboxyl-terminal four helix bundle domain. The connective domain is responsible for dimerisation and harbors most of the active site. A remarkable feature of DXR is its intrinsic flexibility suggesting the necessity to

undergo induced fit upon substrate binding. Residues 186-216 function as a “lid” over the active site, shielding the reactants from the solvent environment.

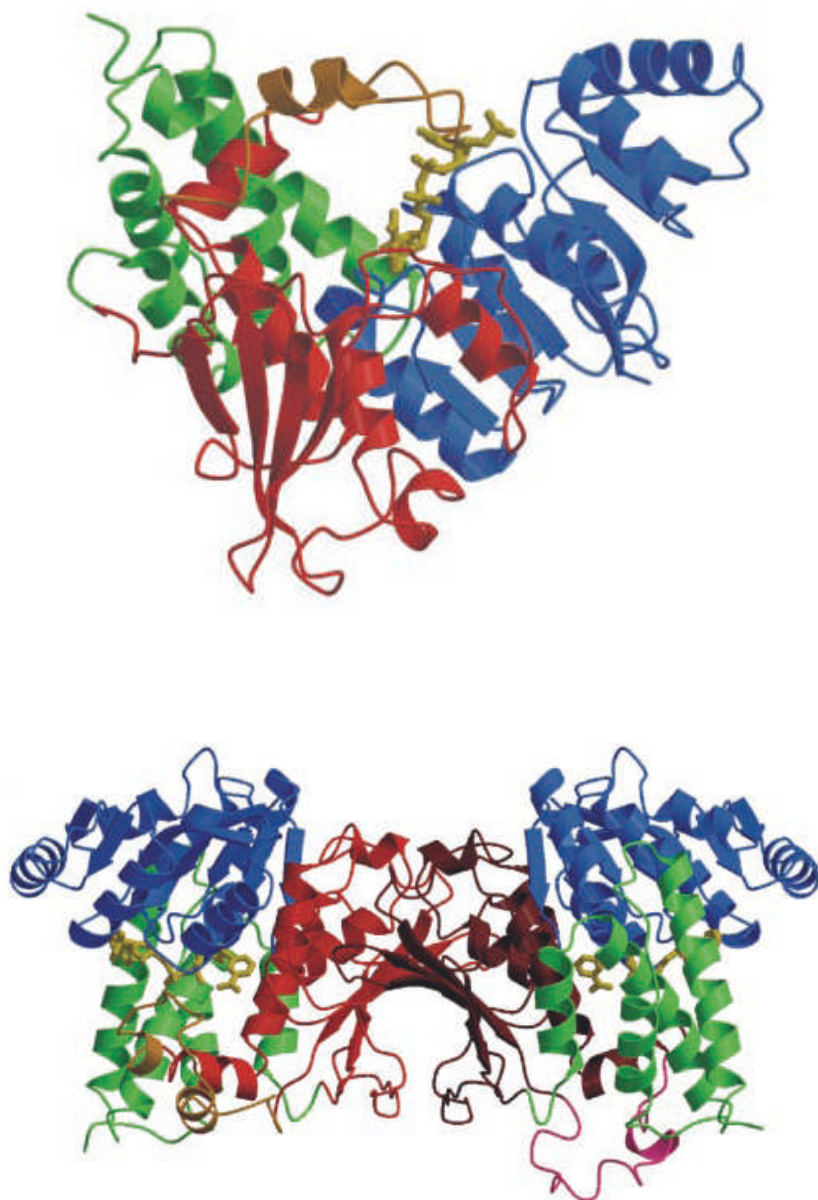


Figure 4.5 A ribbon representation of the DXR; monomer with the NADPH co-substrate modelled into the structure (upper) and the DXR dimer (lower).³⁴

The crystal structure of the ternary complex of DXR, NADPH, and fosmidomycin has been reported.³⁸ This revealed Asp 150, Glu152, Glu231, Glu234, His209 and His257 as conserved active site residues. Residues 206-216 link the connective and C-terminal domains and act as the lid. The substrate binding cavity at the active site consists of three regions: a positively charged pocket, which binds the phosphate moiety of fosmidomycin (Figure 4.6), a hydrophobic region around the carbon backbone, and an amphipathic region, which binds the hydroxamic acid group. Interestingly, fosmidomycin does not form hydrogen bonds with His209, which appears to play an important role in binding the substrate in the correct orientation for catalysis. This is rationalised by the presence of the mono-anionic phosphonate of fosmidomycin resulting from crystallization at pH 5.0.

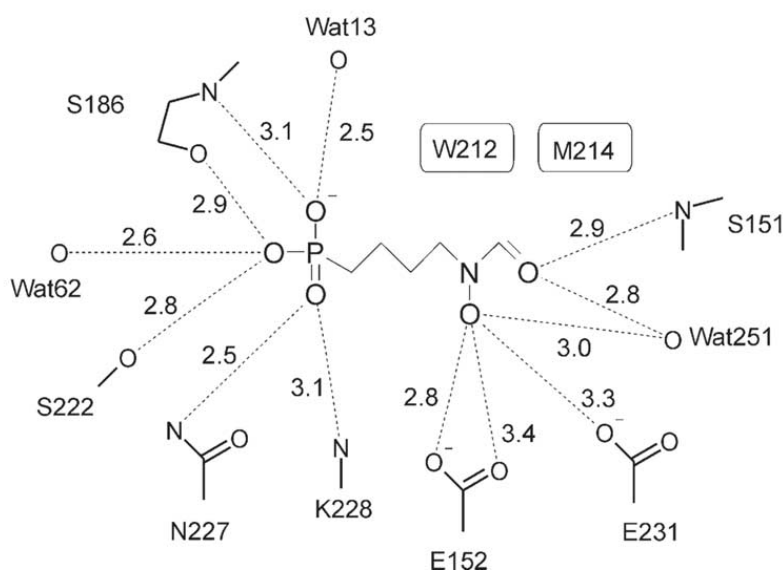


Figure 4.6 Representation of fosmidomycin contacts on binding of the inhibitor to DXR (distances are given in Å).³⁸

A ternary complex of DXR, NADPH, and DXP has been reported.²⁸ The phosphate moiety of the substrate forms hydrogen bonds to Ser186, Asn227, Lys228 and with the catalytically essential His209 (Figure 4.7). The substrate backbone interacts with the β -indole of Trp212 and the carbonyl group of C2 is hydrogen bonded to Glu152 and the backbone NH of Ser151. The hydroxyl group of C3 is involved in hydrogen bonds with Lys125 and Glu231, while the C4 hydroxyl group is hydrogen bonded to Glu152, Asn227 and Lys228. The C3 hydroxyl group of the alternative diastereoisomer is not involved in any hydrogen bonding interactions. The nicotinamide ring of NADPH adopts an orientation that allows the transfer of hydride from the *pro-S* hydrogen at C4 of the nicotinamide ring to C2 of the proposed intermediate, 2-*C*-methylerythrose 4-phosphate **50**.

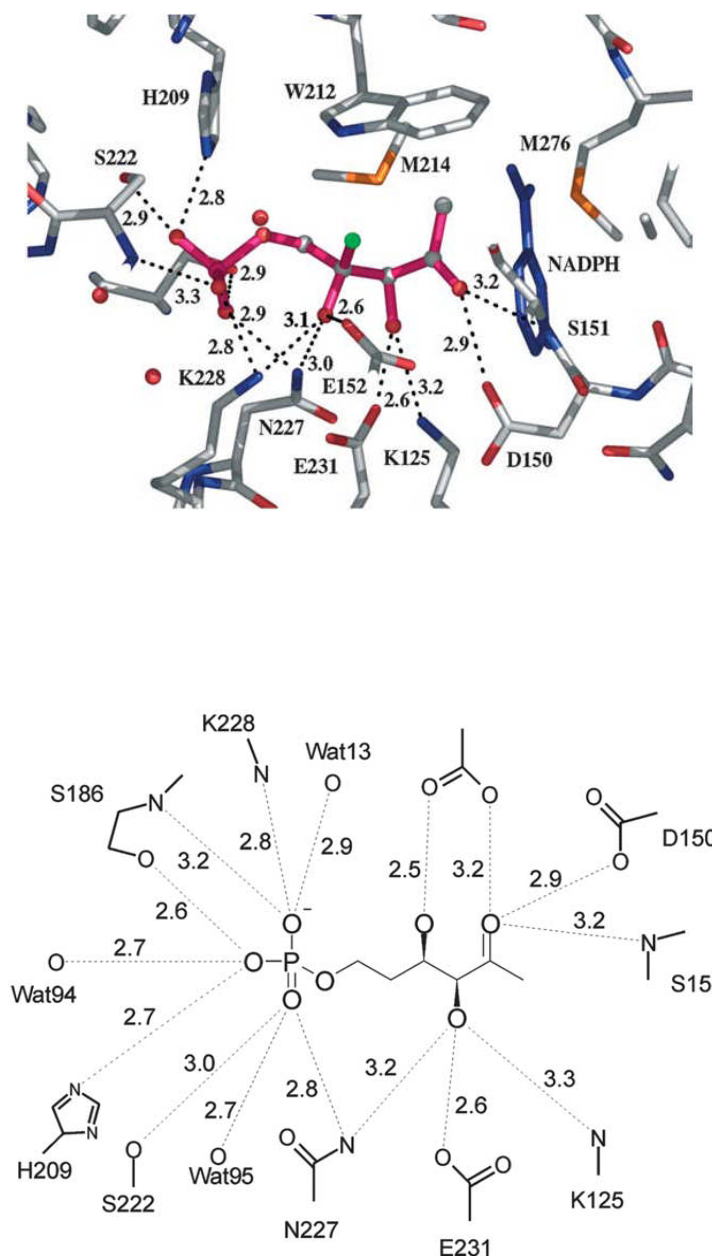


Figure 4.7 Representation of the DXP substrate binding to DXR as deduced from the X-ray structure of the DXR, NADPH, DXP ternary complex (distances are given in Å).³⁸

4.5 Inhibitors of DXR

For some microbial pathogens such as the malaria parasite and the micro-organism responsible for tuberculosis, *Plasmodium falciparum* and *Mycobacterium tuberculosis*, the MEP pathway is the exclusive source of IPP and DMAPP. The pathway is not found in humans. Therefore, each enzyme of the MEP pathway represents an attractive target for the development of new antibacterial, antimalarial, anti-TB agents, and herbicides.^{40, 41} Extensive studies have focused on the biotransformation of DXP to MEP, the reaction mediated by the enzyme DXP reductoisomerase. Fosmidomycin (**224**),⁴² which is a natural antibacterial, displayed a potent inhibitory effect on *E. coli* DXR with an IC₅₀ of 8.2 nM and it also showed strong inhibition of the growth of *P. falciparum* cells. The potent inhibitory effect of this compound may derive from its structural similarity to the hypothetical intermediate **205**. The analogue of fosmidomycin, FR900098 (**225**) showed twice the antimalarial activity *in vitro* and also cures malaria infected-mice.⁴³ To date, the most powerful inhibitor of DXR is the fosmidomycin analogue **226** which shows a 12-fold increase in activity over the parent compound and almost a 4-fold increase over FR900098 in antimalarial activity.⁴⁴ The combination of fosmidomycin with clindamycin is currently being employed in clinical studies against malaria in Gabon and Thailand. Several analogs of DXP, (3*S*)-hydroxypentan-2-one-5-phosphate (**215**, **216**, and **227**) have also shown inhibitory effects but at lower activity than fosmidomycin and its derivatives.

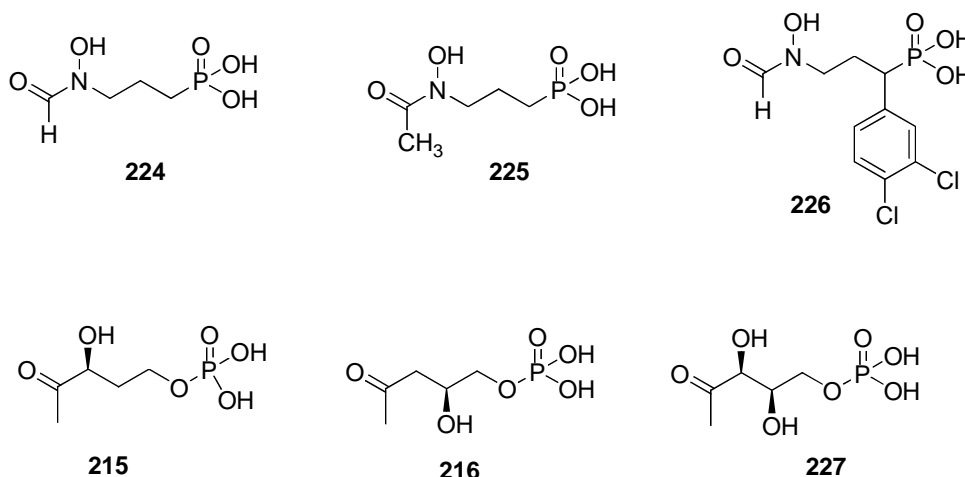
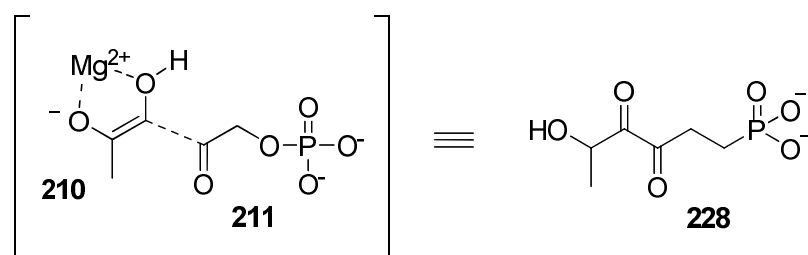


Figure 4.8 Inhibitors of DXR fosmidomycin (**224**), FR900098 (**225**) and DXP analogues.

4.6 Aims of the project

The aim of this study was to prepare 5-hydroxy-3,4-dioxohexylphosphonate (**228**). This phosphonate mimic is close in structure and geometry to the putative intermediates **210** and **211** involved in the retro-aldol/aldol mechanism (Scheme 4.5).

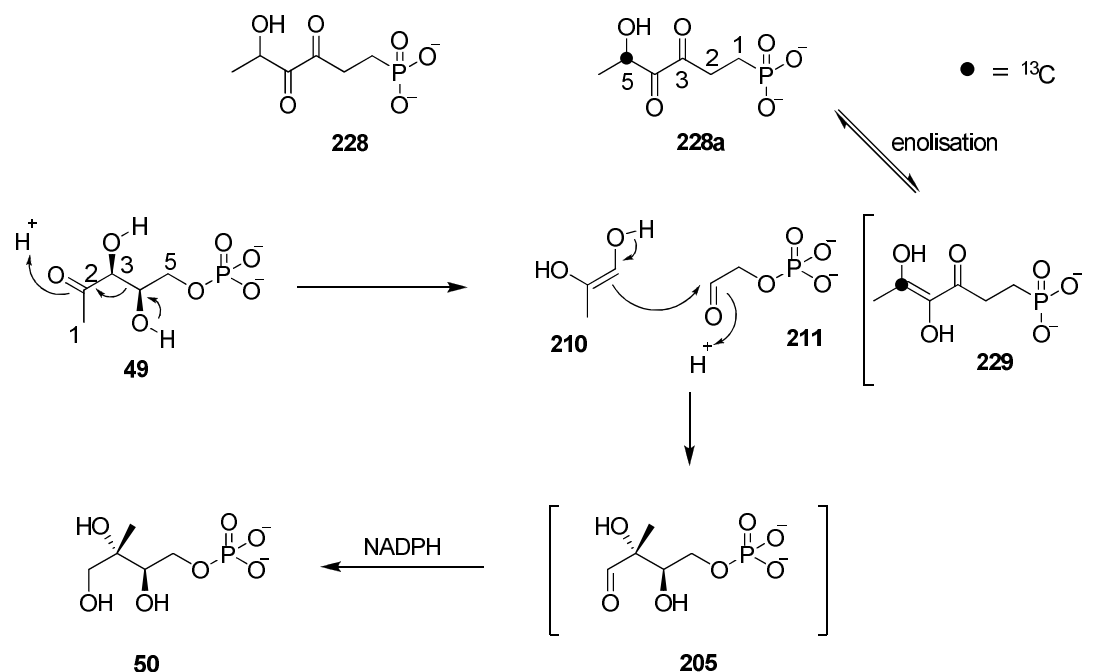


The cleavage of the bond between C3-C4 of DXP (Scheme 4.9) converts these sp^3 carbons into sp^2 in the resultant glycoaldehyde phosphate (**211**) and hydroxy acetone (**210**) fragments. These two fragments then undergo an aldol condensation to form a bond between C2 and C4 to generate the transient aldehyde (**205**) intermediate. The

tautomeric forms of 5-hydroxy-3,4-dioxo-hexyl-phosphonate (**228**) have similar structures to hydroxyacetone (**210**) and glycoaldehyde phosphate (**211**) and therefore **228** represents a possible transition state inhibitor of DXP.

The study aimed to explore if **228** would form tautomeric structures in solution. These tautomers may also be relevant as transition state analogues/inhibitors of DXR. To clarify the ground state content in the product mixtures, a synthesis of [5- ^{13}C]-**228a** was also designed. By enriching the carbonyl at C-5 with the ^{13}C -isotope, tautomeric mixtures in the crude product could potentially be identified by ^{13}C -NMR.

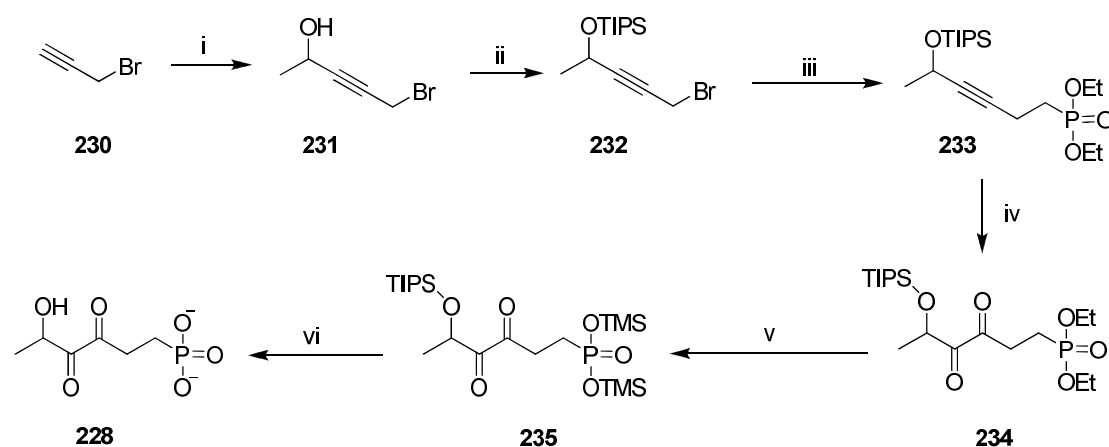
It was also an objective to assess the bioactivity of **228** by incubation with the *E. coli* DXR. A particular tautomer may bind the active site if it approximates the transition state geometry. The study may also reveal details of the enzyme mechanism.



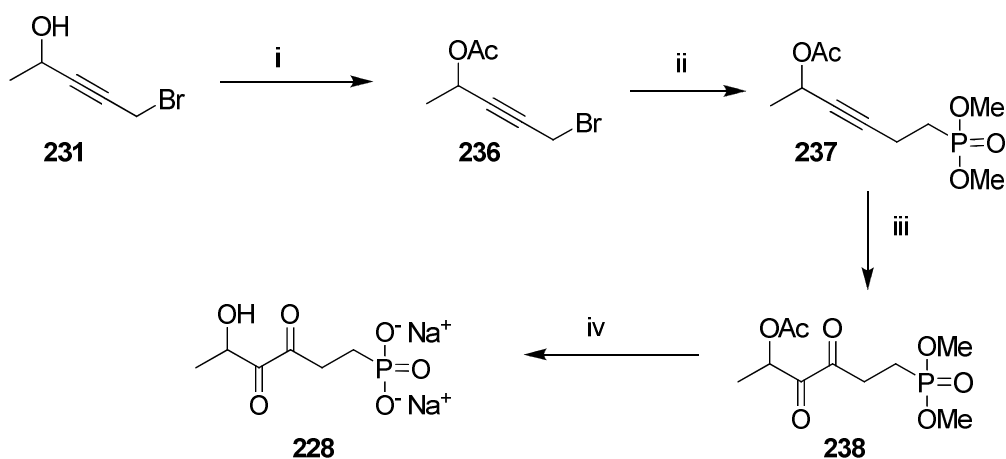
Scheme 4.8 Target molecules, **228** and [5- ^{13}C]-**228a**. Their tautomer (**229**) mimics the transition state of the retro-aldol/aldol mechanism.

4.7 Previous study on synthesis of potential DXR inhibitors.³²

As a potential transition state inhibitor of the retroaldol/aldol mechanism, 5-hydroxy-3,4-dioxohexylphosphonate (**228**) was synthesised in our laboratory by Dr C. D. Cadicamo. Two different synthetic routes to **228** are shown in Schemes 4.9 and 4.10. The first involved the protection of the hydroxyl group as a triisopropylsilyl ether and the second as an acetyl ester. In both cases the target compound showed complex ¹H NMR spectra. A preliminary biological assay suggested that a crude product preparation of **228** was a modest inhibitor of the *E. coli* DXR enzyme. At 1.0 mM it showed about 80% inhibition with a tentative K_i of 0.5 mM. Although not a very potent inhibitor it had a similar affinity to the enzyme as the natural substrate (~0.34 mM). The assay was carried out in the laboratory of Prof. R. J. Cox at the University of Bristol. A definitive conclusion on its inhibition potential was confused as the compound was clearly a complex mixture by ¹H-NMR analysis.



Scheme 4.9 Preparation of **228**; i. 1) BuLi, THF; 2) acetaldehyde, 40-60%; ii. TIPS-triflate, DCM, 2,6-lutidine, ~100; iii. 1) Diethyl methylphosphonate, BuLi, THF; 2) (5-bromopent-3-yn-2-yloxy)triisopropylsilane, 40%; iv. 1) O₃, MeOH; 2) PPh₃, diethyl ether, 70%. v. TMS-Br, DCM; ii H₂O; vi. 0.2 M NaOH until pH ~7. Synthesis carried out by Dr. C. D. Cadicamo (2006).



Scheme 4.10 Preparation of **228**; i. acetic anhydride, DCM/Pyr/DMAP, 60%; ii. 1) Dimethyl methylphosphonate, BuLi, THF; 2) 5-bromopent-3-yn-2-yl acetate, 40%; iii. 1) O₃, CCl₄/acetic acid (4:1); 2) PPh₃, diethyl ether, 70%. V. 1). TMS-Br, DCM; 2) H₂O; 3) NaOH (3 eq.) or lipase, phosphate buffer. Synthesis carried out by Dr. C. D. Cadicamo (2006).

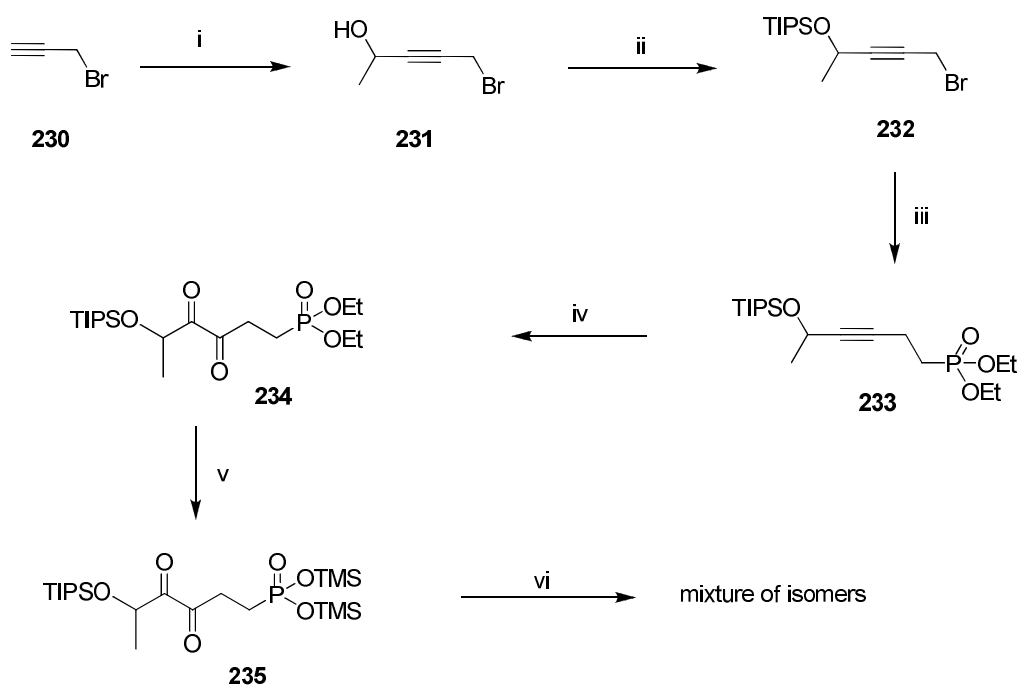
The objective of this study was to modify the synthesis of **228** to prepare a purer product, and also to prepare [5-¹³C]-**228a**, for a more in-depth assessment of the tautomers of this compound by ¹³C-NMR.

4.8 Results

4.8.1 Synthesis

4.8.1.1 Preparation of 5-hydroxy-3,4-dioxohexylphosphonate (**228**)

The preparation of 5-hydroxy-3,4-dioxohexylphosphonate (**228**) was previously described by C. D. Cadicamo. In this project, the synthesis essentially followed that route, however, with a slight modification during installation of the α -diketone (Scheme 4.11). Propargyl bromide was treated with LDA and then acetaldehyde for a condensation reaction to give **231**. The resultant alcohol was then protected as a TIPS ether (**232**). Dimethyl phosphonate was treated with *n*-BuLi to form the lithium phosphonate, which was then reacted with **232** to give the acetylene **233** in moderate yield. In order to install the α -diketone moiety, treatment of the acetylenic phosphonate **233** with NaIO₄/cat.RuO₂ in CHCl₃:ACN:H₂O (1:1:1.5) was employed.⁴⁵ The active species RuO₄ is generated *in situ* from RuO₂ by the action of NaIO₄. Such a reaction with acetylenes has previously been shown to give an α -diketone.^{45, 46} A bright yellow oil was obtained in good yield after chromatography and the resultant ¹H and ¹³C-NMR spectra of the ethyl phosphonate **234** are shown in Figures 4.9A and B. It was envisaged that the ethyl phosphonate esters could be hydrolysed by treatment with TMSBr, however the acidic conditions generated by TMSBr may also hydrolyse the TIPS ether. Therefore, **234** was treated with an excess TMSBr and then with water until a homogeneous solution was obtained. Then the solution was neutralised with 0.2 M NaOH. The product **228** was analysed by ¹H NMR in D₂O. The ¹H NMR spectrum (Figure 4.10) now was extremely complex, unlike that of **234**, indicating that the deprotected product was a complex mixture of isomers.



Scheme 4.11 Summary of synthetic route to 5-hydroxy-3,4-dioxohexylphosphonate (**228**). *Reagents and conditions*: i. 1) LDA, THF; 2) acetaldehyde, 60%; ii. TIPS-triflate, CH₂Cl₂, 2,6-lutidine (quantitative); iii. 1) diethyl methylphosphonate, BuLi, THF; 2) **232**, 40%; iv. RuO₂, NaIO₄, H₂O:CH₃CN:CHCl₃ (1.5:1:1), 60%; v. TMS-Br, DCM; vi. 1) H₂O; 2) 0.2 M NaOH.

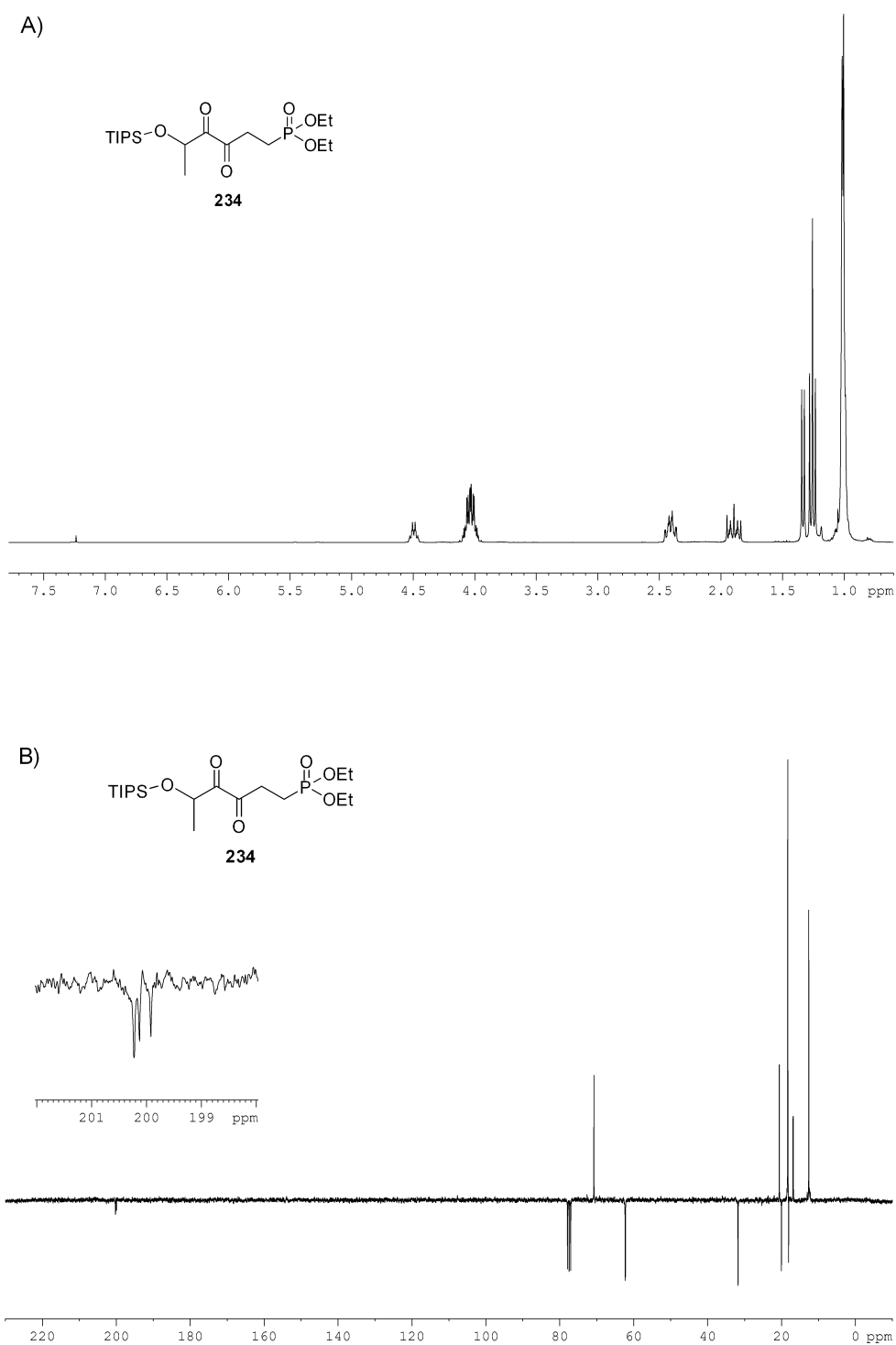


Figure 4.9 A) ^1H -NMR (CDCl₃) spectrum of α -diketone **234**; B) ^{13}C -NMR of α -diketone **234**.

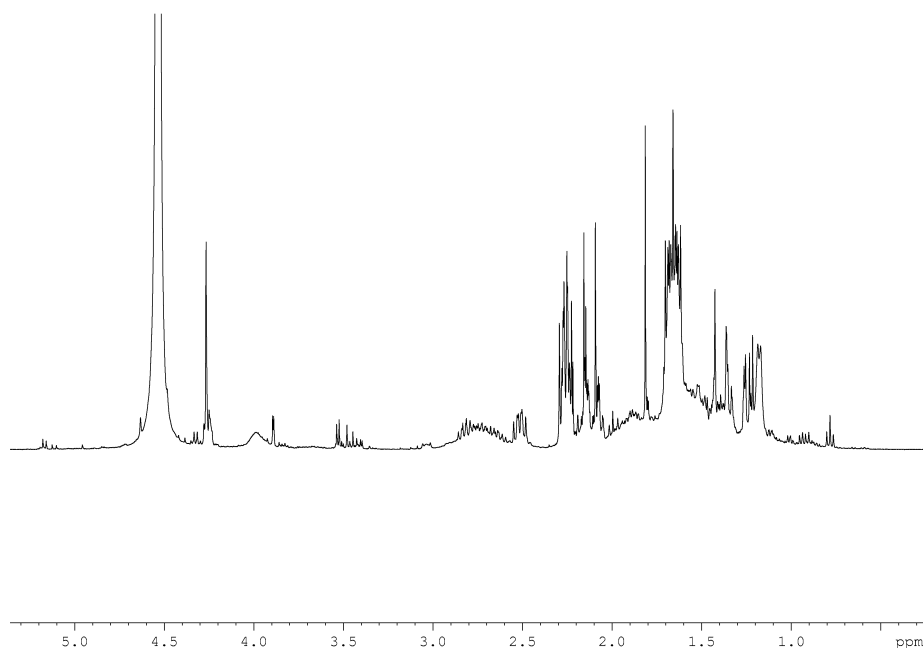
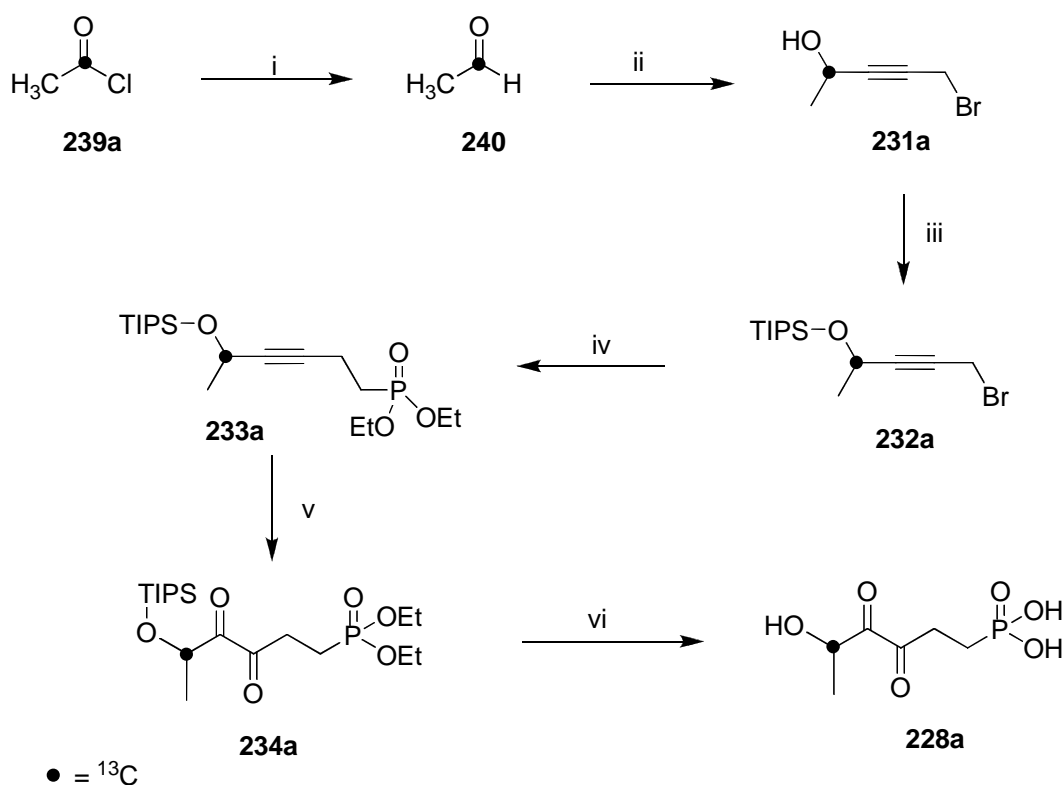


Figure 4.10 Complex ^1H -NMR (D_2O) of **228** obtained after treatment of **234** with TMSBr, H_2O , and neutralised with 0.2 M NaOH. This shows a clear contrast to the relatively clean NMR spectra of the immediate precursor **234** (Figure 4.9 A and B).

4.8.1.2 Preparation of $[5\text{-}^{13}\text{C}]\text{-5-hydroxy-3,4-dioxohexylphosphonate}$ (**228a**)

In order to gain a clearer insight into understanding the complexity of this mixture, it was decided to incorporate a ^{13}C isotope as a probe to explore the extent of the isomerisation. The strategy taken (Scheme 4.12) involved installing ^{13}C at C5 of **228a**. A synthetic route was envisaged that involved treating $[1\text{-}^{13}\text{C}]\text{-acetaldehyde}$ (**240**) with propargyl bromide (**230**). Further synthetic steps then followed the previous synthesis of **228** as illustrated in Scheme 4.12.



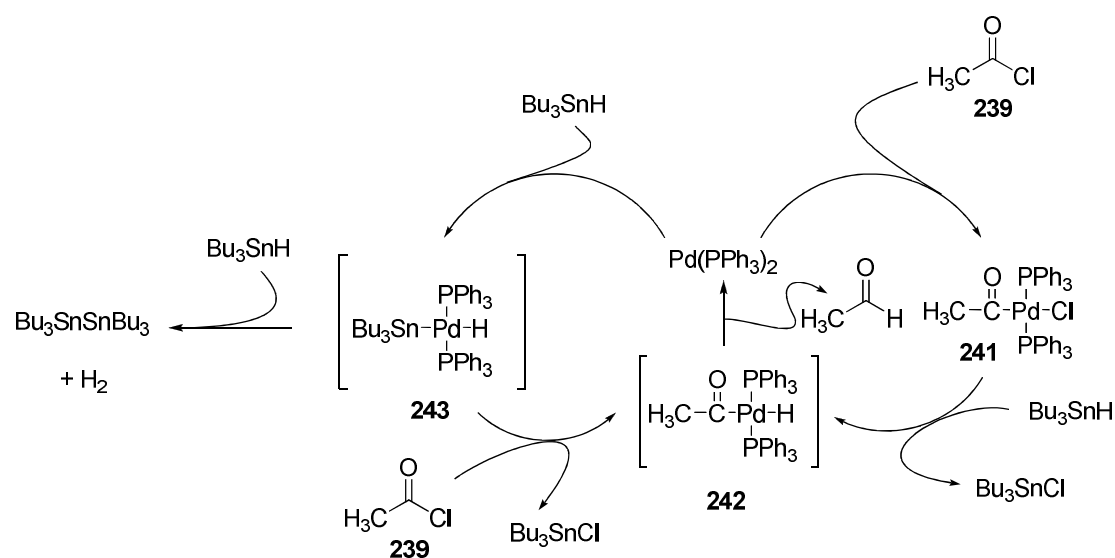
Scheme 4.12 Synthetic route to [5- ^{13}C]-**228a**. *Reagents and conditions:* i. *n*-Bu₃SnH/Pd(0)(PPh₃)₄, toluene, 30 °C; ii. 1) LDA, THF; 2) propargyl bromide (38.1%); iii. TIPS-triflate, CH₂Cl₂, 2,6-lutidine (96.7%); iv. 1) diethyl methyl phosphonate, BuLi, THF; 2) **232a** (56.9%); v. RuO₂, NaIO₄, H₂O:CH₃CN:CHCl₃ (1.5:1:1) (64.6%); vi. 1) TMS-Br, DCM; 1) H₂O.

4.8.1.3 Preparation of [4- ^{13}C]-1-bromo-4-hydroxypent-2-yne (**231a**).

In order to generate a sample of [1- ^{13}C]-acetaldehyde (**240**), [1- ^{13}C]-acetylchloride (**239a**), was treated with Pd(0)(Ph₃)₄ and *n*-Bu₃SnH in toluene at 30°C.⁴⁷ The product was flushed from the reaction mixture by evaporation on a flow of nitrogen gas, and was trapped by condensation in a round bottom flask which contained dry THF at -89°C. The flask was warmed to ambient temperature and the mixture was then transferred *via* a cannular into a round bottom flask containing propargyl bromide

(**230**) which had previously been treated with LDA. The resultant [4-¹³C]-**231a** alcohol was obtained in moderate yield (38%) after chromatography.

The consensus mechanism for the catalytic reduction is shown in Scheme 4.13.⁴⁸ The key acylhydridopalladium (**242**) intermediate may be derived from two possible pathways. Firstly, an oxidative addition of acyl chloride with Pd(PPh₃)₂ to form an acylchloropalladium(II) complex (**241**), followed by a metathesis reaction with *n*-Bu₃SnH. A second possible pathway involves the oxidative addition of *n*-Bu₃SnH with Pd(PPh₃)₂ to generate adduct (**243**), followed by oxidative addition of the acyl chloride to form the acylhydridopalladium (**242**) intermediate. Reductive elimination of **242** would then give the aldehyde and regenerate the catalyst.



Scheme 4.13 Proposed catalytic reduction of acyl chloride to acetaldehyde by Pd(0)(PPh₃)₄/*n*-Bu₃SnH.⁴⁸

4.8.1.4 Preparation [5-¹³C]- α -diketone **234a**.

Following the method for the previous synthesis of **228**, alcohol **231a** was then protected as a TIPS ether, which then underwent a condensation with the ethyl methylphosphonate moiety to give **233a**. Treatment of the acetylene **233a** with NaIO₄/cat.RuO₂ gave the α -diketone [5-¹³C]-**234a** in good yield. The ¹H NMR of [5-¹³C]-**234a** (Figure 4.11) shows a *dq* multiplicity at 5.03 ppm (¹*J*_{CH} 144.3 and ³*J*_{HH} 6.8 Hz) corresponding to the methylene proton directly attached to the carbon-13 isotope. The ¹³C-NMR shows a clear predominant signal at 70.7 ppm, indicating isotope enrichment of the C-5 carbon. These spectra again indicate a relatively clean synthetic phosphonate ester precursor, prior to final deprotection.

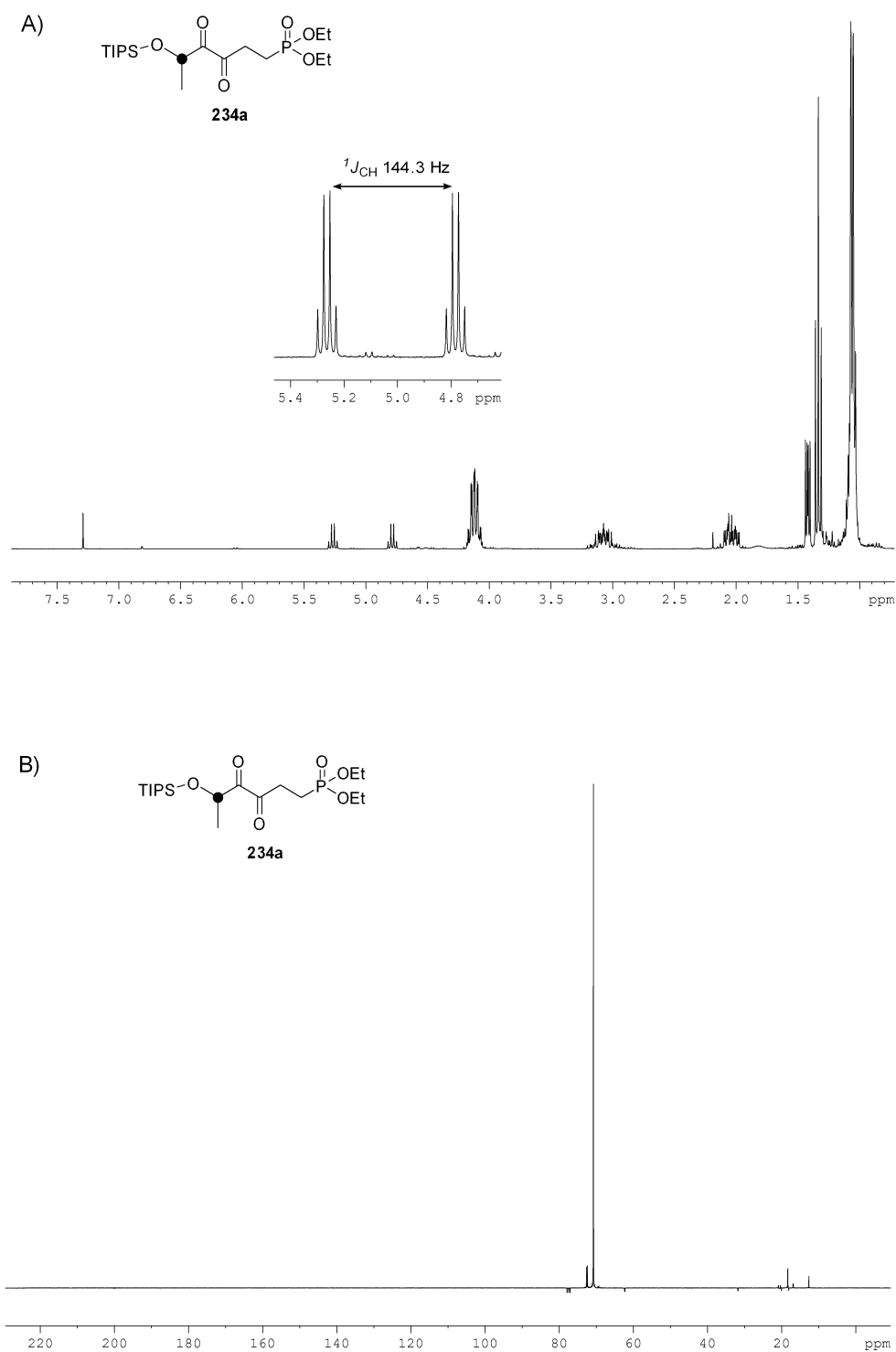
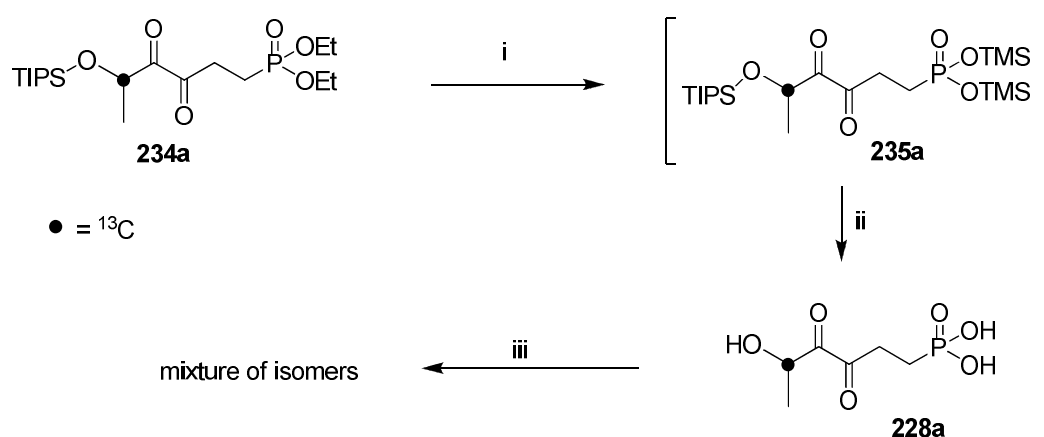


Figure 4.11 ^1H -NMR (A) and ^{13}C -NMR (B) spectra of α -diketone **234a**.

4.8.1.5 Preparation of [5-¹³C]- α -diketone phosphonate **228a**.

Compound [5-¹³C]-**234a** was now treated with an excess TMSBr in DCM, followed by addition of water until a homogeneous solution was obtained, and the solvents were then removed *in vacuo* to give **228a**. The ¹H and ¹³C NMR spectra of the resultant **228a** are shown in Figure 4.12, and they are clearly complex, representing a mixture of tautomers of **228a**.



Scheme 4.14 Deprotection of [5-¹³C]-**234a** gave a mixture of isomers of **228a**.

Reagents and conditions: i) TMSBr, DCM; ii) H₂O; iii) 0.2 M NaOH.

The ¹H NMR (Figure 4.12) of **228a** shows two methylene groups multiplets at 1.53-1.68 ppm and 2.34-2.64 ppm. Methyl groups attached directly to an isotopically enriched carbonyl are identified as two sets of doublets at 1.80 ppm and 1.81 ppm. The ¹³C NMR spectrum (Figure 4.12) revealed that there were at least four different ¹³C-enriched environments in the product indicating a significant level of tautomerisation. Two carbonyl environments were clearly obvious as indicated by the two ¹³C signals at 207.0 ppm and 207.5 ppm. Also signals consistent with carbinols (H¹³COH) appear at 69.8 ppm and 72.5 ppm. This combination of signals suggested that the product contains at least two isomers bearing C5 carbonyls (**244**) and two isomers containing ¹³C-5 enriched carbinol motifs (**245**, Scheme 4.15).

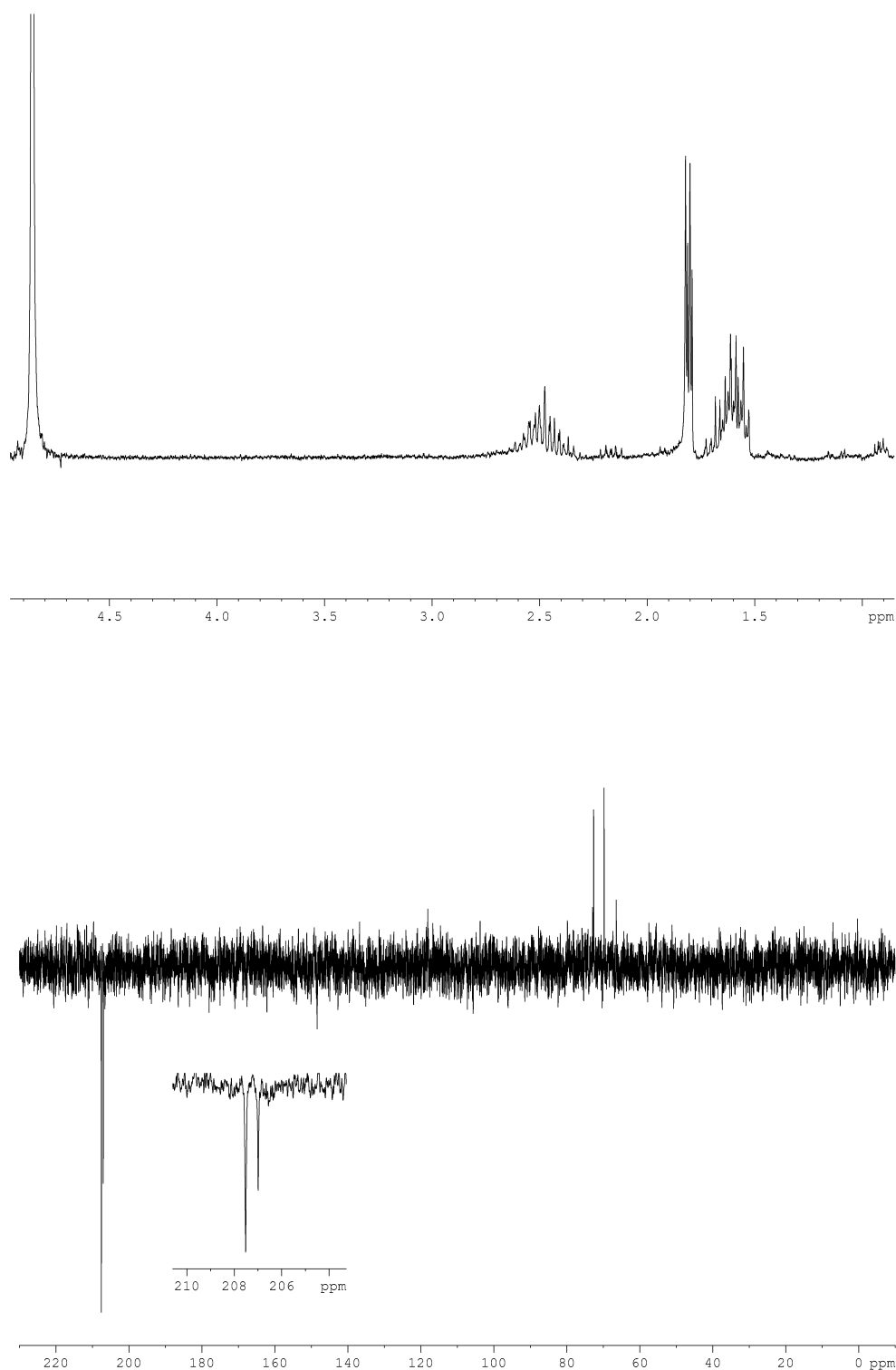
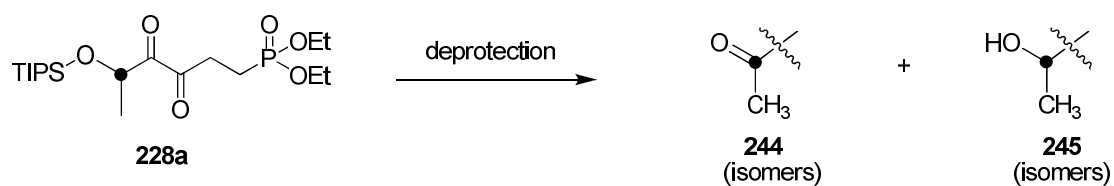


Figure 4.12 A) ^1H -NMR (D_2O) and B) ^{13}C -NMR (D_2O) of **228a** obtained after treatment [5- ^{13}C]-**234a** with an excess $\text{TMSBr}/\text{H}_2\text{O}$.



Scheme 4.15 Possible isomer motifs contained in the product after treatment of $[5-^{13}\text{C}]\text{-234a}$ with TMSBr.

4.8.1.3 Influence of pH on tautomerism of **228a**.

In order to explore tautomerism in the isotopically labelled sample of **228a**, a series of ^{13}C -NMR studies were carried out at different pH's in D_2O . Accordingly, the solution of **228a** was adjusted the pH's to 3.5, 7.0, 10.5, and 12.5 with 0.2 M NaOH. The ^{13}C -NMR spectrum was recorded in D_2O at each pH point to observe the influence of pH on the nature of the carbon-13 signals in product mixture. The ^{13}C NMR for this series of experiments is shown in Figure 4.13 and all possible tautomeric motifs of the isotopically labelled C-5 are shown in Figure 4.14.

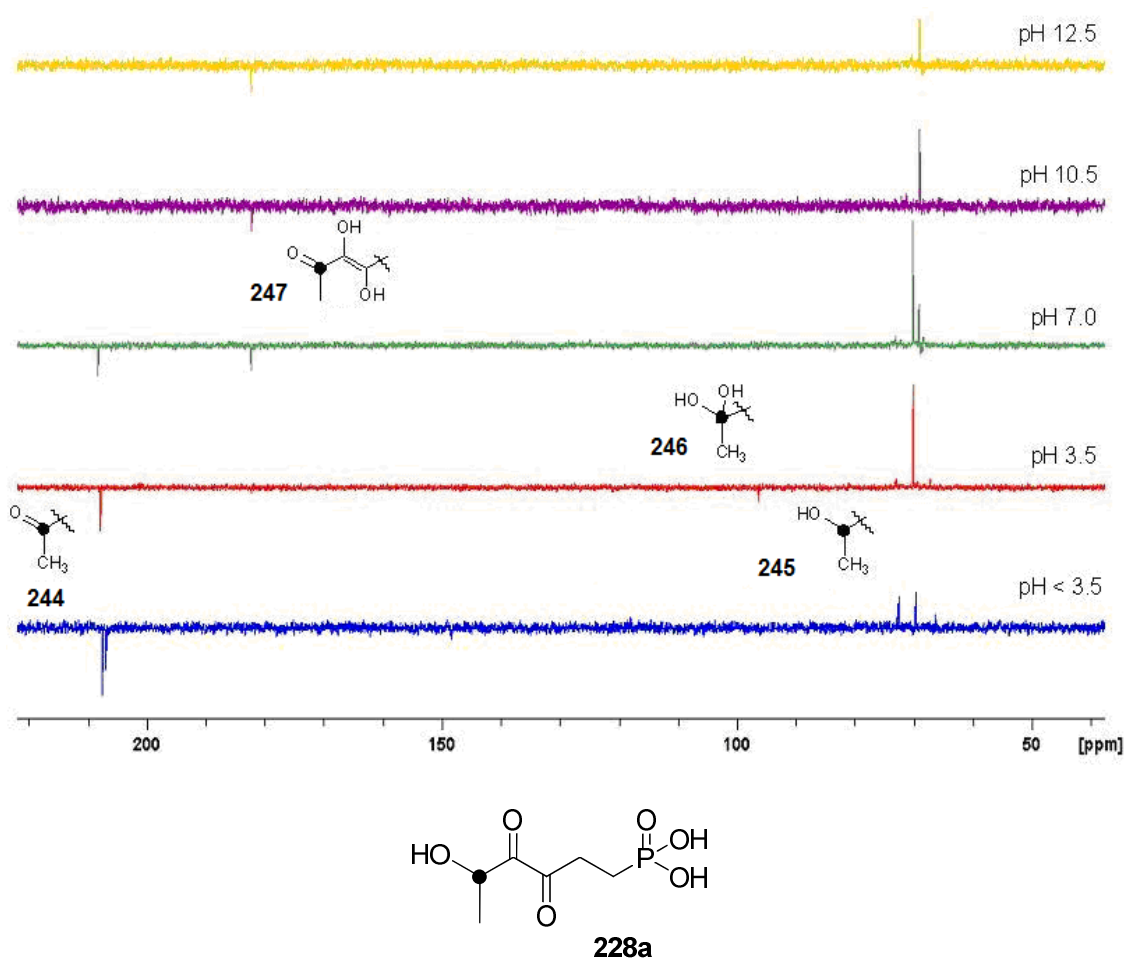


Figure 4.13 ^{13}C NMR of **228a** recorded in D_2O at pH's 3.5, 7.0, 10.5, and 12.5.

The ^{13}C NMR of **228a** adjusted pH to 3.5 showed only one obvious enriched carbonyl signal at 207.8 ppm, a predominant carbinol signal at 70.0 ppm, and a minor signal of a hydrate at 95.7 ppm. These signals are perhaps consistent with the motifs **244**, **245**, and **246**, respectively. Therefore, at this pH there were at least three isotopically enriched C-5 environments. Neutralised **228a** (pH 7.0) exhibited two additional signals relative to pH 3.5. A new carbonyl signal emerged perhaps consistent with an enol motif (**247**), at 182.3 ppm. It was envisaged that **247** may tautomerise to an enol **248**, however there was no apparent ^{13}C signal consistent with this enol motif. The signal for a secondary carbinol also appeared at 69.1 ppm. Under basic conditions (pH 10.5), the carbonyl signal at 207.8 ppm and the carbinol at 70.0 ppm disappeared.

However, two predominant signals consistent with structural motifs **245** and **247** remained. These signals also persisted at pH 12.5. These results clearly demonstrate pH dependent tautomerisation with different tautomers present under acidic and basic conditions.

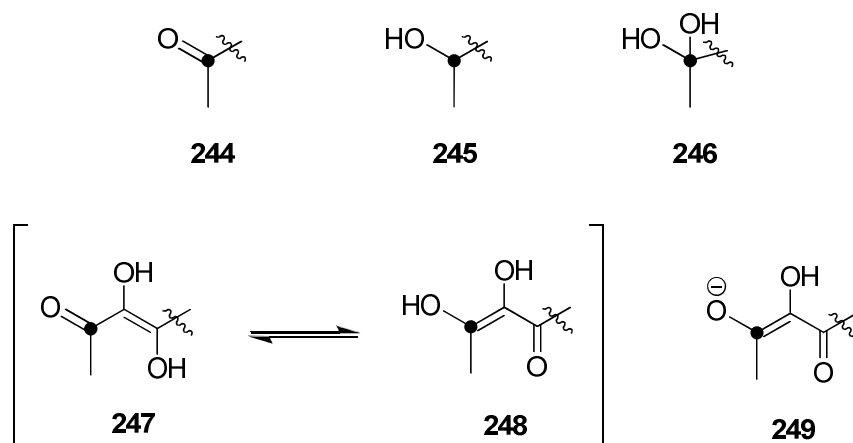


Figure 4.14 Molecular fragments contained in solution of [5-¹³C]-**228a** at different pH's. In an acidic environment, the product contained both ¹³C-enriched C5 carbonyl (**244**) and carbinol (**245**) moieties. At neutral pH, **247** emerged along with **244** and **245**. Under basic conditions, the predominant labelled moiety was **245**.

4.8.2 Incubation of **229a** with *E. coli* DXR

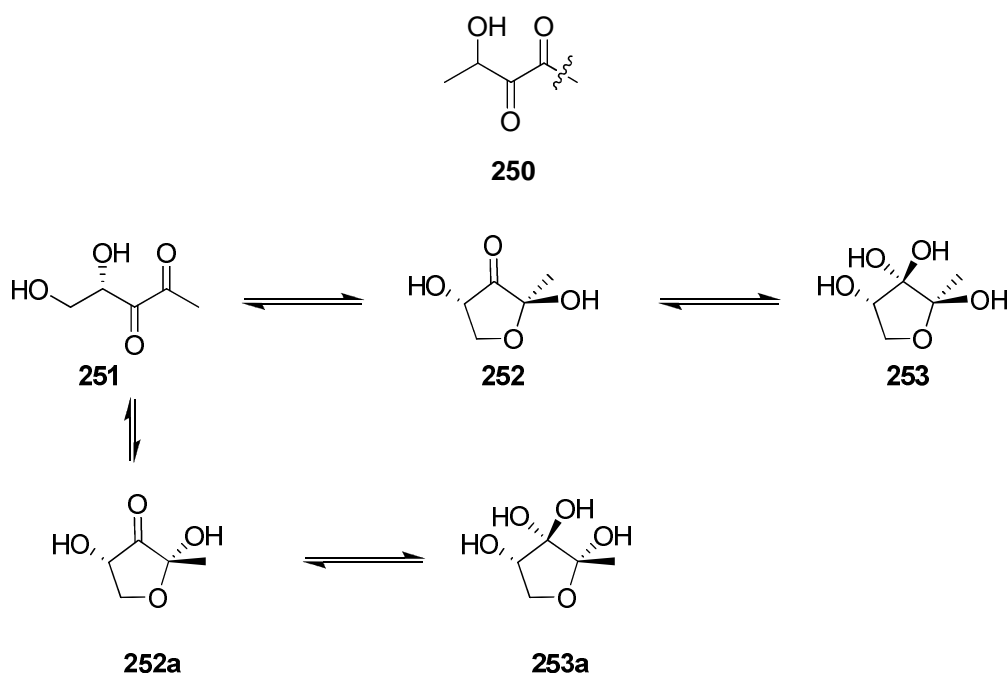
Samples of phosphonate salt **228a** for enzyme assays were obtained by adjusting the pH to 7.0 with 0.2 M NaOH. All incubations with DXR were carried out in collaboration with Prof. M. Rohmer at the University of Strasbourg. Assays were carried out by Denis Tritsch. DXR (2 μL, stock concentration 2.7 μg/μL) was first preincubated with NADPH (0.25 mM final concentration) and the solutions of **228a** at 37°C for 2 min. The enzymatic reaction was then initiated by the addition of DXP (0.5 mM final concentration). The reaction was followed at 340 nm in a UV

spectrometer. The concentrations of inhibitor varied from 10 to 800 μM , however no apparent decrease of the enzymatic rate was observed over this concentration range. Phosphonate **228a** did not appear to inhibit DXR. The compound (400 μM) was also incubated with NADPH and DXR as a potential substrate. However there was no decrease in the absorbance at 340 nm. It is concluded that **228a** is not a substrate or an inhibitor of DXR.

The earlier Bristol assay had been carried out on a small amount of material, and we must conclude that the assay carried out in Strasburg was more rigorous.

4.9 Discussion and conclusion

Based on the retroaldol/aldol mechanism for the rearrangement of DXP to MEP, the phosphonate analogue **228** was designed as a potential transition state mimic. A synthesis of **228** has previously been demonstrated by Dr. Cadicamo in St Andrews, however at that time the nature of the product was not clear. Molecules containing a 1,2-diketone-3-hydroxyl motif (**250**) are anticipated to tautomerise, and are also susceptible to hydration, and therefore assignment by NMR is complicated. For instance, the natural compound 4,5g-dihydroxy-pentane-2,3-dione (DPD, **251**) has never been isolated as a pure compound.⁴⁹⁻⁵¹ It was shown to equilibrate as a mixture of cyclic anomers (**252**, **252a**) and hydrated anomeric forms (**253**, **253a**).^{49, 50}

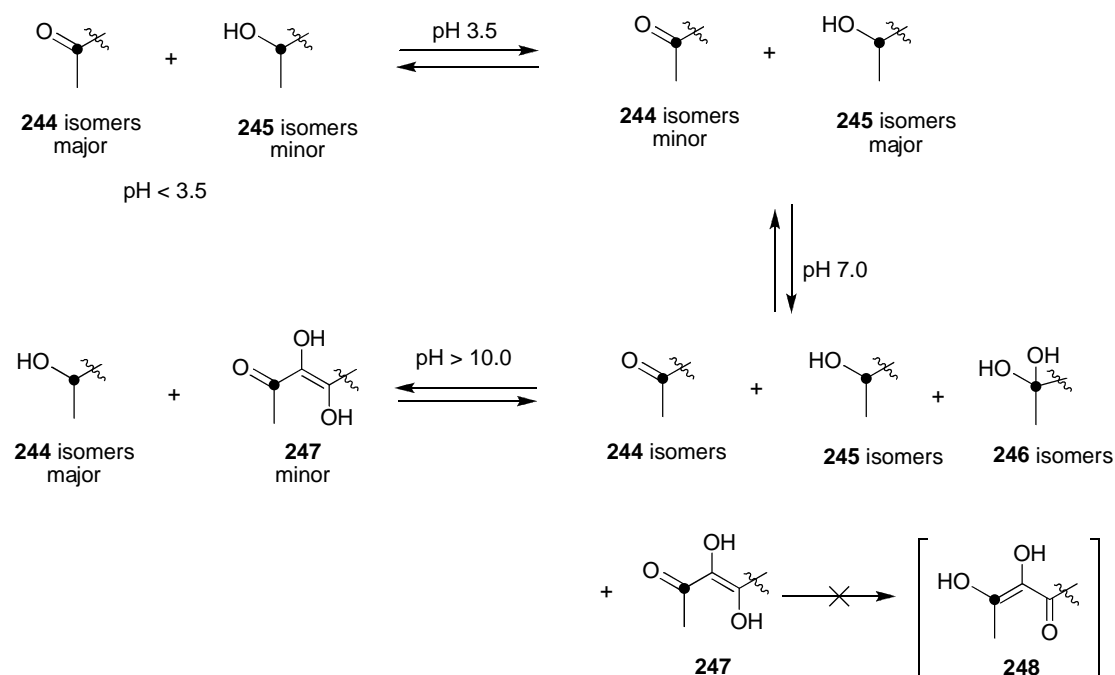


Scheme 4.16 The 1,2-diketone-3-hydroxyl motif (**250**) and the equilibrium of 4,5-dihydroxy-pentane-2,3-dione (**253**).^{49, 50}

Although the precursor to **228** and **228a** could be relatively easily characterised by ^1H NMR, deprotection to the phosphonate salt led to a complex mixture of isomers. It was anticipated that this complex mixture was actually an equilibrium between a number of tautomeric forms, and also with hydrates. A selectively labelled ^{13}C analogue was synthesised to investigate if this carbon could equilibrate between carbonyls and carbinols and hydrates. Isotopic labelling at C-5 was selected. Under an acidic environment ($\text{pH} < 3.5$), the labelled carbon of **228a** was substantially carbonyl (**244**) in nature along with a minor carbinol component (**245**). However, the equilibrium favored ^{13}C -5 carbinol isomers when the pH of the solution was adjusted to 3.5. At neutral pH, an additional ^{13}C -5 carbonyl emerged, suggesting that C-3 and C-4 were perhaps in an enol form (**247**). Thus, there were at least four ^{13}C -5 enriched

environments present at pH 7. Under basic conditions (pH 10.5 and 12.5), tautomeric forms **244** disappeared and a ^{13}C -5 carbinol isomer predominated.

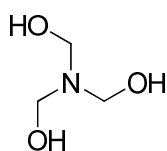
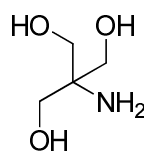
It was envisaged that the tautomeric enol **248** could mimic the putative transition state of the isomerisation of DXP to MEP (Scheme 4.8). The geometry of this tautomer would fit the catalysis reaction of the DXR enzyme. A study of the influence of pH on the tautomerisation of **228a** (Section 4.8.1.3) has revealed that at a neutral pH all tautomeric motifs, **244** and **245** were present in the solution, particularly an enol **247**. This enol can tautomerise to enol **248** in solution. However, there was no obvious signal indicating the presence of the tautomer **248** at all varying pH states.



Scheme 4.17 Fate of the ^{13}C -5 enriched carbon of **228a** with pH variation.

Previous enzyme assays of **228** with the *E. coli* DXR were carried out in Dr. R. Cox's laboratory at the Bristol University in 2006 and suggested some inhibition activity. In

this study, an enzyme assay evaluating the inhibitory effect of **228a** on the production of MEP was carried out in Prof. M. Rohmer's laboratory at the University of Strasbourg. However, triethanolamine buffer (**254**) was employed instead of Tris buffer (Bristol), since Tris buffer (**255**) is able to react with carbonyl compounds. Incubation of the tautomeric forms of **228a** with DXR, and NADPH showed no decrease of absorbance at 340 nm. This result suggested that **228a** was not a substrate for the enzyme. Incubation of the tautomeric forms of **228a** with DXR, DXP, and NADPH suggested also that **228a** was not an inhibitor of DXR even at concentrations up to 8 mM.

**254****255**

Inconsistent bioassay results were somewhat confusing, but the assay carried out in Strasbourg during this research suggests that **228** is not an inhibitor.

4.10 References

1. P. M. Dewick, *Medicinal Natural Products : a biosynthetic approach*, 2 edn., John Wiley & Sons, 2001.
2. Y. V. Ershov, *App. Biochem. Micro.*, 2007, **43**, 115-138.
3. H. K. Lichtenthaler, *Biochem. Soc. Trans.*, 2000, **26**, 785-789.
4. M. Rohmer, M. Knani, P. Simonin, B. Sutter and H. Sahm, *Biochem. J.*, 1993, **295**, 517-524.
5. H. K. Lichtenthaler, J. Schwender, A. Disch and M. Rohmer, *Biochem. J.*, 1996, **316**, 73-80.
6. H. K. Lichtenthaler, J. Schwender, A. Disch and M. Rohmer, *FEBS Lett.*, 1997, **400**, 271-274.
7. D. Arigoni, S. Sagner, C. Latzel, W. Eisenreich, A. Bacher and M. H. Zenk, *Proc. Natl. Acad. Sci. USA*, 1997, **94**, 10600-10605.
8. J. H. Cyjic and M. Rohmer, *Phytochem.*, 2000, **53**, 21-28.
9. H. Jomaa, J. Wiesner, S. Sanderbrand, B. Altincicek, C. Weidemeyer, M. Hintz, I. Turbachova, M. Eberl, J. Zeidler, H. K. Lichtenthaler, D. Soldati and E. Beck, *Science*, 1999, **285**, 1573-1576.
10. G. A. Sprenger, U. Schorken, T. Weigert, S. Grolle, A. A. deGraaf, S. V. Taylor, T. P. Begley, S. Bringer-Meyer and H. Sahm, *Proc. Natl. Acad. Sci. USA*, 1997, **94**, 12857-12862.
11. M. A. Phillips, P. Leon, A. Boronat and M. Rodriguez-Concepcion, *Trend in Plant Science*, 2008, **13**, 619-623.
12. G. A. Sprenger, U. Schorken, T. Weigert, S. Grolle, A. A. D. Graaf, S. V. Taylor, T. P. Begley, S. Bringer-Meyer and H. Sahm, *Proc. Natl. Acad. Sci. USA*, 1997, **94**, 12857-12862.

13. J. F. Hoeffler, D. Tritsch, C. Grosdemange-Billiard and M. Rohmer, *Eur. J. Biochem.*, 2002, **269**, 4446-4457.
14. A. T. Koppisch, D. T. Fox, S. J. B. Blagg and C. D. Poulter, *Biochemistry*, 2002, **41**, 236-243.
15. M. Rohmer, M. Seeman, S. Horbach, S. Bringer-Meyer and H. Sahm, *J. Am. Chem. Soc.*, 1996, **118**, 2564-2566.
16. F. Rohdich, J. Wungsintaweeikul, M. Fellermeirer, S. Sagner, S. Herz, K. Kis, W. Eisenreich, A. Bacher and M. H. Zenk, *Proc. Natl. Acad. Sci. USA*, 1999, **96**, 11758-11763.
17. T. Kuzuyama, M. Takagi, K. Kaneda, T. Dairi and H. Seto, *Tetrahedron Lett.*, 2000, **41**, 703-706.
18. H. Luttgen, F. Rohdich, S. Herz, J. Wungsintaweeikul, S. Hecht, C. A. Schuhr, M. Fellermeirer, S. Sagner, M. H. Zenk, A. Bacher and W. Eisenreich, *Proc. Natl. Acad. Sci. USA*, 2000, **97**, 1062-1067.
19. T. Kuzuyama, M. Takagi, K. Kaneda, H. Watanabe, T. Dairi and H. Seto, *Tetrahedron Lett.*, 2000, **41**, 2925-2928.
20. M. Takagi, T. Kuzuyama, K. Kaneda, H. Watanabe, T. Dairi and H. Seto, *Tetrahedron Lett.*, 2000, **41**, 3395-3398.
21. S. Herz, J. Wungsintaweeikul, C. A. Schuhr, S. Hecht, H. Luttgen, S. Sagner, M. Fellermeirer, W. Eisenreich, M. H. Zenk, A. Bacher and F. Rohdich, *Proc. Natl. Acad. Sci. USA*, 2000, **97**, 2486-2490.
22. S. Hecht, W. Eisenreich, P. Adam, S. Amslinger, K. Kis, A. Bacher and D. Arigoni, *Proc. Natl. Acad. Sci. USA*, 2001, **98**, 4837-4842.
23. L. Charon, C. Pale-Grosdemange and M. Rohmer, *Tetrahedron Lett.*, 1999, **40**, 7231-7234.

24. F. Rohdich, S. Hecht, K. Gartner, P. Adam, C. Krieger, S. Amslinger, D. Arigoni, A. Bacher and W. Eisenreich, *Proc. Natl. Acad. Sci. USA*, 2002, **99**, 1158-1163.
25. T. Grawert, F. Rohdich, I. Span, A. Bacher, W. Eisenreich, J. Eppinger and M. Groll, *Angew. Chem. Int. Ed.*, 2009, **48**, 5756-5759.
26. P. Proteau, *Bioorg. Chem.*, 2004, **32**, 483-493.
27. R. Dumas, V. Bion, F. Halgan, R. Douce and R. G. Duggleby, *Acc. Chem. Res.*, 2001, **34**, 399-408.
28. A. E. Johnson and M. E. Tanner, *Biochemistry*, 1998, **37**, 5746-5754.
29. C. Phaosiri and P. J. Proteau, *Bioorg. Med. Chem. Lett.*, 2004, **14**, 5309-5312.
30. A. Wong, J. W. Munos, V. Devasthali, K. A. Johnson and H.-w. Liu, *Org. Lett.*, 2004, **6**, 3625-3628.
31. D. T. Fox and C. D. Poulter, *Biochemistry*, 2005, **44**, 8360-8368.
32. U. Wong and R. J. Cox, *Angew. Chem. Int. Ed.*, 2007, **46**, 4926-4929.
33. J. W. Munos, X. Pu, S. O. Mansoorabadi, H. J. Kim and H.-w. Liu, *J. Am. Chem. Soc.*, 2009, **131**, 2048-2049.
34. K. Reuter, S. Sanderbrand, H. Jomaa, J. Wiesner, I. Steinbrecher, E. Beck, M. Hintz, G. Klebe and M. T. Stubbs, *J. Biol. Chem.*, 2002, **277**, 5378-5384.
35. S. Yajima, T. Nanoka, T. Kuzuyama and H. Seto, *J. Biochem.*, 2002, **131**, 313-317.
36. S. Steinbacher, J. Kaiser, W. Eisenreich, R. Huber, A. Bacher and F. Rohdich, *J. Biol. Chem.*, 2003, **278**, 18401-18407.
37. S. Yajima, K. Hara, J. S. Sanders, F. Yin, K. Ohsawa, J. Wiesner, H. Jomaa and E. Oldfield, *J. Am. Chem. Soc.*, 2004, **126**, 10824-10825.

38. A. M. Sweeney, R. Lange, R. P. M. Fernandes, H. Schulz, G. E. Dale, A. Douangamath, P. J. Proteau and C. Oefner, *J. Mol. Biol.*, 2005, **345**, 115-127.
39. S. Ricagno, S. Grolle, S. Bringer-Meyer, H. Sahm, Y. Lindqvist and G. Schneider, *Biochim. Biophys. Acta*, 2004, **1698**, 37-44.
40. H. Eoh, P. J. Brennan and D. C. Crick, *Tuberculosis*, 2009, **89**, 1-11.
41. W. Eisenreich, A. Bacher, D. Arigoni and F. Rohdich, *Cell. Mol. Life. Sci.*, 2004, **61**, 1401-1426.
42. T. Kuzuyama, T. Shimizu, S. Takahashi and H. Seto, *Tetrahedron Lett.*, 1998, **39**, 7913-7916.
43. H. Jomaa, J. Wiesner, S. Sanderbrands, A. Altincicek and C. Weide-Meyer, *Science*, 1999, **285**, 1573-1576.
44. T. Haemers, J. Wiesner, S. V. Poecke, J. Geoman, D. Henschker, E. Beck, H. Jomaa and S. V. Calenbergh, *Bioorg. Med. Chem. Lett.*, 2006, **16**, 1888-1891.
45. R. Zibuck and D. Seebach, *Helv. Chim. Acta*, 1988, **71**, 237-240.
46. H. Gopal and A. J. Gordon, *Tetrahedron Lett.*, 1971, **31**, 2941-2944.
47. D. Barbry and D. Couturier, *J. Labelled Comps. Radiopharm.*, 1987, **24**, 603-606.
48. P. Four and F. Guibe, *J. Org. Chem.*, 1981, **46**, 4439-4445.
49. M. M. Meijler, L. G. Hom, G. F. Kaufmann, K. M. McKenzie, C. Sun, J. A. Moss, M. Matsushita and K. D. Janda, *Angew. Chem. Int. Ed.*, 2004, **43**, 2106-2108.
50. M. F. Semmelhack, S. R. Campagna, M. J. Federle and B. L. Bassler, *Org. Letts.*, 2005, **7**, 569-572.
51. M. Frezza, L. Soulere, Y. Queneau and A. Doutheau, *Tetrahedron Lett.*, 2005, **46**, 6495-6498.

Chapter 5

Chemical and biochemical experiments

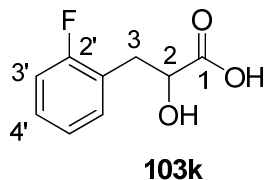
5.1 General methods

Air and moisture sensitive reactions were carried out under a nitrogen atmosphere using oven-dried glassware (140 °C). All reagents of synthetic grade were used as supplied. If further purification was required the procedures are detailed in Armarego and Perrin, *"Purification of laboratory chemicals"* 4th Ed. Dry ether, THF, DCM, and toluene were collected directly from a MBRAUN solvent purification system MB SPS-800. Ambient temperature refers to 20-25 °C. Reaction temperatures of -78 °C to -10 °C were obtained using solid carbon dioxide pellets and acetone or isopropyl alcohol or by using a bath cooling LP technology RP-100-CD. Temperatures of -10 °C to +4 °C were obtained in an ice/water/NaCl bath. Reactions requiring reflux or heating were carried out using an oil bath equipped with a contact thermometer. Nuclear magnetic resonance (NMR) spectra were obtained using Bruker Av-300 and Varian Unity Plus 300 machines operating at 300 MHz for ¹H, 75 MHz for ¹³C, 282 MHz for ¹⁹F, and 121 MHz for ³¹P. A Bruker Advance II 400 machine operating at 400 MHz for ¹H, 100 MHz for ¹³C, 376 MHz for ¹⁹F, and 162 MHz for ³¹P. All chemical shifts (δ) are reported in parts per million (ppm) and are quoted relative to the residual peak of CDCl₃, CFCl₃, D₂O, or CD₃OH or to the internal standard for (CH₃)₄Si. Coupling constants (*J*) are given in Hertz (Hz). ¹³C-NMR spectra were ¹H decoupled. ¹⁹F-NMR and ³¹P-NMR spectra were ¹H coupled. Complete assignment based on 1D and 2D NMR (COSY, NOESY, HSQC, and HMBC). Thin layer chromatography (TLC) was performed using Merck, Kieselgel 60 plates. Compounds were detected by either UV or by the use of a molybdenum based staining agents. Column chromatography was performed using Merck Kieselgel 60 silica gel (230-400 nm mesh). Cation exchange procedures were carried out using Dowex 50W (X8) resin with 50-100 mesh particles. Melting points were determined in Pyrex capillaries using

a Gallenkamp Griffin MPA350.BM2.5 melting point apparatus. All infra red (IR) spectra were recorded in the range 4000-440 cm^{-1} on a Nicolet Avatar 360 FT-IR as a thin film on NaCl plates or on PTFE plates. High-mass resolution spectrometry (HRMS) and low resolution mass spectrometry (LRMS) were performed using a Micromass LCT (Manchester, UK) mass spectrometer with electrospray ionization (ESI) operating in both positive and negative mode. Optical rotations were measured on Perkin-Elmer model 341 polarimeter. Single X-ray diffraction analyses were carried out by Prof. Alex M. Z. Slawin at the University of St Andrews.

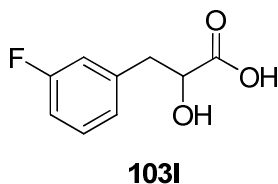
5.2 Synthetic experiment for Chapter 2

5.2.1 (*RS*)-*o*-Fluorophenyllactic acid **103k**



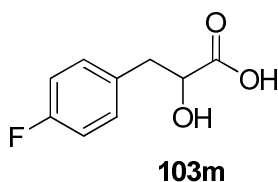
Conc. HCl (6.9 ml, 3 equiv.) was added to a solution of (*RS*)-*o*-fluorophenylalanine (4.98 g, 27.2 mmol) in water (260 ml) and the reaction mixture was stirred until homogenous. The solution was then cooled to 0 °C and NaNO₂ (3.90 g, 2 equiv.) was added portionwise over 4 h maintaining a temperature of 0 °C. The reaction was warmed to ambient temperature and left to stir for a further 48 h. The solution was concentrated under reduced pressure and organic compounds were extracted into ether (3×150 ml). The organic extracts were combined, dried over MgSO₄, and filtered. After removal of solvents under reduced pressure, a crude yellow oil was obtained. Recrystallisation of the crude product from chloroform gave (*RS*)-*o*-fluorophenyllactic acid **103k** as a white crystalline solid (1.62 g, 32.2%). Mp. 80-81 °C (lit.¹ 80-81 °C); δ_{H} (300 MHz, MeOH-d₄) 3.04 (dd, 1H, $^3J_{\text{HH}} = 7.7$, $^2J_{\text{HH}} = 14.2$, H-3), 3.28 (dd, 1H, $^3J_{\text{HH}} = 4.7$, $^2J_{\text{HH}} = 14.2$, H-3), 4.54 (dd, 1H, $^3J_{\text{HH}} = 4.7$, $^3J_{\text{HH}} = 7.7$, H-2), 7.03-7.14 (m, 2H, Ar-H), 7.22-7.31 (m, 2H, Ar-H). δ_{C} (75 MHz, CDCl₃) 33.8 (C-3), 70.1 (C-2), 115.4 (d, $^2J_{\text{CF}} = 22.3$, C-3'), 124.1 (d, $^4J_{\text{CF}} = 3.5$, C-5'), 123.0 (d, $^2J_{\text{CF}} = 15.5$, C-1'), 128.9 (d, $^3J_{\text{CF}} = 8.2$, C-4' or C-6'), 131.9 (d, $^3J_{\text{CF}} = 4.6$, C-6' or C-4'), 161.3 (d, $^1J_{\text{CF}} = 245.5$, C-2'), 177.9 (C-1). δ_{F} (283 MHz, CDCl₃,) -117.9 (m, 1F, Ar-F). ν_{max} (KBr): 3416, 2950, 1703, 1604, 1507, 1450, 1418, 1362, 1230 cm⁻¹.

5.2.2 (RS)-*m*-Fluorophenyllactic acid **103l**



(*RS*)-*m*-Fluorophenyllactic acid **103l** was prepared as procedure described in **5.2.1** to obtain a white crystalline solid (1.25 g, 26.0%). Mp. 106-107 °C (lit.¹ 106-107 °C); δ_{H} (300 MHz, MeOH- d_4) 2.81 (dd, $^3J_{\text{HH}} = 8.0$, $^2J_{\text{HH}} = 14.0$, 1H, H-3), 3.01 (dd, 1H, $^3J_{\text{HH}} = 4.3$, $^2J_{\text{HH}} = 14.0$, H-3), 4.23 (dd, 1H, $^3J_{\text{HH}} = 4.3$, $^3J_{\text{HH}} = 8.0$, H-2), 6.82 (ddt, $^4J_{\text{HH}} = 0.8$, $^4J_{\text{HH}} = 2.6$, $^3J_{\text{HF, HH}} = 9.0$, 1H, H-4'), 6.91 (td, 1H, $^4J_{\text{HH}} = 2.4$, $^3J_{\text{HF}} = 10.2$, H-2'), 6.97 (d, 1H, $^3J_{\text{HH}} = 7.6$, H-6'), 7.14 (dt, 1H, $^4J_{\text{HF}} = 6.1$, $^3J_{\text{HH}} = 7.9$, H-5'). δ_{C} (75 MHz, CDCl_3) 41.1 (C-3), 72.4 (C-2), 114.2 (d, $^2J_{\text{CF}} = 21.5$, C-4'), 117.3 (d, $^2J_{\text{CF}} = 21.5$, C-2'), 126.4 (d, $^4J_{\text{CF}} = 2.8$, C-6'), 130.8 (d, $^3J_{\text{CF}} = 8.3$, C-5'), 141.7 (d, $^3J_{\text{CF}} = 7.6$, C-1'), 164.1 (d, $^1J_{\text{CF}} = 243.2$, C-3'), 176.8 (C-1). δ_{F} (283 MHz, CDCl_3) -116.7 (ddd, $^4J_{\text{HF}} = 6.2$, $^3J_{\text{HF}} = 9.3$, $^3J_{\text{HF}} = 9.3$, 1F, Ar-F). ν_{max} (KBr) 3428, 2940, 1722, 1585, 1486, 1450, 1429, 1324, 1240 cm^{-1} .

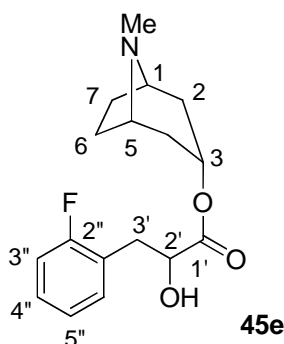
5.2.3 (RS)-*p*-Fluorophenyllactic acid **103m**



(*RS*)-*p*-Fluorophenyllactic acid **103m** was prepared as procedure described in **5.2.1** to obtain a white crystalline solid (1.01 g, 20.5%). Mp. 99-100 °C (lit.¹ 100-101 °C); δ_{H}

(300 MHz, MeOH- d_4) 2.78 (dd, 1H, $^3J_{\text{HH}} = 7.9$, $^2J_{\text{HH}} = 14.0$, H-3), 2.98 (dd, 1H, $^3J_{\text{HH}} = 4.3$, $^2J_{\text{HH}} = 14.0$, H-3), 4.20 (dd, 1H, $^3J_{\text{HH}} = 4.3$, $^3J_{\text{HH}} = 7.9$, H-2), 6.89 (dd, 2H, $^3J_{\text{HF}} = 8.9$, $^3J_{\text{HH}} = 8.9$, H-3', H-5'), 7.17 (dd, 2H, $^4J_{\text{HF}} = 5.6$, $^3J_{\text{HH}} = 8.6$, H-2', H-6'). δ_{C} (75 MHz, MeOH- d_4) 43.2 (C-3), 75.1 (C-2), 118.3 (d, $^2J_{\text{CF}} = 21.5$, C-3', C-5'), 134.8 (d, $^3J_{\text{CF}} = 7.9$, C-2', C-6'), 137.3 (d, $^4J_{\text{CF}} = 3.0$, C-1'), 165.7 (d, $^1J_{\text{CF}} = 243.0$, C-4'), 179.5 (C-1). δ_{F} (283 MHz, MeOH- d_4) -116.1 (dddd, $^4J_{\text{HF}} = 5.4$, $^4J_{\text{HF}} = 5.4$, $^3J_{\text{HF}} = 8.7$, $^3J_{\text{HF}} = 8.7$, 1F, Ar-F). ν_{max} (KBr) 3417, 2950, 1702, 1600, 1507, 1445, 1363, 1228 cm^{-1} .

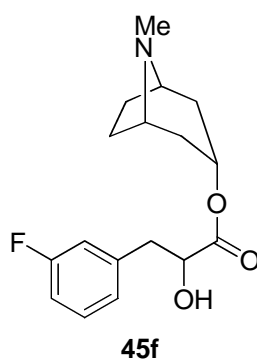
5.2.4 (*rac*)-*o*-Fluorolittorine ((*RS*)-*o*-fluorophenyllactoyltropine, **45e**)¹



Dry (*RS*)-*o*-fluorophenyllactic acid **103k** (0.32 g, 1.71 mmol) and tropine (0.24 g, 1.71 mmol) were mixed intimately under nitrogen in the solid phase. The mixture was heated to 130 °C and a current of dry HCl gas was passed periodically over the reaction for 4 h and the reaction was allowed to cool to ambient temperature. The product was dissolved as completely as possible in 50 mM H₂SO₄ (10 ml), the insoluble material was filtered off. The filtrate was then treated with 10% aqueous ammonium hydroxide until it was basic, and then the organics were extracted into chloroform (3 × 15 ml). The combined organic phases were dried over MgSO₄, and the solvents were evaporated under reduced pressure to give a pale yellow oil. The

product was purified over silica gel column eluting with EtOH:CHCl₃:35%NH₃ (7:7:0.2) to afford **45e** as a colourless viscous oil (0.11 g, 21.0%). δ_{H} (300 MHz, CDCl₃) 1.58 (d, 1H, $^2J_{\text{HH}} = 15.3$, H-4_a), 1.65 (d, 1H, $^2J_{\text{HH}} = 15.3$, H-2_a), 1.74-1.79 (m, 2H, H-6_a, H-7_a), 1.87-1.98 (m, 2H, H-6_e, H-7_e), 2.04-2.15 (m, 2H, H-2_e, H-4_e), 2.22 (s, 3H, NMe), 2.93 (dd, 1H, $^3J_{\text{HH}} = 7.6$, $^2J_{\text{HH}} = 14.0$, H-3'), 3.05-3.06 (br, 2H, H-1, H-5), 3.12 (dd, 1H, $^3J_{\text{HH}} = 5.1$, $^2J_{\text{HH}} = 14.0$, H-3'), 4.33 (dd, $^3J_{\text{HH}} = 5.1$, $^3J_{\text{HH}} = 7.6$, 1H, H-2'), 5.01 (t, $^3J_{\text{HH}} = 5.3$, 1H, H-3_e), 6.93-7.05 (m, 2H, Ar-H), 7.13-7.24 (m, 2H, Ar-H). δ_{C} (CDCl₃) 25.3 (C-6 or C-7), 25.5 (C-6 or C-7), 34.0 (C3'), 36.3 (C-2 or C-4), 36.6 (C-2 or C-4), 40.4 (NCH₃), 59.6 (C-1, C-5), 69.4 (C-3), 70.4 (C-2'), 115.2 (d, $^2J_{\text{HF}} = 22.1$, C-3''), 123.6 (d, $^2J_{\text{HF}} = 15.6$, C-1''), 124.0 (d, $^4J_{\text{HF}} = 3.5$, C-5''), 128.7 (d, $^3J_{\text{HF}} = 8.1$, C-4''), 131.9 (d, $^3J_{\text{HF}} = 4.5$, C-6''), 162.7 (d, $^1J_{\text{HF}} = 245.23$, C-2''), 173.2 (C-1'). δ_{F} (282 MHz, CDCl₃) -118.20 (m, 1F, Ar-F). ν_{max} (neat) 2923, 1739, 1587, 1493, 1461, 1377, 1260 cm⁻¹. m/z (ES⁺): Calcd. for C₁₇H₂₃NFO₃ [M+H]⁺: 308.1662, found 308.1328 100%)

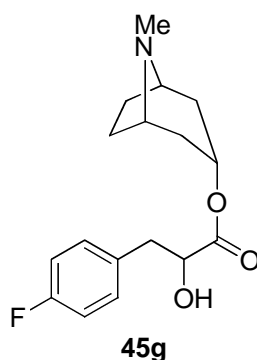
5.2.5 (*rac*)-*m*-Fluorolittorine ((*RS*)-*m*-fluorophenyllactoyltropine, **45f**)¹



The procedure described in **5.2.4** was repeated with (*RS*)-*m*-fluorophenyllactic acid (**103m**, 0.37 g, 1.90 mmol) and tropine (0.27 g, 1.90 mmol) to afford **45f** as colorless

viscous oil (0.12 g, 20%). δ_{H} (300 MHz, CDCl_3) 1.57 (d, $^2J_{\text{HH}} = 15.0$, 2H, H-4_a), 1.60 (d, $^2J_{\text{HH}} = 15.0$, 2H, H-2_a), 1.66-1.73 (m, 2H, H-6_a, H-7_a), 1.92-1.96 (m, 2H, H-6_e, H-7_e), 2.02-2.12 (m, 2H, H-2_e, H-4_e), 2.19 (s, 3H, NMe), 2.89 (dd, $^3J_{\text{HH}} = 7.1$, $^2J_{\text{HH}} = 14.0$, 1H, H-3'), 3.00-3.05 (br, 2H, H-1, H-5), 3.06 (dd, $^3J_{\text{HH}} = 4.7$, $^2J_{\text{HH}} = 14.0$, 1H, H-3'), 4.31 (dd, $^3J_{\text{HH}} = 4.7$, $^3J_{\text{HH}} = 7.1$, 1H, H-2'), 5.00 (t, $^3J_{\text{HH}} = 4.8$, 1H, H-3_e), 6.84-6.92 (m, 2H, H-4'', H-5''), 6.94 (d, $^3J_{\text{HF}} = 7.8$, 1H, H-6''), 7.16-7.23 (m, 1H, H-2''). δ_{C} (75 MHz, CDCl_3) 25.4 (C-7 or C-6), 25.5 (C-6 or C-7), 36.3 (C-2 or C-4), 36.6 (C-4 or C-2), 40.4 (C-3', NMe), 59.6 (C-1, C-5), 69.4 (C-3), 70.4 (C-2'), 115.3 (d, $^2J_{\text{CF}} = 22.0$, C-4''), 123.5 (d, $^3J_{\text{CF}} = 15.5$, C-1''), 124.0 (d, $^4J_{\text{CF}} = 3.4$, C-6''), 128.7 (d, $^3J_{\text{CF}} = 8.1$, C-2''), 131.9 (d, $^3J_{\text{CF}} = 4.5$, C-5''), 161.2 (d, $^1J_{\text{CF}} = 245.5$, C-3''), 173.5 (C-1'). δ_{F} (282 MHz, CDCl_3) -113.8 (ddd, $^4J_{\text{HF}} = 6.2$, $^3J_{\text{HF}} = 9.3$, $^3J_{\text{HF}} = 9.3$, 1F, Ar-F). ν_{max} 2948, 1740, 1620, 1592, 1492, 1452, 1254 cm^{-1} . m/z (ES⁺): Calcd. for $\text{C}_{17}\text{H}_{22}\text{NFO}_3$ $[\text{M}]^+$: 307.1584, found 307.8809.

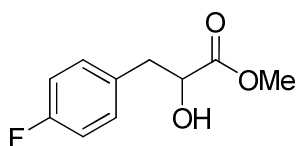
5.2.6 (*rac*)-*p*-Fluorolittorine ((*RS*)-*p*-fluorophenyllactoyltropine, **45g**)¹



The procedure described in **5.2.4** was repeated with (*RS*)-*o*-fluorophenyllactic acid (**103m**, 0.39 g, 2.1 mmol) and tropine (0.29 g, 2.1 mmol) to afford **45g** a colourless viscous oil (0.48 g, 48.1%). δ_{H} (300 MHz, CDCl_3) 1.65 (d, 1H, $^2J_{\text{HH}} = 15.2$, H-4_a),

1.68 (d, 1H, $^2J_{\text{HH}} = 15.2$, H-2_a), 1.74-1.83 (m, 2H, H-6_a, H-7_a), 1.96-2.09 (m, 2H, H-6_e, H-7_e), 2.11-2.23 (m, 2H, H-2_e, H-4_e), 2.38 (s, 3H, -NMe), 2.94 (dd, 1H, $^3J_{\text{HH}} = 6.9$, $^2J_{\text{HH}} = 14.0$, H-3'), 3.12 (dd, 1H, $^3J_{\text{HH}} = 4.7$, $^2J_{\text{HH}} = 14.0$, H-3'), 3.07-3.16 (m, 3H, H-1, H-5, H-3'), 4.36 (dd, 1H, $^3J_{\text{HH}} = 4.7$, $^3J_{\text{HH}} = 6.9$, H-2'), 5.07 (t, 1H, $^3J_{\text{HH}} = 5.3$, H-3_e), 6.99 (t, 2H, $^3J_{\text{HF, HH}} = 8.8$, H-3'', H-5''), 7.21 (dd, 2H, $^4J_{\text{HF}} = 5.4$, $^3J_{\text{HH}} = 8.7$, H-2'', H-6''). δ_{C} (75 MHz, CDCl₃) 25.3 (C-6, C-7), 25.4 (C-6, C-7), 36.1 (C-4 or C-2), 36.2 (C-2 or C-4), 39.7 (C-3'), 40.1 (NMe), 59.7 (C-2, C-5), 68.9 (C-3), 71.4 (C-2'), 115.2 (d, $^2J_{\text{CF}} = 21.4$, C-3'', C-5''), 130.9 (d, $^3J_{\text{CF}} = 7.8$, C-2'', C-6''), 132.2 (d, $^4J_{\text{CF}} = 3.2$, C-1''), 162.7 (d, $^1J_{\text{CF}} = 244.9$, C-4''), 173.2 (C-1'). δ_{F} (CDCl₃, 283 MHz) -116.6 (dddd, $^4J_{\text{HF}} = 5.4$, $^4J_{\text{HF}} = 5.4$, $^3J_{\text{HF}} = 8.7$, $^3J_{\text{HF}} = 8.7$, 1F, Ar-F). ν_{max} (KBr) 2944, 1730, 1601, 1508, 1448, 1418, 1218 cm⁻¹. m/z (ES⁺): Calcd. for C₁₇H₂₂NFO₃ [M]⁺: 307.1584, found 307.8727.

5.2.7 Methyl-(*RS*)-*p*-fluorophenyllactate **124a**

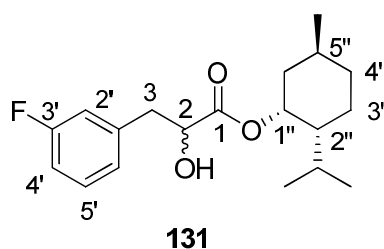


124a

Conc. HCl (0.1 ml, 1.20 mmol) was added to a solution of (*RS*)-*p*-fluorophenyllactic acid **103m** (50 mg, 0.27 mmol) in toluene (5 ml) and MeOH (10 ml) and the reaction mixture was brought to reflux. After 4 h the reaction mixture was neutralised with 5% NaHCO₃ and the mixture was extracted into DCM (3×10 ml). The combined organic phases were washed with water, brine, dried over MgSO₄, and filtered. The solvents

were removed under reduced pressure to yield **124a** as white solid (50 mg, 93.4%). Mp 53-54 °C. δ_{H} (300 MHz, CDCl_3) 2.95 (dd, $^3J_{\text{HH}} = 6.6$, $^2J_{\text{HH}} = 14.0$, 1H, H-3), 3.12 (dd, 1H, $^3J_{\text{HH}} = 4.5$, $^2J_{\text{HH}} = 14.0$, H-3), 3.79 (s, 3H, -OMe), 4.44 (dd, 1H, $^3J_{\text{HH}} = 4.5$, $^3J_{\text{HH}} = 6.6$, H-2), 7.00 (dd, 2H, $^3J_{\text{HF}} = 8.7$, $^3J_{\text{HH}} = 8.7$, H-3', H-5'), 7.19 (dd, 2H, $^4J_{\text{HF}} = 5.6$, $^3J_{\text{HH}} = 8.6$, H-2', H-6'). δ_{C} (75 MHz, CDCl_3) 39.9 (C-3), 52.9 (-OMe), 71.6 (C-2), 115.63 (d, $^2J_{\text{CF}} = 21.2$, C-3', C-5'), 131.4 (d, $^3J_{\text{CF}} = 7.7$, C-2', C-6'), 132.6 (d, $^4J_{\text{CF}} = 3.2$, C-1'), 162.3 (d, $^1J_{\text{CF}} = 244.8$, C-4'). δ_{F} (283 MHz, CDCl_3) -116.6 (dddd, $^4J_{\text{HF}} = 5.5$, $^4J_{\text{HF}} = 5.5$, $^3J_{\text{HF}} = 8.8$, $^3J_{\text{HF}} = 8.8$, 1F, Ar-F). ν_{max} (KBr) 3176, 1748, 1508, 1218, 1154, 503 cm^{-1} .

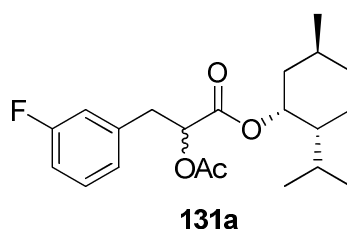
5.2.8 (-)-Menthyl-(*RS*)-*m*-fluorophenyllactate **131**²



The mixture of (*RS*)-*m*-fluorophenyllactic acid **103I** (0.10 g, 0.5 mmol) and (-)-menthol (0.12 g, 0.75 mmol) was heated at 120 °C under a periodically stream of dry HCl gas. After 6 h the reaction was cooled to ambient temperature, dissolved in ether (20 ml), and washed with aq. Na_2CO_3 (5 ml). The ethereal phase was washed with water (10 ml), brine, dried over MgSO_4 , filtered, and evaporated under reduced pressure. The crude product was purified over silica gel eluting with ether:cyclohexane (3:2) to afford a mixture of 1:1 diastereomers **131** as a white solid (0.118 g, 73.2 %). δ_{H} (300 MHz, MeOH-d_4) 0.65 (d, 3H, $^3J_{\text{HH}} = 7.0$, CH_3CHCH_3), 0.66 (d, 3H, $^3J_{\text{HH}} = 7.0$, CH_3CHCH_3), 0.81 (d, 3H, $^3J_{\text{HH}} = 6.5$, CH_3CHCH_3), 0.82 (d,

$^3J_{\text{HH}} = 6.5$, CH_3CHCH_3), 0.84 (d, 3H, $^3J_{\text{HH}} = 7.0$, $-\text{CHCH}_3$), 0.85 (d, 3H, $^3J_{\text{HH}} = 7.0$, $-\text{CHCH}_3$), 0.80-0.95 (m, 6H, H-3_a'', H-4_a'', H-6_a''), 1.27-1.48 (m, 4H, H-2_a'', H-5_a''), 1.57-1.76 (m, 6H, $(\text{CH}_3)_2\text{CH}$, H-3_e'', H-4_e''), 1.79-1.97 (m, 2H, H-2_{6e}'), 2.83 (dd, 1H, $^3J_{\text{HH}} = 7.4$, $^2J_{\text{HH}} = 14.1$, H-3), 2.87 (dd, 1H, $^3J_{\text{HH}} = 7.0$, $^2J_{\text{HH}} = 14.0$, H-3), 3.05 (dd, 1H, $^3J_{\text{HH}} = 4.5$, $^2J_{\text{HH}} = 14.0$, H-3), 3.08 (dd, 1H, $^3J_{\text{HH}} = 4.3$, $^2J_{\text{HH}} = 14.1$, H-3), 4.30-4.37 (m, 2H, H-2), 4.68 (dt, 2H, $^3J_{\text{HH}} = 4.7$, $^3J_{\text{HH}} = 10.9$, H-1''), 6.84 (dd, 2H, $^4J_{\text{HH}} = 2.6$, $^3J_{\text{HF, HH}} = 8.6$, H-4'), 6.91 (dd, 2H, $^4J_{\text{HH}} = 2.3$, $^3J_{\text{HF}} = 9.6$, H-2'), 6.96 (d, 2H, $^3J_{\text{HH}} = 7.6$, H-6'), 7.18 (dt, 2H, $^4J_{\text{HF}} = 2.7$, $^3J_{\text{HH}} = 8.6$, H-5'). δ_{C} (75 MHz, CDCl_3) 15.8, 16.9, (CH_3CHCH_3), 20.7, 20.8 (CH_3CHCH_3), 21.9 ($\text{CH}_3\text{CH}-$), 22.9, 23.3 (C-3''), 25.9, 26.2 (CH_3CHCH_3), 31.4 (C-5''), 34.0 (C-4''), 40.0, 40.1 (C-3), 40.6, 40.8 (C-6''), 46.8, 46.9 (C-2''), 70.7 (C-2), 71.2 (C-2), 76.3 (C-1''), 76.5 (C-1''), 113.7 (d, $^2J_{\text{CF}} = 21.3$, C-4'), 116.3 (d, $^2J_{\text{CF}} = 16.9$, C-2'), 116.6 (d, $^2J_{\text{CF}} = 16.9$, C-2'), 125.1 (d, $^4J_{\text{CF}} = 2.9$, C-6'), 125.3 (d, $^4J_{\text{CF}} = 2.9$, C-6'), 129.6 (d, $^3J_{\text{CF}} = 7.9$, C-5'), 129.7 (d, $^3J_{\text{CF}} = 7.9$, C-5'), 141.7 (d, $^3J_{\text{CF}} = 7.6$, C-1'), 164.1 (d, $^1J_{\text{CF}} = 243.2$, C-3'), 173.6 (C-1), 173.7 (C-1). δ_{F} (283 MHz, CDCl_3) -113.9 (ddd, $^4J_{\text{HF}} = 6.2$, $^3J_{\text{HF}} = 9.5$, $^3J_{\text{HF}} = 9.5$, 1F, Ar-F), -114.2 (ddd, $^4J_{\text{HF}} = 6.2$, $^3J_{\text{HF}} = 9.5$, $^3J_{\text{HF}} = 9.5$, 1F, Ar-F). ν_{max} (KBr) 3478, 2955, 1724, 1616, 1588, 1209, 1152 cm^{-1} . m/z (ES+) 345.14 $[\text{M}+\text{Na}]^+$ (100%).

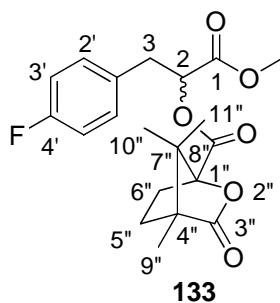
5.2.9 α -Acetyl-(-)-menthyl-(*RS*)-*m*-fluorophenyllactate **131a**



Acetic anhydride (0.2 ml, 0.21 mmol) was added to a solution of (-)-menthyl-(*RS*)-*m*-fluorophenyllactate **131** (50 mg, 0.15 mmol) in dry pyridine (0.5 ml, mmol) at 0 °C. The reaction mixture was then warmed to ambient temperature. After being left overnight, MeOH (3 ml) was added the reaction mixture and was evaporated under reduced pressure. The residue was dissolved in 1 M HCl (5 ml) and the mixture was extracted into DCM (3×10 ml). The combined organic phases were washed with water, brine, dried over MgSO₄, and filtered. The solvents were removed under reduced pressure to afford a mixture of diastereomers **131a** as colourless oil (50 mg, 88.5%). δ_{H} (300 MHz, CDCl₃) 0.62 (d, 3H, $^3J = 7.0$, CH₃CHCH₃), 0.66 (d, 3H, $^3J = 7.0$, CH₃CHCH₃), 0.78 (d, 3H, $^3J = 7.0$, CH₃CHCH₃), 0.79 (d, 3H, $^3J = 7.0$, CH₃CHCH₃), 0.82 (d, 3H, $^3J = 6.5$, -CHCH₃), 0.83 (d, 3H, $^3J = 6.5$, -CHCH₃), 0.86-1.04 (m, 6H, H-3_a", H-4_a", H-6_a"), 1.23-1.46 (m, 4H, H-2_a", H-5_a"), 1.54-1.65 (m, 4H, H-3_e", H-4_e"), 1.67-1.75 (m, 2H, (CH₃)₂CH), 1.76-1.94 (m, 2H, H-6_e"), 2.01 (s, 3H, COCH₃), 2.02 (s, 3H, COCH₃), 2.96-3.12 (m, 4H, H-3), 4.59 (dd, 1H, $^3J_{\text{HH}} = 4.4$, $^3J_{\text{HH}} = 6.9$, H-2), 4.66 (dd, 1H, $^3J_{\text{HH}} = 4.4$, $^3J_{\text{HH}} = 6.9$, H-2), 5.09 (m, 2H, H-1"), 6.83-6.93 (m, 4H, H-2', H-4'), 6.95 (d, 2H, $^3J_{\text{HH}} = 7.8$, H-6'), 7.18 (m, 2H, H-5'). δ_{C} (75 MHz, CDCl₃) 15.8, 16.3 (CH₃CHCH₃), 20.5, 20.6 (O=CCH₃), 20.6, 20.8 (CH₃CHCH₃), 21.9 (CH₃CH-), 23.2, 23.4 (C-3"), 25.9, 26.1 (CH₃CHCH₃), 31.3, 31.4 (C-5"), 34.1 (C-4"), 36.9 (C-3), 40.4, 40.5 (C-6"), 46.8, 46.9 (C-2"), 72.7, 72.9 (C-2), 77.0, 77.5 (C-1"),

113.9 (d, $^2J_{\text{CF}} = 20.9$, C-4'), 116.3, 116.4 (d, $^2J_{\text{CF}} = 21.5$, C-2'), 125.0, 125.1 (d, $^4J_{\text{CF}} = 2.8$, C-6'), 129.8, 129.9 (d, $^3J_{\text{CF}} = 8.3$, C-5'), 138.4, 138.5 (d, $^3J_{\text{CF}} = 2.0$, C-1'), 162.7 (d, $^1J_{\text{CF}} = 245.7$, C-3'), 162.8 (d, $^1J_{\text{CF}} = 246.1$, C-3'), 169.0, 169.1 (C-1''), 170.2, 170.3 (C-1). δ_{F} (283 MHz, CDCl_3) -113.7 (ddd, $^4J_{\text{HF}} = 6.0$, $^3J_{\text{HF}} = 9.3$, $^3J_{\text{HF}} = 9.3$, 1F, Ar-F), -113.9 (ddd, $^4J_{\text{HF}} = 6.2$, $^3J_{\text{HF}} = 9.3$, $^3J_{\text{HF}} = 9.3$, 1F, Ar-F). ν_{max} (KBr) 2956, 1746, 1590, 1452, 1371, 1213 cm^{-1} . m/z (ES+) 428.25 $[\text{M}+\text{Na}+\text{ACN}]$ (100%); m/z (ES-) 225.03 (M-menthyl) (100%)

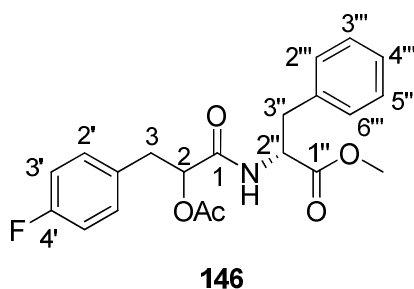
5.2.10 (S)-Camphanoyl-methyl-(RS)-p-fluorophenyllactate **133**



A solution of (RS)-methyl-*p*-fluorophenyllactate **124a** (0.1g, 0.5 mmol) in dry pyridine (0.32 ml, 4 mmol) was slowly added to a solution of (S)-(-)-camphanoyl chloride (0.11 g, 0.5 mmol) in dry DCM (10 ml) at 0 °C. The progress of the reaction was monitored by TLC. After completion, the reaction mixture was diluted with DCM (10 ml), washed successively with 1 M HCl, then washed with water and sat. NaHCO_3 . The organic phase was dried over MgSO_4 , filtered, and evaporated under reduced pressure. The crude product was purified over silica gel eluting with EtOAc:hexane (1:4) to afford a mixture of diastereoisomers **133** as colourless oil (0.17g, 90.2%). δ_{H} (300 MHz, CDCl_3) 0.86 (s, 3H, H-10'' or H-11''), 0.92 (s, 6H, H-

10''or H-11''), 1.03 (s, 3H, H-10''or H-11''), 1.09 (s, 6H, H-9''), 1.66 (m, 2H, H-5_e''), 1.84-2.02 (m, 4H, H-4_a'', H-5_a''), 2.43-2.27 (m, 2H, H-4_e''), 3.10 (dd, $^3J_{\text{HH}} = 4.2$, $^2J_{\text{HH}} = 14.4$, 1H, H-3), 3.13 (dd, $^3J_{\text{HH}} = 4.0$, $^2J_{\text{HH}} = 14.4$, 1H, H-3), 3.24 (dd, $^3J_{\text{HH}} = 3.5$, $^2J_{\text{HH}} = 14.4$, 1H, H-3), 3.73 (s, 3H, OCH₃), 3.74 (s, 3H, OCH₃), 5.32 (m, 2H, H-2), 6.97 (t, $^3J_{\text{HF}} = 8.6$, $^3J_{\text{HH}} = 8.6$, 2H, H-3', H-5'), 7.19 (ddd, $^4J_{\text{HF}} = 5.5$, $^3J_{\text{HH}} = 8.6$, 2H, H-2', H-6'). δ_{C} (75 MHz, CDCl₃) 10.0, 10.1, (C-9''), 16.5, 16.8, 16.9, (C-10'', C-11''), 29.1, 29.4, (C-5''), 30.8, 30.9 (C-4''), 36.6, 36.7 (C-3), 52.8, 52.9 (OCH₃), 54.8, 54.9 (C-7''), 55.2, 55.4 (C-6''), 73.8, 73.9 (C-2), 91.1, 91.2 (C-3''), 115.8 (d, $^2J_{\text{CF}} = 21.4$, C-3', C-5'), 131.4 (d, $^3J_{\text{CF}} = 8.1$, C-2', C-6'), 162.5 (d, $^1J_{\text{CF}} = 245.4$, C-4'), 167.0, 167.4, (C-8''), 169.3, 169.4 (C-1), 178.6, 178.3 (C-1''). δ_{F} (283 MHz, CDCl₃) -115.9 (dddd, $^4J_{\text{HF}} = 5.3$, $^4J_{\text{HF}} = 5.3$, $^3J_{\text{HF}} = 8.7$, $^3J_{\text{HF}} = 8.7$, 1F, Ar-F), -115.8 (dddd, $^4J_{\text{HF}} = 5.5$, $^4J_{\text{HF}} = 5.5$, $^3J_{\text{HF}} = 8.7$, $^3J_{\text{HF}} = 8.7$, 1F, Ar-F). ν_{max} (KBr) 2967, 1789, 1752, 1603, 1510, 1222 and 1159 cm⁻¹. m/z (ESI+) 401.08 [M+Na] (100%).

5.2.11 α -Acetyl-methyl-D-phenylalanyl-(*RS*)-*p*-fluorophenyllactamide 146

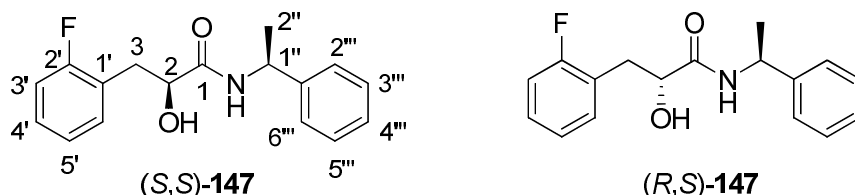


D-phenylalanine methyl ester hydrochloride (45 mg, 0.21 mmol), which was neutralised with NMM (27 μ l) was added a solution of (*RS*)- α -acetyl-*p*-fluorophenyllactic acid **103n** (47 mg, 0.21 mmol) in DMF (2 ml). HOBt (71 mg, 0.53

mmol) was then added and the reaction mixture was cooled to 0 °C. To this mixture, a solution of EDC (0.13 g, 0.69 mmol) in chloroform (3 ml) was slowly added. The reaction mixture was warmed to ambient temperature. After being left stir overnight, water (5 ml) was added and the mixtures were extracted into EtOAc (3×10 ml). The combined organic phases were washed with 1 M HCl (2×10 ml), sat. NaHCO₃ (2×10 ml), and brine. After drying over MgSO₄ and filtered off, the solvents were evaporated under reduced pressure. The residue was purified over silica gel eluting with EtOAc:hexane (2:3) to give a mixture of diastereoisomers of **146** as colourless viscous oil (61 mg, 74.8%); δ_{H} (CDCl₃, 300 MHz) 1.95 (s, 3H, O=CCH₃), 1.96 (s, 3H, O=CCH₃), 2.86-3.12 (m, 8H, H-3, H-3''), 3.61 (s, 3H, OCH₃), 3.64 (s, 3H, OCH₃), 4.74 (dd, 1H, ³*J* = 5.7, ³*J*_{HH} = 8.0, H-2''), 4.77 (dd, 1H, ³*J*_{HH} = 5.7, ³*J*_{HH} = 8.0, H-2''), 5.25 (dd, 1H, ³*J*_{HH} = 4.8, ³*J*_{HH} = 6.5, H-2), 5.27 (dd, 1H, ³*J*_{HH} = 4.7, ³*J*_{HH} = 7.2, H-2), 6.29 (d, 1H, ³*J*_{HH} = 8.0, NH), 6.37 (d, 1H, ³*J*_{HH} = 8.0, NH), 6.79-7.19 (m, 18H, Ar-H). δ_{C} (CDCl₃, 75 MHz) 20.6, 20.7 (O=CCH₃), 36.6, 36.9 (C-3''), 37.6, 38.0 (C-3), 52.3, 52.4 (OCH₃), 52.5, 52.6 (C-2''), 73.9, 74.0 (C-2), 115.2 (d, ²*J*_{CF} = 21.2, C-3', C-5'), 127.2, 127.3 (C-4''), 128.5, 128.6 (C-2'', C-6''), 129.2, 129.3 (C-3''', C-5'''), 131.2, 131.9 (d, ³*J*_{CF} = 7.9, C-2''', C-6'''), 131.5, 131.4 (d, ³*J*_{CF} = 3.3, C-1'), 135.3 (C-1'''), 161.9, 162.0 (d, ¹*J*_{CF} = 245.1, C-4'), 168.3, 168.6 (C=O), 169.2 (C=O), 171.4, 171.3 (C-1). δ_{F} (CDCl₃, 283 MHz) -116.4 (dddd, ⁴*J*_{HF} = 5.4, ⁴*J*_{HF} = 5.4, ³*J*_{HF} = 8.6, ³*J*_{HF} = 8.6, 1F, Ar-F), -116.2 (dddd, ⁴*J*_{HF} = 5.3, ⁴*J*_{HF} = 5.3, ³*J*_{HF} = 8.6, ³*J*_{HF} = 8.6, 1F, Ar-F). ν_{max} (neat): 3422, 3322, 1744, 1678, 1603, 1509, 1371, 1221, 702, 503 cm⁻¹. **HRMS** (**ES**⁺): Calcd. for C₂₁H₂₂FNO₅Na⁺ [M+Na]⁺: 410.1380, found: 410.1369

5.2.12 (*S*)-3-(2-Fluorophenyl)-2-hydroxyl-*N*-((*S*)-1-phenylethyl)

propanamide (*S,S*)-**147** and (*R*)-3-(2-fluorophenyl)-2-hydroxyl-*N*-((*S*)-1-phenylethyl)propanamide (*R,S*)-**147**



(*S*)-Phenylethylamine (0.72 ml, 5.3 mmol) and HOBT (1.8 g, 13.3 mmol) were added to a solution of (*RS*)-*o*-fluorophenyllactic acid (0.98 g, 5.32 mmol) in DMF (3 ml) and the reaction mixture was cooled to 0 °C. A solution of EDC (3.4 g, 17.7 mmol) in CHCl₃ (5 ml) was slowly added. The reaction mixture was warmed to ambient temperature and left stirring overnight. Water (10 ml) was added and the mixture was extracted into EtOAc (3× 20). The combined organic phases were washed with 1 M HCl (2×10 ml), sat. aq. NaHCO₃ (2×10 ml), brine, and dried over MgSO₄. After filtration, the solvents were removed under reduced pressure. The crude product was purified over silica gel eluting with EtOAc:hexane (1:3) to afford (*S,S*)-**147** as colourless needles (0.67g, 44.3%) and (*R,S*)-**147** as a white solid (0.61g, 39.7%).

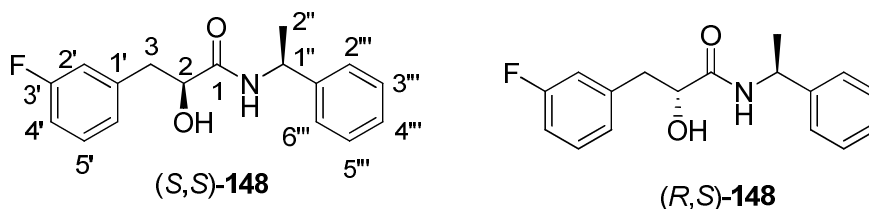
(*S,S*)-**147**: Mp 71-72 °C; $[\alpha]_D^{20}$: -74.0° ($c = 1.0 \times 10^{-3}$, CHCl₃); δ_H (CDCl₃, 300 MHz) 1.36 (d, $^3J_{HH} = 7.0$, 3H, H-1''), 2.92 (dd, 1H, $^3J_{HH} = 7.8$, $^2J_{HH} = 14.2$, H-3), 3.23 (dd, 1H, $^3J_{HH} = 4.4$, $^2J_{HH} = 14.2$, H-3), 4.29 (dd, 1H, $^3J_{HH} = 4.29$, $^3J_{HH} = 7.8$, H-3), 5.04 (quint, 1H, $^3J_{HH} = 7.0$, H-2''), 6.65 (d, 1H, $^3J_{HH} = 6.7$, NH), 6.93-7.03 (m, 2H, Ar-H), 7.12-7.28 (m, 7H, Ar-H); δ_C (CDCl₃, 75 MHz) 21.7 (C-2''), 34.3 (C-3), 48.5 (C-1''), 72.0 (C-2), 115.8 (d, $^3J_{CF} = 22.2$, C-3'), 123.9 (d, $^2J_{CF} = 15.8$, C-1'), 124.3 (d, $^3J_{CF} = 8.1$, C-4' or C-6'), 126.2 (C-2''', C-6'''), 127.4 (C-4'''), 128.6 (C-3''', C-5'''), 128.7 (d,

$^3J_{\text{CF}} = 8.1$, C-4' or C-6'), 132.0 (d, $^3J_{\text{CF}} = 4.6$, C-4' or C-6'), 142.8 (C-1'''), 161.7 (d, $^1J_{\text{CF}} = 244.2$, C-2'), 171.4 (C-1); δ_{F} (CDCl₃, 283 MHz) -117.3 (ddd, $^4J_{\text{HF}} = 6.5$, $^4J_{\text{HF}} = 6.5$, $^3J_{\text{HF}} = 9.8$, 1F, Ar-F); ν_{max} (KBr): 3335, 2972, 1647, 1583, 1451, 1229, 1075, 758 cm⁻¹. **HRMS (ES+)**: Calcd. for: C₁₇H₁₈FNO₂Na [M+Na]⁺: 310.1219, found 310.1222.

(*R,S*)-**147**: Mp 76-77 °C; $[\alpha]_{\text{D}}^{20}$: +14.0° (c = 2.0×10⁻³, CHCl₃); δ_{H} (CDCl₃, 300 MHz) 1.36 (d, 3H, $^3J_{\text{HH}} = 7.0$, H-1''), 2.92 (dd, 1H, $^3J_{\text{HH}} = 7.8$, $^2J_{\text{HH}} = 14.0$, H-3), 3.23 (dd, 1H, $^3J_{\text{HH}} = 4.4$, $^2J_{\text{HH}} = 14.2$, H-3), 4.31 (t, 1H, $^3J_{\text{HH}} = 5.4$, $^3J_{\text{HH}} = 7.8$, H-3), 5.02 (quint, 1H, $^3J_{\text{HH}} = 7.1$, H-2''), 6.52 (d, 1H, $^3J_{\text{HH}} = 7.4$, NH), 6.49-6.99 (m, 2H, Ar-H), 7.10-7.25 (m, 7H, Ar-H); δ_{C} (CDCl₃, 75 MHz) 21.8 (C-2''), 34.3 (C-3), 48.5 (C-1''), 72.1 (C-2), 115.4 (d, $^3J_{\text{CF}} = 22.2$, C-3'), 123.7 (d, $^2J_{\text{CF}} = 15.6$, C-1'), 124.4 (d, $^3J_{\text{CF}} = 3.3$, C-5'), 126.1 (C-2''', C-6'''), 127.3 (C-4'''), 128.7 (C-3''', C-5'''), 128.8 (d, $^3J_{\text{CF}} = 8.9$, C-4' or C-6'), 132.1 (d, $^3J_{\text{CF}} = 4.6$, C-4' or C-6'), 142.8 (C-1'''), 161.4 (d, $^1J_{\text{CF}} = 244.7$, C-2'), 171.4 (C-1). δ_{F} (CDCl₃, 283 MHz) -117.9 (ddd, $^4J_{\text{HF}} = 6.8$, $^4J_{\text{HF}} = 6.8$, $^3J_{\text{HF}} = 10.6$, 1F, Ar-F). ν_{max} (KBr): 3330, 2969, 1646, 1580, 1450, 1230, 1067, 755 cm⁻¹. **HRMS (ES+)**: Calcd. for C₁₇H₁₈FNO₂Na [M+Na]⁺: 310.1219, found 310.1221.

5.2.13 (*S,S*)-3-(3-Fluorophenyl)-2-hydroxyl-*N*-((*S*)-1-phenylethyl)

propanamide (*S,S*)-**148** and (*R,S*)-3-(3-fluorophenyl)-2-hydroxyl-*N*-((*S*)-1-phenylethyl)propanamide (*R,S*)-**148**



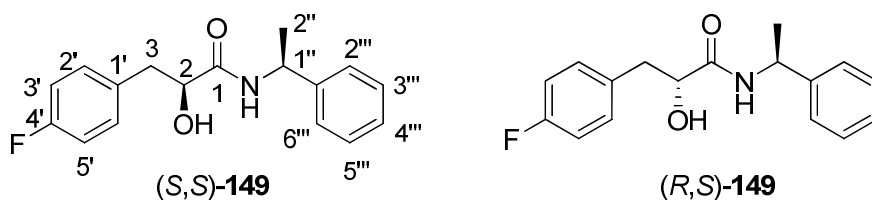
The same procedure as described in 5.2.12 was repeated with (*RS*)-*m*-fluorophenyllactic acid **103l** to yield (*S,S*)-**148** as viscous oil (46.8%) and (*R,S*)-**148** as white solid (44.1%).

(*S,S*)-**148**: $[\alpha]_{\text{D}}^{20}$: -93.88° ($c = 4.90 \times 10^{-3}$, CHCl_3); δ_{H} (CDCl_3 , 300 MHz) 1.32 (d, 3H, $^3J_{\text{HH}} = 6.9$, H-1''), 2.85 (dd, 1H, $^3J_{\text{HH}} = 7.7$, $^2J_{\text{HH}} = 13.9$, H-3), 3.09 (dd, 1H, $^3J_{\text{HH}} = 4.1$, $^2J_{\text{HH}} = 13.9$, H-3), 4.19 (dd, 1H, $^3J_{\text{HH}} = 4.1$, $^3J_{\text{HH}} = 7.7$, H-3), 4.99 (quint, 1H, $^3J_{\text{HH}} = 7.0$, H-2''), 6.66 (d, 1H, $^3J_{\text{HH}} = 7.9$, NH), 6.84-6.93 (m, 3H, Ar-H), 7.14-7.27 (m, 6H, Ar-H). δ_{C} (CDCl_3 , 75 MHz) 22.1 (C-2''), 40.8 (C-3), 48.9 (C-1''), 72.8 (C-2), 114.1 (d, $^2J_{\text{CF}} = 21.0$, C-4'), 117.0 (d, $^2J_{\text{CF}} = 21.3$, C-2'), 125.7 (d, $^4J_{\text{CF}} = 2.7$, C-6'), 126.5 (C-2''', C-6'''), 127.8 (C-4'''), 129.1 (C-3''', C-5'''), 130.3 (d, $^3J_{\text{CF}} = 8.2$, C-5'), 139.8 (d, $^3J_{\text{CF}} = 7.3$, C-1'), 143.1 (C-1'''), 163.2 (d, $^1J_{\text{CF}} = 246.5$, C-4'), 172.0 (C-1). δ_{F} (CDCl_3 , 283 MHz) -113.5 (ddd, $^4J_{\text{HF}} = 6.0$, $^3J_{\text{HF}} = 9.1$, $^3J_{\text{HF}} = 9.1$, 1F, Ar-F). ν_{max} (KBr): 3393, 3263, 1645, 1586, 1483, 1190, 1080, 765 cm^{-1} . HRMS (ES⁺): Calcd. for: $\text{C}_{17}\text{H}_{18}\text{FNO}_2\text{Na}$ $[\text{M}+\text{Na}]^+$: 310.1219, found 310.1210.

(*R,S*)-**148**: Mp 110- 111 °C. $[\alpha]_D^{20}$: +16.47° ($c = 1.05 \times 10^{-3}$, CHCl₃). δ_H (CDCl₃, 300 MHz) 1.32 (d, 3H, $^3J_{HH} = 6.9$, H-1''), 2.84 (dd, 1H, $^3J_{HH} = 7.6$, $^2J_{HH} = 14.0$, H-3), 3.07 (dd, $^3J_{HH} = 4.3$, 1H, $^2J_{HH} = 14.0$, H-3), 4.23 (dd, $^3J_{HH} = 4.3$, $^3J_{HH} = 7.6$, 1H, H-3), 5.00 (quint, 1H, $^3J_{HH} = 7.0$, H-2''), 6.68 (d, 1H, $^3J_{HH} = 7.4$, NH), 6.83-6.90 (m, 3H, Ar-H), 7.08-7.27 (m, 6H, Ar-H). δ_C (CDCl₃, 75 MHz) 22.1 (C-2''), 40.8 (C-3), 48.9 (C-1''), 72.7 (C-2), 114.0 (d, $^2J_{CF} = 21.1$, C-4'), 117.0 (d, $^2J_{CF} = 21.2$, C-2'), 125.6 (d, $^4J_{CF} = 2.7$, C-6'), 126.5 (C-2''', C-6'''), 127.8 (C-4'''), 129.1 (C-3''', C-5'''), 130.1 (d, $^3J_{CF} = 8.1$, C-5'), 139.8 (d, $^3J_{CF} = 7.8$, C-1'), 143.1 (C-1'''), 163.2 (d, $^1J_{CF} = 246.5$, C-4'), 172.0 (C-1). δ_F (CDCl₃, 283 MHz) -113.3 (ddd, $^4J_{HF} = 6.3$, $^3J_{HF} = 9.1$, $^3J_{HF} = 9.1$, 1F, Ar-F). ν_{max} (KBr): 3393, 3263, 1647, 1586, 1487, 1187, 1086, 765 cm⁻¹. **HRMS** (**ES**⁺): Calcd. for: C₁₇H₁₈FNO₂Na [M+Na]⁺: 310.1219, found 310.1218.

5.2.14 (*S*)-3-(4-Fluorophenyl)-2-hydroxyl-*N*-((*S*)-1-phenylethyl)

propanamide (*S,S*)-**149** and (*R*)-3-(4-fluorophenyl)-2-hydroxyl-*N*-((*S*)-1-phenylethyl)propanamide (*R,S*)-**149**

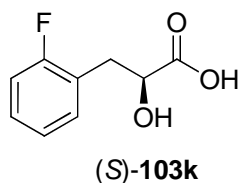


The same procedure as described in **5.2.12** was repeated with (*RS*)-*p*-fluorophenyllactic acid **103m** to yield (*S,S*)-**149** as white solid (48.4%) and (*R,S*)-**149** as white solid (36.6%).

(*S,S*)-**149**: Mp 92.0-93.0 °C; $[\alpha]_D^{20}$: -101.6° ($c = 1.25 \times 10^{-3}$, CHCl₃). δ_H (CDCl₃, 300 MHz) 1.40 (d, 3H, $^3J_{HH} = 6.9$, H-1''), 2.92 (dd, 1H, $^3J_{HH} = 7.5$, $^2J_{HH} = 14.0$, H-3), 3.14 (dd, 1H, $^3J_{HH} = 4.1$, $^2J_{HH} = 14.0$, H-3), 4.24 (dd, 1H, $^3J_{HH} = 4.1$, $^3J_{HH} = 7.5$, H-3), 5.08 (quint, 1H, $^3J_{HH} = 7.2$, H-2''), 6.74 (d, 1H, $^3J_{HH} = 7.8$, NH), 6.95-7.35 (m, 9H, Ar-H); δ_C (CDCl₃, 75 MHz) 22.1 (C-2''), 40.5 (C-3), 48.84 (C-1''), 73.0 (C-2), 115.8 (d, $^3J_{CF} = 21.2$, C-3', C-5'), 126.6 (C-2''', C-6'''), 127.9 (C-4'''), 129.1 (C-3''', C-5''') 131.5 (d, $^3J_{CF} = 7.9$, C-2', C-6'), 132.7 (d, $^4J_{CF} = 3.2$, C-1'), 143.4 (C-1'''), 162.4 (d, $^1J_{CF} = 244.9$, C-4'), 171.6 (C-1). δ_F (CDCl₃, 283 MHz) -116.3 (dddd, $^4J_{HF} = 5.4$, $^4J_{HF} = 5.4$, $^3J_{HF} = 8.8$, $^3J_{HF} = 8.8$, 1F, Ar-F). ν_{max} (KBr): 3392, 3208, 1643, 1535, 1214 cm⁻¹; **HRMS (ES⁺)**: Calcd. for: C₁₇H₁₈FNO₂Na [M+Na]⁺: 310.1219, found 310.1221.

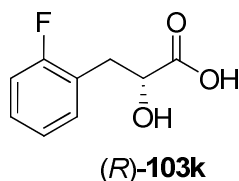
(*R,S*)-**149**: Mp 116.0-117.5 °C; $[\alpha]_D^{20}$: +11.43° ($c = 1.05 \times 10^{-3}$, CHCl₃); δ_H (CDCl₃, 300 MHz) 1.49 (d, 3H, $^3J_{HH} = 6.9$, H-1''), 2.98 (dd, 1H, $^3J_{HH} = 7.3$, $^2J_{HH} = 14.$, H-3), 3.15 (dd, 1H, $^3J_{HH} = 4.5$, $^2J_{HH} = 14.1$, H-3), 4.34 (dd, 1H, $^3J_{HH} = 4.5$, $^3J_{HH} = 7.3$, H-3), 5.12 (quint, 1H, $^3J_{HH} = 7.4$, H-2''), 6.65 (d, 1H, $^3J_{HH} = 6.9$, NH), 6.92-7.37 (m, 9H, Ar-H). δ_C (CDCl₃, 75 MHz) 22.2 (C-2''), 40.3 (C-3), 48.5 (C-1''), 73.1 (C-2), 115.9 (d, $^3J_{CF} = 21.2$, C-3', C-5'), 126.5 (C-2''', C-6'''), 127.8 (C-4'''), 129.1 (C-3''', C-5'''), 131.6 (d, $^3J_{CF} = 8.1$, C-2', C-6'), 132.7 (d, $^4J_{CF} = 3.2$, C-1'), 143.4 (C-1'''), 162.4 (d, $^1J_{CF} = 244.7$, C-4'), 171.6 (C-1). δ_F (CDCl₃, 283 MHz) -116.3 (dddd, $^4J_{HF} = 5.4$, $^4J_{HF} = 5.4$, $^3J_{HF} = 8.6$, $^3J_{HF} = 8.6$, 1F, Ar-F). ν_{max} (KBr): 3390, 3210, 1644, 1535, 1211 cm⁻¹. **HRMS (ES⁺)**: Calcd. for: C₁₇H₁₈FNO₂Na [M+Na]⁺: 310.1219, found 310.1219.

5.2.15 (*S*)-*o*-Fluorophenyllactic acid (*S*)-103k



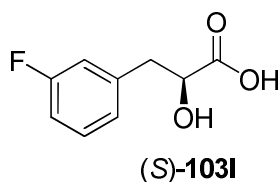
A solution of (*S*)-3-(2-fluorophenyl)-2-hydroxyl-*N*-((*S*)-1-phenylethyl)propanamide **147** (0.49 g, 1.71 mmol) in 6 M HCl (20 ml) was refluxed for 24 h. The reaction mixture was allowed to cool to ambient temperature, and then was extracted into ether (3 × 30ml), washed with water (10 ml), brine (10 ml), dried over MgSO₄, and filtered. The solvent was removed under reduced pressure to give a white solid. Recrystallisation from EtOAc/Hexane gave (*S*)-**103k** as a white solid (0.30 g, 93.7%). Mp 76-77 °C; $[\alpha]_D^{20}$: -26.7° ($c = 1.30 \times 10^{-3}$, CHCl₃); δ_H (400 MHz, MeOH-*d*₄) 2.93 (dd, 1H, $^2J_{HH} = 8.5$, $^2J_{HH} = 13.9$, H-3), 3.19 (dd, 1H, $^3J_{HH} = 4.5$, $^2J_{HH} = 13.9$, H-3), 4.36 (dd, 1H, $^3J_{HH} = 4.5$, $^3J_{HH} = 8.5$, H-2), 7.02-7.13 (m, 2H, Ar-H), 7.21-7.36 (m, 2H, Ar-H). δ_C (CDCl₃, 75 MHz) 34.9 (C-3), 71.6 (C-2), 116.0 (d, $^2J_{CF} = 22.4$, C-3'), 125.0 (d, $^3J_{CF} = 3.5$, C-5'), 125.8 (d, $^2J_{CF} = 15.7$, C-1'), 129.6 (d, $^3J_{CF} = 8.1$, C-4' or C-6'), 133.1 (d, $^4J_{CF} = 4.7$, C-6' or C-4'), 162.8 (d, $^1J_{CF} = 243.69$, C-2'), 176.9 (C-1). δ_F (CDCl₃, 283 MHz) -120.5 (m, 1F, Ar-F). ν_{max} (KBr): 3427, 2940, 1733, 1578, 1490, 1110, 1068, 760 cm⁻¹. HRMS (ES⁺): Calcd. for: C₉H₈FO₃ [M-H]⁺: 183.0457, found 183.0460.

5.2.16 (*R*)-*o*-Fluorophenyllactic acid (*R*)-103k



The same procedure as described in **5.2.15** was repeated with (*R*)-3-(2-fluorophenyl)-2-hydroxyl-*N*-((*S*)-1-phenylethyl)propanamide **147** to afford (*R*)-**103k** as a white solid (93.7%). Mp 76-77 °C; $[\alpha]_{\text{D}}^{20}$: +27.0° ($c = 1.35 \times 10^{-3}$, CHCl₃); δ_{H} (MeOH-*d*₄, 400 MHz) 2.92 (dd, 1H, $^2J_{\text{H,H}} = 8.4$, $^2J_{\text{H,H}} = 14.0$, H-3), 3.19 (dd, 1H, $^3J_{\text{H,H}} = 4.6$, $^2J_{\text{H,H}} = 14.0$, H-3), 4.36 (dd, 1H, $^3J_{\text{H,H}} = 4.6$, $^3J_{\text{H,H}} = 8.4$, H-2), 7.02-7.13 (m, 2H, Ar-H), 7.21-7.36 (m, 2H, Ar-H); δ_{C} (CDCl₃, 75 MHz) 34.9 (C-3), 125.0 (d, $^3J_{\text{C,F}} = 3.6$, C-5'), 115.9 (d, $^2J_{\text{C,F}} = 22.6$, C-3'), 71.6 (C-2), 125.8 (d, $^2J_{\text{C,F}} = 15.8$, C-1'), 129.6 (d, $^3J_{\text{C,F}} = 8.2$, C-4' or C-6'), 133.1 (d, $^4J_{\text{C,F}} = 4.45$, C-6' or C-4'), 163.0 (d, $^1J_{\text{C,F}} = 243.7$, C-2'), 176.9 (C-1); δ_{F} (CDCl₃, 283 MHz) -120.5 (m, 1F, Ar-F); ν_{max} (KBr): 3429, 2934, 1738, 1581, 1491, 1257, 1110, 1070, 760 cm⁻¹; **HRMS (ESI+)**: Calcd. for: C₉H₈FO₃ [M-H]⁺: 183.0457, found 183.0457.

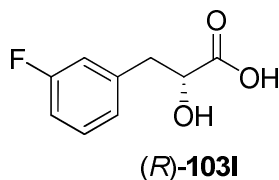
5.2.17 (*S*)-*m*-Fluorophenyllactic acid (*S*)-103l



The same procedure as described in **5.2.15** was repeated with (*S*)-3-(3-fluorophenyl)-2-hydroxyl-*N*-((*S*)-1-phenylethyl)propanamide **148** to yield (*S*)-**103l** as a white solid

(96.21%). Mp 89-90 °C; $[\alpha]_D^{20}$: -33.0° ($c = 1.15 \times 10^{-3}$, CHCl₃). δ_H (400 MHz, MeOH-d₄) 2.92 (dd, 1H, $^2J_{HH} = 8.0$, $^2J_{HH} = 13.9$, H-3), 3.11 (dd, 1H, $^3J_{HH} = 4.3$, $^2J_{HH} = 13.9$, H-3), 4.34 (dd, 1H, $^3J_{HH} = 4.3$, $^3J_{HH} = 8.0$, H-2), 6.93 (ddt, 1H, $^4J_{HH} = 0.8$, $^4J_{HH} = 2.4$, $^3J_{HH} = 9.16$, $^3J_{HF} = 9.1$, H-4'), 7.02 (td, 1H, $^4J_{HH} = 2.4$, $^3J_{HF} = 10.1$, H-2'), 7.08 (d, 1H, $^3J_{HH} = 7.9$, H-6'), 7.27 (dt, 1H, $^4J_{HF} = 6.1$, $^3J_{HH} = 7.9$, H-5'). δ_C (CDCl₃, 75 MHz) 41.1 (C-3), 72.4 (C-2), 114.2 (d, $^2J_{CF} = 21.4$, C-4'), 117.3 (d, $^2J_{CF} = 21.3$, C-2'), 126.5 (d, $^4J_{CF} = 2.3$, C-6'), 130.8 (d, $^3J_{CF} = 8.3$, C-5'), 141.7 (d, $^3J_{CF} = 7.9$, C-1'), 164.1 (d, $^1J_{CF} = 243.3$, C-3'), 176.8 (C-1). δ_F (CDCl₃, 283 MHz) -116.7 (ddd, $^4J_{HF} = 6.4$, $^3J_{HF} = 9.6$, $^3J_{HF} = 9.7$, 1F, Ar-F). ν_{max} (KBr): 3450, 2928, 1731, 1587, 1487, 1098, 801 cm⁻¹. **HRMS (ES⁺)**: Calcd. for: C₉H₉FO₃Na [M+Na]⁺: 207.0433, found 207.0432.

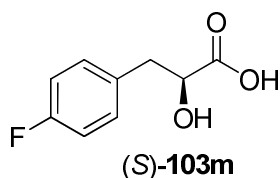
5.2.18 (*R*)-*m*-Fluorophenyllactic acid (*R*)-1031



The same procedure as described in **5.2.15** was repeated with (*R*)-3-(3-fluorophenyl)-2-hydroxyl-*N*-((*S*)-1-phenylethyl)propanamide **148** to afford (*R*)-**1031** as white solid (93.5 %). Mp 89-90 °C; $[\alpha]_D^{20}$: +33.0° ($c = 1.15 \times 10^{-3}$, CHCl₃). δ_H (MeOH-d₄, 400 MHz) 2.91 (dd, 1H, $^2J_{H,H} = 8.0$, $^2J_{H,H} = 13.9$, H-3), 3.11 (dd, 1H, $^3J_{H,H} = 4.3$, $^2J_{H,H} = 13.9$, H-3), 4.34 (dd, 1H, $^3J_{H,H} = 4.3$, $^3J_{H,H} = 8.0$, H-2), 6.93 (ddt, 1H, $^4J_{H,H} = 0.9$, $^4J_{H,H} = 2.3$, $^3J_{H,F; H,H} = 9.0$, H-4'), 7.02 (td, 1H, $^4J_{H,H} = 2.3$, $^3J_{H,F} = 10.2$, H-2'), 7.07 (d, 1H, $^3J_{H,H} = 7.7$, H-6'), 7.27 (dt, 1H, $^4J_{H,F} = 6.1$, $^3J_{H,H} = 7.9$, H-5'); δ_C (CDCl₃, 75 MHz) 41.7 (C-3), 72.4 (C-2), 114.1 (d, $^2J_{C,F} = 21.5$, C-4'), 117.3 (d, $^2J_{C,F} = 21.4$, C-2'), 126.4

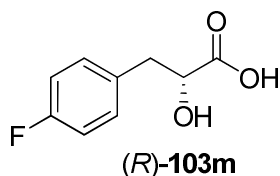
(d, $^4J_{\text{C,F}} = 2.7$, C-6'), 130.8 (d, $^3J_{\text{C,F}} = 8.5$, C-5'), 141.7 (d, $^3J_{\text{C,F}} = 7.7$, C-1'), 164.1 (d, $^1J_{\text{C,F}} = 242.5$, C-3'), 176.8 (C-1); δ_{F} (CDCl₃, 283 MHz) -116.7 (ddd, $^4J_{\text{H,F}} = 6.3$, $^3J_{\text{H,F}} = 9.5$, 9.5, 1F, Ar-F); ν_{max} (KBr): 3445, 2926, 1731, 1587, 1488, 1096, 799 cm⁻¹. **HRMS (ESI+)**: Calcd. for: C₉H₉FO₃Na [M+Na]⁺: 207.0433, found 207.0430.

5.2.19 (S)-*p*-Fluorophenyllactic acid (S)-103m



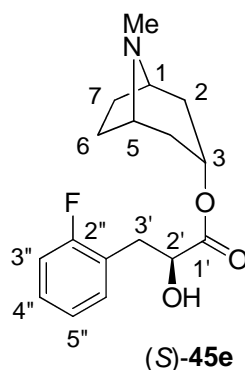
The same procedure as described in **5.2.15** was repeated with (S)-3-(4-fluorophenyl)-2-hydroxyl-*N*-((S)-1-phenylethyl)propanamide **149** to afford (S)-**103m** as a white solid (93.60%). Mp 71-72 °C; $[\alpha]_{\text{D}}^{20}$: -35.6° ($c = 1.35 \times 10^{-3}$, CHCl₃). δ_{H} (MeOH-*d*₄, 400 MHz) 2.98 (dd, 1H, $^2J_{\text{H,H}} = 7.9$ Hz, $^2J_{\text{H,H}} = 14.0$, H-3), 3.08 (dd, 1H, $^3J_{\text{H,H}} = 4.4$, $^2J_{\text{H,H}} = 14.0$, H-3), 4.34 (dd, 1H, $^3J_{\text{H,H}} = 4.4$, $^3J_{\text{H,H}} = 7.9$, H-2), 6.99 (t, 2H, $^3J_{\text{H,F}} = 8.9$, $^3J_{\text{H,H}} = 8.9$, H-3', H-5'), 7.28 (dd, 2H, $^4J_{\text{H,F}} = 5.5$, $^3J_{\text{H,H}} = 8.8$, H-2', H-6'); δ_{C} (CDCl₃, 75 MHz) 42.1 (C-3), 73.0 (C-2), 116.2 (d, $^2J_{\text{C,F}} = 21.5$, C-3', C-5'), 135.2 (d, $^4J_{\text{C,F}} = 3.1$, C-1'), 132.7 (d, $^3J_{\text{C,F}} = 7.9$, C-2', C-6'), 163.6 (d, $^1J_{\text{C,F}} = 243.1$, C-4'), 177.4 (C-1); δ_{F} (CDCl₃, 283 MHz) -116.3 (dddd, $^4J_{\text{H,F}} = 5.4$, 5.4, $^3J_{\text{H,F}} = 9.0$, 9.0, 1F, Ar-F); ν_{max} (KBr): 3474, 1737, 1508, 1240 cm⁻¹. **HRMS (ES+)**: Calcd. for: C₉H₉FO₃Na [M+Na]⁺: 207.0433, found 207.0437.

5.2.20 (*R*)-*p*-Fluorophenyllactic acid (*R*)-103m



The same procedure as described in **5.2.15** was repeated with (*R*)-3-(4-fluorophenyl)-2-hydroxyl-*N*-((*S*)-1-phenylethyl)propanamide **149** to afford (*R*)-**103m** as a white solid (95.04 %). Mp 71-72 °C; $[\alpha]_{\text{D}}^{20}$: +34.8° ($c = 1.35 \times 10^{-3}$, CHCl₃); δ_{H} (MeOH-*d*₄, 400 MHz) 7.28 (dd, 2H, $^4J_{\text{H,F}} = 5.5$, $^3J_{\text{H,H}} = 8.7$, H-2', H-6'), 6.99 (t, $^3J_{\text{H,F}} = 8.9$, 2H, $^3J_{\text{H,H}} = 8.9$, H-3', H-5'), 4.32 (dd, 1H, $^3J_{\text{H,H}} = 4.3$, $^3J_{\text{H,H}} = 7.9$, H-2), 3.08 (dd, 1H, $^3J_{\text{H,H}} = 4.3$, $^2J_{\text{H,H}} = 14.0$, H-3), 2.90 (dd, 1H, $^2J_{\text{H,H}} = 7.9$, $^2J_{\text{H,H}} = 14.0$, H-3); δ_{C} (CDCl₃, 75 MHz) 40.1 (C-3), 73.0 (C-2), 116.2 (d, $^2J_{\text{C,F}} = 21.4$, C-3', C-5'), 132.7 (d, $^3J_{\text{C,F}} = 8.0$, C-2', C-6'), 135.2 (d, $^4J_{\text{C,F}} = 3.0$, C-1'), 163.6 (d, $^1J_{\text{C,F}} = 243.9$, C-4'), 177.4 (C-1); δ_{F} (CDCl₃, 283 MHz) -119.7 (dddd, $^4J_{\text{H,F}} = 5.8$, 5.8, $^3J_{\text{H,F}} = 9.6$, 9.6, 1F, Ar-F); ν_{max} (KBr): 3473, 1735, 1506, 1240 cm⁻¹; **HRMS** (ESI⁺): Calcd. for: C₉H₉FO₃Na [M+Na]⁺: 207.0433, found 207.0434.

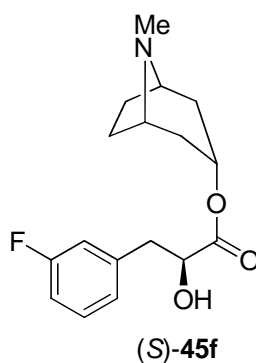
5.2.21 (*S*)-*o*-Fluorolittorine (*S*)-45e



Dry (*S*)-*o*-fluorophenyllactic acid **103k** (0.18 g, 0.98 mmol) and tropine (0.17 g, 1.17 mmol) were mixed intimately under nitrogen in the solid phase. The mixture was heated to 130 °C and a current of dry HCl gas was passed periodically over the reaction for 4 h and the reaction was allowed to cool to room temperature. The product was dissolved in 50 mM H₂SO₄ as much as possible and filtered. The filtrate was treated with 10% aqueous ammonium hydroxide until it was basic. The organics were extracted into chloroform (3 x 15 ml), dried over MgSO₄, and evaporated to give pale yellow oil. The product was purified over silica gel eluting with EtOH:CHCl₃: 35%NH₃ (7:7:0.2) to afford (*S*)-**45e** as a white solid (0.15 g, 49.8 %). Mp 75-76 °C; $[\alpha]_D^{20}$: -9.39° (c = 3.3 × 10⁻³, CHCl₃); δ_H (CDCl₃, 400 MHz) 1.51 (d, 1H, ²*J*_{H,H} = 15.0, H-4_a), 1.62 (d, 1H, ²*J*_{H,H} = 15.6, H-2_a), 1.68-1.79 (m, 2H, H-6_a, H-7_a), 1.83-1.95 (m, 2H, H-6_e, H-7_e), 2.16 (s, 3H, NMe), 1.99-2.10 (m, 2H, H-2_e, H-4_e), 2.91 (dd, 1H, ³*J*_{H,H} = 7.6, ²*J*_{H,H} = 14.1, H-3'), 2.95-3.04 (m, 2H, H-1, H-5), 3.10 (dd, 1H, ³*J*_{H,H} = 5.2, ²*J*_{H,H} = 14.0, H-3'), 4.13 (br, OH), 4.30 (dd, 1H, ³*J*_{H,H} = 5.2, ³*J*_{H,H} = 7.6, H-2'), 4.96 (t, 1H, ³*J*_{H,H} = 5.3, H-3_e), 6.91-7.03 (m, 2H, Ar-H), 7.11-7.23 (m, 2H, Ar-H); δ_C (CDCl₃, 75 MHz) 25.3 (C-7 or C-6), 25.5 (C-6 or C-7), 34.1 (C-3'), 36.1 (C-2 or C-4), 36.4 (C-4 or C-2), 40.7 (NMe), 59.6 (C-1, C-5), 69.1 (C-3), 70.4 (C-2'), 115.2 (d, ²*J*_{C,F} = 22.0,

(d, $^3J_{\text{C,F}} = 15.8$, C-1''), 124.0 (d, $^3J_{\text{C,F}} = 3.6$, C-5''), 128.6 (d, $^3J_{\text{C,F}} = 8.1$, C-6'', C-4''), 131.9 (d, $^3J_{\text{C,F}} = 4.5$, C-4'' or C-6''), 161.2 (d, $^1J_{\text{C,F}} = 244.7$, C-2''), 173.4 (C-1'); δ_{C} (CDCl₃, 283 MHz) -118.3 (m, 1F, Ar-F); ν_{max} (KBr): 2963, 1734, 1580, 1488, 1113, 1029, 752 cm⁻¹; **HRMS (ES+)**: Calcd. for: C₁₇H₂₃NFO₃ [M+H]⁺: 308.1662, found 308.1655.

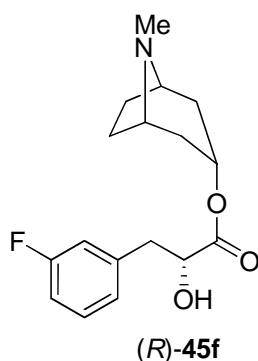
5.2.23 (*S*)-*m*-Fluorolittorine (*S*)-45f



The same procedure as described in 5.2.21 was repeated with (*S*)-*m*-fluorophenyllactic acid **103l** to obtain (*S*)-45f as a white solid (42.5%). Mp 83-83 °C; $[\alpha]_{\text{D}}^{20}$: -16.08° (c = 2.3 × 10⁻³, CHCl₃); δ_{H} (CDCl₃, 300 MHz) 1.57 (d, 2H, $^2J_{\text{H,H}} = 16.1$, H-2_a, H-4_a), 1.68-1.75 (m, 2H, H-6_a, H-7_a), 1.86-1.99 (m, 2H, H-6_e, H-7_e), 2.05-2.17 (m, 2H, H-2_e, H-4_e), 2.20 (s, 3H, NMe), 2.88 (dd, 1H, $^3J_{\text{H,H}} = 7.2$, $^2J_{\text{H,H}} = 14.0$, H-3'), 3.03 (dd, 1H, $^3J_{\text{H,H}} = 4.8$, $^2J_{\text{H,H}} = 14.0$, H-3'), 3.03-3.108 (br, 2H, H-1, H-5), 4.28 (dd, 1H, $^3J_{\text{H,H}} = 4.8$, $^3J_{\text{H,H}} = 7.2$, H-2'), 4.34 (br, OH), 4.97 (t, 1H, $^3J_{\text{H,H}} = 5.2$, H-3_e), 6.28-6.92 (m, 2H, H-2'', H-4''), 6.94 (d, 1H, $^3J_{\text{H,F}} = 7.7$, H-6''), 7.18 (dt, 1H, $^4J_{\text{H,F}} = 6.2$, $^3J_{\text{H,H}} = 7.8$, H-5''); δ_{C} (CDCl₃, 75 MHz) 25.7 (C-7 or C-6), 25.8 (C-6 or C-7), 36.6 (C-2 or C-4), 36.7 (C-4 or C-2), 40.5 (C-3', NMe), 60.0 (C-1, C-5), 69.4 (C-3),

71.6 (C-2'), 114.1 (d, $^2J_{\text{C,F}} = 21.0$, C-4''), 116.7 (d, $^2J_{\text{C,F}} = 21.5$, C-2''), 125.5 (d, $^4J_{\text{C,F}} = 2.7$, C-6''), 130.2 (d, $^3J_{\text{C,F}} = 8.3$, C-5''), 139.5 (d, $^3J_{\text{C,F}} = 7.4$, C-1''), 163.1 (d, $^1J_{\text{C,F}} = 245.8$, C-2''), 173.5 (C-1'); δ_{F} (CDCl₃, 283 MHz) -113.8 (ddd, $^4J_{\text{H,F}} = 6.1$, $^3J_{\text{H,F}} = 9.2$, 1F, Ar-F); ν_{max} (KBr): 2929, 1728, 1583, 1485, 1197, 1032, 693 cm⁻¹; **HRMS** (ES⁺): Calcd. for: C₁₇H₂₃NFO₃ [M+H]⁺: 308.1662, found 308.1657.

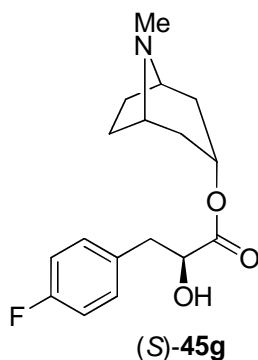
5.2.24 (*R*)-*m*-Fluorolittorine (*R*)-45f



The same procedure as described in 5.2.21 was repeated with (*R*)-*m*-fluorophenyllactic acid **103l** to obtain (*R*)-**45f** as a white solid (31.9%). Mp 76-77 °C; $[\alpha]_{\text{D}}^{20}$: +16.08° (c = 2.3×10⁻³, CHCl₃); δ_{H} (CDCl₃, 300 MHz) 1.59 (d, 2H, $^2J_{\text{H,H}} = 16.2$, H-2_a, H-4_a), 1.70-1.77 (m, 2H, H-6_a, H-7_a), 1.90-1.99 (m, 2H, H-6_e, H-7_e), 2.12-2.21 (m, 2H, H-2_e, H-4_e), 2.23 (s, 3H, NMe), 2.87 (dd, 1H, $^3J_{\text{H,H}} = 7.2$, $^2J_{\text{H,H}} = 14.0$, H-3'), 3.04 (dd, 1H, $^3J_{\text{H,H}} = 4.8$, $^2J_{\text{H,H}} = 14.0$, H-3'), 3.06-3.13 (br, 2H, H-1, H-5), 4.29 (dd, 1H, $^3J_{\text{H,H}} = 4.83$ Hz, $^3J_{\text{H,H}} = 7.2$, H-2'), 4.79 (br, OH), 4.98 (t, 1H, $^3J_{\text{H,H}} = 5.2$, H-3_e), 6.83-6.91 (m, 2H, H-2'', H-4''), 6.94 (d, 1H, $^3J_{\text{H,F}} = 8.6$, H-6''), 7.18 (dt, 1H, $^4J_{\text{H,F}} = 6.2$, $^3J_{\text{H,H}} = 7.9$, H-5''); δ_{C} (CDCl₃, 75 MHz) 25.7 (C-7 or C-6), 25.8 (C-6 or C-7), 36.4 (C-2 or C-4), 36.5 (C-4 or C-2), 40.4 (C-3'), 40.5 (NMe), 60.1 (C-1, C-5), 69.3 (C-3), 71.6 (C-2'), 114.1 (d, $^2J_{\text{C,F}} = 21.1$, C-4'), 116.8 (d, $^2J_{\text{C,F}} = 21.5$, C-2'), 125.5 (d, $^4J_{\text{C,F}} = 2.7$, C-6'), 130.2 (d, $^3J_{\text{C,F}} = 8.3$, C-5'), 139.5 (d, $^3J_{\text{C,F}} = 7.5$, C-1'), 163.1 (d, $^1J_{\text{C,F}} =$

245.6, C-2''), 173.5 (C-1'); δ_F (CDCl₃, 283 MHz) -113.8 (ddd, $^4J_{H,F} = 6.2$, $^3J_{H,F} = 9.3$, 9.3, 1F, Ar-F); ν_{max} (KBr): 2952, 1728, 1586, 1485, 1197, 1029, 693 cm⁻¹; **HRMS** (ESI⁺): Calcd. for: C₁₇H₂₃NFO₃ [M+H]⁺: 308.1662, found 308.1661.

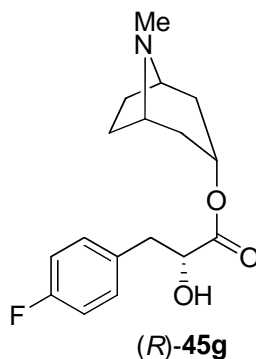
5.2.25 (*S*)-*p*-Fluorolittorine (*S*)-45g



The same procedure as described in **5.2.21** was repeated with (*S*)-*p*-fluorophenyllactic acid **103m** to obtain (*S*)-**45g** as a white solid (41.7 %). Mp 93-94 °C; $[\alpha]_D^{20}$: -15.2° (c = 1.25×10⁻³, CHCl₃); δ_H (CDCl₃, 400 MHz) 1.57 (d, $^3J_{H,H} = 13.5$, 2H, H-2_a, H-4_a), 1.66-1.76 (m, 2H, H-6_a, H-7_a), 1.88-1.99 (m, 2H, H-6_e, H-7_e), 2.04-2.13 (m, 2H, H-2_e, H-4_e), 2.19 (s, 3H, NMe), 2.87 (dd, $^3J_{H,H} = 7.1$, $^2J_{H,H} = 14.0$, 1H, H-3'), 2.99-3.06 (m, 3H, H-1, H-5, H-3'), 4.27 (dd, $^3J_{H,H} = 4.1$, $^3J_{H,H} = 7.1$, 1H, H-2'), 4.97 (t, $^3J_{H,H} = 5.3$, 1H, H-3_e), 6.91 (t, $^3J_{H,F; H,H} = 8.7$, 2H, H-3'', H-5''), 7.13 (dd, $^4J_{H,F} = 5.5$, $^3J_{H,H} = 8.5$, 2H, H-2'', H-6''); δ_C (CDCl₃, 75 MHz) 25.9 (C-6, C-7), 36.8 (C-4 or C-2), 36.9 (C-2 or C-4), 40.0 (C-3'), 40.7 (NMe), 60.0 (C-2, C-5), 69.7 (C-3), 71.8 (C-2'), 115.6 (d, $^2J_{C,F} = 21.3$, C-3'', C-5''), 131.3 (d, $^3J_{C,F} = 7.9$, C-2'', C-6''), 132.6 (d, $^4J_{C,F} = 3.0$, C-1''), 162.3 (d, $^1J_{C,F} = 244.7$, C-4''), 173.7 (C-1'); δ_F (CDCl₃, 283 MHz) -116.6 (dddd, $^4J_{H,F} = 5.7$, 5.7, $^3J_{H,F} = 8.9$, 8.9, 1F, Ar-F); ν_{max} (KBr): 2946, 1730, 1597, 1508, 1328,

1197, 1032 cm^{-1} ; **HRMS (ESI+)**: Calcd. for: $\text{C}_{17}\text{H}_{23}\text{FO}_3\text{N}$ $[\text{M}+\text{H}]^+$: 308.1662, found 308.1660.

5.2.26 (*R*)-*p*-Fluorolittorine (*R*)-45g

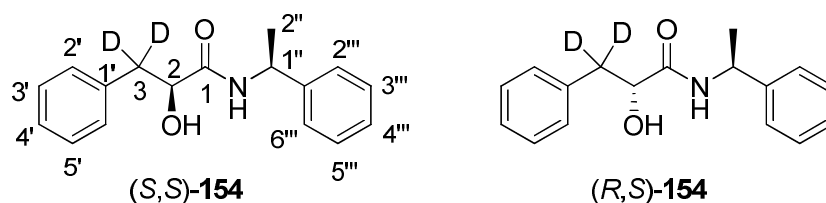


The same procedure as described in **5.2.21** was repeated with (*R*)-*m*-fluorophenyllactic acid **103m** to obtain (*R*)-**45g** as a white solid (43.2 %). Mp 82-84 °C; $[\alpha]_{\text{D}}^{20}$: +15.2° ($c = 1.25 \times 10^{-3}$, CHCl_3); δ_{H} (CDCl_3 , 400 MHz) 1.57 (d, 2H, $^3J_{\text{H,H}} = 14.8$, H-2_a, H-4_a), 1.68-1.75 (m, 2H, H-6_a, H-7_a), 1.86-1.97 (m, 2H, H-6_e, H-7_e), 2.06-2.15 (m, 2H, H-2_e, H-4_e), 2.19 (s, 3H, NMe), 2.86 (dd, 1H, $^3J_{\text{H,H}} = 7.1$, $^2J_{\text{H,H}} = 14.0$, H-3'), 3.01 (dd, 1H, $^3J_{\text{H,H}} = 4.8$, $^2J_{\text{H,H}} = 14.0$, H-3'), 3.02-3.08 (m, 2H, H-1, H-5), 4.26 (dd, 1H, $^3J_{\text{H,H}} = 4.8$, $^3J_{\text{H,H}} = 7.1$, H-2'), 4.96 (t, 1H, $^3J_{\text{H,H}} = 5.3$, H-3_e), 6.91 (t, 2H, $^3J_{\text{H,F}} = 8.7$, H-3'', H-5''), 7.13 (dd, 2H, $^4J_{\text{H,F}} = 5.5$, $^3J_{\text{H,H}} = 8.6$, H-2'', H-6''); δ_{C} (CDCl_3 , 75 MHz) 25.8 (C-7, C-6), 25.9 (C-6, C-7), 36.7 (C-4 or C-2), 36.8 (C-2 or C-4), 40.1 (C-3'), 40.6 (NMe), 60.0 (C-2, C-5), 69.5 (C-3), 71.9 (C-2'), 115.6 (d, $^2J_{\text{C,F}} = 21.2$, C-3'', C-5''), 131.3 (d, $^3J_{\text{C,F}} = 7.9$, C-2'', C-6''), 132.8 (d, $^4J_{\text{C,F}} = 3.2$, C-1''), 162.3 (d, $^1J_{\text{C,F}} = 244.8$, C-4''), 173.7 (C-1'); δ_{F} (CDCl_3 , 283 MHz) -116.6 (dddd, $^4J_{\text{H,F}} = 5.4$, $^3J_{\text{H,F}} = 8.8$, 8.8, 1F, Ar-F); ν_{max} (KBr): 2950, 1730, 1599, 1328, 1197, 1033 cm^{-1} ; **HRMS (ES+)**: Calcd. for: $\text{C}_{17}\text{H}_{23}\text{FO}_3\text{N}$ $[\text{M}+\text{H}]^+$: 308.1662, found 308.1654.

5.2.27 (2*S*,2'*S*)-[3,3-²H₂]-3-Phenyl-2-hydroxyl-*N*-(1-phenylethyl)

propanamide (*S,S*)-**154** and (2*R*,2'*S*)-[3,3-²H₂]-3-phenyl-2-hydroxyl-

N-(1-phenylethyl) propanamide (*R,S*)-**154**



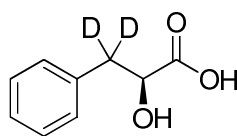
A solution of phenylpyruvic acid **104** (1 g, 6.09 mmol) in D₂O (30 ml) was adjusted to pH 11 with K₂CO₃ and left at 4 °C for 48 h. After acidification with D₂SO₄, the reaction mixture was extracted into ether (3×30 ml). The combined organic extracts were dried over MgSO₄, filtered and evaporated under reduced pressure to yield [3,3-²H₂]-phenylpyruvic acid. The crude product was then dissolved in MeOD (10 ml) at 0 °C and a solution of NaBH₄ (1.73 g, 40.2 mmol) in D₂O (15 ml) and 1M KOD (10 ml) was added dropwise, maintaining temperature below 5 °C during the addition. The reaction was then allowed to warm to ambient temperature and left to stir overnight. Methanol was evaporated, the residue dissolved in 10% HCl and the solution extracted into ether (3×30 ml). The combined organic extracts were dried over MgSO₄, filtered and evaporated under reduced pressure to yield crude (*rac*)-[3,3-²H₂]-phenyllactic acid **104a**. This product was then coupled with (*S*)-phenylethylamine **145** using the same procedure as described for the preparation of (*S,S*)-**147** in 5.2.12 to give (*S,S*)-**154** as a viscous oil (0.23 g, 13.9%, 3 steps) and separately (*R,S*)-**154** as a white solid (0.19 g, 12%, 3 steps).

(*S,S*)-**154**: $[\alpha]_{\text{D}}^{20}$: -88.9° ($c = 4.05 \times 10^{-3}$, CHCl₃); δ_{H} (CDCl₃, 300 MHz) 1.28 (d, 3H, $^3J_{\text{H,H}} = 6.9$, H-1''), 4.13 (s, 1H, H-2), 4.96 (quint, 1H, $^3J_{\text{H,H}} = 7.1$, H-2''), 6.73 (d, 1H,

$^3J_{\text{H,H}} = 7.7$, NH), 7.10-7.22 (m, 10H, Ar-H); δ_{C} (CDCl₃, 75 MHz) 22.8 (C-2''), 40.1 (m, C-3), 48.5 (C-1''), 72.7 (C-2), 126.2, 126.9, 127.4, 128.6, 128.7, 129.7 (Ar-C), 136.8 (C-1''' or C-1'), 142.8 (C-1' or C-1'''), 172.1 (C-1); ν_{max} (KBr): 3397, 3193, 1644, 1538, 1104, 697 cm⁻¹; **HRMS (ESI+)**: Calcd. for: C₁₇H₁₇D₂FNO₂Na [M+Na]⁺: 294.1439, found 294.1435.

(*R,S*)-**154**: Mp 116.0-117.5 °C; $[\alpha]_{\text{D}}^{20}$: +16.4° (c = 1.40×10⁻³, CHCl₃); δ_{H} (CDCl₃, 300 MHz) 1.47 (d, 3H, $^3J_{\text{H,H}} = 7.0$, H-1''), 3.17-3.28 (br, -OH), 4.30 (s, 1H, H-2), 5.10 (quint, 1H, $^3J_{\text{H,H}} = 6.9$, H-2''), 6.83 (d, 1H, $^3J_{\text{H,H}} = 7.9$, NH), 7.18-7.34 (m, 10H, Ar-H); δ_{C} (CDCl₃, 75 MHz) 21.8 (C-2''), 40.1 (m, C-3), 48.4 (C-1''), 72.6 (C-2), 126.1, 126.9, 127.3, 128.6, 128.7, 129.7 (Ar-C), 136.7 (C-1''' or C-1'), 142.8 (C-1' or C-1'''), 171.9 (C-1); ν_{max} (KBr): 3397, 3195, 1644, 1538, 1104, 697 cm⁻¹; **HRMS (ESI+)**: Calcd. for: C₁₇H₁₇D₂FNO₂Na [M+Na]⁺: 294.1439, found 294.1433.

5.2.28 (*S*)-[3,3-²H₂]-Phenyllactic acid (*S*)-**103i**



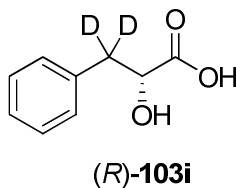
(*S*)-**103i**

The same procedure as described in **5.2.15** was repeated with (*S*)-[3,3-²H₂]-3-phenyl-2-hydroxyl-*N*-((*S*)-1-phenylethyl)propanamide **154** to afford (*S*)-**103i** as colourless needles (95.5%). Mp 118-119 °C; $[\alpha]_{\text{D}}^{20}$: -39.0° (c 1.05×10⁻³, CHCl₃); δ_{H} (MeOH-d₄, 400 MHz) 4.33 (s, 1H, H-2), 7.21 (m, 1H, Ar-H), 7.26-7.29 (m, 4H, Ar-H); δ_{C} (CDCl₃, 75 MHz) 39.5 (quint, $^1J_{\text{C,D}} = 19.1$, C-3), 71.3 (C-2), 126.1 127.8, 129.1, (Ar-

C), 137.4 (C-1'), 175.7 (C-1); ν_{max} (KBr): 3447, 2644, 1731, 1490, 1110, 700 cm^{-1} ;

HRMS (ES⁺): Calcd. for: $\text{C}_9\text{H}_8\text{D}_2\text{O}_3\text{Na}$ $[\text{M}+\text{Na}]^+$: 191.0653, found 191.0657.

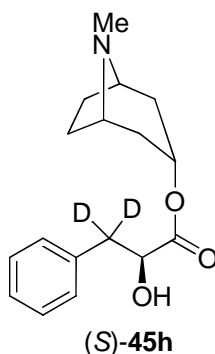
5.2.29 (*R*)-[3,3-²H₂]-Phenyllactic acid (*R*)-**103i**



The same procedure as described in **5.2.15** was repeated with (*R*)-[3,3-²H₂]-3-phenyl-2-hydroxyl-*N*-((*S*)-1-phenylethyl)propanamide **154** to afford (*R*)-**103i** as colourless needles (95.5%). Mp 118-119 °C. $[\alpha]_{\text{D}}^{20}$: -39.0° (c 1.05×10⁻³, CHCl_3). δ_{H} (MeOH- d_4 , 400 MHz) 4.33 (s, 1H, H-2), 7.21 (m, 1H, Ar-H), 7.26-7.29 (m, 4H, Ar-H). δ_{C} (CDCl_3 , 75 MHz) 39.5 (qt, $^1J_{\text{CD}} = 19.1$, C -3), 71.3 (C-2), 112.6, 127.8, 129.1 (Ar-C), 137.4 (C-1'), 175.7 (C-1). ν_{max} (KBr): 3447, 2644, 1731, 1490, 1110, 700 cm^{-1} .

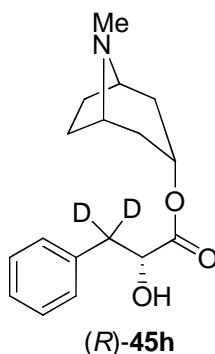
HRMS (ES⁺): Calcd. for $\text{C}_9\text{H}_8\text{D}_2\text{O}_3\text{Na}^+$ $[\text{M}+\text{Na}]^+$: 191.0653, found: 191.0657.

5.2.30 (S)-[3',3'-²H₂]-Littorine (S)-45h



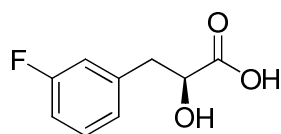
The same procedure as described in **5.2.21** was repeated with (S)-[3,3-²H₂]-phenyllactic acid **103i** to obtain (S)-**45h** as white solid (39.54%). Mp 116-117 °C; $[\alpha]_D^{20}$: -8.6° ($c = 2.3 \times 10^{-3}$, CHCl₃); δ_H (CDCl₃, 300 MHz) 1.53 (d, 1H, $^2J_{H,H} = 15.3$, H-4_a), 1.59 (d, 1H, $^2J_{H,H} = 15.5$, H-2_a), 1.68-1.73 (m, 2H, H-6_a, H-7_a), 1.88-1.94 (m, 2H, H-6_e, H-7_e), 2.06-2.14 (m, 2H, H-2_e, H-4_e), 2.20 (s, 3H, NMe), 3.01-3.07 (br, 2H, H-1, H-5), 4.29 (s, 1H, H-2'), 4.97 (t, 1H, $^3J_{H,H} = 5.3$, H-3_e), 7.15-7.18 (m, 3H, Ar-H), 7.20-7.24 (m, 2H, Ar-H); δ_C (CDCl₃, 75 MHz) 25.4 (C-7 or C-6), 25.5 (C-6 or C-7), 36.1 (C-2 or C-4), 36.2 (C-4 or C-2), 40.1 (NMe), 40.1 (C-3'), 59.6 (C-1, C-5), 68.9 (C-3), 71.5 (C-2'), 126.9, 128.5, 129.4, (Ar-C), 136.4 (C-1''), 173.4 (C-1'); ν_{max} (KBr): 2952, 1731, 1580, 1172, 738 cm⁻¹. **HRMS (ES⁺)**: Calcd. for: C₁₇H₂₂D₂NO₃ [M+H]⁺: 292.1882, found 292.1880.

5.2.31 (*R*)-[3',3'-²H₂]-Littorine (*R*)-45h

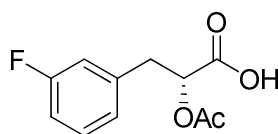


The same procedure as described in **5.2.21** was repeated with (*R*)-[3,3-²H₂]-phenyllactic acid **103i** to obtain (*R*)-**45h** as white solid (41.2%). Mp 116.0-117.5 °C; $[\alpha]_{\text{D}}^{20}$: +8.60° ($c = 2.3 \times 10^{-3}$, CHCl₃); δ_{H} (CDCl₃, 300 MHz) 1.53 (d, $^2J_{\text{H,H}} = 15.2$, 1H, H-4_a), 1.59 (d, $^2J_{\text{H,H}} = 15.3$, 1H, H-2_a), 1.68-1.73 (m, 2H, H-6_a, H-7_a), 1.88-1.94 (m, 2H, H-6_e, H-7_e), 2.06-2.14 (m, 2H, H-2_e, H-4_e), 2.20 (s, 3H, NMe), 3.02-3.07 (br, 2H, H-1, H-5), 4.29 (s, 1H, H-2'), 4.97 (t, $^3J_{\text{H,H}} = 5.3$, 1H, H-3_e), 7.14-7.18 (m, 3H, Ar-H), 7.20-7.24 (m, 2H, Ar-H); δ_{C} (CDCl₃, 75 MHz) 25.3 (C-7 or C-6), 25.4 (C-6 or C-7), 36.1 (C-2 or C-4), 36.2 (C-4 or C-2), 40.1 (NMe), 40.1 (C-3'), 59.8 (C-1, C-5), 68.9 (C-3), 71.5 (C-2'), 126.9, 128.5, 129.5 (Ar-C), 136.3 (C-1''), 173.4 (C-1'); ν_{max} (KBr): 2952, 1728, 1583, 1172, 735 cm⁻¹. **HRMS (ES⁺)**: Calcd. for: C₁₇H₂₂D₂NO₃ [M+H]⁺: 292.1882, found 292.1881.

5.2.32 Enzymatic resolution of fluorophenyllactic acids³



(S)-**103l**



(R)-**103o**

To a 250 ml Erlenmeyer flask was added (*RS*)- α -acetyl-*m*-fluorophenyllactic acid **103o** (0.1 g, 0.44 mmol), acetone (20 ml), and phosphate buffer (pH 7.5, 35 ml, 50 mmol). Porcine pancreatic lipase (EC 3.1.1.3, Sigma type II, crude) was then added and the flask was shaken at 30 °C and 150 rpm and the progress of the reaction was monitored every 6 h by TLC (50% EtOAc/hexane) and ¹H NMR. After 24 h, the content of the flask then transferred to a centrifuge tube. After centrifugation, the solvent was removed under reduced pressure and the residue was acidified with 3 M HCl to pH 1-2. The reaction mixture was extracted into DCM (2×20 ml). The combined organic phases were dried over MgSO₄, filtered, and the solvents were removed under reduced pressure. The product was purified over silica gel eluting with a gradient of 0-10% MeOH/DCM to afford (*R*)- α -acetyl-*m*-fluorophenyllactic acid (*R*)-**103o** as oil (34.5%) and (*S*)-*m*-fluorophenyllactic acid **103l** as colourless needles (28.9%).

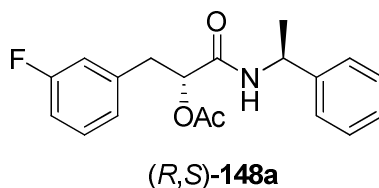
(*R*)-**103o**: $[\alpha]_D^{20}$: +10.0° (c = 11 × 10⁻³, CHCl₃). δ_H 2.02 (s, 3H, CH₃CO), 3.04 (dd, 1H, ²*J*_{HH} = 8.8, ²*J*_{HH} = 14.4, H-3), 3.16 (dd, 1H, ³*J*_{HH} = 4.29, ²*J*_{HH} = 14.4, H-3), 5.17 (dd, 1H, ³*J*_{HH} = 4.3, ³*J*_{HH} = 8.8, H-2), 6.84-6.92 (m, 2H, H-2', H-4'), 6.95 (d, 1H, ³*J*_{HH} = 7.9, H-6'), 7.17-7.24 (m, 1H, H-5'); δ_C (CDCl₃, 75 MHz) 20.5 (CH₃C=O), 36.7 (C-3), 72.1 (C-2), 114.2 (d, ²*J*_{CF} = 21.0, C-4'), 116.3 (d, ²*J*_{CF} = 21.3, C-2'), 124.9 (d, ⁴*J*_{CF} = 2.7, C-6'), 130.1 (d, ³*J*_{CF} = 8.4, C-5'), 138.1 (d, ³*J*_{CF} = 7.5, C-1'), 162.8 (d, ¹*J*_{CF} =

246.2, C-3'), 170.3 (C-1), 174.8 (CH₃C=O); δ_F (CDCl₃, 283 MHz) -113.6 (ddd, $^4J_{HF}$ = 6.1, $^3J_{HF}$ = 9.0, $^3J_{HF}$ = 9.0, 1F, Ar-F). ν_{max} (KBr): 2921, 1735, 1588, 1214, 1152 cm⁻¹.

HRMS (ES⁺): Calcd. for: C₉H₉FO₃Na⁺ [M+Na]⁺: 207.0433, found: 207.0432.

(S)-103l: Mp 101-102 °C. $[\alpha]_D^{20}$: -40.0° (c = 1.35×10⁻³, CHCl₃). δ_H (CDCl₃, 300 MHz) 3.01 (dd, 1H, $^2J_{HH}$ = 7.0, $^2J_{HH}$ = 14.1, H-3). 3.21 (dd, 1H, $^3J_{HH}$ = 4.3, $^2J_{HH}$ = 14.1, H-3), 4.54 (dd, 1H, $^3J_{HH}$ = 4.3, $^3J_{HH}$ = 7.0, H-2), 6.94-7.02 (m, 2H, H-2', H-4') 7.04 (d, 1H, $^3J_{HH}$ = 7.7, H-6'), 7.25-7.32 (m, 1H, H-5'); δ_C (CDCl₃, 75 MHz) 40.2 (C-3), 71.9 (C-2), 114.5 (d, $^2J_{CF}$ = 21.1, C-4'), 116.9 (d, $^2J_{CF}$ = 21.3, C-2'), 125.6 (d, $^4J_{CF}$ = 2.9, C-6'), 130.4 (d, $^3J_{CF}$ = 8.3, C-5'), 141.5 (d, $^3J_{CF}$ = 7.9, C-1'), 164.1 (d, $^1J_{CF}$ = 243.7, C-3'), 177.5 (C-1); δ_F (CDCl₃, 283 MHz) -113.5 (ddd, $^4J_{HF}$ = 6.1, $^3J_{HF}$ = 9.4, $^3J_{HF}$ = 9.4, 1F, Ar-F). ν_{max} (KBr): 3457, 2926, 1732, 1587, 1487, 1098, 801 cm⁻¹. **HRMS (ES⁺):** Calcd. for: C₉H₉FO₃Na⁺ [M+Na]⁺: 207.0433, found: 207.0432.

5.2.33 (R)-2-Acetoxy-3-(3-fluorophenyl)-2-hydroxyl-N-((S)-1-phenylethyl)propanamide (R,S)-148a

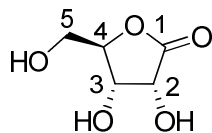


The procedure described in Section 5.2.12 was repeated with (R)-2-acetoxy-*m*-fluorophenyllactic acid ((R)-103o) (29.6 mg, 0.13 mmol) to obtain (R,S)-148a as colourless needles (39.8 mg, 90.7%). $[\alpha]_D^{20}$: +16.5° (c = 1.05×10⁻³, CHCl₃). δ_H (CDCl₃, 300 MHz) 1.35 (d, 3H, 3J = 6.9, H-1''), 2.02 (s, 3H, CH₃C=O), 3.10 (d, 2H,

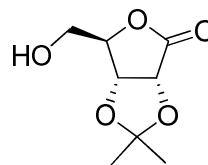
$^3J_{\text{HH}} = 5.6$, H-3), 5.02 (qt, 1H, $^3J_{\text{HH}} = 7.4$, H-2''), 5.32 (t, 1H, $^3J_{\text{HH}} = 5.6$, H-2), 6.05 (d, 1H, $^3J_{\text{HH}} = 7.79$, NH), 6.75-6.89 (m, 3H, Ar-H), 7.01-7.27 (m, 6H, Ar-H); δ_{C} (CDCl_3 , 75 MHz) 21.4 ($\text{CH}_3\text{C}=\text{O}$), 21.8 (C-1''), 37.6 (C-3), 48.9 (C-2''), 74.4 (C-2), 114.3 (d, $^2J_{\text{CF}} = 20.8$, C-4'), 117.0 (d, $^2J_{\text{CF}} = 21.3$, C-2'), 125.8 (d, $^4J_{\text{CF}} = 2.8$, C-6'), 126.5 (C-2''', C-6'''), 127.8 (C-4'''), 129.1 (C-3''', C-5'''), 130.3 (d, $^3J_{\text{CF}} = 8.3$, C-5'), 138.6 (d, $^3J_{\text{CF}} = 7.7$, C-1'), 142.7 (C-1'''), 163.1 (d, $^1J_{\text{CF}} = 245.7$, C-4'), 168.0 ($\text{CH}_3\text{C}=\text{O}$), 169.8 (C-1); δ_{F} (CDCl_3 , 283 MHz) -113.7 (ddd, $^4J_{\text{HF}} = 6.0$, $^3J_{\text{HF}} = 9.1$, $^3J_{\text{HF}} = 9.1$, 1F, Ar-F). ν_{max} (KBr): 3393, 3263, 1647, 1586, 1487, 1187, 1086, 765 cm^{-1} . HRMS (ES⁺): Calcd. for: $\text{C}_{17}\text{H}_{18}\text{FNO}_2\text{Na}^+$ $[\text{M}+\text{Na}]^+$: 310.1219, found: 310.1218.

5.3 Synthetic experiments for Chapter 3

5.3.1 2,3-*O*-Isopropylidene-D-ribo-1,4-lactone **184**⁴



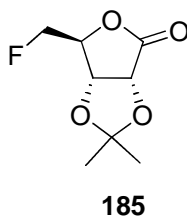
176



184

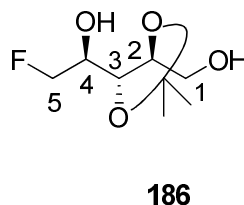
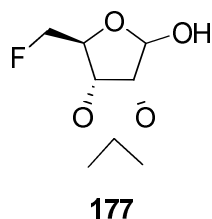
A catalytic amount of concentrated sulfuric acid was added to a suspension of D-ribo- γ -1,4-lactone **176** (2.92 g, 19.75 mmol) in acetone (100 ml) at 0 °C. After warming to ambient temperature the reaction was stirred for further 4 h. NH₃ was slowly added until the solution was neutralised, and the precipitate resultant was then filtered off. Recrystallisation of the product from benzene yielded **184** as colourless needles (3.19 g, 86%); Mp: 136-137 °C. (lit.⁴ 138-139 °C), $[\alpha]_D^{20}$: -62.3° (c 0.05, acetone) (lit.¹ $[\alpha]_D^{20}$: -84.2 (c 0.9, acetone); δ_H (Acetone-d₆, 400 MHz) 1.35 (s, 3H, CH₃), 1.39 (s, 3H, CH₃), 3.83 (m, 2H, H-5), 4.59 (t, 1H, $^3J_{HH}$ = 2.3, H -4), 4.77 (d, 1H, $^3J_{HH}$ = 5.6, H-3), 4.85 (d, 1H, $^3J_{HH}$ = 5.6, H-2). δ_C (100 MHz; Acetone-D₆) 25.5 (CH₃), 27.1 (CH₃), 62.1 (C-5), 79.3 (C-4), 83.1 (C-2), 76.4 (C-3), 112.9 (C(CH₃)₂), 206.3 (C-1). ν_{max} (KBr): 3460, 1771, 1201, 1088, 968 cm⁻¹. m/z (ES+) 210.99 [M+Na] (100%).

5.3.2 5-Deoxy-5-fluoro-2,3-*O*-isopropylidene-D-ribo-1,4-lactone **185**⁵



Deoxo-Fluor™ (3.06 ml, 16.58 mmol) was slowly added to a stirred solution of 2,3-*O*-isopropylidene-D-ribo-1,4-lactone **184** (1.04 g, 5.53 mmol) in DCM (10 ml) at ambient temperature. After stirring at 40 °C for 30 min, the reaction mixture was cooled down to ambient temperature and silica gel (0.5 g) was carefully added. After removal of the solvent, the silica gel was applied to a silica gel eluting with EtOAc:hexane (1:3) to afford **185** as white solid (0.88 g, 84%); Mp: 60-62 °C; $[\alpha]_D^{20}$: -82.8° (c 5.0×10⁻³, CHCl₃). δ_H (CDCl₃, 400 MHz) 1.39 (s, 3H, CH₃), 1.48 (s, 3H, CH₃), 4.67 (ddd, 1H, $^3J_{HH}$ = 1.9, $^2J_{HH}$ = 11.0, $^2J_{HF}$ = 46.1, H-5), 4.72 (dddd, 1H, $^3J_{HH}$ = 1.7, $^3J_{HH}$ = 1.7, $^3J_{HH}$ = 1.7, $^3J_{HF}$ = 34.57, H-4), 4.74 (ddd, 1H, $^3J_{HH}$ = 1.8, $^2J_{HH}$ = 11.0, $^2J_{HF}$ = 48.1, H-5), 4.81 (dd, 1H, $^3J_{HH}$ = 3.3, $^3J_{HH}$ = 5.6, H-3), 4.85 (d, 1H, $^3J_{HH}$ = 5.7, H-2); δ_C (CDCl₃, 100 MHz;) 25.5 (CH₃), 26.8 (CH₃), 75.1 (d, $^4J_{CF}$ = 3.9, C-2), 77.2 (d, $^3J_{CF}$ = 5.1, C-3), 80.3 (d, $^2J_{CF}$ = 19.2, C-4), 82.2 (d, $^1J_{CF}$ = 171.3, C-5), 113.9 (C(CH₃)₂), 173.6 (C-1); δ_F (282 MHz, CDCl₃) -236.0 (ddd, $^3J_{HF}$ = 3.3, $^2J_{HF}$ = 34.8, $^2J_{HF}$ = 46.3). ν_{max} (KBr): 3563, 2993, 1804, 1455, 1384, 1272, 1054, 849, 610, 513. **HRMS (ES⁺)**: Calcd. for: C₈H₁₁FO₄Na⁺ [M+Na]⁺: 213.0539, found: 231.0537.

5.3.3 5-Deoxy-5-fluoro-2,3-*O*-isopropylidene-D-ribofuranose 177 and (2*S*,3*S*,4*S*)-5-fluoro-2,3-(*O*-isopropylidenedioxy)pentan-1,4-diol 186



5.3.3.1 Synthesis with NaBH₄

NaBH₄ (11.18 mg, 0.3 mmol) was added to a vigorously stirred solution of 5-fluoro-2,3-*O*-isopropylidene-D-ribo-1,4-lactone **185** (22.5 mg, 0.12 mmol) in absolute ethanol (3 ml) at 0 °C. After stirring for 2 h, excess AcOH was added, and the volatiles were evaporated under reduced pressure. The residue was dissolved in EtOAc (20 ml), the solution was washed with H₂O, dried over Mg₂SO₄. After removal of solvent, the residue was purified over silica gel eluting with EtOAc:cyclohexane (1:4) to afford **186** as colourless oil (14.97 mg, 65.3%). $[\alpha]_D^{20}$: +19.6° (c 4.55×10⁻³, CHCl₃). δ_H (CDCl₃, 400 MHz): 1.35 (s, 3H, CH₃), 1.41 (s, 3H, CH₃), 3.73 (dd, 1H, $^3J_{HH} = 4.7$, $^2J_{HH} = 11.6$, H-1), 3.81 (dd, 1H, $^3J_{HH} = 3.8$, $^2J_{HH} = 11.6$, H-1), 3.96 (dddd, $^3J_{HH} = 2.3$, $^3J_{HH} = 5.5$, $^3J_{HH} = 9.7$, $^3J_{HF} = 21.7$, H-4), 4.07 (dd, $^3J_{HH} = 5.8$, $^3J_{HH} = 9.7$, H-3), 4.29 (dddd, 1H, $^3J_{HH} = 5.3$, $^3J_{HH} = 5.3$, $^3J_{HH} = 7.6$, $^3J_{HH} = 9.7$, H-2), 4.48 (ddd, 1H, $^3J_{HH} = 5.5$, $^2J_{HH} = 9.7$, $^2J_{HF} = 47.5$, H-5), 4.60 (ddd, 1H, $^3J_{HH} = 2.3$, $^2J_{HH} = 9.7$, $^2J_{HF} = 49.8$, H-5); δ_C (100 MHz; CDCl₃) 25.5 (CH₃), 26.8 (CH₃), 61.1 (C-1), 69.2 (d, $^2J_{CF} = 17.7$, C-4), 75.8 (d, $^3J_{CF} = 6.7$, C-3), 77.5 (C-2), 85.5 (d, $^1J_{CF} = 163.8$, C-5), 109.5 (C(CH₃)₂); δ_F (282 MHz; CDCl₃) -236.5 (ddd, $^3J_{HF} = 22.1$, $^2J_{HF} = 47.4$, $^2J_{HF} = 47.4$). ν_{max} (neat): 3384, 2988, 1373, 1043, 874, 507. **HRMS (ES⁺)**: Calcd. for: C₈H₁₅FO₄Na⁺ [M+Na]⁺: 217.0852, found: 217.0848.

5.3.3.2 Synthesis with DIBAL-H⁶

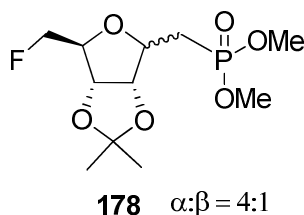
A solution of DIBAL-H (1 M in hexane, 2.20 ml, 2.18 mmol) was carefully added to a solution of 5-deoxy-5-fluoro-2,3-*O*-isopropylidene-D-ribo-1,4-lactone **185** (0.42 g, 2.18 mmol) in dry toluene (10 ml) at 40 °C and the reaction was monitored by ¹⁹F NMR. After completion, MeOH (2 ml) was added. The slurry gel was broken by adding sat. aq. solution of sodium potassium tartrate (1 ml). After extracted into ether (3×10 ml), the combined organic phases were washed with brine and dried over MgSO₄. After removal of solvent under reduced pressure the residue was purified over silica gel eluting with 60% EtOAc/hexane to afford **177** as colourless oil (0.26 g, α/β ; 7.6/1, 63.6%) and **186** (25.4 mg, 6.0%) .

177: δ_{H} (CDCl₃, 300 MHz), α -anomer: 1.27 (s, CH₃), 1.43 (s, CH₃), 3.27 (t, $^3J_{\text{HH}} = 5.17$, -OH), 4.31-4.41 (m, 2H, H-4, H-5, (overlap with β , H-4, H-5)), 4.44-4.61 (m, 2H, H-3, H-5 (overlap with β , H-3, H-5)), 4.71 (d, $^3J_{\text{HH}} = 5.9$, H-2), 5.38 (dd, 1H, $^3J_{\text{HH}} = 2.5$, $^3J_{\text{HH}} = 5.3$, H-1); δ_{C} (CDCl₃, 75 MHz) 24.9 (CH₃), 26.5 (CH₃), 81.2 (d, $^3J_{\text{CF}} = 5.5$, C-4), 82.2 (d, $^1J_{\text{CF}} = 171.3$, C-5), 84.8 (C-3 or C-2), 86.1 (C-2 or C-3), 103.3 (C-1), 112.7 (C(CH₃)₂). δ_{F} (CDCl₃, 282 MHz) -230.8 (dddd, $^4J_{\text{HF}} = 3.3$, $^3J_{\text{HF}} = 37.5$, $^2J_{\text{HF}} = 47.3$, $^2J_{\text{HF}} = 47.3$, 1F).

β - anomer: 1.50 (s, CH₃), 1.33 (s, CH₃), 3.93 (d, $^3J_{\text{HH}} = 10.9$, -OH), 4.31-4.41 (m, 2H, H-4, H-5, (overlap with α , H-4, H-5)), 4.44-4.61 (m, 2H, H-3, H-5 (overlap with α , H-3, H-5)), 4.74 (ddd, 1H, $^3J_{\text{HH}} = 0.8$, $^3J_{\text{HH}} = 1.5$, $^3J_{\text{HH}} = 6.4$, H-4), 5.33 (ddd, 1H, $^3J_{\text{HH}} = 3.7$, $^3J_{\text{HH}} = 3.7$, $^3J_{\text{HH}} = 10.9$, H-1); δ_{C} (CDCl₃, 75 MHz) 24.7 (CH₃), 26.1 (CH₃), 79.5 (C-2), 79.6 (d, $^2J_{\text{CF}} = 17.8$, C-4), 80.7 (d, $^3J_{\text{CF}} = 6.7$, C-3), 85.1 (d, $^1J = 170.5$, C-5), 97.7 (C-1), 114.2 (C(CH₃)₂). δ_{F} (CDCl₃, 283 MHz) -225.4 (dddd, $^4J_{\text{HF}} = 3.2$, $^3J_{\text{HF}} =$

23.1, $^2J_{\text{HF}} = 46.5$, $^2J_{\text{HF}} = 46.5$, 1F). ν_{max} (neat): 3426, 2944, 1376, 1211, 1072, 868, 504. **HRMS (ES⁺)**: Calcd. for: C₈H₁₃FO₄Na⁺ [M+Na]⁺: 215.0696, found: 215.0691.

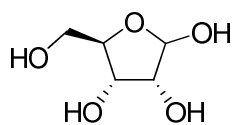
5.3.4 5-Deoxy-5-fluoro-1-deoxy-2,3-*O*-isopropylidene-1-(dimethoxyphosphinyl)-D-ribofuranose **178**⁷



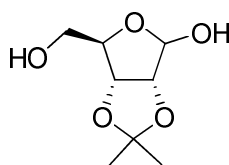
A 50% aq.NaOH solution (3 ml) was slowly added to a vigorously stirring mixture of 5-deoxy-5-fluoro-2,3-*O*-isopropylidene-D-ribofuranose **177** (0.125 g, 0.63 mmol) and tetramethyl methylenediphosphonate (0.16 g, 0.69 mmol) in DCM (3 ml) at ambient temperature. After 18 h, the reaction mixture was diluted with DCM (10 ml) and the aq. phase was extracted with DCM (2×10 ml). The combined organic phases were dried over MgSO₄, and filtered. After removal of solvent, the residue was purified over silica gel eluting with 5% MeOH:DCM to afford a mixture of epimers **7** as colourless oil (0.11 g, α/β; 3.2/1, 58.5%).

δ_{H} (CDCl₃, 400 MHz) 1.19 (C(CH₃)₂), 1.33 (C(CH₃)₂), 1.95-2.20 (m, 2H, H-1), 3.58-3.63 (m, POCH₃), 3.95-4.69 (m, 6H); δ_{P} (CDCl₃, 162 MHz) 30.3-31.1 (m, P_α), 31.7-32.4 (m, P_β); δ_{F} (CDCl₃, 283 MHz) -231.1 (ddd, $^3J = 28.90$, $^2J = 47.32$, $^2J = 47.32$, 1F_α), -229.3 (dddd, $^4J = 2.26$, $^3J = 32.94$, $^2J = 47.29$, $^2J = 47.29$, 1F_β). ν_{max} (neat): 3466, 2955, 1644, 1459, 1374, 1213, 1023, 822, 537 **HRMS (ES⁺)**: Calcd. for: C₁₁H₂₀O₄FPNa [M+Na]⁺: 321.0879, found: 321.0874.

5.3.5 2,3-*O*-Isopropylidene-D-ribofuranose **189**



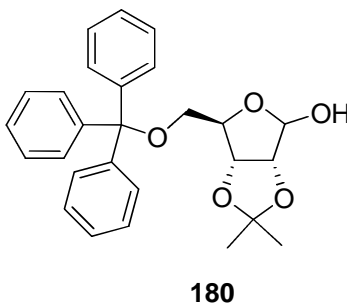
179



189

Catalytic amount of concentrated sulfuric acid was added to a suspension of D-ribonolactone **179** (2.92 g, 19.75 mmol) in acetone (100 ml) at 0 °C. After warming to ambient temperature the reaction was stirred for a further 4 h. 35% NH₃ was then slowly added until the solution was neutralised. The resultant precipitate was then filtered off. Recrystallisation of the solid from toluene yielded **189** as colourless needle (3.19 g, 86%); Mp: 136-137 °C. (lit.¹ 138-139 °C), $[\alpha]_D^{20}$: -62.3° (c 0.05, acetone) (lit.¹ $[\alpha]_D^{20}$ -84.2° (c 0.9, acetone); δ_H (Acetone-d₆, 400 MHz) 1.35 (s, 3H, CH₃), 1.39 (s, 3 H, CH₃), 3.83 (d, 2H, $^3J_{HH}$ = 2.1, H-5), 4.59 (t, 1H, $^3J_{HH}$ = 2.3, H-4), 4.77 (d, 1 H, $^3J_{HH}$ = 5.6, H-3), 4.85 (d, 1H, $^3J_{HH}$ = 5.6, H-2); δ_C (Acetone-d₆, 100 MHz) 25.5 (CH₃), 27.1 (CH₃), 62.1 (C-5), 76.4 (C-3), 79.3 (C-4), 83.1 (C-2), 112.9 (CMe₂), 206.3 (C-1). ν_{max} 3445, 2986, 1372, 1212, m/z (ES+) 322.12 [M+H] (40%).

5.3.6 2,3-*O*-Isopropylidene-5-*O*-trityl-D-ribofuranose **180**



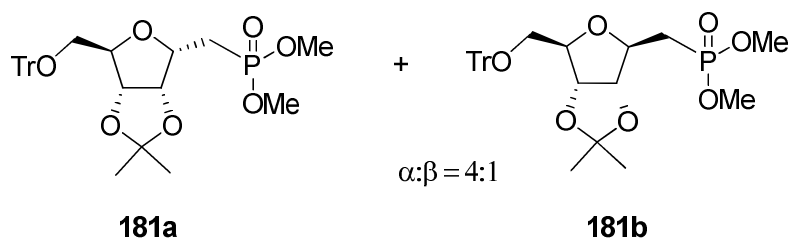
Trityl chloride (3.67 g, 13.14 mmol) was added portionwise to a solution of 2,3-*O*-isopropylidene-D-ribofuranose **189** (2.50 g, 13.14 mmol) in triethylamine (3.67 ml, 26.28 mmol). A catalytic amount of DMAP was then added. After stirring overnight, water (20 ml) was added and the mixture was extracted with EtOAc (3 × 20 ml). The combined organic extracts were washed with water and brine and then dried over MgSO₄. After removal of the solvent, the residue was purified over silica gel eluting with EtOAc:hexane (1:4) to afford **180** as viscous oil (5.30g, 93.6%, α/β; 1/4.3).

α-anomer: δ_H (CDCl₃, 300 MHz) 1.29 (s, CH₃), 1.48 (s, CH₃), 2.94 (dd, 1H, ³J_{HH} = 2.8, ²J_{HH} = 10.2, H-5), 3.38 (dd, 1H, ³J_{HH} = 3.1, ²J_{HH} = 10.2, H-5), 3.93 (d, 1H, ³J_{HH} = 11.3, -OH), 4.12 (t, 1H, ³J_{HH} = 2.6, H-4), 4.51 (dd, 1H, ³J_{HH} = 0.9, ³J_{HH} = 6.3, H-3), 4.67 (dd, 1H, ³J_{HH} = 4.1, ³J_{HH} = 6.3, H-2), 5.67 (dd, 1H, ³J_{HH} = 4.1, ³J_{HH} = 11.3, H-1), 7.17-7.35 (m, 15H, Ar-H, overlap with β-anomer); δ_C (CDCl₃, 75 MHz) 25.2 (CH₃), 26.6 (CH₃), 65.8 (C-5), 79.9 (C-3), 82.6 (C-4), 86.5 (C-2), 98.5 (C-1), 113.5 (C(CH₃)₂), 127.6 (Ar-C), 128.4 (Ar-C), 129.0 (Ar-C), 143.9 (Ar-C_{quat}).

β-anomer: δ_H (CDCl₃, 300 MHz) 1.28 (s, CH₃), 1.41 (s, CH₃), 3.27 (dd, 1H, ³J_{HH} = 3.8, ²J_{HH} = 10.4, H-5), 3.35 (dd, 1H, ³J_{HH} = 3.5, ²J_{HH} = 10.4, H-5), 3.86 (d, 1H, ³J_{HH} = 9.1, -OH), 4.28 (t, 1H, ³J_{HH} = 3.5, H-4), 4.59 (d, 1H, ³J_{HH} = 5.9, H-3), 4.71 (dd, 1H, ³J_{HH} = 0.6, ³J_{HH} = 5.9, H-2), 5.26 (d, 1H, ³J_{HH} = 9.1, H-1), 7.17-7.35 (m, 15H, Ar-H,

overlap with α -anomer); δ_{C} (CDCl_3 , 75 MHz) 25.5 (CH_3), 26.9 (CH_3), 65.5 (C-5), 80.5 (C-3), 82.4 (C-4), 87.5 (C-2), 103.9 (C-1), 112.7 ($\text{C}(\text{CH}_3)_2$), 127.9 (Ar-C), 128.5 (Ar-C), 129.1 (Ar-C), 143.2 (Ar-C_{quat}). ν_{max} (neat): 3439, 3058, 2339, 1569, 1491, 1448, 1374, 1212, 1072, 870, 705, 648. m/z (ES+) 455.06 [$\text{M}+\text{Na}$] (40%); 243.03 [Ph_3C] (100%).

5.3.7 2,5-Anhydro-1-deoxy-2,3-*O*-isopropylidene-1-(dimethoxyphosphinyl)-5-*O*-trityl-D-altritol **181a** and D-allitol **181b**⁷



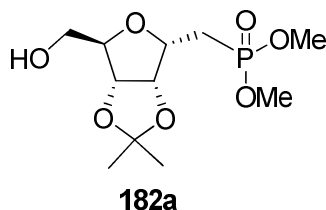
The same procedure as described for preparation of **7** was repeated with 2,3-*O*-isopropylidene-5-*O*-trityl-D-ribofuranose **180** (2.1g, 5 mmol). After chromatographic separation, **181a** (1.36g, 50.64%) and **181b** (0.32 g, 13.39%) were obtained as viscous colourless oil.

181a: $[\alpha]_{\text{D}}^{20}$: +2.9° ($c = 11.45 \times 10^{-3}$, CHCl_3), δ_{H} (CDCl_3 , 300 MHz) 1.35 (s, 3H, CH_3), 1.51 (s, 3H, CH_3), 2.26 (ddd, 1H, $^3J_{\text{HH}} = 7.0$, $^2J_{\text{HH}} = 15.5$, $^2J_{\text{HP}} = 17.6$, H-1), 2.36 (ddd, 1H, $^3J_{\text{HH}} = 6.2$, $^2J_{\text{HH}} = 15.5$, $^2J_{\text{HP}} = 18.5$, H-1), 3.15 (dd, 1H, $^3J_{\text{HH}} = 4.8$, $^2J_{\text{HH}} = 10.1$, H-6), 3.28 (dd, 1H, $^3J_{\text{HH}} = 4.2$, $^2J_{\text{HH}} = 10.1$, H-6), 3.75 (d, 3H, $^3J_{\text{HP}} = 3.8$, POCH_3), 3.79 (d, 3H, $^3J_{\text{HP}} = 3.8$, POCH_3), 4.23 (t, 1H, $^3J_{\text{HH}} = 4.4$, H-5), 4.57 (dddd, 1H, $^3J_{\text{HH}} = 3.8$, $^3J_{\text{HH}} = 6.4$, $^3J_{\text{HH}} = 6.4$, $^3J_{\text{HP}} = 10.1$, H-2), 4.69 (d, $^3J_{\text{HH}} = 6.0$, 1H, H-4), 4.76 (dd, $^3J_{\text{HH}} = 3.9$, $^3J_{\text{HH}} = 6.0$, 1H, H-3), 7.23-7.28 (m, 3H, Ar-H), 7.30-7.36 (m, 6H, Ar-H),

7.41-7.46 (m, 6H, Ar-H); δ_{C} (CDCl₃, 75 MHz) 25.6 (CH₃), 26.1 (d, $^1J_{\text{PC}} = 141.2$, C-1), 27.0 (CH₃), 52.6 (d, $^2J_{\text{CP}} = 6.3$, OCH₃), 53.2 (d, $^2J_{\text{CP}} = 6.3$, OCH₃), 64.8 (C-6) 77.1 (C-3)), 82.4 (d, $^2J_{\text{CP}} = 8.3$, C-2), 83.7 (C-4), 83.8 (C-5), 112.8 (C(CH₃)₂), 127.5 (Ar-C), 128.3 (Ar-C), 129.0 (Ar-C), 143.9 (Ar-C); δ_{P} (CDCl₃, 121 MHz) 32.3-33.0 (m, P). ν_{max} (neat): 2949, 1489, 1447, 1371, 1209, 1029, 705, 503. **HRMS (ES+)**: Calcd. for: C₃₀H₃₅O₇PNa⁺ [M+Na]⁺: 561.2018, found: 561.2021.

181b: $[\alpha]_{\text{D}}^{20}$: -8.3° (c = 12.85×10⁻³, CHCl₃), δ_{H} (CDCl₃, 300 MHz) 1.35 (s, 3H, CH₃), 1.55 (s, 3H, CH₃), 2.16 (ddd, 1H, $^3J_{\text{HH}} = 7.7$, $^2J_{\text{HH}} = 15.3$, $^2J_{\text{HP}} = 17.8$, H-1), 2.24 (ddd, 1H, $^3J_{\text{HH}} = 5.6$, $^2J_{\text{HH}} = 15.3$, $^2J_{\text{HP}} = 19.1$, H-1), 3.19 (dd, 1H, $^3J_{\text{HH}} = 4.8$, $^2J_{\text{HH}} = 11.1$, H-6), 3.33 (dd, 1H, $^3J_{\text{HH}} = 3.7$, $^2J_{\text{HH}} = 11.0$, H-6) 3.74 (d, 3H, $^3J_{\text{HP}} = 11.0$, POCH₃), 3.78 (d, 3H, $^3J_{\text{HP}} = 11.0$, POCH₃), 4.20 (dd, 1H, $^3J_{\text{HH}} = 3.4$, $^3J_{\text{HH}} = 8.3$, H-5), 4.26 (dddd, 1H, $^3J_{\text{HH}} = 5.3$, $^3J_{\text{HH}} = 5.3$, $^3J_{\text{HH}} = 7.7$, $^3J_{\text{HP}} = 10.3$, H-2), 4.54 (dd, 1H, $^3J_{\text{HH}} = 5.1$, $^3J_{\text{HH}} = 6.6$, H-3), 4.62 (dd, $^3J_{\text{HH}} = 3.5$, $^3J_{\text{HH}} = 6.6$, 1H, H-4), 7.22-7.28 (m, 3H, Ar-H), 7.28-7.35 (m, 6H, Ar-H), 7.44-7.48 (m, 6H, Ar-H); δ_{C} (CDCl₃, 75 MHz) 26.1 (CH₃), 27.1 (CH₃), 30.4 (d, $^1J_{\text{CP}} = 141.1$, C-1), 52.7 (d, $^2J_{\text{CP}} = 6.4$, OCH₃), 53.1 (d, $^2J_{\text{CP}} = 6.4$, OCH₃), 64.7 (C-6), 79.9 (d, $^2J_{\text{CP}} = 3.6$, C-3), 82.7 (C-4), 83.9 (C-5), 85.7 (d, $^2J_{\text{CP}} = 12.6$, C-2), 114.9 (C(CH₃)₂), 127.5 (Ar-C), 128.3 (Ar-C), 129.1 (Ar-C), 144.1 (Ar-C); δ_{P} (CDCl₃, 121 MHz) 30.6-31.7 (m, P). ν_{max} (neat): 2955, 1486, 1442, 1374, 1211, 1032, 711, 513. **HRMS (ES+)**: Calcd. for: C₃₀H₃₅O₇PNa⁺ [M+Na]⁺: 561.2018, found: 561.2018.

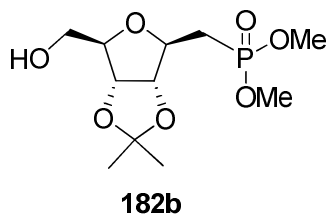
5.3.8 2,5-Anhydro-1-deoxy-2,3-*O*-isopropylidene-1-(dimethoxyphosphinyl)-5-*O*-D-altrohexitol **182a.⁸**



Anhydrous ZnCl_2 (3.1g, 22.6 mmol) was added portionwise to a solution of **181a** (1.22 g, 2.26 mmol) in DCM (40 ml) over 1 h. The reaction was monitored by TLC until the starting material was consumed. After completion of the reaction, sat. NH_4Cl (10 ml) was added and the reaction mixture was extracted into DCM (3×10 ml). The combined organic phases were washed with water and brine, and dried over MgSO_4 . After removal of solvent, the residue was purified over silica gel eluting with $\text{MeOH}:\text{DCM}$ (1:20) to afford **182a** as viscous oil (0.53 g, 78.2%).

$[\alpha]_{\text{D}}^{20}$: $+1.7^\circ$ ($c = 10.85 \times 10^{-3}$, CHCl_3), δ_{H} (CDCl_3 , 400 MHz) 1.27 (s, 3H, CH_3), 1.42 (s, 3H, CH_3), 2.14 (ddd, 1H, $^3J_{\text{HH}} = 7.3$, $^2J_{\text{HH}} = 15.5$, $^2J_{\text{HP}} = 17.7$, H-1), 2.18 (ddd, 1H, $^3J_{\text{HH}} = 6.2$, $^2J_{\text{HH}} = 15.3$, $^2J_{\text{HP}} = 18.5$, H-1), 3.56 (d, 2H, $^3J_{\text{HH}} = 5.5$, H-6), 3.68 (d, 3H, $^3J_{\text{HP}} = 10.9$, POCH_3), 3.70 (d, 3H, $^3J_{\text{HP}} = 10.9$, POCH_3), 4.06 (t, 1H, $^3J_{\text{HH}} = 5.2$, H-5), 4.25 (dddd, 1H, $^3J_{\text{HH}} = 3.8$, $^3J_{\text{HH}} = 6.5$, $^3J_{\text{HH}} = 6.5$, $^3J_{\text{HP}} = 10.1$, H-2), 4.61 (dd, $^3J_{\text{HH}} = 3.7$, $^3J_{\text{HH}} = 6.2$, 1H, H-3), 4.65 (d, $^3J_{\text{HH}} = 6.2$, 1H, H-4); δ_{C} (CDCl_3 , 100 MHz) 25.0 (CH_3), 26.3 (d, $^1J_{\text{CP}} = 141.8$, C-1), 26.4 (CH_3), 52.2 (d, $^2J_{\text{PC}} = 6.5$, OCH_3), 52.9 (d, $^2J_{\text{PC}} = 6.1$, OCH_3), 62.1 (C-6), 75.8 (C-2), 81.8 (d, $^2J_{\text{PC}} = 9.3$, C-3), 82.7 (C-4), 84.7 (C-5), 112.5 ($\text{C}(\text{CH}_3)_2$); δ_{P} (CDCl_3 , 162 MHz) 31.5–32.1.0 (m, P). $\nu_{\text{max}}(\text{neat})$: 3385, 2954, 1373, 1212, 1032, 826, 537. **HRMS (ES⁺)**: Calcd. for: $\text{C}_{11}\text{H}_{21}\text{O}_7\text{PNa}^+$ $[\text{M}+\text{Na}]^+$: 319.0923, found: 319.0927.

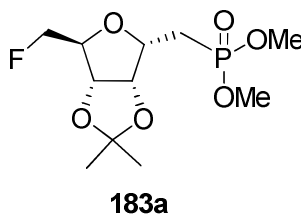
5.3.9 2,5-Anhydro-1-deoxy-2,3-*O*-isopropylidene-1-(dimethoxyphosphinyl)-5-*O*-D-allohexitol **182b.**



The same procedure as described in **5.3.8** was repeated with **181b** (0.29 g, 0.54 mmol) to afford **182b** as a viscous colourless oil (0.13 g, 80.6 %).

$[\alpha]_D^{20}$: -21.5° ($c = 9.75 \times 10^{-3}$, CHCl_3), δ_{H} (CDCl_3 , 400 MHz) 1.27 (s, 3H, CH_3), 1.46 (s, 3H, CH_3), 2.12 (ddd, 1H, $^3J_{\text{HH}} = 6.4$, $^2J_{\text{HH}} = 15.5$, $^2J_{\text{HP}} = 18.1$, H-1), 2.19 (ddd, 1H, $^3J_{\text{HH}} = 5.6$, $^2J_{\text{HH}} = 15.5$, $^2J_{\text{HP}} = 18.9$, H-1), 3.56 (dd, 1H, $^3J_{\text{HH}} = 2.8$, $^2J_{\text{HH}} = 12.5$, H-6), 3.67 (d, 3H, $^3J_{\text{HP}} = 11.0$, POCH_3), 3.71 (d, 3H, $^3J_{\text{HP}} = 11.0$, POCH_3), 3.72 (dd, 1H, $^3J_{\text{HH}} = 2.9$, $^2J_{\text{HH}} = 12.2$, H-6), 4.08 (dd, 1H, $^3J_{\text{HH}} = 3.1$, $^3J_{\text{HH}} = 6.2$, H-5), 4.17 (dddd, 1H, $^3J_{\text{HH}} = 5.7$, $^3J_{\text{HH}} = 5.7$, $^3J_{\text{HH}} = 5.7$, $^3J_{\text{HP}} = 19.3$, H-2), 4.53 (dd, 1H, $^3J_{\text{HH}} = 4.7$, $^3J_{\text{HH}} = 6.4$, H-3), 4.71 (dd, $^3J_{\text{HH}} = 2.9$, $^3J_{\text{HH}} = 6.4$, 1H, H-4); δ_{C} (CDCl_3 , 100 MHz) 25.4 (CH_3), 27.3 (CH_3), 29.1 (d, $^2J_{\text{PC}} = 141.9$, C-1), 52.1 (d, $^2J_{\text{PC}} = 6.3$, POCH_3), 52.9 (d, $^2J_{\text{PC}} = 6.3$, POCH_3), 62.7 (C-6), 79.3 (d, $^2J_{\text{PC}} = 6.5$, C-2), 81.7 (C-4), 84.9 (d, $^3J_{\text{PC}} = 10.4$, C-3), 85.4 (C-5), 113.8 (CCH_3)₂; δ_{P} (CDCl_3 , 162 MHz) 30.80-31.43 (m, P). ν_{max} : 3386, 2936, 1381, 1031, 826. **HRMS (ES⁺)**: Calcd. for: $\text{C}_{11}\text{H}_{21}\text{O}_7\text{PNa}^+$ $[\text{M}+\text{Na}]^+$: 319.0923, found: 319.0925.

5.3.10 2,5-Anhydro-1-deoxy-5-fluoro-2,3-*O*-isopropylidene-1-(dimethoxyphosphinyl)-D-altrohexitol 183a.^{9,10}

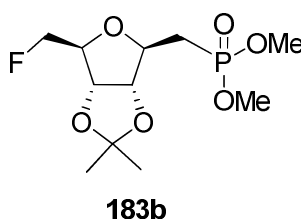


A solution of TBAF (1 M in THF, 2.16 ml, 2.16 mmol) was added to a mixture of **182a** (0.16 g, 0.54 mmol) and TsF (0.28g, 1.62 mmol) in THF (15 ml) and then the reaction mixture was brought to reflux. After refluxing for 18h, the reaction was cooled to ambient temperature and the product filtered through a short pad of silica gel washing with EtOAc. After removal of solvent the residue was purified over silica gel eluting with MeOH:DCM (1:20) to afford **183a** as colourless oil (0.148g, 92.3%).

$[\alpha]_D^{20}$: -16.4° ($c = 2.25 \times 10^{-3}$, CHCl₃). δ_H (CDCl₃, 300 MHz) 1.28 (s, 3H, C(CH₃)₂), 1.42 (s, 3H, C(CH₃)₂), 2.13 (ddd, 1H, $^3J_{HH} = 6.7$, $^2J_{HH} = 15.4$, $^2J_{HP} = 18.1$, H-1), 2.23 (ddd, 1H, $^3J_{HH} = 6.6$, $^2J_{HH} = 15.4$, $^2J_{HP} = 18.4$, H-1), 3.68 (d, 3H, $^3J_{HH} = 3.9$, POCH₃), 3.70 (d, 3H, $^3J_{HH} = 3.9$, POCH₃), 4.12 (ddd, 1H, $^3J_{HH} = 2.9$, $^3J_{HH} = 2.9$, $^3J_{HF} = 33.1$, H-5), 4.26 (dddd, 1H, $^3J_{HH} = 3.2$, $^3J_{HH} = 6.6$, $^3J_{HH} = 6.6$, $^3J_{HP} = 10.3$, H-2), 4.44 (ddd, 1H, $^3J_{HH} = 3.4$, $^2J_{HH} = 10.2$, $^2J_{HF} = 46.8$, H-5), 4.48 (ddd, 1H, $^3J_{HH} = 3.2$, $^2J_{HH} = 10.2$, $^2J_{HF} = 47.6$, H-5), 4.65 (dd, $^3J_{HH} = 3.9$, $^3J_{HH} = 6.0$, 1H, H-3), 4.77 (d, $^3J_{HH} = 6.0$, 1H, H-4); δ_C (CDCl₃, 75 MHz) 24.9 (CH₃), 25.5 (d, $^2J_{PC} = 141.9$, C-1), 26.2 (CH₃), 52.3 (d, $^2J_{PC} = 6.4$, POCH₃), 52.6 (d, $^2J_{PC} = 6.2$, POCH₃), 76.9 (d, $^2J_{CF} = 1.9$, C-2), 81.7 (d, $^2J_{PC} = 7.5$, C-3), 82.1 (d, $^2J_{CF} = 6.4$, C-4), 82.5 (d, $^2J_{CF} = 17.8$, C-5), 84.8 (d, $^1J_{CF} = 172.4$, C-6), 112.7 (C(CH₃)₂); δ_P (CDCl₃, 121 MHz) 31.65-32.38 (m, P); δ_F (CDCl₃, 282 MHz) -229.3 (ddd, $^3J_{HF} = 2.2$, $^3J_{HF} = 33.2$, $^2J_{HF} = 33.2$, $^2J_{HF} = 47.1$, 1F). ν_{max}

(neat): 2954, 1372, 1209, 1025, 819, 503. **HRMS (ES⁺)**: Calcd. for: C₁₁H₂₀O₄FPNa⁺
[M+Na]⁺: 321.0879, found: 321.0879.

5.3.11 2,5-Anhydro-1-deoxy-5-fluoro-2,3-O-isopropylidene-1-(dimethoxyphosphinyl)-D-allohexitol 183b.^{9, 10}



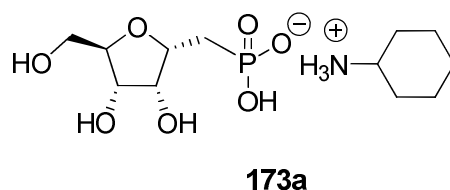
The same procedure as described for **183a** was repeated with **182b** (70 mg, 0.23 mmol) to afford **183b** as a colourless oil (60 mg, 83.1%).

$[\alpha]_D^{20}$: -18.8° (c = 2.45×10⁻³, CHCl₃). δ_H (CDCl₃, 300 MHz) 1.28 (s, 3H, C(CH₃)₂), 1.47 (s, 3H, C(CH₃)₂), 2.13 (dd, 1H, ³J_{HH} = 0.9, ²J_{HP} = 18.4, H-1), 2.09 (d, 1H, ²J_{HP} = 18.4, H-1), 3.67 (d, 3H, ³J_{HH} = 2.3, POCH₃), 3.71 (d, 3H, ³J_{HH} = 2.2, POCH₃), 4.09 (ddd, 1H, ³J_{HH} = 3.4, ³J_{HH} = 3.4, ²J_{HF} = 28.3, H-5), 4.23 (dddd, 1H, ³J_{HH} = 4.2, ³J_{HH} = 6.7, ³J_{HH} = 6.7, ³J_{HP} = 11.1, H-2), 4.45 (ddd, 1H, ³J_{HH} = 3.5, ²J_{HH} = 10.8, ²J_{HF} = 47.0, H-6), 4.48 (dd, 1H, ³J_{HH} = 4.3, ³J_{HH} = 6.6, H-3), 4.49 (ddd, 1H, ³J_{HH} = 2.8, ²J_{HH} = 10.4, ²J_{HF} = 47.6, H-6), 4.64 (dd, ³J_{HH} = 3.9, ³J_{HH} = 6.6, 1H, H-4); δ_C (CDCl₃, 75 MHz) 25.9 (CH₃), 27.7 (CH₃), 30.1 (d, ²J_{CP} = 141.1, C-1), 52.7 (d, ²J_{CP} = 6.5, OCH₃), 52.9 (d, ²J_{CP} = 6.5, OCH₃), 80.5 (d, ²J_{CF} = 3.4, C-2), 81.2 (d, ³J_{CF} = 7.4, C-4), 83.2 (d, ²J_{CF} = 172.7, C-6), 83.5 (d, ²J_{CF} = 18.3, C-5), 85.7 (d, ⁴J_{CF} = 11.3, C-3), 114.9 (C(CH₃)₂); δ_P (CDCl₃, 162 MHz) 30.33-31.09 (m, P); δ_F (CDCl₃, 282 MHz) -231.0 (ddd, ³J_{HF} =

28.8, $^2J_{\text{HF}} = 47.3$, $^2J_{\text{HF}} = 47.3$, 1F₁). ν_{max} (neat): 3464, 2956, 1383, 1214, 1030, 822, 513. **HRMS (ES⁺)**: Calcd. for: C₁₁H₂₀O₄FPNa [M+Na]⁺: 321.0879, found: 321.0875.

5.3.12 2,5-Anhydro-1-deoxy-1-phosphono-D-altritol

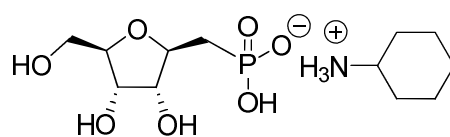
cyclohexylammonium salt 173a^{7, 11}



TMSBr (0.08 ml, 0.64 mmol) was added to a solution of **182a** (44.8 mg, 0.16 mmol) in DCM (5 ml). The progress of the reaction was monitored by ³¹P NMR. On completion, a solution of TFA:H₂O (1:1, 1 ml) was added to the reaction mixture. After 30 min, water (5 ml) was added, the solvent was removed under reduced pressure. Water (5 ml) was added and was removed under reduced pressure a process that was repeated until all traces of TFA were gone. To this residue water (5 ml) was added and adjusted pH to 11 with cyclohexylamine. After removal of solvent, the residue was dissolved in EtOH and about 0.5 volume of acetone was added. The precipitate was filtered off to afford **173a** as a white solid (43.8 mg, 83.7%). $[\alpha]_{\text{D}}^{20}$: +4.4° (c = 5.05×10⁻³, MeOH). δ_{H} (MeOH-d₄, 400 MHz) 1.18-1.27 (m, 1H, cyclohexyl), 1.31-1.44 (m, 4H, cyclohexyl), 1.71 (br d, 1H, $^2J_{\text{HH}} = 12.6$, cyclohexyl), 1.80-2.07 (m, 6H, 2H-1 overlap with 4H-cyclohexyl), 3.06 (br, s, 1H, cyclohexyl), 3.54 (dd, 1H, $^3J_{\text{HH}} = 5.0$, $^2J_{\text{HH}} = 11.9$, H-5), 3.68 (dd, 1H, $^3J_{\text{HH}} = 3.5$, $^2J_{\text{HH}} = 11.9$, H-5), 3.78-3.82 (m, 2H, H-3 and H-5), 4.01 (t, 1H, $^3J_{\text{HH}} = 5.0$, H-4), 4.06 (quintet, 1H, $^3J_{\text{HH}} = 6.9$, H-2); δ_{C} (MeOH-d₄, 75 MHz) 25.7 (2 × C), 25.4 (C), 32.4 (2 × C), 51.8 (C-

1cyclohexyl), 35.4 (d, $^1J_{CP} = 130.8$, C-1), 64.0 (C-6), 73.5 (C-4), 77.9 (d, $^2J_{CP} = 6.5$, C-2), 80.7 (C-3), 86.3 (C-5); δ_P (MeOH- d_4 , 162 MHz) 19.4 (ddd, $^3J_{HP} = 6.9$, $^2J_{HP} = 17.5$, $^2J_{HP} = 17.5$). ν_{max} (KBr): 2938, 2013, 1638, 1389, 1123, 1050, 906. **HRMS** (**ES**⁺): Calcd. for: C₁₂H₂₇NO₇P [M+H]⁺: 328.1525, found: 328.1522.

5.3.13 2,5-Anhydro-1-deoxy-1-phophon-D-allitol cyclohexylammonium salt **173b**

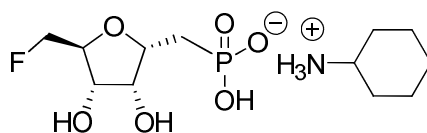


173b

The same procedure as described for preparation of **173a** was repeated for **182b** (83.2 mg, 0.3 mmol) to afford **173b** (84.1 mg, 85.6%). $[\alpha]_D^{20}$: +1.6° (c = 5.65×10⁻³, MeOH), δ_H (MeOH- d_4 , 400 MHz) 1.07-1.15 (m, 1H, cyclohexyl), 1.21-1.32 (m, 4H, cyclohexyl), 1.59 (br d, 1H, $^2J_{HH} = 12.5$, cyclohexyl), 1.68-1.98 (m, 6H, 2H-1 overlap with 4H-cyclohexyl), 2.95 (br s, 1H, cyclohexyl), 3.45 (dd, 1H, $^3J_{HH} = 5.3$, $^2J_{HH} = 11.9$, H-5), 3.59 (dd, 1H, $^3J_{HH} = 3.5$, $^2J_{HH} = 11.9$, H-5), 3.67-3.72 (m, 2H, H-4 and H-5), 3.09 (t, 1H, $^3J_{HH} = 4.9$, H-3), 3.96 (quintet, 1H, $^3J_{HH} = 6.8$, H-2); δ_C (MeOH- d_4 , 75 MHz) 25.5 (2 × C), 25.9 (1C), 32.0 (2 × C), 35.1 (d, $^1J_{CP} = 129.9$, C-1), 51.3 (C-1-cyclohex), 63.7 (C-6), 73.0 (C-4), 77.6 (d, $^2J_{CP} = 7.1$, C-2), 80.4 (C-3), 85.6 (C-5); δ_P (MeOH- d_4 , 162 MHz) 19.4 (ddd, $^3J_{HP} = 6.9$, $^2J_{HP} = 17.5$, $^2J_{HP} = 17.5$). ν_{max} : 3200, 2938, 2060, 2021, 1596, 1492, 1389, 1018. **HRMS** (**ES**⁺): Calcd. for: C₁₂H₂₇NO₇P [M+H]⁺: 328.1525, found: 328.1515.

5.3.14 2,5-Anhydro-1-deoxy-5-fluoro-1-phosphono-D-alltritol

cyclohexylammonium salt **174a**¹



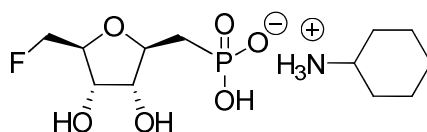
174a

The same procedure as described for preparation of **173a** was repeated for **183a** (94.8 mg, 0.34 mmol) to afford **174a** as colourless needles (97.6 mg, 87.2%). Mp. 168-170 °C, $[\alpha]_D^{20}$: +18.7° ($c = 1.50 \times 10^{-3}$, MeOH). δ_H (MeOH- d_4 , 400 MHz) 1.07-1.16 (m, 1H, cyclohexyl), 1.19-1.34 (m, 4H, cyclohexyl), 1.57-1.64 (m, 1H, cyclohexyl), 1.70-1.79 (m, 2H, cyclohexyl), 1.88-1.94 (m, 2H, cyclohexyl), 1.87 (ddd, 1H, $^3J_{HH} = 4.9$, $^2J_{HH} = 10.1$, $^2J_{HP} = 19.1$, H-1), 2.04 (ddd, 1H, $^3J_{HH} = 10.1$, $^2J_{HH} = 14.2$, $^2J_{HP} = 17.1$, H-1), 2.91-2.98 (m, 1H, H-1, cyclohexyl), 3.83 (dddd, 1H, $^3J_{HH} = 2.0$, $^3J_{HH} = 4.6$, $^3J_{HH} = 8.7$, $^3J_{HF} = 25.5$, H-5), 4.01 (dd, 1H, $^3J_{HH} = 4.6$, $^3J_{HH} = 8.7$, H-4), 4.10-4.14 (br, 1H, H-3), 4.17 (dddd, 1H, $^3J_{HH} = 2.9$, $^3J_{HH} = 4.5$, $^3J_{HH} = 4.5$, $^3J_{HP} = 9.7$, H-2), 4.34 (ddd, 1H, $^3J_{HH} = 4.7$, $^2J_{HH} = 10.3$, $^2J_{HF} = 47.7$, H-6), 4.56 (ddd, 1H, $^3J_{HH} = 2.1$, $^2J_{HH} = 10.3$, $^2J_{HF} = 48.4$, H-6); δ_C (MeOH- d_4 , 100 MHz) 25.4 ($2 \times C$, cyclohexyl), 25.9 (C, cyclohexyl), 31.2 (d, $^1J_{CP} = 129.5$, C-1), 31.9 ($2 \times C$, cyclohexyl), 51.5 (C-1, cyclohexyl), 72.9 (d, $^3J_{CF} = 7.9$, C-4), 73.4 (C-3), 79.7 (d, $^2J_{CP} = 2.7$, C-2), 81.0 (d, $^2J_{CF} = 17.6$, C-5), 84.3 (d, $^1J_{CF} = 170.9$, C-6); δ_P (MeOH- d_4 , 162 MHz) 18.7 (ddd, $^3J_{HP} = 2.9$, $^2J_{HP} = 18.1$, $^2J_{HP} = 18.1$); δ_F (MeOH- d_4 , 376 MHz) -232.4 (ddd, $^3J_{HF} = 25.5$, $^2J_{HF} = 47.4$, $^2J_{HF} = 47.4$, 1F). ν_{max} (KBr): 3199, 2939, 2720, 2012, 1597, 1429, 1389,

1121, 1018, 925. **HRMS (ES+)**: Calcd. for: C₁₂H₂₆NO₆FP [M+H]⁺: 330.1482, found: 330.1492.

5.3.15 2,5-Anhydro-1-deoxy-5-fluoro-1-phophon-D-allitol

cyclohexylammonium salt **174b**¹

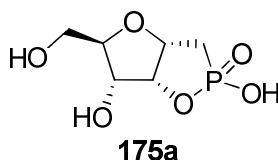


174b

The same procedure as described for preparation of **173a** was repeated with **183b** (53.1 mg, 0.19 mmol) to afford **174b** as a white solid (52.1 mg, 83.3%). Mp. 146-148 °C, $[\alpha]_D^{20}$: +3.1° ($c = 3.55 \times 10^{-3}$, MeOH). δ_H (MeOH- d_4 , 400 MHz) 1.05-1.32 (m, 5H, cyclohexyl), 1.54-1.74 (m, 5H, 1H-1 overlap with 4H-cyclohexyl), 1.87-1.90 (m, 2H, cyclohexyl), 1.99 (ddd, 1H, $^3J_{HH} = 3.7$, $^2J_{HH} = 14.1$, $^2J_{HP} = 18.8$, H-1), 2.83-2.91 (m, 1H, H-1, cyclohexyl), 3.96 (t, $^3J_{HH} = 6.3$, H-3), 3.83 (dddd, 1H, $^3J_{HH} = 3.7$, $^3J_{HH} = 3.7$, $^3J_{HH} = 3.7$, $^3J_{HF} = 25.9$, H-5), 3.97 (dd, 1H, $^3J_{HH} = 3.9$, $^3J_{HH} = 5.5$, H-4), 3.95-4.01 (m, 1H, H-2), 4.31 (ddd, 1H, $^3J_{HH} = 4.1$, $^2J_{HH} = 10.2$, $^2J_{HF} = 47.4$, H-6), 4.36 (ddd, 1H, $^3J_{HH} = 3.2$, $^2J_{HH} = 10.2$, $^2J_{HF} = 47.9$, H-6); δ_C (MeOH- d_4 , 100 MHz) 25.5 (2 × C, cyclohexyl), 26.1 (C, cyclohexyl), 32.8 (2 × C, cyclohexyl), 35.9 (d, $^1J_{CP} = 127.0$, C-1), 51.4 (C-1, cyclohexyl), 73.1 (d, $^3J_{CF} = 5.1$, C-4), 77.4 (C-3), 80.7 (d, $^2J_{CP} = 2.6$, C-2), 84.1 (d, $^2J_{CF} = 18.5$, C-5), 84.3 (d, $^1J_{CF} = 170.5$, C-6); δ_P (MeOH- d_4 , 162 MHz) 17.9 (ddd, $^3J_{HP} = 3.9$, $^2J_{HP} = 17.8$, $^2J_{HP} = 17.8$); δ_F (MeOH- d_4 , 376 MHz) -231.6 (ddd, 1F, $^3J_{HF} = 25.6$, $^2J_{HF} = 47.7$, $^2J_{HF} = 47.7$). ν_{max} (KBr): 3436, 2937, 2561, 2012, 1618,

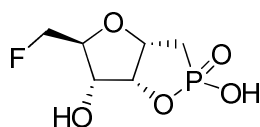
1454, 1389, 1051, 974. **HRMS (ES⁺)**: Calcd. for: C₁₂H₂₆NO₆FP [M+H]⁺: 330.1482, found: 330.1485.

5.3.16 Phostonic acid **175a**¹²



Deprotection as described in **5.3.12** was repeated for **182a** (50 mg, 0.17 mmol) in DCM (5 ml). The residue was dissolved in dry pyridine (1 ml) and acetic anhydride (0.027 ml, 0.28 mmol) was then added. An emergence of a ³¹P-NMR signal at 45 ppm and a disappearance of the signal at 27 ppm indicated that the reaction had gone to completion. After removal of the solvent under reduced pressure, the product was purified over silica gel eluting with MeOH:DCM (3:2) to afford **175a** as white solid (16 mg, 47.1%). Mp. 168-170 °C. [α]_D²⁰: +10.5° (c = 2.05×10⁻³, MeOH), δ_H (MeOH-d₄, 300 MHz) 1.84 (ddd, 1H, ³J_{HH} = 2.1, ²J_{HP} = 12.5, ²J_{HH} = 15.2, H-1), 1.98 (ddd, 1H, ³J_{HH} = 6.9, ²J_{HP} = 13.7, ²J_{HH} = 15.2, H-1), 3.58 (dd, 1H, ³J_{HH} = 4.5, ²J_{HH} = 12.1, H-6), 3.75 (dd, 1H, ³J_{HH} = 2.3, ²J_{HH} = 12.1, H-6), 3.95 (ddd, 1H, ³J_{HH} = 2.5, ³J_{HH} = 4.4, ³J_{HP} = 8.6, H-5), 4.05 (ddd, 1H, ³J_{HH} = 1.8, ³J_{HH} = 4.4, ³J_{HP} = 8.5, H-4), 4.51 (ddd, 1H, ³J_{HH} = 2.8, ³J_{HH} = 4.2, ³J_{HH} = 4.2, H-3), 4.77 (dddd, 1H, ³J_{HH} = 2.1, ³J_{HH} = 4.1, ³J_{HH} = 6.4, ³J_{HP} = 22.9, H-2); δ_C (MeOH-d₄, 75 MHz) 30.5 (d, ¹J_{CP} = 119.1, C-1), 62.9 (C-6), 74.1 (d, ⁴J_{CP} = 6.9, C-4), 80.6 (d, ³J_{CP} = 3.3, C-3), 80.7 (d, ²J_{CP} = 14.9, C-2), 83.2 (C-5); δ_P (MeOH-d₄, 162 MHz) 43.1-44.5 (br, m). ν_{max} (PTFE): 3570, 1736, 1215, 1154, 503. **HRMS (ES⁻)**: Calcd. for C₆H₁₀O₆P [M]: 209.0215, found: 209.0211.

5.3.17 5-fluorophostonic acid **175b**

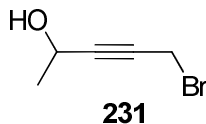


175b

The same procedure as described in **5.3.16** was repeated for **183a** to obtain **175b** as an amorphous white solid. Mp. 180-182 °C. $[\alpha]_D^{20}$: +103.0° (c = 1.0×10⁻³, MeOH). δ_H (MeOH-d₄, 300 MHz) 1.73-1.98 (m, 2H, H-1), 4.25 (dddd, 1H, $^3J_{HH}$ = 2.10, $^3J_{HH}$ = 3.90, $^3J_{HH}$ = 8.30, $^3J_{HF}$ = 26.32, H-1, H-5), 4.36 (ddd, 1H, $^3J_{HH}$ = 3.90, $^2J_{HH}$ = 10.63, $^2J_{HF}$ = 47.18, H-6), 4.48 (ddd, 1H, $^3J_{HH}$ = 2.10, $^2J_{HH}$ = 10.63, $^2J_{HF}$ = 48.14, H-6), 4.67-4.71 (m, 1H, H-3), 4.72-4.82 (m, 1H, H-2), 4.88 (ddd, 1H, $^3J_{HH}$ = 1.91, $^3J_{HH}$ = 4.61, $^3J_{HP}$ = 8.34, H-4); δ_C (MeOH-d₄, 75 MHz) 29.6 (d, $^1J_{CP}$ = 119.5, C-1), 74.4 (d, $^4J_{CF}$ = 7.15, C-4), 77.8 (d, $^4J_{CF}$ = 8.8, C-3), 79.5 (d, $^3J_{CF}$ = 18.36, C-5), 81.2 (d, $^2J_{CP}$ = 4.0, C-2), 83.2 (d, $^1J_{CF}$ = 172.1, C-6); δ_F (MeOH-d₄, 282 MHz) -234.3 (ddd, 1F, $^3J_{HF}$ = 26.4, $^2J_{HF}$ = 47.4, $^2J_{HF}$ = 47.7); δ_P (MeOH-d₄, 162 MHz) 41.9-42.6 (br, m). ν_{max} (PTFE): 3419, 1214, 1154, 799, 503. **HRMS (ES-)**: Calcd. for: C₆H₉FO₅P [M-H]: 211.0172, found: 211.0166

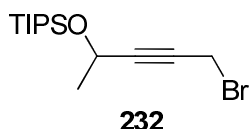
5.4 Synthetic experiments for Chapter 4

5.4.1 5-Bromo-3-pentyn-2-ol **231**¹³



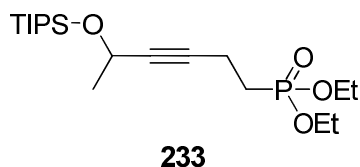
A solution of LDA (2.0 M in THF/*n*-heptane, 9.5 ml, 19.0 mmol) was added to a THF (30 ml) solution of propargyl bromide (2.4 g 19.0 mmol) in toluene (2.11 ml), at $-78\text{ }^{\circ}\text{C}$, and the mixture was stirred for 5 min. Acetaldehyde (1.2 ml, 20.4 mmol) was then added, and the reaction mixture was warmed to $0\text{ }^{\circ}\text{C}$ and stirred for 2 h. A sat. NH_4Cl solution (25 ml) was then added and the mixture was extracted into EtOAc (2 x 50 ml). The organic layer was dried over MgSO_4 , evaporated and the organic residue purified over silica gel, eluting with hexane:EtOAc (80:20) to afford **231** as dark yellow oil (1.64 g, 60%); δ_{H} (CDCl_3 , 300 MHz) 1.44 (d, 3H, $^3J_{\text{HH}} = 6.6$, CHCH_3), 3.93 (d, 2H, $^5J_{\text{HH}} = 1.8$, CH_2Br), 4.58 (q, 1H, $^3J_{\text{HH}} = 6.5$, CHCH_3); δ_{C} (CDCl_3 , 75 MHz) 14.4 (CH_2), 24.0 (CH_3), 58.2 (CH), 79.1 ($\text{C}\equiv\text{CCH}_2$), 90.1 ($\text{C}\equiv\text{CCHOH}$). ν_{max} (neat): 3345, 2983, 2252, 1079 cm^{-1} . m/z (ES+) 184.93 (^{79}Br , 90%) and 186.93 (^{81}Br , 100%) $[\text{M} + \text{Na}]^+$.

5.4.2 4-(Triisopropylsilanoyloxy)-1-bromopent-2-yne **232**



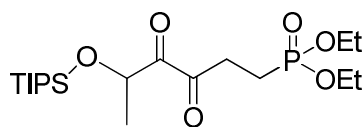
TIPS-triflate (1.12 ml, 3.65 mmol) was added dropwise to a solution of 5-bromopent-3-yn-2-ol **231** (0.54 g, 3.32 mmol) in DCM (10 ml) and 2,6-lutidine (1.16 ml, 9.96 mmol), at 0 °C. The mixture was left to warm to ambient temperature. After 45 min water (2 ml) was added, and the solvent was evaporated. The residue was dissolved in EtOAc (20 ml) and was washed with water (20 ml). The organic layer was then dried over MgSO₄, evaporated and the organic residue purified over silica gel eluting with EtOAc:hexane (2:98) to give **232** as colourless oil (~100%). δ_{H} (CDCl₃, 300 MHz) 0.99-1.01 (m, 21H, 3 \times CH(CH₃)₂), 1.37 (d, 3H, $^3J_{\text{HH}} = 6.5$, CHCH₃), 3.86 (d, 2H, $^5J_{\text{HH}} = 1.9$, CH₂Br), 4.58 (qt, 1H, $^3J_{\text{HH}} = 6.5$, $^5J_{\text{HH}} = 1.9$, CHCH₃); δ_{C} (CDCl₃, 75 MHz) 12.5 (3 \times CH(CH₃)₂), 15.0 (CH₂Br), 18.3 and 18.4 (3 \times CH(CH₃)₂), 26.6 (CHCH₃), 59.4 (CHCH₃), 78.4 (C \equiv CCH₂), 90.1 (C \equiv CCHOTIPS). ν_{max} (neat): 2944, 2235, 1464, 1104, 1029, 761, 682 cm⁻¹. m/z (ES⁺): 341.0924 [M+Na] C₁₄H₂₇⁷⁹BrOSiNa (55%) and 343.0901 [M+Na]. C₁₄H₂₇⁸¹BrOSiNa (52%).

5.4.3 Diethyl 5-(triisopropylsilanoyloxy)-hex-3-ynylphosphonate **233**



A solution of *n*-BuLi (2.5 M in hexane, 0.40 ml, 1.0 mmol) was added to a THF (20 ml) solution of diethyl methylphosphonate (0.152 g, 1.0 mmol) at -78 °C, and the mixture was stirred for 15 min. A solution of 4-(triisopropylsilanoyloxy)-1-bromopent-2-yne **232** (0.319 g, 1.0 mmol) in THF was then added, and the reaction mixture was warmed to ambient temperature and stirred for 2 h. A sat.aq.NH₄Cl solution (25 ml) was then added and the mixture was extracted into EtOAc (2 × 50 ml). The organic layer was then dried over MgSO₄, evaporated and the organic residue purified over silica gel eluting with EtOAc:hexane (80:20) to afford **233** as colourless oil (0.156 g, 40%). δ_{H} (CDCl₃, 300 MHz) 1.04-1.10 (m, 21H, 3 × CH(CH₃)₂), 1.33 (t, 6H, *J* 7.1, 2 × CH₂CH₃), 1.40 (d, 3H, ³*J*_{HH} = 6.4, CHCH₃), 1.87-2.05 (m, 2H, CH₂P), 2.43-2.52 (m, 2H, C≡CCH₂), 4.02-4.16 (m, 4H, 2 × CH₂CH₃), 4.56 (tq, 1H, ⁵*J*_{HH} = 1.8, ³*J*_{HH} = 6.4, CHCH₃); δ_{C} (CDCl₃, 75 MHz) 12.5 (3 × CH(CH₃)₂), 13.1 (d, ³*J*_{CP} = 3.1, CH₂CH₂P), 16.8 (d, ³*J*_{CP} = 6.0, 2 × POCH₂CH₃), 18.3, 18.4 (3 × CH(CH₃)₂), 25.3 (d, ¹*J*_{CP} = 140.7, CH₂P), 26.1 (CHCH₃), 59.4 (CHCH₃), 62.1 (d, ²*J*_{CP} = 6.4, 2 × POCH₂CH₃), 81.9 (d, ³*J*_{CP} = 23.0, C≡CCH₂CH₂P), 84.1 (C≡CCHOH); δ_{P} (CDCl₃, 121.5 MHz) 30.6 (m). ν_{max} (neat): 2941, 2229, 1463, 1247, 1099, 1029 cm⁻¹. **HRMS (ES⁺)**: Calcd. For C₁₉H₃₉O₄PSiNa [M+Na]⁺: 413.2253, found: 413.2247.

5.4.4 Diethyl 5-(triisopropylsilanoyloxy)-3,4-dioxohexyl-phosphonate **234**

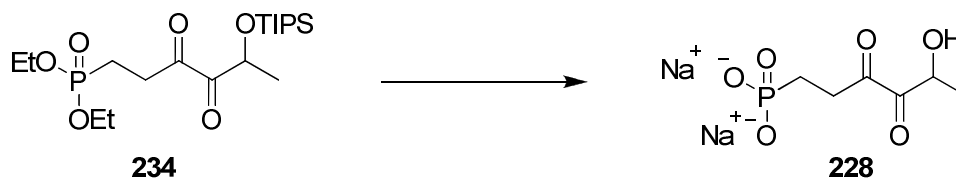


234

To a solution of **233** (0.31 g, 0.79 mmol) in $\text{CHCl}_3/\text{CH}_3\text{CN}/\text{H}_2\text{O}$ (1:1:1.5) was added NaIO_4 (4.1 equiv.). The mixture was stirred vigorously at room temperature and then RuO_2 (0.022 equiv.) was added. Two clear phases partitioned.³⁴ The reaction mixture turned from black to bright yellow and a white precipitate formed. The mixture was poured into a separatory funnel, and water (10 ml) was added. The aq. phase was extracted into CH_2Cl_2 (3 x 20 ml) and the combined organic phases were dried over MgSO_4 , and filtrated through a column of Celite (6 cm high, Ø 2 cm). The solvents were evaporated under reduced pressure and the residue was purified over silica gel (EtOAc:hexane, 30:70) to afford **234** as yellow oil (0.19 g, 60%); δ_{H} (CDCl_3 , 300 MHz) 1.00-1.10 (m, 21H, $3 \times \text{CH}(\text{CH}_3)_2$), 1.32 (t, 6H, $^3J_{\text{HH}} = 7.1$, $2 \times \text{CH}_2\text{CH}_3$), 1.41 (d, 3H, $^3J_{\text{HH}} = 6.9$, CHCH_3), 1.96-2.08 (m, 2H, CH_2P), 2.93-3.18 (m, 2H, $\text{O}=\text{CCH}_2$), 4.04-4.19 (m, 4H, $2 \times \text{POCH}_2\text{CH}_3$), 5.01 (q, 1H, $^3J_{\text{HH}} = 6.8$, OCHCH_3); δ_{C} (75 MHz; CDCl_3) 12.6 [$3 \times \text{CH}(\text{CH}_3)_2$], 16.8 (d, $^3J_{\text{CP}} = 6.0$, $2 \times \text{POCH}_2\text{CH}_3$), 18.2, 18.3 ($3 \times \text{CH}(\text{CH}_3)_2$), 19.0 (d, $^1J_{\text{CP}} = 146.0$, CH_2P), 20.5 (CHCH_3), 37.3 (d, $^2J_{\text{CP}} = 3.5$, $\text{CH}_2\text{CH}_2\text{P}$), 62.2 (d, $^2J_{\text{CP}} = 6.0$, $2 \times \text{POCH}_2\text{CH}_3$), 70.7 (CHCH_3), 200.0 (d, $^3J_{\text{CP}} = 15.4$, $\text{COCH}_2\text{CH}_2\text{P}$), 200.2 (C=O); δ_{P} (121.5 MHz; CDCl_3) 31.5; ν_{max} (neat): 2943, 1719, 1218, 1507, 1026 cm^{-1} . **HRMS** (ES^+): Calcd. For $\text{C}_{19}\text{H}_{39}\text{O}_6\text{PSiNa}$ $[\text{M}+\text{Na}]^+$: 445.2151, found: 445.2160.

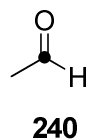
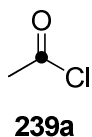
5.4.5 Deprotection of diethyl-5-(triisopropylsilanoyloxy)-3,4-

dioxohexyl phosphonate **234**³⁷



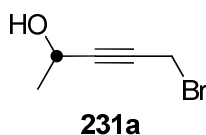
TMS-bromide (0.26ml, 1.96 mmol) was added to a solution of diethyl 5-(triisopropylsilanoyloxy)-3,4-dioxohexyl-phosphonate **234** (0.21 g, 0.49 mmol) in DCM (2 ml) at ambient temperature and under an inert atmosphere. After 6 h the solvent was removed and the residue was dried under reduced pressure. Water (5 ml) was then added and the mixture was stirred for 20 min until the solid completely dissolved. The solution was then neutralized with 0.2 M NaOH until pH ~7 and the solvent was finally removed to afford **228** as crude product as white amorphous solid. ^1H and ^{13}C NMR are shown in Figure 4.9. δ_{P} (D_2O , 121.5 MHz;) 25.6; m/z (ES+) 432.72 (100%).

5.4.6 [1-¹³C]-acetaldehyde **240**^{14, 15}



Pd(0)P(Ph₃)₄ (0.15g, 0.13 mmol) was added to a 2-necked flask equipped with condenser and a receiving flask containing dry THF (3 ml) cooling at -89 °C under N₂. Dry toluene (5 ml) was then added. [1-¹³C]acetyl chloride (1g, 6.24 mmol) was slowly added and the reaction was stirred for 5 min and then a solution of *n*-Bu₄SnH (4.40 ml, 1.29 mmol) was added dropwise. After 10 min, N₂ was bubbled through the reaction mixture and this was continued for 45 min after the addition of *n*-Bu₄SnH was finished. [1-¹³C]-acetaldehyde was used immediately in Section 5.4.7.

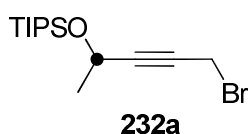
5.4.7 [2-¹³C]-5-Bromo-3-pentyn-2-ol **231a**^{14, 15}



Propargyl bromide (80% solution in toluene, 1.05 ml, 11.8 mmol) in THF was treated with LDA (2.0 M in THF/*n*-heptane, 5.70 ml, 11.4 mmol) at -78 °C. A solution of [1-¹³C]-acetaldehyde in THF was then added to the reaction *via* a cannular. After stirring at 78 °C for 15 min, the reaction mixture was warmed to 0 °C and stirred for a further 2 h. A sat. NH₄Cl solution (25 ml) was added and the mixture was extracted into EtOAc (2 × 50 ml). The organic layer was dried over MgSO₄, evaporated and the organic residue purified over silica gel, eluting with hexane:EtOAc (80:20) to afford **231a** as dark yellow oil (0.39 g, 38.1%).

δ_{H} (CDCl₃, 400 MHz) 1.38 (dd, 3H, $^3J_{\text{HH}} = 6.6$, $^2J_{\text{CH}} = 4.7$, CHCH₃), 3.88 (br, 2H, CH₂Br), 4.52 (dqt, 1H, $^5J_{\text{HH}} = 1.8$, $^3J_{\text{HH}} = 6.6$, $^1J_{\text{CH}} = 148.7$, CHCH₃); δ_{C} (CDCl₃, 100 MHz) 14.4 (CH₂), 24.0 ($^1J_{\text{CC}} = 40.3$, CH₃), 58.2 (CH), 79.1 (C \equiv CCH₂), 90.1 (C \equiv CCHOH). ν_{max} (neat): 3340, 2983, 2250, 1081 cm⁻¹.

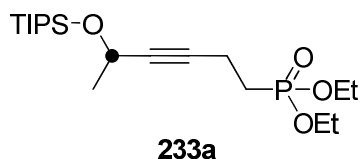
5.4.7 [4-¹³C]-4-(Triisopropylsilyloxy)-1-bromopent-2-yne **232a**



The procedure described in **5.4.2** was repeated for **231a** (0.39 g, 2.39 mmol) to afford **232a** as colourless oil (0.74g, 96.7%).

δ_{H} (CDCl₃, 400 MHz) 0.99-1.04 (m, 21H, 3 \times CH(CH₃)₂), 1.36 (dd, 3H, $^3J_{\text{HH}} = 6.5$, $^2J_{\text{CH}} = 4.5$, CHCH₃), 3.86 (dd, 2H, $^3J_{\text{CH}} = 6.5$, $^5J_{\text{HH}} = 1.8$, CH₂Br), **4.56 (dqt, 1H, $^5J_{\text{HH}} = 1.8$, $^3J_{\text{HH}} = 6.5$, $^1J_{\text{CH}} = 144.8$, ¹³CH(OH)CH₃)**; δ_{C} (CDCl₃, 100 MHz) 12.2 (3 \times CH(CH₃)₂), 14.6 (CH₂Br), 17.9, 18.0 (3 \times CH(CH₃)₂), 25.4 (d, $^2J_{\text{CC}} = 41.6$, CH(OH)CH₃), 59.0 (¹³CH(OH)CH₃), 78.1 ($^2J_{\text{CC}} = 13.1$, C \equiv CCH₂), 89.7 ($^1J_{\text{CC}} = 75.5$, C \equiv CCHOTIPS). ν_{max} (neat): 2944, 2233, 1464, 1100, 1031, 760 cm⁻¹.

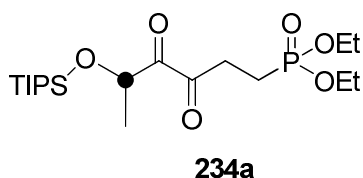
5.4.8 [5-¹³C]-Diethyl-5-(triisopropylsilylanoyloxy)-hex-3-ynyl-phosphonate **233a**



The procedure described in **5.4.3** was repeated for **232a** (0.61g, 1.90 mmol) to afford **233a** as a colourless oil (0.42 g, 56.9%).

δ_{H} (CDCl₃, 300 MHz) 0.98-1.02 (m, 21H, 3 × CH(CH₃)₂), 1.26 (t, 6H, ³*J*_{HH} = 7.1, 2 × CH₂CH₃), 1.33 (dd, 3H, ³*J*_{HH} = 6.5, ²*J*_{CH} = 4.5, CH(OH)CH₃), 1.84-1.95 (m, 2H, CH₂P=O), 2.35-2.45 (m, 2H, CH₂CH₂C≡C), 3.96-4.09 (m, 4H, 2 × CH₂CH₃), **4.50** (dtq, 1H, ⁵*J*_{HH} = 1.9, ³*J*_{HH} = 6.5, ¹*J*_{CH} = 144.5, ¹³CHCH₃); δ_{C} (CDCl₃, 75 MHz) 12.5 (3 × CH(CH₃)₂), 16.8 (d, ³*J*_{CP} = 6.0, 2 × CH₃CH₂OP=O), 18.3, 18.4 (3 × CH(CH₃)₂), 25.8 (d, ¹*J*_{CP} = 140.7, CH₂CH₂P=O), 26.1 (d, ¹*J*_{CP} = 41.1, CH₃CH(OH)), 31.3 (CH₂CH₂P=O), 59.4 (¹³CH(HO)CH₃), 62.1 (d, ²*J*_{CP} = 6.5, 2 × POCH₂CH₃); δ_{P} (CDCl₃, 121.5 MHz) 30.2-30.8 (m). ν_{max} (neat): 2946, 1719, 1221, 1108, 1027 cm⁻¹.

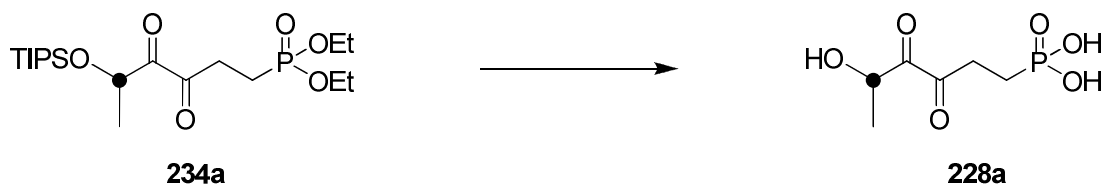
5.4.9 [5-¹³C]-Diethyl-5-(triisopropylsilylanoyloxy)-3,4-dioxohexyl-phosphonate **234a**



The procedure described in **5.4.3** was repeated for **233a** (0.25g, 0.65 mmol) to afford **234a** as a bright yellow oil (0.18 g, 64.6%).

δ_{H} (CDCl_3 , 300 MHz) 0.95-1.01 (m, 21H, $3 \times \text{CH}(\text{CH}_3)_2$), 1.25 (t, 6H, $^3J_{\text{HH}} = 7.1$, $2 \times \text{CH}_2\text{CH}_3$), 1.34 (dd, 3H, $^3J_{\text{HH}} = 6.4$, $^2J_{\text{CH}} = 4.3$, CHCH_3), 1.90-2.00 (m, 2H, $\text{CH}_2\text{P}=\text{O}$), 2.88-3.09 (m, 2H, $\text{CH}_2\text{CH}_2\text{C}=\text{O}$), 3.99-4.09 (m, 4H, $2 \times \text{CH}_2\text{CH}_3$), **4.95 (dq, 1H, $^3J_{\text{HH}} = 6.9$, $^1J_{\text{CH}} = 144.5$, $^{13}\text{CH}(\text{OH})\text{CH}_3$)**; δ_{C} (CDCl_3 , 75 MHz) 12.6 ($3 \times \text{CH}(\text{CH}_3)_2$), 16.8 (d, $^3J_{\text{CP}} = 6.1$, $2 \times \text{CH}_3\text{CH}_2\text{P}=\text{O}$), 18.2, 18.3 ($3 \times \text{CH}(\text{CH}_3)_2$), 19.1 (d, $^1J_{\text{CP}} = 146.2$, $\text{CH}_2\text{P}=\text{O}$), 20.5 (d, $^1J_{\text{CP}} = 38.9$, $\text{CH}_3\text{CH}(\text{OH})$), 31.7 (d, $^2J_{\text{CP}} = 3.3$, $\text{CH}_2\text{CH}_2\text{P}=\text{O}$), 62.2 (d, $^2J_{\text{CP}} = 6.5$, $2 \times \text{POCH}_2\text{CH}_3$), 70.3 ($^{13}\text{CH}(\text{HO})\text{CH}_3$); δ_{P} (CDCl_3 , 121.5 MHz) 30.0-30.6 (m). ν_{max} (neat): 2945, 1720, 1212, 1105, 1025 cm^{-1} . **HRMS (ES⁺)**: Calcd. For $^{12}\text{C}_{18}^{13}\text{C}_1\text{H}_{39}\text{O}_6\text{PSiNa} [\text{M}+\text{Na}]^+$: 446.2185, found: 446.2192.

5.4.10 Deprotection of [5- ^{13}C]-diethyl-5-(triisopropylsilanoyloxy)-3,4-dioxohexyl-phosphonate **228a**



The same procedure described in **5.4.5** was repeated for **234a** (28 mg, 0.7 mmol) to obtain crude **228a**. Only the isotopically enriched signals are reported in the ^{13}C -NMR. δ_{C} (D_2O , 75 MHz) 207.5, 207.0 ($\text{C}=\text{O}$), 72.6 69.7 ($\text{CH}(\text{OH})$); δ_{P} (D_2O , 121.5 MHz) 30.9-31.7 (br, m).

This product was dissolved in D_2O (3 ml) and the solution was basicified to pH 3.5 with 0.2 M NaOH. After removal of solvents, the ^1H , ^{13}C and ^{31}P NMR spectra were then recorded. The process was repeated at pH 7.0, 10.5, and 12.5.

pH 3.5: δ_C (D₂O, 100 MHz) 207.9 (C=O), 96.3 (C(OH)₂), 70.1 (CH(OH)); δ_P (D₂O, 121.5 MHz) 25.1-26.1 (br, m). m/z (ES⁻): 156.94 (100%).

pH 7.0: δ_C (D₂O, 100 MHz) 208.3, 182.3 (C=O), 70.2, 69.1 (CH(OH)); δ_P (D₂O, 121.5 MHz) 24.5-25.6 (br, m), 26.1-27.0 (br, m). m/z (ES⁺): 275.97 [M+3Na] (100%). m/z (ES⁻): 156.96 (100%)

pH 10.5: δ_C (D₂O, 100 MHz) 182.2 (C=O), 67.0 (CH(OH)); δ_P (D₂O, 121.5 MHz) 21.7-22.0 (br, m), 22.5-23.0 (br, m), 23.2-23.7 (br, m). m/z (ES⁺): 275.94 [M+3Na] (100%). m/z (ES⁻): 181.98 (100%)

pH 12.5: δ_C (D₂O, 100 MHz) 182.3 (C=O), 69.1 (CH(OH)); δ_P (D₂O, 121.5 MHz) 22.7-23.1 (br, m), 23.4-23.7 (br, m). m/z (ES⁺): 275.95 [M+3Na] (100%). m/z (ES⁻): 156.98 (100%).

5.5 Biochemical experiments

5.5.1 Bioassay for Chapter 2

Bioassays were carried out by Dr. Darwin W Reed, Plant Biotechnology Institute, 110 Gymnasium Place, Saskatoon, SK, Canada, S7N OW9.

5.5.1.1 Preparation of yeast microsomes

Yeast microsomes were prepared according to Katavic *et al.*¹⁶ and the microsomal membrane pellet was re-suspended in storage buffer containing 100 mM potassium phosphate buffer, pH 7.5, 1 mM EDTA, 20% (v/v) glycerol. Protein concentration was determined by Bradford assay (Bio-Rad, Hercules, CA).

5.5.1.2 GC/MS analysis

GC/MS analysis of the alkaloids was accomplished using an Agilent 5973 Mass Selective Detector coupled to an Agilent 6890N Gas Chromatograph equipped with a 30 m X 0.25 mm DB-5MS column with 0.25 μ m film thickness (J&W Scientific). The chromatograph conditions were a split injection (20:1) using a helium flow of 0.4 ml/min, an initial temperature of 175°C for 1 min, followed by a temperature ramp at 5°C/min to 300°C. The mass selective detector was run under standard EI⁺ conditions (70 eV) scanning an effective mass range of 40 to 700 amu at 2.26 scan/s.

5.5.1.3 CYP80F1 enzyme assays with fluorolittorines

The complete reaction mixture (200 μ l) contained 264 μ g microsomal protein, 100 mM potassium phosphate buffer, pH 7.4, 3 mM NADPH, and 865 mM alkaloid substrate. Reactions were initiated by the addition of substrate and carried out at 30°C for 10 mins with gentle shaking. Reactions were stopped by adding 800 μ l of 100 mM sodium carbonate buffer (pH 10.8) containing 1 μ g of internal standard (scopolamine, Sigma, Oakville, ON) to bring the final pH to 8.5. The reaction mixture was immediately applied to an Extrelut QE column (EM Science, Gibbstown, NJ). After 5 min, the alkaloids were eluted with 12 ml of DCM and the solvent was removed under a nitrogen stream. For GC/MS analysis the residue was dissolved in 20 μ l of BSA/pyridine (1:1).

Hyoscyamine aldehydes were monitored at m/z 359 (M⁺ of O-TMS derivative of enol) and 3'-hydroxylittorines were monitored at m/z 449 (M⁺ of (O-TMS)₂ derivative). Fluorohyoscyamine aldehydes were monitored at m/z 377 ((M⁺ of O-TMS derivative of enol)) and fluoro-3'-hydroxylittorines were monitored at m/z 467

(M⁺ of (O-TMS)₂ derivative). Internal standard quantitation was done by comparison of SIM (single ion monitoring) integrations (m/z 124) on peaks identified as products using the integrated area of m/z 138 of scopolamine as 1 µg (a correction factor of 1.0 was used).

5.5.1.4 CYP80F1 enzyme assays for isotope effect experiments

The complete reaction mixture (200 µl) contained 64 µg microsomal protein, 100 mM potassium phosphate buffer, pH 7.4, 3 mM NADPH, and 0.87 mM alkaloid substrate. Reactions were initiated by the addition of NADPH and carried out at 30°C for 15 minutes with gentle shaking. Reactions were stopped by adding 800 µl of 100 mM sodium carbonate buffer (pH 10.8) containing 2.5 µg of internal standard (scopolamine) to bring the final pH to 8.5 and then the reaction mixture was immediately applied to an Extrelut QE column (EM Science, Gibbstown, NJ). After 5 min, the alkaloids were eluted with 12 ml of dichloromethane and the solvent was removed under a nitrogen stream. For GC/MS analysis the residue was dissolved in 25 µl of BSA/pyridine (1:1).

For competitive isotope effect experiments, a 1:1 mixture of [2',2'-d₂]- and [d₀]- (*S*)-littorines was used. Substrates were monitored at m/z 363 and 361 and products at m/z 179 (d₀) and 180 (d₁). The m/z = 180 was corrected by subtraction of the m/z 179 + 1 isotope peak. Competitive isotope effect were calculated using KIE (k_H/k_D) = (d₀ product / d₁ product) / (d₀ substrate / d₂ substrate).

For non-competitive isotope effect experiments with (*S*)-littorine the same ions were monitored with no need for natural isotopic abundance correction of m/z 180. For

noncompetitive experiments on the oxidation/rearrangement of (*R*)-littorine, production of the hyoscyamine aldehyde was determined by comparing integrated signals for *m/z* 124 and *m/z* 138 (scopolamine internal standard and correction factor 1.0).

5.5.2 Bioassay for Chapter 3

The enzyme assays were carried out by Dr. Stuart M. Cross, at the University of St Andrews.¹⁷

5.5.3 Bioassay for Chapter 4

The enzyme assays were carried out by Dr. Denis Tritsch, Université Louis Pasteur/Centre National de la Recherche Scientifique, Institut de Chimie de Strasbourg, LC3-UMR 7177, 67070 Strasbourg cedex, France.

His-Tagged DXR from *E. coli* was purified as described in Kuntz et al.¹⁸ Assays were performed in a 50 mM triethanolamine buffer pH 7.7 containing 3 mM MgCl₂, 2 mM dithiothreitol (triethanolamine was preferred over Tris buffer, which is able to react with α -dicarbonyl compounds) at 37 °C. The final volume was 500 μ L. The compound (35.5 mg) was dissolved in 0.7 mL H₂O (concentration 200 mM).

DXR (2 μ L, stock concentration 2.7 μ g/ μ L) was first preincubated with NADPH (0.25 mM final concentration) and **228a** at 37 °C for 2 min. The enzymatic reaction was then initiated by addition of DXP (0.5 mM final concentration). The reaction was followed at 340 nm with a Uvikon 933 spectrometer. The concentrations of inhibitor varied from 10 to 800 μ M and no decrease of the enzymatic rate was observed.

Compound did not inhibit DXR. **228a** (400 μ M) was also incubated with NADPH and DXR. No decrease of the absorbance at 340 nm was detected. It is not substrate of the enzyme.

5.6 References

1. D. O'Hagan, R. J. Robins, M. Wilson, C. W. Wong, M. Berry and I. Zebatakis, *J. Chem. Soc., Perkin trans. 1*, 1999, 2117-2120.
2. H. Wren and E. Wright, *J. Chem. Soc., Trans.*, 1921, **119**, 798-803.
3. B. Larissegger-Schnell, S. M. Glueck, W. Kroutil and K. Faber, *Tetrahedron*, 2006, **62**, 2912-2916.
4. A. A. Kandil and K. N. Slessor, *J. Org. Chem.*, 1985, **50**, 5649-5655.
5. Y. Oogo, A. M. Ono and M. Kainosho, *Tetrahedron Lett.*, 1998, **39**, 2873-2876.
6. S. J. Baker and D. W. Young, *J. Labelled Cpd. Radiopharm.*, 2000, **43**, 1023-1032.
7. R. B. Mayer, T. E. Stone and P. K. Jesthi, *J. Med. Chem.*, 1984, **27**, 1095-1098.
8. V. Kohli and H. Blocker, *Tetrahedron Lett.*, 1980, **21**, 2683-2686.
9. M. Shimizu, Y. Nakahara and H. Yoshioka, *Tetrahedron Lett.*, 1985, **26**, 4207-4210.
10. T. D. Ashton and P. J. Scammells, *Bioorg. Med. Chem. Lett.*, 2005, **15**, 3361-3363.
11. R. W. McClard and J. F. Witte, *Bioorg. Med. Chem. Lett.*, 1994, **4**, 1537-1538.
12. M. Bosco, P. Bissereet and J. Eustache, *Tetrahedron Lett.*, 2003, **44**, 2347-2349.
13. C. D. Cardicamo, University of St Andrews, 2006.
14. P. Four and F. Guibe, *J. Org. Chem.*, 1981, **46**, 4439-4445.

15. D. Barbry and D. Couturier, *J. Labelled Cpd. Radiopharm.*, 1987, **24**, 603-606.
16. V. Katavic, E. Miethiewska, D. L. Barton, E. M. Giblin, D. W. Reed and D. C. Taylor, *Eur. J. Biochem.*, 2002, **269**, 5625-5631.
17. S. M. Cross, University of St Andrews, 2008.
18. L. Kuntz, D. Tritsch, C. Grosdemange-Billiard, A. Hemmerlin, A. Willem, T. J. Bach and M. Rohmer, *Biochem. J.*, 2005, **386**, 127-135.

Appendix I

Crystallographic data for (*S,S*)-147

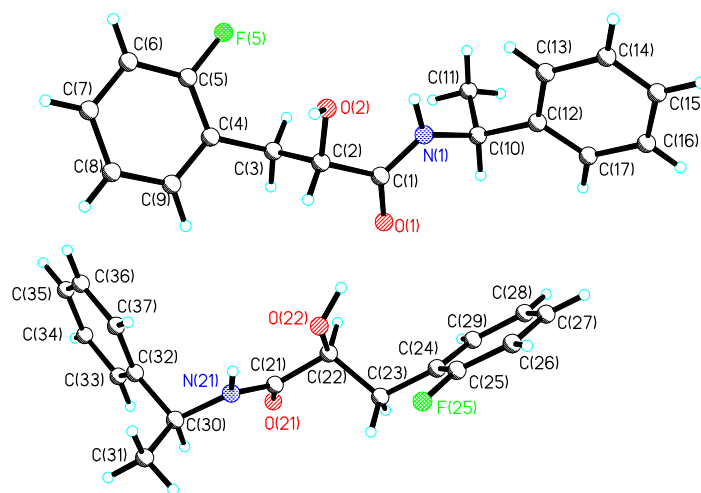


Table 1. Crystal data and structure refinement for (S,S)-**147**.

Identification code	pndh6	
Empirical formula	C ₁₇ H ₁₈ F N O ₂	
Formula weight	287.32	
Temperature	93(2) K	
Wavelength	0.71073 Å	
Crystal system	Monoclinic	
Space group	P2(1)	
Unit cell dimensions	a = 5.531(2) Å	α = 90°.
	b = 22.228(9) Å	β = 101.881(5)°.
	c = 12.362(5) Å	γ = 90°.
Volume	1487.1(10) Å ³	
Z	4	
Density (calculated)	1.283 Mg/m ³	
Absorption coefficient	0.092 mm ⁻¹	
F(000)	608	
Crystal size	0.2000 x 0.0300 x 0.0100 mm ³	
Theta range for data collection	1.68 to 25.32°.	
Index ranges	-6 ≤ h ≤ 6, -26 ≤ k ≤ 26, -14 ≤ l ≤ 14	
Reflections collected	14791	
Independent reflections	5369 [R(int) = 0.0389]	
Completeness to theta = 25.00°	99.5 %	
Absorption correction	Multiscan	
Max. and min. transmission	1.0000 and 0.8638	
Refinement method	Full-matrix least-squares on F ²	
Data / restraints / parameters	5369 / 5 / 397	
Goodness-of-fit on F ²	1.045	
Final R indices [I > 2σ(I)]	R1 = 0.0566, wR2 = 0.1439	
R indices (all data)	R1 = 0.0649, wR2 = 0.1515	
Absolute structure parameter	-0.2(9)	
Extinction coefficient	0.010(4)	
Largest diff. peak and hole	1.455 and -0.355 e.Å ⁻³	

Crystallographic data for (*R,S*)-149

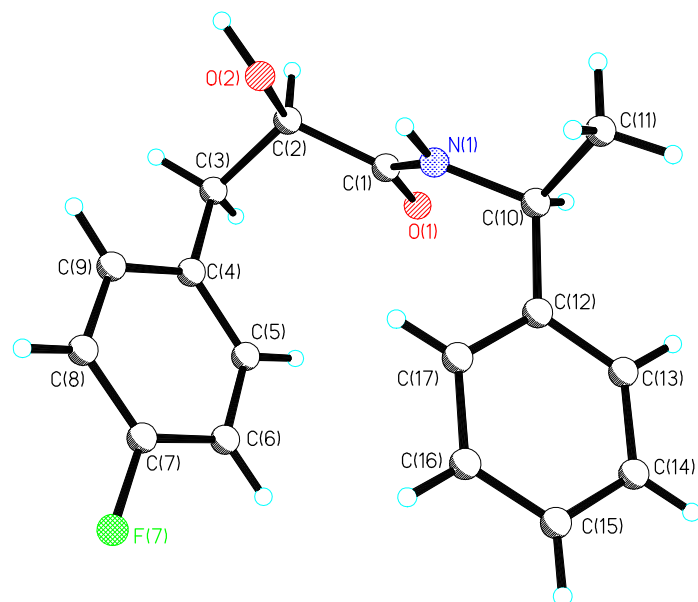


Table 1. Crystal data and structure refinement for (R,S)-**149**.

Identification code	pndh5	
Empirical formula	C ₁₇ H ₁₈ F N O ₂	
Formula weight	287.32	
Temperature	93(2) K	
Wavelength	0.71073 Å	
Crystal system	Orthorhombic	
Space group	P2(1)2(1)2(1)	
Unit cell dimensions	a = 8.9265(8) Å	$\alpha = 90^\circ$.
	b = 9.0292(8) Å	$\beta = 90^\circ$.
	c = 19.3276(18) Å	$\gamma = 90^\circ$.
Volume	1557.8(2) Å ³	
Z	4	
Density (calculated)	1.225 Mg/m ³	
Absorption coefficient	0.088 mm ⁻¹	
F(000)	608	
Crystal size	0.200 x 0.200 x 0.030 mm ³	
Theta range for data collection	2.49 to 25.35°.	
Index ranges	-10 ≤ h ≤ 7, -10 ≤ k ≤ 10, -22 ≤ l ≤ 22	
Reflections collected	12750	
Independent reflections	2746 [R(int) = 0.0280]	
Completeness to theta = 25.00°	97.6 %	
Absorption correction	Multiscan	
Max. and min. transmission	1.0000 and 0.9539	
Refinement method	Full-matrix least-squares on F ²	
Data / restraints / parameters	2746 / 2 / 199	
Goodness-of-fit on F ²	1.083	
Final R indices [I > 2σ(I)]	R1 = 0.0261, wR2 = 0.0626	
R indices (all data)	R1 = 0.0271, wR2 = 0.0633	
Absolute structure parameter	-0.2(6)	
Largest diff. peak and hole	0.138 and -0.133 e.Å ⁻³	

Crystallographic data for (*R,S*)-148a

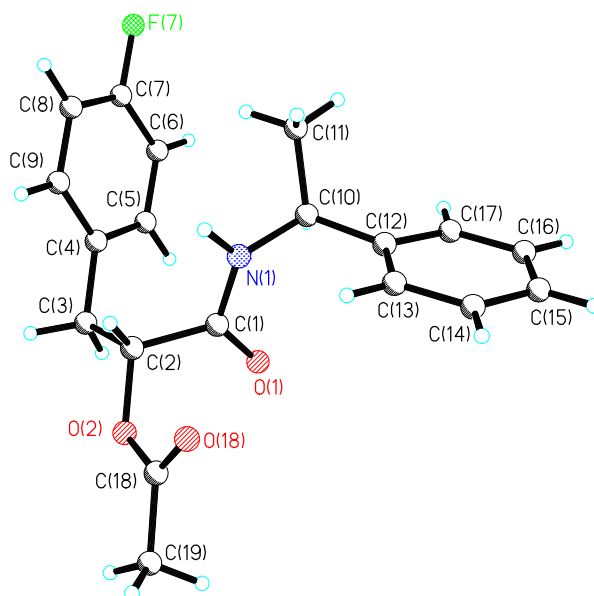


Table 1. Crystal data and structure refinement for (R,S)-**148a**.

Identification code	pndh2	
Empirical formula	C ₁₉ H ₂₀ F N O ₃	
Formula weight	329.36	
Temperature	93(2) K	
Wavelength	0.71073 Å	
Crystal system	Orthorhombic	
Space group	P2(1)2(1)2(1)	
Unit cell dimensions	a = 9.2837(10) Å	$\alpha = 90^\circ$.
	b = 12.9755(15) Å	$\beta = 90^\circ$.
	c = 14.5401(17) Å	$\gamma = 90^\circ$.
Volume	1751.5(3) Å ³	
Z	4	
Density (calculated)	1.249 Mg/m ³	
Absorption coefficient	0.091 mm ⁻¹	
F(000)	696	
Crystal size	0.1000 x 0.0500 x 0.0500 mm ³	
Theta range for data collection	2.60 to 25.34°.	
Index ranges	-10 ≤ h ≤ 9, -12 ≤ k ≤ 15, -17 ≤ l ≤ 17	
Reflections collected	11629	
Independent reflections	3099 [R(int) = 0.0459]	
Completeness to theta = 25.00°	97.7 %	
Absorption correction	Multiscan	
Max. and min. transmission	1.0000 and 0.9740	
Refinement method	Full-matrix least-squares on F ²	
Data / restraints / parameters	3099 / 1 / 224	
Goodness-of-fit on F ²	1.016	
Final R indices [I > 2σ(I)]	R1 = 0.0431, wR2 = 0.0814	
R indices (all data)	R1 = 0.0564, wR2 = 0.0875	
Absolute structure parameter	0.8(10)	
Extinction coefficient	0.0150(15)	
Largest diff. peak and hole	0.182 and -0.184 e.Å ⁻³	

Crystallographic data for 174a

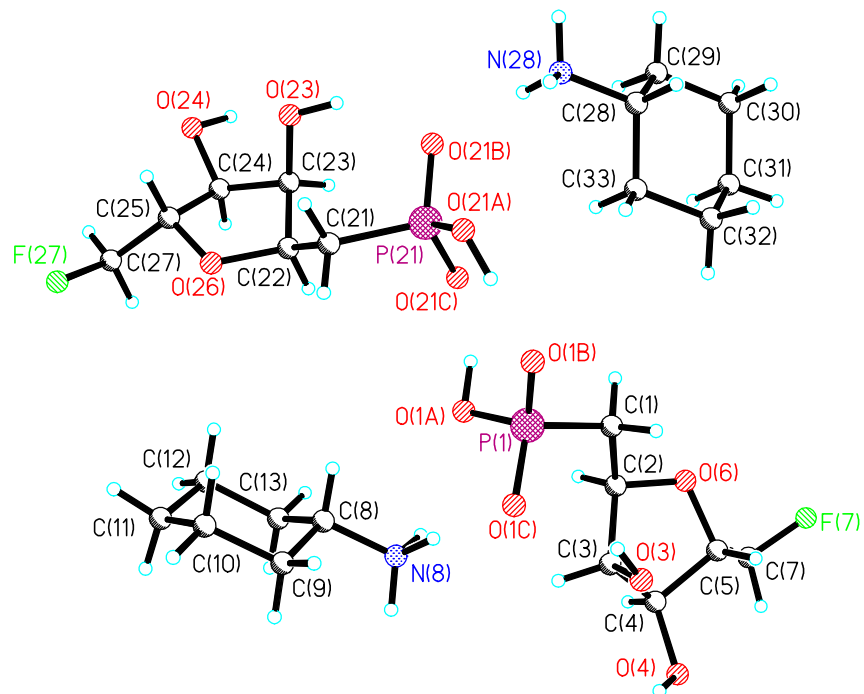


Table 1. Crystal data and structure refinement for **174a**.

Identification code	pndh7	
Empirical formula	C ₁₂ H ₂₅ F N O ₆ P	
Formula weight	329.30	
Temperature	93(2) K	
Wavelength	0.71073 Å	
Crystal system	Triclinic	
Space group	P1	
Unit cell dimensions	a = 5.6457(14) Å	$\alpha = 85.28(2)^\circ$.
	b = 11.273(4) Å	$\beta = 81.582(18)^\circ$.
	c = 12.867(4) Å	$\gamma = 76.950(18)^\circ$.
Volume	788.2(4) Å ³	
Z	2	
Density (calculated)	1.388 Mg/m ³	
Absorption coefficient	0.211 mm ⁻¹	
F(000)	352	
Crystal size	0.1500 x 0.1500 x 0.0100 mm ³	
Theta range for data collection	1.86 to 25.35°.	
Index ranges	-6 ≤ h ≤ 6, -13 ≤ k ≤ 12, -15 ≤ l ≤ 15	
Reflections collected	6205	
Independent reflections	4337 [R(int) = 0.0519]	
Completeness to theta = 25.00°	99.3 %	
Absorption correction	Multiscan	
Max. and min. transmission	1.0000 and 0.9734	
Refinement method	Full-matrix least-squares on F ²	
Data / restraints / parameters	4337 / 15 / 429	
Goodness-of-fit on F ²	1.032	
Final R indices [I > 2σ(I)]	R1 = 0.0530, wR2 = 0.1401	
R indices (all data)	R1 = 0.0552, wR2 = 0.1467	
Absolute structure parameter	-0.03(13)	
Extinction coefficient	0.058(7)	
Largest diff. peak and hole	0.428 and -0.394 e.Å ⁻³	

Appendix II

List of Publications

“Tropic acid biosynthesis: Mechanistic insights into the P-450 mediated isomerisation of littorine to hyoscyamine in *Hyoscyamus niger*”

Pitak Nasomjai, Darwin W Reed, David Tozer, Michael Peach, Alex M. Z. Slawin, Patrick S Covello and David O’Hagan, *ChemBioChem*, 2009, **10**, 2382-2393.

“Synthesis of phosphonate and phostone analogues of ribose-1-phosphates”

Pitak Nasomjai, David O’Hagan, and Alexandra M Z Slawin, *Beilstein J Org Chem.*, 2009; **5**.

Conferences attended

- 238th ACS National Meeting & Exposition, Washington DC (USA), Aug 2009. Poster presentation
- Organic Chemistry Final Year PhD Symposium, St Andrews (UK), June, 2009. Oral Presentation
- 38th RSC Scottish Organic Division Meeting, Aberdeen (UK), Dec 2008. Poster presentation
- 8th RSC Fluorine Group Meeting, Henderson Hall, Newcastle University (UK), Sep 2008. Oral presentation
- RSC Drugs from Natural Products IV, New Hall, Cambridge, Apr 2008. Poster presentation

- 36th RSC Scottish Organic Division Meeting, Glasgow (UK), Dec 2007.
- RSC Bio-Organic Group Meeting: Biosynthesis in Unexpected Places, Fribush (UK), Sep 2007.
- 6th Annual RSC Fluorine Subject Group Meeting, Hulme Hall, University of Manchester, 31 Aug-01 Sep 2006.
- 35th RSC Scottish Organic Division Meeting, Glasgow (UK), Dec 2005.